Aerobic and Electrochemical Treatment of Process Water from Hydrothermal Carbonization of Sewage Sludge

vom Fachbereich 13
Bau- und Umweltingenieurwissenschaften
der Technischen Universität Darmstadt

Zur Erlangung des akademischen Grades eines
Doktor-Ingenieurs (Dr.-Ing.)
genehmigte

DISSERTATION

von
Tobias Blach, M.Sc.

Erstgutachter:	Prof. Dr.-Ing. Markus Engelhart
Zweitgutachterin:	Prof. Dr.-Ing. Heidrun Steinmetz

Darmstadt 2024

Tobias Blach, M.Sc.

Aerobic and Electrochemical Treatment of Process Water from Hydrothermal Carbonization of Sewage Sludge

Darmstadt, Technische Universität Darmstadt

Jahr der Veröffentlichung der Dissertation auf TUprints: 2025

URN: urn:nbn:de:tuda-tuprints-273565

URI: https://tuprints.ulb.tu-darmstadt.de/id/eprint/27356

Erstgutachter: Prof. Dr.-Ing. Markus Engelhart

Zweitgutachterin: Prof. Dr.-Ing. Heidrun Steinmetz

Tag der schriftlichen Einreichung: 10.01.2024

Tag der mündlichen Prüfung: 25.04.2024

Abstract

This dissertation demonstrates possibilities and limitations of aerobic and electrochemical processes for the treatment of process water from the hydrothermal carbonisation (HTC) of sewage sludge. During HTC, sewage sludge is heated to around 190 to 250 °C, causing various reaction mechanisms to turn sewage sludge into a brown coal-like solid. The so-called hydrochar or biochar has a higher calorific value and better dewaterability compared to the untreated sewage sludge. This enables thermal utilisation, use as an adsorbent, or for carbon sequestration. However, the reaction mechanisms also release a large number of organic substances from the solids and partially transform them into substances that are difficult to biodegrade, inhibitory or toxic. Current research focuses primarily on optimizing the HTC process and only secondarily on treating the highly contaminated process water. Nevertheless, previous studies have shown that biodegradability of process water contaminats is limited and hindered by various inhibitors. This raises the issue of the robustness of aerobic processes and the efficiency of electrochemical oxidation to remove refractory substances. The main findings are summarized in four international publications.

Paper 1 visualizes the correlation of the process water load on various reaction parameters. For this purpose, the effect of the parameters reaction temperature (190 to 250 °C), reaction time (0.5 to 4 h) and pH value (3.9 to 6.1) on calorific value, dissolved organic carbon (DOC), and ammonium was tested using design of experiments and the Box-Behnken design. The temperature turned out to be the decisive parameter of the HTC reaction. The higher the temperature, the higher was the calorific value of the hydrochars and the lower was the concentration of DOC in the process water. Higher temperature also increased the percentage of ammonium in the total nitrogen due to the mineralisation of dissolved organic nitrogen (DON).

As the reaction temperature emerged as the decisive reaction parameter from paper 1, paper 2 focuses on the effect of temperature on aerobic bio-degradability. In Zahn-Wellens tests, the DOC removal for temperatures from 190 to 249 °C was about 81%. Continuous lab-scale tests in sequencing batch reactors (SBR, V=0.3 L) also showed similar DOC removals of 72% for different temperatures (190 °C and 217 °C). Due to the strong inhibition by substances formed during HTC, nitrification was only possible by diluting the process water 1:10. Inhibition tests according to DIN EN ISO 9509 (2006) revealed a stronger

inhibition for process water at 217 °C than at 190 °C. However, the overall effect of temperature on aerobic biodegradability can be considered low. In addition, an exemplary mix calculation for a municipal wastewater treatment plant showed that the refractory organics could increase the effluent concentration of chemical oxygen demand (COD) by 24 mg/L in the worst case.

Paper 3 takes up the findings of paper 2 and transfers them to the operation of a pilot plant in order to determine the limits of nitrification performance and organic removal. For this purpose, the sludge loading of a membrane bioreactor (MBR, V=170 L) and an SBR (V=300 L) was successively increased. In addition, reducing the dilution of the process water from 1:20 to 1:1 led to an increase in inhibitor concentration. The maximum sludge loading for nitrification as total nitrogen (TN) per mixed liquor suspended solids (MLSS) was 20 - 25 mg TN/(g MLSS·d) in both reactors. The nitrogen sludge loading during treatment of the undiluted process water was too high for nitrification. With nitrification, COD removal was 74.8 ± 1.9% (MBR) and 71.4 ± 2.6% (SBR). The activated sludge from the SBR adapted to inhibitors in the process water to a certain degree. The nitrification rate was inhibited by 50% at 50 mg DON (i.e. 4% v/v process water share), compared to 6.6 mg DON (i.e. 0.4% v/v process water share) for activated sludge from a municipal wastewater treatment plant. Although different process waters were treated in paper 2 and 3, both the COD removal and the inhibition of nitrification were similar.

Paper 2 and paper 3 have demonstrated that 20 to 30% of the COD was not biodegradable. Following this, paper 4 presents results from the electrochemical oxidation (EO) of refractory COD using a boron-doped diamond electrode and introduced three possible treatment scenarios: (I) EO alone, (II) aerobic COD removal + EO, and (III) nitrification/denitrification + EO. In all scenarios, EO proved to be very effective and even reduced the COD to below 10 mg/L in scenario III. This low concentration was associated with an energy consumption of up to 534 kWh/kg COD. As the energy consumption of the EO largely depends on the COD concentration, it was significantly lower in scenario I and II with 31.3 and 46.6 kWh/kg COD. A concluding mass balance showed that scenario II had the lowest overall energy consumption due to the reduced COD load and yet high energy efficiency.

The result of this dissertation suggest that aerobic treatment with downstream electrochemical oxidation is a conceivable solution for treating HTC process water. However, due to high inhibitor concentration, nitrification can in fact only be established by diluting the process water.

Kurzfassung

Diese Dissertation zeigt Möglichkeiten und Grenzen aerober und elektrochemischer Verfahren zur Behandlung von Prozesswasser aus der hydrothermalen Karbonisierung (engl. hydrothermal carbonization, HTC) von Klärschlamm auf. Während der HTC wird Klärschlamm auf etwa 190 bis 250 °C erhitzt, wodurch diverse Reaktionsmechnismen aus Klärschlamm einen braunkohleartigen Feststoff formen. Die sogenannte Hydrokohle oder Biokohle weist einen im Vergleich zu Klärschlamm höheren Brennwert und eine bessere Entwässerbarkeit auf. Dies ermöglicht eine thermische Verwertung, den Einsatz als Adsorbens oder zur Sequestrierung von Kohlenstoff. Die Reaktions-mechanismen lösen jedoch auch eine Vielzahl an organischen Stoffen aus dem Feststoff heraus und formen daraus teilweise biologisch schwer abbaubare, hemmende oder toxische Stoffe. Der Fokus der Forschung lag bislang primär auf der Optimierung des HTC Prozesses und nur sekundär auf der Behandlung der hoch belasteten Prozesswässer. Bisherige Studien zeigen jedoch, dass die biologische Abbaubarkeit der Stoffe im Prozesswasser limitiert ist und durch Hemmstoffe erschwert wird. Hieraus ergibt sich die Fragestellung wie robust aerobe Verfahren sind und inwiefern eine elektrischemische Oxidation refraktäre Stoffe entfernen kann. Die wesentlichen Erkenntnisse werden in vier Papern zusammengefasst.

Paper 1 veranschaulicht die Abhängigkeit der Prozesswasserbelastung von verschiedenen Reaktionsparametern. Hierzu wurde mittels statistischer Versuchsplanung und Box-Behnken Design der Einfluss der Parameter Reaktionstemperatur (190 bis 250 °C), Reaktionsdauer (0,5 bis 4 h) sowie pH-Wert (3,9 bis 6,1) auf Brennwert der Hydrokohle, gelöstem Kohlenstoff (engl. dissolved organic carbon, DOC) und Ammonium untersucht. Hierbei erwies sich die Temperatur als maßgebender Parameter der HTC Reaktion. Je höher die Temperatur, desto höher war der Brennwert der Hydrokohle und desto geringer war die DOC-Konzentration im Prozesswasser. Mit höherer Temperatur nahm der prozentuale Anteil von Ammonium am gesamten Stickstoff durch Mineralisierung gelöster organischer Stickstoffverbindungen (engl. dissolved organic nitrogen, DON) zu.

Da aus Paper 1 die Temperatur als maßgebender Reaktionsparameter hervorging, thematisiert Paper 2 die Auswirkung der Temperatur auf die aerobe Abbaubarkeit. In Zahn-Wellens Tests betrug die DOC Entfernung für Temperaturen von 190 bis 249 °C etwa 81%. In kontinuierlichen Laborversuchen

in Sequencing Batch Reaktoren (SBR, V=0.3 L) wurden mit 72% DOC Entfernung ebenfalls ähnliche Werte für unterschiedliche HTC Temperaturen (190 °C und 217 °C) festgestellt. Aufgrund der starken Hemmung von während der HTC gebildeten Stoffen, war eine Nitrifikation nur durch Verdünnung des Prozesswassers (1:10) möglich. Hemmtests nach DIN EN ISO 9509 (2006) wiesen für Prozesswasser bei 217 °C eine stärkere Hemmung als bei 190 °C nach. Insgesamt ist der Einfluss der Temperatur auf die aerobe Abbaubarkeit jedoch als gering einzustufen. Weiterhin zeigte eine exemplarische Mischungsrechnung für eine kommunale Kläranlage, dass die refraktäre Organik die Ablaufkonzentration des chemischen Sauerstoffbedarfs (engl. chemical oxygen demand, COD) im ungünstigsten Fall um 24 mg/L erhöhen könnte.

Paper 3 greift die Erkenntnise aus Paper 2 auf und überträgt diese in den Betrieb einer Pilotanlage mit dem Ziel die Grenzen der Nitrifikationsleistung und der Organikentfernung zu ermitteln. Hierzu wurde die Schlammbelastung eines Membran Bioreaktor (MBR, V=170 L) und eines SBR (V=300 L) sukzessive gesteigert. Zudem führte die Rücknahme der Verdünnung des Prozesswassers von 1:20 auf 1:1 zur Steigerung der Hemmstoffkonzentration. Die für eine Nitrifikation maximale Schlammbelastung als Gesamtsickstoff (engl. total nitrogen, TN) pro Trockensubstanz (engl. mixed liquor suspended solids, MLSS) lag in beiden Reaktoren bei 20 - 25 mg TN/(g MLSS·d). Die Stickstoff-schlammbelastung bei der Behandlung des unverdünnten Prozesswassers war zu hoch für eine Nitrifikation. Mit Nitrifikation betrug die COD-Entfernung 74.8 ± 1.9% (MBR) und 71.4 ± 2.6% (SBR). Der Belebtschlamm aus dem SBR konnte sich an Hemmstoffe im Prozesswasser in gewissem Umfang anpassen. Die Nitrifikationsrate wurde bei 50 mg DON (bzw. 4 vol.-% Prozesswasser) um 50% gehemmt, im Vergleich zu 6,6 mg DON (bzw. 0.4 vol.-% Prozesswasser) für Belebtschlamm aus einer kommunalen Kläranlage. Obwohl in Paper 2 und 3 verschiedene Prozesswässer behandelt wurden, lag sowohl die COD-Entfernung als auch die Hemmung der Nitrifikation in einer ähnlichen Größenordnung.

Paper 2 und Paper 3 demonstrierten, dass zwischen 20 und 30% des COD biologisch nicht abbaubar sind. Daran anknüpfend legt Paper 4 die Ergebnisse der elektrochemischen Oxidation (EO) des refraktären COD mittels bor-dotierter Diamantelektrode dar und stellt drei mögliche Behandlungsszenarien vor: (I) alleinige EO, (II) aerobe Kohlenstoffelimination + EO und (III) Nitrifikation/ Denitrifikation + EO. In allen Szenarien erwies sich die EO als sehr effektiv und reduzierte den COD in Szenario III sogar auf unter 10 mg/L. Diese niedrige Konzentration war mit einem Energieaufwand von bis zu 534 kWh/kg COD

verbunden. Da der Strombedarf der EO maßgebend von der COD-Konzentration abhängt, war der Energiebedarf in Szenario I und II mit 31,3 und 46,6 kWh/kg COD deutlich geringer. Eine abschließende Massenbilanz zeigte auf, dass Szenario II aufgrund reduzierter COD-Fracht und dennoch hoher energetischer Effizienz den insgesamt geringsten Energiebedarf besaß.

Die Ergebnisse dieser Arbeit legen nahe, dass eine aerobe Behandlung mit nachgeschalteter elektrochemischer Oxidation eine Lösung zur Behandlung von HTC-Prozesswasser ist. Aufgrund der hohen Hemmstoff-Konzentration kann eine Nitrifikation jedoch nur durch Verdünnung des Prozesswassers erzielt werden.

Acknowledgment

Diese Dissertation ist während meiner Zeit als wissenschaftlicher Mitarbeiter am Institut IWAR der Technischen Universität Darmstadt entstanden. Die Untersuchungen fanden überwiegend im Rahmen des Projekts „IntenKS“ statt und wurden durch das Bundesministerium für Bildung und Forschung gefördert.

An erster Stelle möchte ich mich bei Prof. Dr.-Ing. Markus Engelhart für die Betreuung meiner Dissertation, die fachlichen Diskussionen sowie die vertrauensvolle gemeinsame Arbeit sehr herzlich bedanken. Prof. Dr.-Ing. Heidrun Steinmetz danke ich für die freundliche Übernahme des Korreferats. Herrn Prof. Dr.-Ing. habil. Martin Wagner danke ich für seine Unterstützung, insbesondere hinsichtlich diverser Reisen nach China.

Meinen ehemaligen Kolleginnen und Kollegen am IWAR möchte ich für die angenehme Zusammenarbeit und die abwechslungsreiche Zeit danken. Sinem Fundneider-Kale danke ich für die Unterstützung in Labor und Technikum sowie die vielen Flachwitze, die jederzeit einen guten Start in den Büro-Tag bedeuteten. Johannes Rühl gilt mein Dank für die vielen fachlichen Diskussionen und sein Engagement mich an seinen Erfahrungen teilhaben zu lassen. Bei Luisa Barkmann-Metaj, Thomas Fundneider, Maximilian Schwarz, Jana Trippel, Justus Behnisch und Maro Atzorn bedanke ich mich für die zahlreichen herzlichen Einladungen zu gemeinsamen Unternehmungen. Hajo Bitter und Philipp Bunse danke ich für den Einsatz auf und neben dem Fußballplatz. Franziska Kirchen möchte ich für die Unterstützung und die Ermunterung während der Pilotierung in Darmstadt-Eberstadt danken. Bei Bingxiang Wang bedanke ich mich für die gemeinsamen Abende mit vorzüglichem chinesischem Essen. Michel Harder danke ich für angehme und produktive Diskussionen zur Bearbeitung des gemeinsamen Forschungsprojekts. Thu Ngyuen und Gregor Knopp möchte ich für den Einstieg in die Abwassertechnik auf dem Versuchsfeld, insbesondere aber in Vietnam bedanken. Robert Lutze danke ich für viele lebhafte Diskussionen und den guten Start am IWAR.

Die vorliegende Arbeit wäre ohne die Mithilfe zahlreicher Studierender, ob als studentische Hilfskraft oder im Rahmen einer Abschlussarbeit, nicht möglich gewesen. Für den herausragenden Einsatz gilt mein Dank insbesondere Lea Hennemann, Pierre Lechevallier, Abdul Mateen, Lara Schreiber, Wibke de Boer und Patrick Grobecker sowie Katharina Aupperle, Miguel Ospina und Victoria Breidling.

Für die tatkräftige Unterstützung bei dem Bau und der Programmierung der Pilotanlage möchte ich mich herzlich bei Florian Bleffert und Manuel Hesse der

Firma HST Systemtechnik bedanken. Christian Georg und Ewa Freitag danke ich für die Unterstützung beim Betrieb der Pilotanlage. Vom Labor des IWAR danke ich insbesondere Harald Grund, der mir stets mit Rat und Tat zur Seite stand. Ein besonderer Dank gilt Vera Soedradjat und Renate Schäfer, ohne deren unermüdlicher Einsatz der Alltag am Institut deutlicher grauer gewesen wäre.

Zuletzt möchte ich mich bei meiner Familie bedanken. Meine Eltern und meine Schwester Patricia haben mir erst die Möglichkeit einer Promotion gegeben und mich fortwährend unterstützt. Meiner Freundin Rebecca danke ich für die nie endende Unterstützung, das Verständnis und den Freiraum, mich an Abenden und Wochenenden dieser Arbeit widmen zu können.

Table of contents

List of figures

List of tables

List of abbreviations

Abbreviation	Description, Unit
AC	Activated carbon
ADD	Absolute average deviation
ADS	Anaerobically digested sludge
ANOVA	Analysis of variance
AOB	Ammonium oxidizing bacteria
BBD	Box-Behnken design
BDD	Boron-doped diamond electrode
COD	Chemical oxygen demand
DF	Degrees of freedom
DO	Dissolved oxygen in mg/L
DOC	Dissolved organic carbon in mg/L or g/L
DON	Dissolved organic nitrogen in mg/L or g/L
EC_{50}	50% inhibitition
EC	Energy consumption in kWh
EC/ECO	Electrical conductivity in mS/cm, μS/cm
EO	Electrochemical oxidation
F/M_X	Sludge loading for X = COD, DOC, TN in mg/(g MLSS·d)
Fe^{2+}/PS	Ferrous/persulphate
FA	Free ammonia in mg/L
FNA	Free nitrous acid in mg/L
G_L	Dilution level causing less than 20% toxicity to *Vibrio fischeri*
HHV	Higher heating value in MJ/kg TS
HMF	5-hydroxymethylfurfural
HRT	Hydraulic retention time in d
HTC	Hydrothermal carbonization
HTG	Hydrothermal gasification
HTL	Hydrothermal liquefaction

IC_{50}	50% nitrification inhibition
ICE	Instantaneous current efficiency in %
MBR	Membrane bioreactor
MBR 1-1	MBR effluent (without dilution and nitrication/denitrification)
MBR 1-10	MBR effluent (with 1:10 dilution and nitrification/denitrification)
MLSS	Mixed liquor suspended solids in g/L
MLVSS	Mixed liquor volatile suspended solids in g/L
MS	Mean squares
NOB	Nitrite oxidizing bacteria
OLR	Organic loading rate in g/(L·d)
ON	Oxidized nitrogen in mg/L
ORP	Redox potential in mV
PAH	Polycyclic aromatic hydrocarbons
PS	Primary sludge
PW	HTC process water
PW-AD	HTC process water
RCS	Reactive chlorine species
rCOD	Recalcitrant chemical oxygen demand in mg/L
rDOC	Recalcitrant dissolved organic carbon in mg/L
rDON	Recalcitrant dissolved organic nitrogen in mg/L
RS1	Raw sewage sludge 1
RS2	Raw sewage sludge 2
RS3	Raw sewage sludge 3
RSM	Response surface methodology
SBR	Sequencing batch reactor
SBR190	SBR operating with process water generated at 190 °C
SBR217	SBR operating with process water generated at 217 °C
SUVA	Ratio of UV_{254} to DOC in L/(mg·m)

SRT	Sludge retention time in d
SS	Sum of squares
SVI	Sludge volume index in mL/g
TKN	Total Kjeldahl nitrogen in mg/L or g/L
TN	Total nitrogen in mg/L or g/L
TOC	Total organic carbon in mg/L or g/L
TS	Total solids in %
$UV_{254,\ 475}$	UV absorbance at 254 or 475 nm
VFA	Volatile fatty acids in mg/L or g/L
VS	Volatile solids in %
WAS	Waste activated sludge
WWTP	Wastewater treatment plant
ZW190	Zahn-Wellens test with process water generated at 190 °C
ZW218	Zahn-Wellens test with process water generated at 218 °C
ZW218*	Similar to ZW218 but with adapted inoculum
ZW249	Zahn-Wellens test with process water generated at 249 °C
β_0	Intercept, dimensionless
β_i	Linear constant, dimensionless
β_{ii}	Quadratic constant, dimensionless
β_{ij}	Interactive constant, dimensionless
$y_{i,exp}$	Experimental results in mg/L
$y_{i,cal}$	Calculated results in mg/L
p	Number of HTC runs, dimensionless
f	Reaction intensity, dimensionless
c_X	Concentration of a substance X in mg/L or g/L
I_N	Inhibition of nitrification in %
R_N	Nitrification rate in mg N/(g MLSS·h)
R_{AOB}	AOB rate in mg N/(g MLSS·h)
Q_X	Volume flow of a stream X in m^3/d

Re	Reynold's number, dimensionless
ρ	Density in kg/m^3
η	Viscosity in mPa·s
d	Hydraulic diameter in cm
F	Faraday's constant in C/mol
i_{app}	Applied specific current in A/m^2
i_{lim}	Limiting current in A/m^2
k_m	Mass transport coefficient in m/s
α	Ratio of applied specific current and limiting current, dimensionless
A	Anode area in m^2
t	Time in s or min or h
T	Temperatur in °C or K
V_X	Volume of a reactor X in L or m^3
I	Applied current in A
j	Current density in mA/cm^2 or A/m^2
COD_t	COD at time t in mg/L
EE/M	Electrical energy per mass of COD in kWh/kg COD
U	Voltage in V

1 Introduction

Reusing resources from waste streams is a necessary step towards a sustainable society and a circular economy. Sewage sludge, which is a residual material from wastewater treatment, is one of these waste streams. In 2021, around 1.7 million tons of sewage sludge (dry mass) had to be disposed of in Germany (Destatis 2021). The German Sewage Sludge Ordinance and the German Fertilizer Ordinance provide the legal foundation for the disposal of sewage sludge in Germany. Their amendment in 2017 has significantly restricted the agricultural use of sewage sludge as a fertilizer by introducing an obligation to recover phosphorus and by limiting the use of polymers, and stricter regulations on the maximum content of heavy metals. As a result, new and sustainable ways of recycling sewage sludge and recovering phosphorus are urgently needed. So far, sewage sludge incineration followed by phosphorus recovery is a promising approach whose full scale potential is being intensively tested (FiW e.V. 2023). However, the thermal drying required prior to incineration is a very energy-intensive process step.

Hydrothermal carbonization (HTC) is an alternative process for the treatment of sewage sludge. At elevated temperatures, this process transforms sewage sludge into a brown coal-like solid, known as hydrochar (or biochar). This hydrochar-slurry can be dewatered very well, reducing the energy consumption for thermal drying. In addition, other utilization possibilities of the hydrochars as an adsorbent or carbon sequestration material are being discussed (Reißmann et al. 2018). So far, the focus has been on optimizing the HTC process itself and the production of hydrochars. However, a key issue in developing the HTC is how to deal with the process water that is separated during dewatering the hydrochar-slurry. Due to the thermochemical conversion processes, HTC process water is contaminated with carbonaceous and nitrogenous substances, but also phosphorus (Ohlert 2015; Wang et al. 2019b). Some of these substances, such as volatile fatty acids, are readily biodegradable, while others, e.g. pyrazines or pyridines, are poorly biodegradable. These refractory substances are generated in particular when nitrogen-rich feedstock such as sewage sludge is used for HTC (Wang et al. 2019a). For process water treatment, progress has already been made and various processes have been investigated, including anaerobic digestion, wet oxidation, Fe^{2+}/persulfate oxidation, adsorption, coagulation, or membrane processes. (Reza et al. 2016; Wirth 2021; Liu et al. 2022; Hu et al. 2022a; Urbanowska et al. 2020). Nevertheless, the reported treatment approaches were not sufficient regarding the attained effluent qualities. The

treatment of the process water is one of the most crucial issues for an ecological and economical implementation of the HTC, apart from phosphorus recycling and the energetic balance (Reißmann et al. 2021).

2 Hydrothermal carbonization

Hydrothermal carbonization is a hydrothermal process for producing a brown coal-like solid from organic matter. The carbonization process takes a long time in nature, but in 1913, Friedrich Bergius discovered how to accelerate the natural process in a technical application (Bergius 1913). For this purpose, biomass is subjected to elevated temperatures and corresponding steam pressures in a pressure reactor in an aqueous environment. The water content is typically around 40 to 85% and is essential for the reaction (Vogel 2016). Water suppresses undesirable pyrolytic processes and ensures an even temperature distribution. Furthermore, water changes its physical properties at high temperatures and serves as a reaction medium. The dielectric constant, which is an indicator of polarity, decreases, water becomes more nonpolar than at room temperature and therefore behaves like an organic solvent. Due to the increasing ion product, water has a catalyzing effect on the reactions that take place (Peterson et al. 2008; Akiya and Savage 2002). For efficient process performance, however, the water content should be as low as possible, since additional water must also be heated and more organic material undesirably dissolves into the water (Stemann 2013).

The temperature is the most important process parameter of the HTC and is usually set between 180 and 250 °C. HTC has the lowest temperature of all hydrothermal processes compared to hydrothermal liquefaction (HTL, about 330 °C) and hydrothermal gasification (HTG, about 400 to 600 °C) (Vogel 2016). During HTC, the carbon content of the produced hydrochar increases with higher temperatures, while the mass yield is lowered. The reactant mainly governs the maximum achievable carbon content and the required temperature (Funke 2012). Furthermore, longer reaction times lead to higher carbon contents, although the influence is smaller than that of the temperature. Reaction times range from 1 to 72 h, while periods of less than 5 h being typical (Funke and Ziegler 2010). The term reaction intensity generally refers to the intensity of hydrothermal treatment without distinguishing between temperature and reaction time. Besides various analytical parameters, the higher degree of coalification with increasing reaction intensity can also be observed visually (Figure 1).

Figure 1: Raw sewage sludge (I) and hydrochars with increasing reaction intensity (II: 190°C, 0,5h; III: 220°C, 1h; IV: 250°C, 4h)

In addition to the targeted hydrochar, a liquid phase and process gas are produced during HTC. While the process gas is usually less important, composition and treatment of the liquid phase take a key role.

2.1 Main reactions

The formation of hydrochar under hydrothermal conditions is governed by several different reactions. On the one hand, these cause the solid itself to be converted into hydrochar and, on the other hand, dissolved substances to polymerize and form very fine hydrochar particles (Kruse et al. 2013).

During hydrolysis, biopolymers are degraded by reacting with water. These are further broken down into smaller components or extracted from the biomass and decomposed. In this way, the chemical bonds of carbohydrates, lipids, proteins, or lignin can be cleaved under hydrothermal conditions (Funke 2012). The type of bond determines the temperature required for hydrolysis. Peptide, ester, and glycosidic bonds, which are present in proteins, lipids, hemicelluloses, and cellulose, are easily hydrolyzable (<180 °C). In contrast, ether bonds in lignin are much more stable and can only hydrolyze at higher temperatures (approx. 340 °C). Hydrolysis is the basis for subsequent reactions, as solubilized substances are further decomposed and transformed (Vogel 2016).

In the dehydration process, water is split off from molecules. This removal of chemically bound water greatly decreases the oxygen content of the solids. In addition, intermediates are formed which ultimately lead to the generation of HTC hydrochars (Titirici et al. 2007a). Although dehydration is a highly exothermic process, the exothermicity is often overestimated which means HTC requires an external heat supply (Vogel 2016; Funke 2012). Decarboxylation

describes the removal of carboxyl groups from carboxylic acids with the release of carbon dioxide. Decarboxylation and dehydration often occur simultaneously (Lachos-Perez et al. 2022). Reaction products are alcohols, short fatty acids, organic acids, or furans, for example (Blöhse 2016).

The key reaction of HTC is the polymerization of the solubilized decomposition products into hydrochar. The terms "polymerization reactions", "polymerization" and "polyreaction" are often used synonymously for reactions in which monomers are converted into polymers. Polymerization further includes reactions such as polyaddition and polycondensation (Takagi 2015). For the formation of solids, aldol condensation is considered as an important mechanism (Sevilla and Fuertes 2009; Kruse and Dinjus 2007). Higher temperatures generally favor the solid formation, but depending on the reactant, polymerization reactions already start at 180 - 210 °C (Dinjus et al. 2011).

In addition, several other reactions occur. For example, aromatization reactions form aromatic and phenolic components, especially at higher temperatures and alkaline pH values (Falco et al. 2011; Nelson et al. 1984). During the carbonization of protein-containing biomass such as sewage sludge, Maillard reactions take place. These reactions of an amino acid or peptide with a reduced sugar form yellow-brown melanoidins. Due to the high nitrogen content, these are undesirable (Vogel 2016) and are often found in the liquid phase rather than in the HTC char (Fettig and Liebe 2013). Moreover, the presence of proteins induces deamination reactions in which ammonia or ammonium is released (Liebeck 2015).

2.2 HTC of sewage sludge

The reaction mechanisms during HTC change the elemental composition of the solids. The degree of coalification is plotted as the molar ratio of O/C versus H/C in a so called Van-Krevelen diagram (Figure 2). Using sewage sludge as an example, the graph illustrates that the hydrochars produced have a slightly higher hydrogen content, but are comparable to lignin. The more intense the HTC process, the more the hydrochars become similar to brown coal. In the compiled studies, the temperature ranged from 180 to 240 °C and the reaction time from 15 to 240 min.

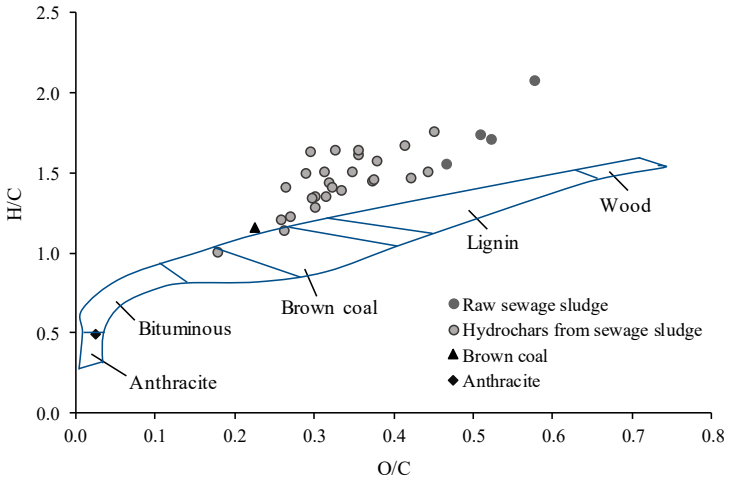

Figure 2: Molar ratios of O/C versus H/C in the so-called Van-Krevelen diagram. Data from Wilk et al. (2022), Zhao et al. (2014), Franck und Knop (1979), Smith et al. (2016), Wang et al. (2020), blue area from Vogel (2016)

In principle, the hydrochars produced from sewage sludge HTC allow a variety of recycling opportunities. In addition to incineration, direct land application as well as use for carbon sequestration, as an adsorbent or as a catalyst were investigated (Hu et al. 2022a; Fang et al. 2018; Hu et al. 2010). Compared to HTC hydrochars from carbohydrate-based feedstock, hydrochars from sewage sludge often have a lower carbon content and a higher ash content. As a result, these hydrochars are not universally suitable for carbon sequestration or as a catalyst. Although they potentially contain high phosphorus concentrations, agricultural utilization is very limited or not possible at all due to legal regulations in Germany (Schnell et al. 2020; Reißmann et al. 2018). Some studies have already used hydrochars as adsorbents and obtained promising results, but further research seems necessary (Ferrentino et al. 2020; Spataru et al. 2016).

Despite the many recycling opportunities for hydrochars from sewage sludge, incineration appears to be the most appropriate use at the moment. This is due to the energetic advantages of incinerating hydrochars compared to dewatered sewage sludge. The main reason for this is the significantly higher total solids (TS) that can be achieved in mechanical dewatering. Furthermore, the carbon content and hence the calorific value of the hydrochars can be increased if the sludge composition is suitable. This allows to completely or at least partially avoid thermal drying, which is usually required before the incineration of sewage sludge. The energy savings during thermal drying can lead to economic advantages of an HTC in a sewage sludge treatment concept. A study by Krebs et al. (2013) suggests incineration in a cement factory, for which the authors

assume drying to 92% dry matter (Figure 3). However, since sewage sludge can burn autothermally at 50 - 55% TS, further drying is not necessarily required (Roskosch and Heidecke 2019).

Figure 3: Suggested integration of an HTC before thermal drying and incineration according to Krebs et al. (2013)

2.2.1 Dewatering properties

In addition to these significant energy savings, the higher TS contents achievable in mechanical dewatering reduce the volume of the hydrochars and thus transport costs. The improved water separability in hydrochars is largely due to the cleavage of polar functional groups during HTC. For proteins, humic substances, and polysaccharides, these functional groups cause a negative surface charge and thus a high water-binding capacity (Wilén et al. 2003). Due to the breakdown of these substances, the surface charge changes and the water binding capacity decreases (Neyens et al. 2004). Furthermore, the reduction in hydrophilicity removes vicinal water, i.e. water molecules that adhere to the particle surface by adhesion and adsorption (Wang et al. 2014; Vesilind 1994). Since the breakdown of polymeric substances increases with higher reaction intensity, higher dewatering results can be achieved (Wang and Li 2015). This is also shown by comparing different studies on dewatering, in which TS contents between (18) 39 and 70% were achieved (Table 1). As temperature is the most important parameter for the HTC, elevating the temperature increases the TS more than prolonging the reaction time. This trend is obvious even though the studies were carried out with different types of sewage sludge and dewatering devices. Generally, filter presses often achieve higher TS compared to centrifuges due to the very fine particles (Klima et al. 2011). By optimizing, for instance, the addition of polymers or the dewatering temperature, it should be possible to achieve TS contents in the upper range of the studies. On a large scale, the company TerraNova Energy GmbH claims to achieve a TS of 65 - 70% (TerraNova Energy GmbH 2023).

Table 1: TS after dewatering hydrochars from sewage sludge in lab scale (Mean values ± STD[a])

Temperature [°C]	Reaction time [min]	TS [%]	Remarks	Reference
190	30	48	Centrifuge at 1.900 rpm	(Meng et al. 2012)
210	30	39	Filter press: 1 bar for 5 min, 4 bar for 10 min, 15 bar final pressure	(Hämäläinen et al. 2021)
230	30	44		
250	30	60		
200 - 260	<60 to 240	42 to 58	Vacuum filtration, afterward filter press 15 bar	(Blöhse 2017)
205[b]	420	52±5,5	Centrifuge 4.400 rpm, afterward filter press 40 bar	(Escala et al. 2013)
205[c]	420	70±8,0	Centrifuge 4.400 rpm, afterward filter press 40 bar	
220	30	18	Centrifuge 4.000 rpm	(Kim et al. 2014)

[a]Standard deviation
[b]Anaerobically digested sewage sludge
[c]Waste activated sludge

2.2.2 Hydochar and energy yields

The decomposition of substances and their dissolving in the liquid phase during HTC lead to a loss of solid mass compared to the feedstock. According to literature data, mass loss reaches between 12 and 70% for sewage sludge, giving a hydrochar yield of 30 to 88%. (Table 2). On the one hand, the yield depends on the character of the sewage sludge and on the other hand on the reaction intensity or the temperature. With increasing temperature, decarboxylation and dehydration lead to increased cleavage of functional groups, and the hydrochar yield decreases. Contrary to expectations, the higher heating values (HHV) of the hydrochars do not increase consistently in all studies. Compared to the raw sewage sludge, the HHV shows a drop at temperatures up to about 220 °C and an increase at temperatures above 240 °C. The results of Oliveira et al. (2022) stand out, as the HHV increases already at 170 °C. It is noticeable that the HHV of the raw sewage sludge in this study is higher than in the other studies, indicating a higher organic content. The HHV often cannot be increased if the

organic content is too low because the few organics are split off during HTC and inorganics accumulate (Zhuang et al. 2018). As a rule of thumb, no increase in HHV is to be expected above 30% inorganic content (Blöhse 2017). The mass loss and the possibility of a decrease in HHV reduce the energy yield, in some cases significantly. In the analyzed studies, the energy yield was reduced to between 90 and 36% of the input value.

Table 2: Hydrochar yields and energetic yields after HTC of sewage sludge

Sewage sludge/ Hydrochar[a]	char yield[b] [%]	HHV [MJ/kg]	Energy yield[c] [%]	Reference
SS	-	18.5	-	(Oliveira et al. 2022)
170	49	20.6	54	
240	30	22.4	36	
SS	-	14.3	-	(Wilk et al. 2022)
200	52	11.4	41	
220	55	13.4	51	
SS	-	11.5	-	(Hämäläinen et al. 2021)
210	86	11.3	85	
230	82	11.6	83	
250	72	11.9	75	
SS	-	14.9	-	(Marin-Batista et al. 2020)
180	74	14.7	73	
210	68	14.9	68	
240	52	15.1	52	
SS	-	16.0	-	(Merzari et al. 2020)
190	88	16.3	90	
220	75	15.7	74	
250	68	16.0	67	

[a]The reaction time has been excluded from this table for better clarity and its small effect

[b]Hydrochar yield = $mass_{Hydrochar}/mass_{Sewage\ sludge} \cdot 100$ (dry basis)

[c]Energy yield = $(HHV_{Hydrochar} \cdot \text{Hydrochar yield})/HHV_{Sewage\ sludge}$

The comparison shows that the HHV in hydrochars from sewage sludge can be increased with appropriate preconditions. However, the energy yield is lower due to the mass loss.

2.2.3 Energy considerations

The lower water content of the hydrochars after mechanical dewatering leads to a reduction in energy consumption (EC) of disposal pathways, in particular the thermal EC of subsequent drying. Several studies focused on specific energy

consumption of HTC and determined a range of 2.6 to 6.9 MJ/kg TS (Table 3). The ECs vary considerably and are determined by different boundary conditions and assumptions. For example, some studies assumed the recovery of heat, which is essential for the energy-efficient operation of an HTC. In the subsequent thermal drying, the energy consumption ranges from 3.2 to 14.2 MJ/kg TS, depending to a large extent on the dry matter after dewatering and the dry matter to be reached in thermal drying. This also applies to thermal drying alone, where the specific energy consumption is between 6.8 and 33.9 MJ/kg TS.

Table 3: Overview of energy consumption for HTC and thermal drying in MJ/kg TS

Process technology	EC	Remarks	Reference
HTC	2.6	Dewatering (70% TS)	(Krebs et al. 2013)
HTC + thermal drying	3.2	Dewatering (70% TS), thermal drying (92% TS)	
Thermal drying	6.8	21.3% TS to 92% TS	
HTC	5.9	HTC at 250 °C, assuming 85% heat recovery	(Aragón-Briceño et al. 2021)
HTC	5.7	Dewatering (80%), HTC at 210 °C, assuming heat recovery	(Wang et al. 2014)
HTC	6.9	Dewatering (50% TS), assuming preheating of reactors	(Zhao et al. 2014)
HTC + thermal drying	14.2	Dewatering (50% TS), thermal drying (>99% TS)	
Thermal drying	33.9	14% TS to >99% TS	
HTC	3.8	Dewatering (>60% TS)	(Blöhse 2017)
HTC + thermal drying	5.1	Dewatering (>60% TS), thermal drying (>90% TS)	
Thermal drying	11.7	>90% TS	

Zhao et al. (2014) reported that the energy contained in the sewage sludge was not sufficient for thermal drying of sewage sludge. However, an upstream HTC with mechanical dewatering even produced a surplus of energy. The authors calculated an energy surplus between 27 and 50%. Overall, they estimated a 58% lower energy consumption for HTC and thermal drying compared to thermal drying alone. They suggested 200 °C and 30 min as optimum hydrothermal conditions. A similar conclusion was reached by Krebs et al. (2013), who predicted a 53% reduction in energy consumption by HTC and dewatering before thermal drying. Blöhse (2017) reported energy savings of 56% using this process combination. So far, the studies have compared sewage sludge drying of >90% TS with HTC. As sewage sludge burns already at lower dry

matter contents, comparing partial drying of sewage sludge with the combustion of HTC coal after dewatering without further drying would probably be more realistic for large-scale application.

2.3 HTC process water

The performance and the associated costs for the treatment of HTC process water are key elements for the practical feasibility of HTC for sewage sludge treatment (Reißmann et al. 2021). The reaction mechanisms during HTC (section 2.1) lead to the decomposition of solids and the formation of various dissolved substances. Although some of the conversion products polymerize to form hydrochar, a significant amount remains in the liquid phase, the HTC process water. As a consequence, the process water is highly contaminated with carbonaceous and nitrogenous substances and is brown to dark brown in color (Figure 4). Phosphorus is of minor concern for the treatment of process water, as most of it remains in the hydrochars, and phosphorus does not form problematic substances during HTC. For this reason, phosphorus and its recovery will not be discussed in greater detail.

Figure 4: Process waters from the HTC of sewage sludge with different brownish colors

The carbon balance (Figure 5) based on data of Blöhse (2017) reveals that about two-thirds of the initial carbon is found in the hydrochar and about 5% in the process gas. The remaining 27.5% is dissolved in the process water. The percentage of carbon that passes into the process water is strongly dependent on the biomass used. In the case of biomass rich in fat and protein, such as sewage sludge, the proportion of carbon dissolved in the process water is higher than in the case of biomass with high carbohydrate content, such as lignocellulosic biomass (Blöhse 2017). Roy et al (2021) found a similar distribution of carbon

for the HTC of sewage sludge. With 69%, the share was highest in the hydrochars, followed by process water with 24% and process gas with 7%.

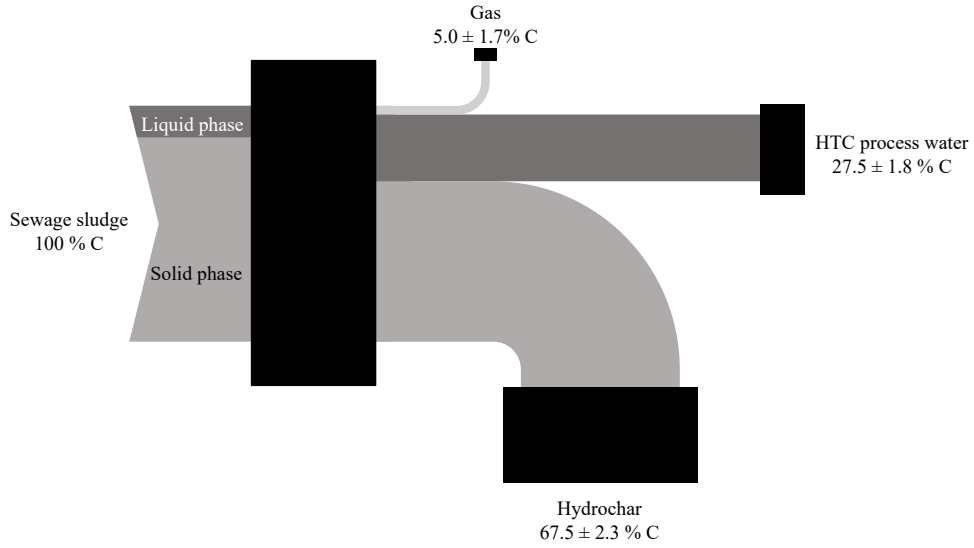

Figure 5: Carbon balance for HTC of sewage sludge between 200 and 260 °C and <60 min to 240 min without pH modification, Mean values ± STD, n = 23. Data from (Blöhse 2017)

During HTC, about 40% of the nitrogen remains in the hydrochar and the other 60% is transferred to the process water (Figure 6). This shows that the nitrogen compounds in sewage sludge are released and formed to a large extent from the solids during HTC. The dissolved nitrogen is mainly present as organically bound nitrogen and ammonium. As nitrogen is not significantly transferred to the gas phase, gas phase nitrogen was not taken into account in the balance. With rising temperature during HTC, the nitrogen in the process water gradually builds up (Huang et al. 2021b).

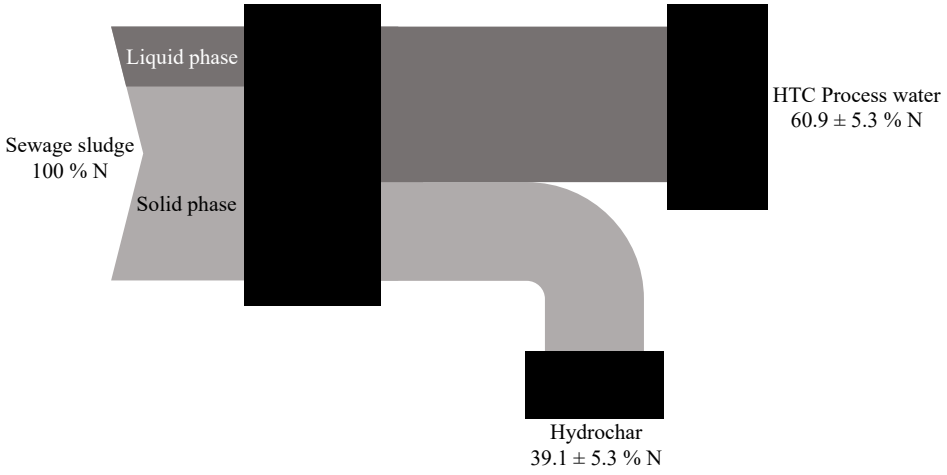

Figure 6: Nitrogen balance for HTC of sewage sludge between 200 and 260 °C and <60 min to 240 min without pH modification, Mean values ± STD, n = 23. Data from (Blöhse 2017)

2.3.1 Reaction mechanisms

The reaction network for the formation of substances dissolved in the process water is extremely complex and not yet fully elucidated. Although reaction pathways for single substances have been largely identified, many paths for multicomponent mixtures like sewage sludge are still unclear. First kinetic models have already been developed for describing the pathways, although the interaction between the different substances cannot yet be represented, not to mention that it is not yet understood (Yang et al. 2022a).

An overview of the most important reaction pathways during the hydrothermal carbonization of single compounds, which are incorporated in sewage sludge, is given in Figure 7. The substances which are not further decomposed or do not react further are highlighted in dark gray. The reactions in the upper area are the result of hydrolysis, while the conversion products in the middle area are formed by dehydration, decarboxylation, and deamination. Polymerization, condensation, and aromatization are mainly located in the lower part of the graph.

Condensation and polymerization of the desired hydrochars result from aldehydes, furfural and 5-hydroxymethylfurfural (HMF), which are formed mainly from carbohydrates. However, furfural and HMF can also be decomposed to organic acids by dehydration, and decarboxylation. Organic acids are additionally split off directly from carbohydrates or their monomers as well as from lignin and lipids. As organic acids do not react further, they remain solubilized in the process water. Moreover, the decomposition of HMF and furfural forms phenols, which also do not react further and are dissolved in the process water. The presence of proteins in sewage sludge induces a variety of reactions leading to the formation of N-heterocyclic compounds. Melanoidins from the Maillard reaction are the most well-known and have a dark brown color and a characteristic odour (Matissek 2016). The melanoidins primarily cause the colouring of the process water (see Figure 4). In addition, the amino acids contained in proteins can reduce char formation by forming melanoidins from HMF and furfural or aldehydes, for example. Ammonia and ultimately ammonium are further broken down from proteins. The reaction scheme demonstrates that lipids contribute to the formation of hydrochar only at high temperatures and are primarily decomposed to organic acids. Likewise, proteins do not form solids, however, protein fragments can be incorporated into solids (Liebeck 2015).

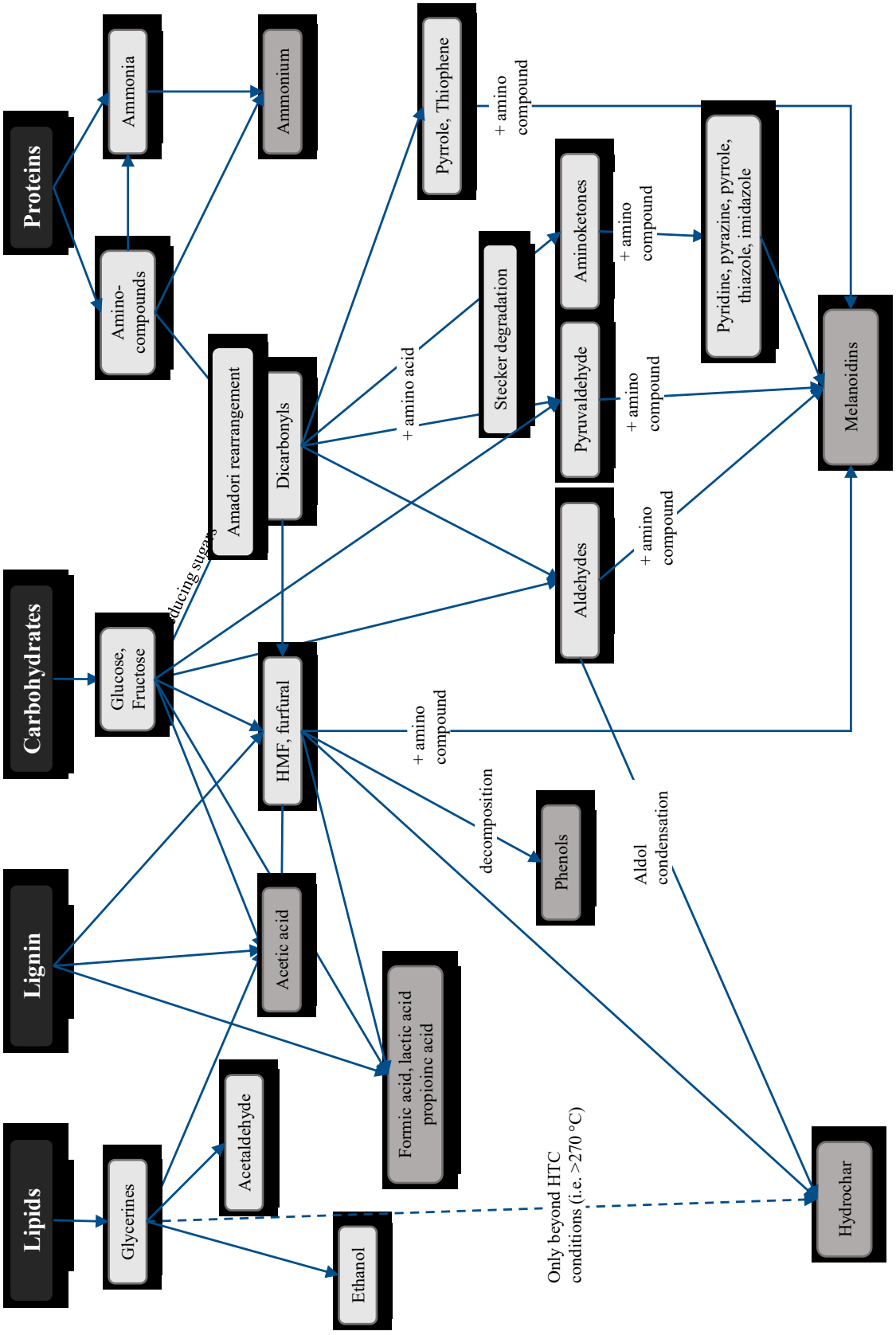

Figure 7: Simplified reaction scheme for HTC of the single substances lipids, lignin, carbohydrates and proteins, which are also present in sewage sludge. Substances that do not decompose or continue to react are highlighted in dark gray. Based on (Liebeck 2015; Baccile et al. 2009; Antal et al. 1990; Bär 2018; Sevilla and Fuertes 2009; Asghari and Yoshida 2006; Zhuang et al. 2017; Hodge 1953; Großkopf 2009; Xu et al. 2022c)

The complex reaction network gives an idea of the multitude of substances that can be present in HTC process water. According to the literature, process waters from HTC of sewage sludge contain aromatics, N-containing compounds, acids, esters, aldehydes, ketones, and more than 50% of unknown substances (Zheng et al. 2021). N-containing compounds include, for example, pyrazines, pyrimidines, phenols, amides, and pyridines as well as various subclasses of these (Villamil et al. 2018; González-Arias et al. 2023). At the same time, organic acids are present such as acetic acid, butanoic acid, pentanoic acid, propanoic acid, or formic acid (Danso-Boateng et al. 2015b; Langone and Basso 2020).

2.3.2 Characteristics

Process water pollutants and inhibitors

Some of the substances formed in the numerous reactions are readily biodegradable. These include primarily organic acids or volatile fatty acids (VFA) such as acetic acid, or monomers such as sugars, which are broken down from carbohydrates (Scherzinger and Kaltschmitt 2021). For this reason, biological processes are an obvious approach for HTC process water treatment. With elevating temperatures, however, more substances that are toxic, inhibitory, and poorly or non-biodegradable are formed (Mottet et al. 2009). Above 160 °C, Maillard reactions take place to a greater extent and lead to the formation of toxic or refractory Melanoidins (Dwyer et al. 2008). Moreover, humic-like acids with a high degree of aromatic condensation are formed as the temperature rises (Huang et al. 2021a). In addition, sugars and hemicelluloses form phenolic components, furan derivatives, and furfurals (Miyazawa et al. 2008; Horn et al. 2011). Their decomposition leads to poorer biodegradability in two ways. On the one hand, sugars and hemicelluloses are easily biodegradable, and on the other hand they are converted into non-degradable substances (Bauer et al. 2014). Seyedi et al. (2021) compiled various substances in a review that have been identified in studies to cause toxicity to biodegradation:

- Phenols
- Benzoic acid
- HMF
- Humic-like substances
- Furane
- Ketones
- Benzene
- Pyridine
- Pyrrolidine
- N-heterocyclic compounds
- Aromatic amides
- Straight amides

Due to the high concentration of readily biodegradable substances, anaerobic digestion processes have been used to produce biogas and improve the energy efficiency (Aragón-Briceño et al. 2021; Mannarino et al. 2022). However, the

biodegradability of N-heterocyclic compounds is largely determined by their physicochemical properties. Anaerobic and aerobic microorganisms metabolize organic substances differently. Since the aerobic degradation of aromatic compounds is often less complex than anaerobic degradation, aerobic biological processes are more resilient (Fuchs et al. 1993; Schwarz and Lingens 1993). Nevertheless, the substances formed during HTC also inhibit aerobic microorganisms as various studies on model organisms have shown. Phenols, for instance, inhibited the growth of *Chlorella vulgaris* by 40% starting at 400 mg/L (Scragg 2006). Towards *Pseudokirchneriella subcapitata*, different derivatives of phenol showed 50% growth inhibition at 2.1 to 145 mg/L (Aruoja et al. 2011).

Pham et al. (2013) studied process water produced from the hydrothermal carbonization of Spirulina. Algae could reduce the strong toxicity by 30%, although algal growth itself was inhibited. Their study further showed that the inhibition by the various nitrogen-containing organic compounds is synergistic. The significant inhibition of Gram-negative *E. coli* and Gram-positive *S. aureus* by HTC process water started from 200 °C (Xu et al. 2022a). In a follow-up study, Xu et al. (2022b) extensively studied its toxic effects. Using *E. coli* and *S. aureus* again, several toxic and inhibitory mechanisms were identified. These included disordering the metabolic pathways, destruction and damaging of cell walls and membranes, and changes in the physiochemical properties of the cell surface. These mechanisms are also suggested in other studies as inhibiton effects of N-heterocylic and aromatic compounds, and phenols (Foladori et al. 2014; Yuan et al. 2019). Xu et al. (2022b) also suspected synergistic inhibition by the substances in process water. This seems only plausible, assuming that single substances disrupt different mechanisms. Consequently, considering real process waters to evaluate inhibition appears to be more targeted than considering isolated substances only.

Process water load

The analytical methods for determining single substances in process water are complex and literature rarely provides data of concentrations, but often only qualitative information on the presence of substances (Chen et al. 2019b). Therefore, it is useful to measure these substances with different sum parameters such as total organic carbon (TOC), chemical oxygen demand (COD), and dissolved organic nitrogen (DON). Literature provides countless data on the concentration of these parameters, which cannot be directly compared with each other due to varying HTC conditions, different sewage sludge compositions and different TS contents. As a representative example, a study is discussed here that

covers a wide range of concentrations and also summarizes the concentrations as a function of TS. The comprehensive study by Aragón-Briceno et al. (2020) showed a maximum TOC concentration of almost 30,000 mg/L in process water at an original TS of 30% (Figure 8 a). Conversely, the solubilization of TOC behaved oppositely with increasing TS and stagnated at about 80 mg/g TS. This effect has already been confirmed in other studies (Stemann 2013; Knežević 2009). Accordingly, a higher TS concentration should be targeted to achieve a specifically lower loading of the process water. Nevertheless, loading of process water will increase with higher TS. COD ranged from 9,600 to 72,300 mg/L and VFAs were present in COD equivalents ranging from 900 to 4,600 mg/L.

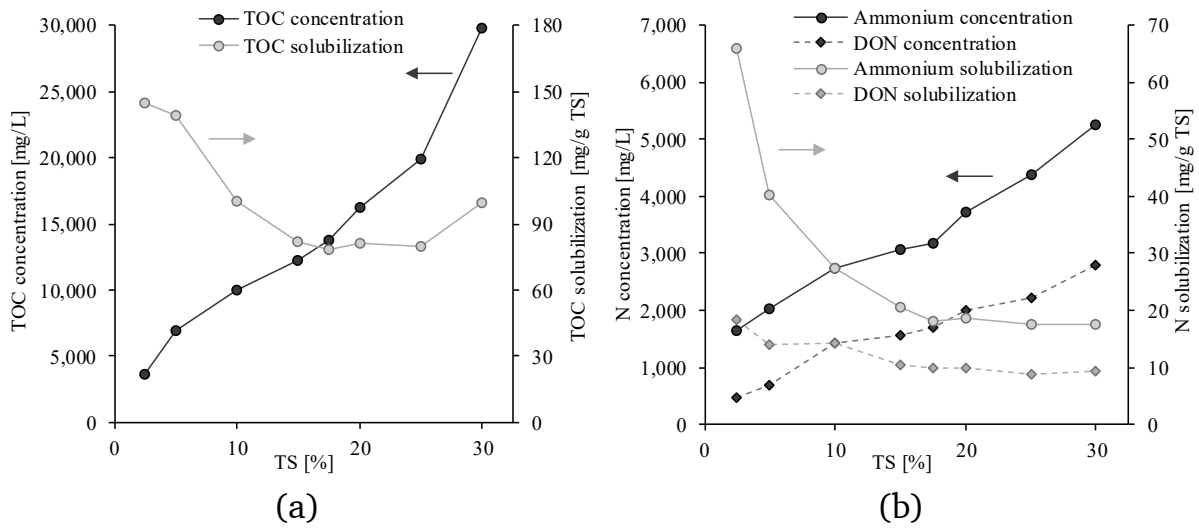

Figure 8: a) TOC and b) ammonium as well as DON in HTC process water of sewage sludge depending on TS content at 250 °C and 30 min. DON was calculated as the difference between Total Kjehldahl Nitrogen and ammonium. Data from (Aragón-Briceño et al. 2020)

The release of ammonium and DON behaved similarly to TOC, where decreasing solubilization also remained constant above 15% TS (Figure 8 b). At 30% TS, the maximum concentrations were 5,300 mg/L for ammonium and 2,800 mg/L for DON.

2.3.3 Treatment strategies

Biological processes

Anaerobic batch tests have very often been carried out to determine the methane potential of HTC process water. The highest biogas production can be achieved at temperatures up to 180 °C and short reaction times. However, this temperature range is rather characteristic for thermal hydrolysis than for HTC. At temperatures significantly above 180 °C, which are more typical for HTC, the

formation of toxic and non-degradable substances leads to a significant drop in biogas yield (Gaur et al. 2020; Chen et al. 2019a; Park et al. 2021).

Studies on the continuous anaerobic digestion of HTC process water are scarce. They report COD removal in the range of 52 to 80% using various anaerobic processes (Table 4). During operation, however, unstable conditions, characterized by an accumulation of VFA or a decrease in gas production, were regularly observed. This could be attributed to inhibitory or toxic substances in the process water. However, the studies did not include anaerobic inhibition tests.

Table 4: Studies on continuous anaerobic digestion of HTC process water

OLR[a] [g COD/(L·d)]	COD removal [%]	Anaerobic process	Reference
5	68 to 75	anaerobic filter (fixed bed reactor)	(Wirth et al. 2015)
7	<80	anaerobic filter, anaerobic moving bed bioreactor	(Fettig et al. 2017)
0.88	52 to 58	continuously stirred tank reactor with sludge recirculation	(Weide et al. 2019)

[a]Organic loading rate

Wirth et al. (2015) treated undiluted process water from sewage sludge carbonization. Despite acceptable COD removal, effluent COD was 11 g COD/L and also effluent DON appeared quite high with 1 g/L. The organic loading rate (OLR) ranged below average organic loading rates of anaerobic filters compared to industrial applications with 5.3 to 10.5 g COD/(L·d) (Young 1991; Rosenwinkel et al. 2015), which indicates an inhibition of anaerobic digestion. Fettig et al. (2017) used various feedstock to generate HTC process water, all with a low nitrogen content. Accordingly, less melanoidins and therefore less inhibiting substances could be formed during HTC. Even though, the percentage of process water in the feed had to be diluted to 50% v/v using tap water and an easily degradable co-substrate. Regardless of the HTC substrate, no stable long-term operation of the reactors was possible. Weide et al. (2019) used sewage sludge and wood for HTC. The buffer capacity had to be increased by adding 5.6 g $NaHCO_3$/L to the reactor. This resulted in stable operation, even though the OLR was significantly below typical industrial applications of continuously stirred tank reactors with 1.5 to 6.4 g COD/(L·d) (DWA-IG-5.1 2012).

Aerobic processes have been considered mainly for post-treatment, and previous studies did not explore limitations of sludge loading (g COD per g mixed liquor suspended solids (MLSS)). In the study by Weide et al. (2019), aerobic post-treatment further reduced the COD, resulting in a COD removal of 75% COD using the combination anaerobic – aerobic. Fettig et al. (2017) also investigated aerobic post-treatment in their study using a membrane bioreactor (MBR) after anaerobic digestion. 60% COD could be removed at a sludge loading up to 0.11 g COD/(g MLSS·d). Lagone et al. (2021) suggested treating the process water in the main stream of a wastewater treatment plant, as inhibitors would be sufficiently diluted and the COD would be easily degradable with 82%. However, the study is based on batch tests and neglects the effect of the refractory COD on the effluent of the wastewater treatment plant. Ferrentino et al. (2021) also focussed on treating HTC process water in a municipal wastewater treatment plant by recreating real wastewater mixtures in a lab-scale sequencing batch reactor (SBR). Even though the process was stable, they found an increase in the COD effluent of 11 mg/L. Complete nitrification was achived due to the dilution of the process waters.

Fettig et al. (2017) revealed a strong inhibition of nitrification, which was around 65% at a volumetric percentage of process water of 1% v/v. Anaerobic pre-treatment significantly reduced the inhibition at the same percentage to around 15 to 35%. Macêdo et al. (2023) found a 50% inhibition of nitrification for different HTL process waters at 0.5% v/v. They confirmed that ammonium oxidizing bacteria were more susceptible to inhibition than nitrite oxidizing bacteria. In addition, the inhibition was limited to nitrifiers, while denitrifiers were not or hardly inhibited. As the inhibition by the process waters is largely determined by the HTC feedstock, further research is required. In addition, no adaptation of biomass to inhibitors has been investigated to date.

Physical-chemical processes

The previous review shows that some substances in HTC process water are not biodegradable. Nevertheless, few studies on the post-treatment of HTC process water have been published to date. Oxidative and adsorptive post-treatment was again investigated by Fettig et al. (2019). They mineralized the COD by 4 and 36% using a specific ozone dose of 0.1 to 0.6 kg O_3/kg COD_0. Furthermore, the ratio of biochemical oxygen demand in 30 days to COD increased from 0.06 to 0.33. Despite the limited COD removal, ozonation could make the refractory COD available for biodegradation. Nevertheless, downstream activated carbon adsorption was necessary in order to safely comply with the

discharge limits. The authors suggested the process chain anaerobic – aerobic – optional ozonation and aerobic – activated carbon for sufficient treatment of HTC process water. A high reduction of melanoidins with the combination ozonation – aerobic was also observed by Sangave et al. (2007).

Although chemical-physical processes are often more expensive than biological processes, various studies have investigated chemical-physical treatment of raw HTC process water (Table 5). The relatively low COD removal could be attributed to the high COD concentration of the process water. Taking into account the quite high dosage of additives, some of these processes reach the limits of their applicability. Excessive coagulant dosing, for example, destabilizes colloids and affects coagulation (Hu et al. 2022a). In the case of activated carbon, wet air oxidation and electro-oxidation, however, higher dosages were simply not tested.

Table 5: Studies on chemical-physical processes for treating HTC process water

Process	Dosing rate	Removal [%]	Reference
coagulation/oxidation using ferrous/persulphate[a]	Fe^{2+}: 150 mM PS: 150 mM	34% DOC	(Liu et al. 2022)
coagulation using poly aluminum ferric sulphate	6 g/L	27% COD	(Hu et al. 2022a)
Activated carbon adsorption	30 g/L 100 g/L	28% COD 56% COD	(Hu et al. 2022a)
Wet oxidation of hydrochar slurry w/o solids separation	104 g H_2O_2/L	30% COD	(Baskyr et al. 2014)
Electrochemical oxidation	28.4 Ah/L	28% COD	(González-Arias et al. 2023)

[a] Fe^{2+}/PS

Liu et al. (2022) combined coagulation and oxidation and showed, that a Fe^{2+}/PS ratio <1 prevails oxidation and removes more organic matter than coagulation. Hu et al. (2022a) dosed 6 g/L poly aluminum ferric sulfate for maximum COD removal, while further dosing disturbed colloid formation and lowered the COD removal. The authors also investigated the adsorption onto activated carbon (AC). Their dosages correspond to an activated carbon capacity of 0.38 g COD/g AC for 28% COD removal. The higher COD removal of 56% was associated with a reduction in capacity to 0.23 g COD/g AC. Even though these

adsorption capacities are common for activated carbon, the high load of the HTC process water would require large amounts of activated carbon making the viability questionable. Wet oxidation of the hydrochar slurry without solids separation by gaseous oxygen at 170 and 200 °C was investigated by Baskyr et al. (2014). However, they obtained a COD removal of only 30%, as hydrochars were destroyed to a larger extent than organic matter in the process water was oxidized.

González-Arias et al. (2023) investigated the electrochemical oxidation (EO) using a boron doped diamond electrode. They oxidized up to a charge input of only 28.4 Ah/L, but a higher reduction in COD can be expected with more intensive oxidation. Ciarlini et al. (2020) confirmed the viability of EO by achieving almost complete decomposition of COD, and N-heterocyclic compounds (99%) in HTL process water. Therefore, EO could be a suitable process for treating HTC process water, as the process is more efficient at organic concentrations above 5 g COD/L, achieves low effluent concentrations, and is robust and easy to automate (Garcia-Rodriguez et al. 2020; Särkkä et al. 2015).

3 Research question and outline of the papers

The objective of this work is to investigate treatment technologies for process water generated from hydrothermal carbonization of sewage sludge. The literature review has revealed that a variety of reactions occur under hydrothermal conditions. This results in the production of various organic substances, which accumulate in high concentrations in the liquid phase. While some of these compounds are easily biodegradable, others are non-biodegradable and potentially toxic to microorganisms. Therefore, the removal of biodegradable substances as well as ammonium will be investigated using aerobic biological processes, which have been poorly studied for HTC process water. For removing refractory substances, electrochemical oxidation will be used. This leads to the key research question:

What is the effectiveness of aerobic biological processes and electrochemical oxidation in treating process water generated from hydrothermal carbonization of sewage sludge?

For answering this question, the following challenges have been identified and studied:

Challenge 1	*How do different HTC operating parameters affect the process water contamination?*
Challenge 2	*What is the effect of reaction temperature as a key parameter of HTC on biodegradability and nitrification?*
Challenge 3	*Can the discharge of biologically pretreated HTC process water deteriorate the effluent quality of municipal wastewater treatment plants?*
Challenge 4	*What are the limitations of biological side-stream treatment of process water using MBR and SBR?*
Challenge 5	*Can nitrifying microorganisms acclimatize to process water contaminants?*
Challenge 6	*What is the efficiency of removing refractory compounds using electrochemical oxidation?*
Challenge 7	*Which process combinations of biological treatment and oxidation are suitable for the treatment of HTC process water?*

These challenges were examined in lab scale (challenge 1 - 3, 6, 7) and pilot scale (challenge 4, 5). Since this thesis is a cumulative dissertation, the sections 4 to 7 are based on reviewed papers published in or submitted to scientific

journals. Section 8 ties the single papers together and places them in an overall context.

Section 4 deals with challenge 1 and discusses the process water composition depending on the main reaction parameters temperature, reaction time, and pH. The section points out their effect by using the three-factorial Box-Behnken design. Furthermore, it focuses on the solubilization of carbon and nitrogen from the solids into the process water. Section 4 is based on the publication:

Blach, T., Engelhart, M., Optimizing the Hydrothermal Carbonization of Sewage Sludge - Response Surface Methodology and the Effect of Volatile Solids. Water 2021, 13, 1225.https://doi.org/10.3390/w13091225

Section 5 examines challenges 2 and 3, taking up the previous findings by evaluating the aerobic biodegradability of the reaction products. The paper examines the effect of HTC temperature on biodegradation and nitrification in batch and continuous tests. Additionally, an approximation reveals that the high level of refractory substances can negatively affect the effluent of a municipal wastewater treatment plant. The basis for section 5 is the publication:

Blach, T., Lechevallier, P., Engelhart, M., Effect of temperature during the hydrothermal carbonization of sewage sludge on the aerobic treatment of the produced process waters. Journal of Water Process Engineering 2023, Volume 51, 103368. https://doi.org/10.1016/j.jwpe.2022.103368

Section 6 focuses on challenge 4 and 5 and transfers the findings from section 5 to pilot scale. An MBR and an SBR treated HTC process water simultaneously for exploring the limits of biodegradation by investigating different operating modes regarding the COD and TN sludge loading. Moreover, batch tests revealed the degree to which nitrifying microorganisms can adapt to the process water. The following publication is the basis for section 6:

Blach, T., Engelhart, M., Limitations of treating hydrothermal carbonization process water in a membrane bio-reactor and a sequencing batch reactor on pilot scale. Journal of Environmental Chemical Engineering 2025, Volume 13, 115304. https://doi.org/10.1016/j.jece.2024.115304

Section 7 addresses challenges 6 and 7 and focuses on the high concentrations of refractory compounds. Electrochemical oxidation using a boron-doped diamond electrode was capable of removing COD to a very high degree. The results suggest three process combinations for treating the HTC process water: (i) the oxidation of raw process water, (ii) the oxidation of biologically treated

process water without nitrification and denitrification, and (iii) the oxidation of process water biologically treated with nitrification and denitrification. The basis for section 7 is the publication:

Blach, T., Engelhart, M., Electrochemical oxidation of refractory compounds from hydrothermal carbonization process waters. Chemosphere 2024, Volume 352, 141310. https://doi.org/10.1016/j.chemosphere.2024.141310

Section 8 also ties in with challenge 7 and combines the findings of sections 6 and 7 to answer the key research question. Comparing the performance and the energy consumption of biodegradation and oxidation leads to a discussion of the most promising combination of processes. Section 9 summarizes the key findings of this dissertation and answers the challenges 1 to 7.

4 Optimizing the hydrothermal carbonization of sewage sludge - response surface methodology and the effect of volatile solids

Authors:	Blach, T.; Engelhart, M.
Keywords:	Box-Behnken Design; hydrothermal carbonization; process water; sewage sludge
Published in:	Water 2021, 13(9), 1225
	https://doi.org/10.3390/w13091225
Received:	23 March 2021
Accepted:	25 April 2021
Published:	28 April 2021

Abstract:

This study focuses on identifying the optimum conditions of sewage sludge hydrothermal carbonization by Box–Behnken Design and on the effects of volatile solids on heating value and process water load. To get insight into the solid and process water characteristics, we applied the Box–Behnken Design on the hydrothermal reaction temperature (190, 220, 250 °C), reaction time (0.5, 2.25, 4 h) and pH (3.9, 5, 6.1). The response surface of the liquid phase revealed decreasing dissolved organic carbon (DOC) concentrations with increasing temperature from 9,446 mg/L (190 °C) to 7,402 mg/L (250 °C) at 4 h reaction time. For the same hydrothermal conditions, NH_4-N concentration increased from 754 to 1,230 mg/L. The reaction temperature was identified as the most important process parameter, whereas reaction time and pH had only minor effects. Moreover, the linear coefficients of the models were more decisive than the interrelation and quadratic coefficients. Volatile solids (VS) of the feedstock were found to significantly influence both the load of the process water and the change in heating value of the hydrochars. Process water load increased steadily with higher VS. The heating value only increased with more than around 65 - 80% VS in the feedstock.

4.1 Introduction

In municipal wastewater treatment the main distinction is made between primary sewage sludge (PS), waste activated sludge (WAS), including precipitation sludge from phosphorus removal, and anaerobically digested

sludge (ADS). The type of sludge as well as several of process parameters determine its elementary main components, which are in the range from 3.4 - 6.64% H, 22.8 - 51.20% C, 1.9 - 8.85% N, 13.86 - 52.30% O and usually <1.37% S (Zhai et al. 2017; Zhao et al. 2014; Danso-Boateng et al. 2015; Zhang et al. 2014; Paneque et al. 2017). In recent years, the treatment and disposal of sewage sludge is gaining more and more attention as its components, especially phosphorus and the chemically bound energy, are considered valuable and worth recovering. To this end, technologies like anaerobic digestion, phosphorus extraction and combustion are widely used for sewage sludge treatment. Current trends towards renewable energies, further optimization of sewage sludge treatment processes and carbon sequestration promote alternative technologies like hydrothermal carbonization (HTC), which reproduces the natural coalification of organic matter in the presence of water in a technical application (Bergius 1913).

Both temperature and feedstock significantly determine chemical pathways and the thermochemical breakdown of the biomass structure into lower-weight molecules. Due to the diverse composition of sewage sludge including polysaccharides, proteins, and lipids, it is still a challenge to define the pathways and kinetics during its hydrothermal treatment (Wang et al. 2019a). The hydrothermal carbonization changes the elemental composition of sewage sludge significantly, as dehydration and decarboxylation lead to higher C content and in contrast to lower N, H and O content (Escala et al. 2013). A review of several studies by Wang et al. (2019a) shows increasing carbon content with increasing reaction temperature and reaction time of the hydrothermal treatment. The breakdown of molecules via dehydration and decarboxylation leads to a mass loss during HTC, resulting in a reduction of volatile solids and consequently an accumulation of inorganic material (Wang et al. 2019a; Wang and Li 2015). The mass loss is generally in a wide range of up to 33%, depending on the sewage sludge properties and the hydrothermal conditions (Paneque et al. 2017; Danso-Boateng et al. 2015).

Depending on the temperature, roughly more than 60% C remains in the solids during hydrothermal treatment. A minor amount of less than 5% C enters the gas phase as CO_2 and consequently the difference of 35 - 40% C is found in the process water (Escala et al. 2013). Accordingly, the reported TOC and COD concentrations vary in a wide range between 4,500 - 24,900 mg/L C and 13,000 - 66,300 mg/L O_2, respectively (Aragón-Briceño et al. 2017; Weiner et al. 2018). Carbonaceous compounds like lipids were reported to hydrolyze almost

completely to free fatty acids during hydrothermal treatment up to 280 °C within 15 - 20 minutes. These fatty acids have been identified mainly as acetic acid and propionic acid and are predominantly derived from unsaturated lipids (Holliday et al. 1997; Wilson and Novak 2009). With increasing reaction times, aldehydes, ketones and monosaccharides have been found to be degraded, while organic acids, mainly formic, lactic and acetic acid, are formed (Asghari and Yoshida 2006). Sugars, 5-HMF and Furfural have also been proven to degrade with longer reaction times and reaction temperatures (Reza et al. 2014).

Dissolved nitrogen is predominantly present as organic nitrogen (DON, containing proteins, amino acids, melanoidins) and ammonium (NH_4-N). The release of NH_4-N results from the deamination and decarboxylation of amino acids, which in turn are degraded from proteins (Klingler et al. 2007). Dote et al. (1998) determined 19 amino acids which are almost completely present in the liquid phase as NH_4-N and organic nitrogen. Increasing shares of NH_4-N with increasing reaction temperatures and reaction times indicate an intensification of deamination processes (Toor et al. 2011). Elevating temperatures from 150 °C to 270 °C increased the ratio of 30% N to over 70% N of the total nitrogen present in the process water (Zhuang et al. 2017). Similar results were obtained with dewatered sewage sludge by Chen et al. (2019b), which show a decline of amino acids and a doubling of NH_4-N concentration in process water as temperature increases from 170 °C to 320 °C. A simultaneous decrease of carbohydrates was attributed to the Maillard's reaction and the associated formation of its refractory products. Melanoidins like aldehydes, furans, pyrroles, pyrazines and pyridines are the brownish colored reaction products of amino acids and sugars under hydrothermal conditions, which mainly contribute to the dissolved nitrogen as their polarity and consequently their solubility is higher than for proteins (Dwyer et al. 2008; Fan et al. 2018). On the other hand, melanoidins were proven to decompose to char, gas, NH_4-N and other decomposed products at temperatures above 200 °C (Minowa et al. 2004). Nitrogen concentrations, in process water after hydrothermal treatment of sewage sludge, range from 700 - 4,900 mg NH_4-N/L and total nitrogen (TN) 1,500 - 5,500 mg TN/L (Wang et al. 2019b; Sun et al. 2014).

The hydrothermal carbonization of sewage sludge has received growing attention in recent years. Literature shows, that numerous works deal with the optimization of the process and use of the hydrochars, energy balances or the question of how to handle the resulting highly loaded process water. Still, the results of studies regarding the interrelation between the loads and process

parameters, as well as the load level and the change in the higher heating value (HHV) are very heterogeneous and demands further investigations. With this in mind, this study aims firstly to provide structured insight into the characteristics of the hydrochars and process water and their dependence on the reaction temperature, the reaction time and the feedstock pH. A three-level full factorial design is intended to highlight the interrelation of all three parameters on the migration and transformation of carbon and nitrogen during hydrothermal carbonization. Secondly, the mass fraction of volatile solids before hydrothermal treatment is correlated with the process water load and the increase or decrease of the HHV after hydrothermal treatment. Since the hydrothermal carbonization transfers parts of the sewage sludge's organic and inorganic components into the liquid phase, the organics mainly determine the load of the process water and the HHV. Thus, our experiments improve the understanding of HTC of sewage sludge and contribute to the optimization of process water treatment.

4.2 Materials and methods

4.2.1 Sampling

Sewage sludge samples were obtained from two municipal wastewater treatment plants (WWTP) in Germany (Table 6).

Table 6: Overview of the tested sewage sludges. The spread of the measuring values was evaluated using the mean value and the deviation of each measured value to the mean value. The maximum deviations are ±7.1% for TS, ±8.6% for VS, ±0.7% for C, ±2.2% for H, ±2.1% for N, ±0.8% for COD and ±1.5% for HHV.

Tested sewage sludges	**TS**	**VS**	**C**	**H**	**N**	**HHV**	**COD**
	%	**%**	**%**	**%**	**%**	**MJ/kg TS**	**g O_2/kg TS**
WWTP A							
Raw sewage sludge 1 (RS1)	5.9	4.6	41.6	5.9	5.0	18.0	1,201
WWTP B							
Primary sewage sludge (PS)	4.5	3.7	42.5	6.4	1.3	17.5	1,177
Waste activated sludge (WAS)	9.2	6.6	36.9	6.0	6.5	16.2	1,026
2nd batch WAS	9.1	6.8	36.7	5.7	6.4	16.1	1,022
WAS diluted 2.33:3 w/w	7.1	5.1	36.4	5.8	6.4	16.3	1,034
WAS diluted 1.67:3 w/w	5.1	3.6	37.0	5.5	6.5	16.3	1,035
WAS diluted 1:3 w/w	3.1	2.2	36.6	5.4	6.4	16.1	1,015
Raw sewage sludge 2 (RS2)	6.6	5.0	-	-	-	-	-
Raw sewage sludge 3 (RS3)	7.9	5.9	38.1	5.8	5.3	16.4	1,197
Anaerobically digested sewage sludge (ADS)	4.2	2.4	30.9	4.6	4.4	13.1	850

The raw sewage sludge of WWTP A (RS1) contained PS and WAS and was used for the Box–Behnken Design. Additionally, PS and WAS samples were taken from WWTP B and mixed to obtain raw sewage sludge RS2 (⅓ w/w PS and ⅔ w/w WAS) and RS3 (⅔ w/w PS and ⅓ w/w WAS). WAS of WWTP B was diluted to 3%, 5% and 7% TS using the effluent of the same WWTP. After preparation, all samples were frozen in portions at -20 °C to avoid degradation processes in feedstock before HTC. Samples were thawed overnight at an ambient temperature just before each hydrothermal run.

4.2.2 Experimental procedure

The hydrothermal experiments were performed using a 0.5 L batch reactor (midiclave Typ 3E/0.5lt, Büchi, AG, Switzerland), which is electrically heated and water cooled. The stirrer was set to 2000 rpm. A 95 - 98% w/w sulfuric acid was added to RS1 before the runs to adjust pH 3.9 and pH 5. The reaction time of the experiment was counted when the difference to the set temperature was <1%. Reaction temperature remained constant ±1% of set value during the whole experiment. It took the reactor about 0.75 - 2.0 h to heat up (corresponding to 1.92 ± 0.38 °C/min) and after the desired reaction time approx. 0.75 h to cool down to ambient conditions. The pressure was equal to the vapor pressure at a given temperature (up to 41 bar max.). the total solids (TS) and the total volatile solids (VS) were analyzed and the coal slurry was centrifuged at 19,500 rpm (rcf: 22,319 g) at 20 °C for 30 min (Sigma 3K30, Sigma Laborzentrifugen GmbH, Osterode am Harz, Germany). For the following analysis of the solids, the dewatered samples were used and the liquid was analyzed from the supernatant of centrifugation. Throughout the experiments, especially at higher temperatures, strong caking occurred on the inner reactor wall, which was removed by scraping and rinsing after each run.

4.2.3 Hydrochar analysis

Solid outputs were analyzed in terms of TS and VS according to DIN EN 12880:2000 and DIN EN 15936:2012 and dried at 105 °C before further analysis. A calorimeter was used to determine the higher heating value (IKA C200, IKA®-Werke GmbH & CO. KG, Staufen, Germany) and an elemental analyzer to obtain the CHN-composition (VarioEL III CHN, Elementar Analysensysteme GmbH, Langenselbold, Germany). The chemical oxygen demand (COD) of the dried solids was measured according to DIN 38414 S9:1986. The analysis of each parameter was performed as duplicate or triplicate.

4.2.4 Process water analysis

Process water samples were filtered via 0.45 μm PES syringe filters before analysis. To determine dissolved organic carbon (DOC), chemical oxygen demand (COD) total nitrogen (TN) and ammonium (NH_4-N) HACH tests LCK 387, LCK 514, LCK 338, LCK 303 and a HACH Photometer DR 3900 were used (Hach Lange GmbH, Düsseldorf, Germany). UV_{254} was determined with a HACH Photometer DR 5000 at a cell length of 10 mm (100-QS, Hellma GmbH, Müllheim, Germany), pH and conductivity by inoLab Multi 9620 IDS (Xylem Analytics Germany Sales GmbH & Co. KG, Weilheim, Germany). The ratio of UV254 to DOC was defined as the specific UV absorbance (SUVA) in L/(mg·m).

4.2.5 Determination of the reaction intensity

The reaction intensity, as introduced by Ruyter (1982), was used to evaluate the correlation of the reaction temperature and reaction time equation (1). This semi-empirical approach showed a good fit for experimental data and considers the greater impact of the reaction temperature compared to reaction time (Dunne and Agnew 1992).

$$\mathrm{f} = 50t^{0.2}e^{-\frac{3500}{T}} \qquad (1)$$

where f is the reaction intensity, t is the reaction time in seconds and T is the temperature in Kelvin. To consider varying heating times (see section 4.2.2), the mean temperature and the mean reaction times above 180 °C were used to calculate reaction intensity.

4.2.6 Experimental design

To point out the effects of various process parameters and their interaction on the process water, we used response surface methodology (RSM) with Box–Behnken Design (BBD) (e.g. Montgomery 2001) and three factors (reaction temperature T, reaction time t, pH) at three levels for RS1. The tested temperature was 190, 220 and 250 °C, the time was 0.5, 2.25 and 4 h and the pH was 3.9, 5, 6.1. These process parameters were chosen, since they cover a wide range of typical and technically feasible process parameters of hydrothermal treatment of sewage sludge. The runs were performed randomly. A second-order polynomial equation according to equation (2) was used to model the investigated parameters.

$$y = \beta_0 + \sum_{i=1}^{k} \beta_i x_i + \sum_{i=1}^{k} \beta_{ii} {x_i}^2 + \sum \sum_{i<j} \beta_{ij} x_i x_j \quad (2)$$

where y is the calculated response value (DOC, NH_4-N, NH_4-N/TN), x_i and x_j are the investigated variables (in this study T, t, pH), β_0 is the intercept, β_i the linear, β_{ii} the quadratic and β_{ij} the interactive constant. The model's constants were fitted to the experimental data using Microsoft Excel 2016 and Minitab 19. The coefficient of determination R^2 as the ratio of the sum of squared errors SSE to the sum of squared total deviations SST according to equation (3) was used to evaluate the model's accuracy.

$$R^2 = \frac{\sum(\hat{y}_i - \bar{y})^2}{\sum(y_i - \bar{y})^2} \quad (3)$$

Since R^2 alone does not measure the accuracy and large values of R^2 are not equivalent to a good fit of the model, Baş and Hoyaci (2007) suggested also taking the absolute average deviation (ADD) into account (Equation (4)).

$$AAD = \frac{\sum_{i=1}^{p} \frac{|y_{i,exp} - y_{i,cal}|}{y_{i,exp}}}{p} \cdot 100 \quad (4)$$

Therein, p is the number of runs, $y_{i,exp}$ and $y_{i,cal}$ are the experimental and the calculated results. To evaluate the model's accuracy further, the common interpretation of R^2 and *AAD* should be carried out. R^2 should be close to 1.0 and *AAD* should be as small as possible. The statistical significance of the parameters was determined by analysis of variance (ANOVA) with a *p*-test using Minitab 19.

4.3 Results and discussion

4.3.1 Results of Box-Behnken Design (Raw sewage sludge 1)

The results for each run for the analyzed parameters of the hydrochars (HHV) and the liquid phase (DOC, NH_4-N and NH_4-N/TN) are summarized in Table 7. Table 8 depicts the coefficients fitted to equation (2). High R^2 and low AAD were determined for all model fits, indicating a valid correlation between measured values and modelled values.

Table 7: Variables of the BBD and the results for the solid phase and the liquid phase of RS1. The spread of the measuring values was evaluated using the mean value and the deviation of each measured value to the mean value. The maximum deviations are ±0.8% for HHV, ±3.7% for DOC and ±1.7% for NH_4-N

	Operation settings			Hydrochar	Liquid phase		
Run	**T**	**t**	**pH**	**HHV**	**DOC**	**NH_4-N**	**NH_4-N/TN**
	°C	**h**	**-**	**MJ/kg TS**	**mg/L**	**mg/L**	**%**
untreated	-	-	-	18.04	1,458	92	26
HTC-1	220	2.25	5	20.30	8,510	975	40
HTC-2	190	0.5	5	18.74	9,160	575	26
HTC-3	190	4	5	19.07	9,395	730	32
HTC-4	250	0.5	5	21.27	8,055	980	45
HTC-5	250	4	5	22.12	7,640	1,223	54
HTC-6	220	0.5	6.1	19.25	9,160	783	35
HTC-7	220	4	6.1	20.08	8,520	1,045	44
HTC-8	220	0.5	3.9	20.34	8,650	858	38
HTC-9	220	4	3.9	21.40	8,335	995	44
HTC-10	190	2.25	6.1	18.75	9,320	630	27
HTC-11	250	2.25	6.1	21.70	7,545	1058	47
HTC-12	190	2.25	3.9	19.41	8,655	658	32
HTC-13	250	2.25	3.9	21.57	7,395	1,110	52
HTC-14	220	2.25	5	20.55	8,365	893	40
HTC-15	220	2.25	5	20.36	8,890	905	39

Table 8: Decoded constants, coefficients of the BBD and the corresponding R^2 and AAD for RS1

Coefficient	**Hydrochar**	**Liquid phase**		
	HHV	**DOC**	**NH_4-N**	**NH_4-N/TN**
β_0	17,834	-7,743	-3,549	-56.6
β_1	13.1	115.2	32.73	0.709
β_2	-27	508	-122.5	-4.2
β_3	-1,259	2,182	65	-5.24
β_{12}	2.45	-3.1	0.417	0.0186
β_{13}	5.94	-3.9	-0.189	-0.0058
β_{23}	-30.1	-42.2	16.23	0.331
β_{11}	-0.009	-0.257	-0.0575	-0.000872
β_{22}	-31.9	67.2	1.46	0.134
β_{33}	-32	-105.7	-7.1	0.435
R^2	0.97	0.96	0.99	0.99
AAD (%)	0.600	1.210	1.369	1.546

The analysis of variance (ANOVA) can be found in the appendix (Section 4.6).

4.3.2 Surface analysis of hydrochars (Raw sewage sludge 1)

The HHV at intensifying hydrothermal conditions was mainly driven by the reaction's temperature (Figure 9 a) and increased from 18.1 MJ/kg TS at 190 °C for 0.5 h to 21.0 MJ/kg TS at 250 °C for 0.5 h. Reaction time became more influential at higher temperatures, since the HHV for 4 h elevated by 1.1 MJ/kg TS at 250 °C but only by 0.6 MJ/kg TS at 190 °C. This indicates that soluble compounds from hydrolysis polymerize and aromatize, which leads to the formation of additional solids, as also described by Sevilla and Fuertes (2009). Consequently, the longer the reaction time, the more polymerization reactions take place and the higher the HHV. Furthermore, the increase in reaction temperature and reaction time resulted in an almost linear increase in HHV. Comparing the HHV of the hydrochars with that of the feedstock with 18.04 MJ/kg TS (see Table 7), almost no positive effect could be observed at mild hydrothermal conditions. At the most intense HTC conditions at 250 °C for 4 h, the HHV increased by 21% to 21.9 MJ/kg TS.

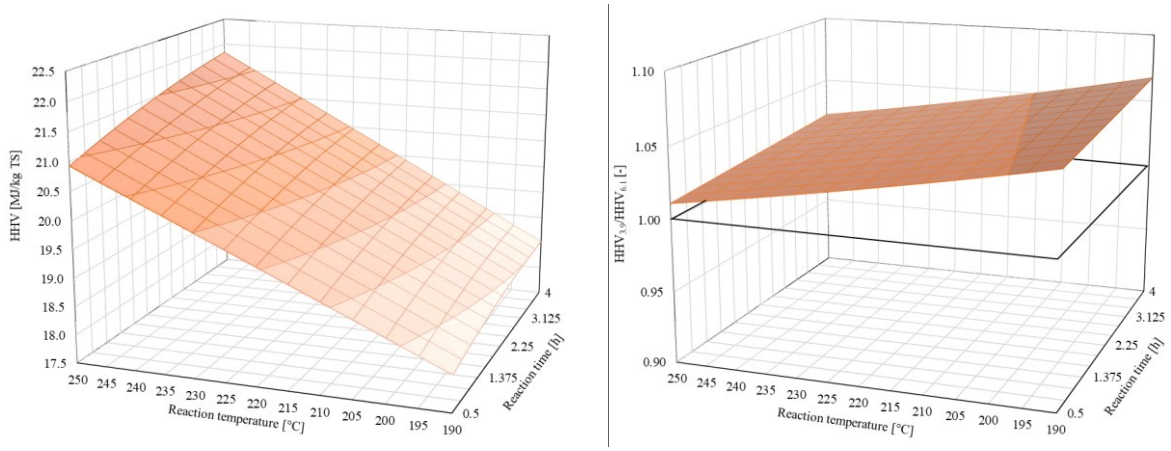

(a) (b)

Figure 9: Response surface plots of a) the HHV at pH = 6.1 and b) the effect of different pH values on the HHV

The ratio of $HHV_{3.9}/HHV_{6.1}$ in Figure 9 b shows, that the reduction of pH promoted a slight HHV increase. This was more pronounced at 190 °C since the HHV was about 6% higher at pH 3.9, while at 250 °C it was only about 2%. As the model shows no minimum at 250 °C, an ongoing impact of acid beyond 250 °C seems likely. Acidic milieus support the formation of carbonaceous products in general. Arrhenius acids like the used H_2SO_4 generally promote hydrolysis, dehydration and condensation reactions (Peterson et al. 2008; Watanabe et al. 2005), which potentially accelerate polymerization and lead to higher carbon content of the solids. An acidic environment at 200 °C has been reported to accelerate dehydration and coalification reactions while suppressing

decarboxylation and hydride transfer reactions (Titirici et al. 2007a). Titirici et al. (2007b) recommend thermal conditions below 200 °C in an acidic milieu as most of the carbon in the feedstock remains bound in the solid phase. Our findings confirm a greater benefit of an acidic environment at lower reaction conditions.

4.3.3 Surface analysis of process water load (Raw sewage sludge 1)

Figure 10 a shows the response surface plot for DOC and the interaction between temperature and time for a fixed pH of 6.1. In general, the DOC concentration in process water decreased with higher reaction temperature and longer reaction times. Since temperature mainly governs hydrothermal reactions, the DOC concentration declined from 9,558 mg/L at 190 °C to 8,161 mg/L at 250 °C (0.5 h). Lower temperatures cause more degradation and hydrolysis processes, whereas higher temperatures lead to more polymerization reactions (Akhtar and Amin 2011). Polymerization reactions and the associated formation of solids reduced the DOC concentration in the liquid phase and correspond to the rising HHV in Figure 9 a. For a reaction time of 4 h and an elevation in temperature from 190 to 250°C, the reactions that took place reduced the DOC concentration by 28%. The extension of the reaction time at 190 °C and 2.25 h showed a minor local minimum of 9,303 mg/L, which does not follow the overall trend. This may be attributed to the chosen design of experiments, since no corner points are tested in the experiments of the BBD (Montgomery 2001). Nevertheless, the model highlights the general dependencies and the interrelation between the parameters.

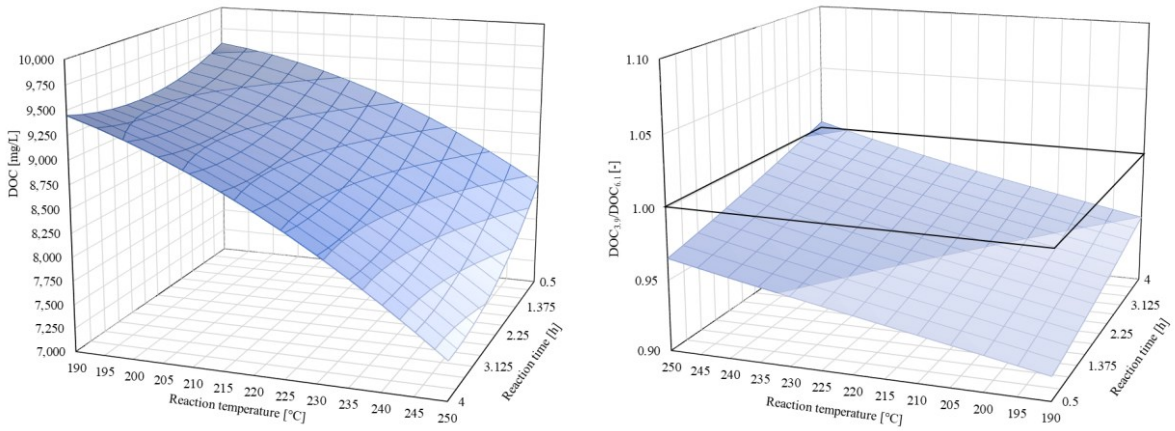

(**a**) (**b**)

Figure 10: Response surface plots of a) DOC at pH = 6.1 and b) the effect of different pH on the DOC concentration

Prolonging the reaction time from 0.5 h to 4 h reduced the DOC concentration depending on the reaction temperature. At 220 °C the DOC concentration was reduced by 5% from 9,107 mg/L to 8,655 mg/L and at 250 °C by 10% from 8,179 mg/L to 7,402 mg/L. This reduction was more distinctive for higher temperatures and thus enhanced polymerization reactions at higher temperatures and fits the previous observation of the hydrochars. To minimize DOC in process water, high temperatures in combination with long reaction times seem favorable. The same trends were observed at 300 °C and 350 °C and the extension of the reaction time from 0.5 to 60 minutes by Shanableh (2000). In contrast, the general findings of our study are somewhat different from the results of Sun et al. (2013), who found higher impacts on the DOC yields for lower temperatures. Nevertheless, the effect of the time was also less dominant than that of the temperature.

The impact of adding H_2SO_4 to the feedstock on the DOC concentration is referred to by the ratio $DOC_{3.9}/DOC_{6.1}$. Figure 10 b shows, that the catalyst reduced the DOC concentration by 0.92 for T = 190 °C and t = 0.5 h. Its effect became less significant for higher hydrothermal conditions and at 250 °C for 4 h an even larger negative effect became apparent. These findings correspond to the previous observations of a higher HHV in reverse order (Figure 9 b). The decreasing effects of an acidic catalyst with increasing reaction temperature were also observed by Rogalinski et al. (2008). They observed increased liquefaction yields using CO_2 up to 260 °C and attributed this to already increased reaction rate at temperatures above 260 °C. A study by Zou et al. (2009) with marine microalgae suggests, that the catalytic impact at lower catalytic concentration might be negated by the organic acids formed during HTC as stated by Asghari and Yoshida (2006). In accordance with our study, they observed lower liquefaction yields for temperatures up to 195 °C and reaction times up to 60 minutes, which was attributed to polymerization. In the present study only minor differences in the DOC concentration at pH 5 and pH 6.1 were observed. Therefore, results at pH 5 are not depicted.

To get an overview of the load of the process water before and after hydrothermal treatment without considering the different process conditions, all 15 hydrothermal runs of the BBD are summarized (Table 6). Apparently, the hydrothermal treatment of the sewage sludge was associated with a massive additional process water load compared to untreated sewage sludge. The concentration of COD was higher by a factor of 5.8, the DOC concentration by a factor 6.7 and the absorption at 254 nm (UV_{254}) was 11.7 times higher. Looking

at the COD/DOC ratio, a shift from 2.68 to 3.10 mg O_2/mg C was observed, which shows that the organic liquid compounds of the HTC process were in a less oxidized form. Furthermore, at higher temperatures the COD/DOC ratio was greater than at low temperatures, indicating ongoing dehydration and decarboxylation reactions. Consequently, less oxygen is bound in the aromatic compounds formed during HTC and more oxygen is needed to oxidize the products of the HTC reaction. The SUVA approximately doubled with the hydrothermal carbonization from 0.82 to 1.63 L/(mg·m). The UV_{254} reflects aromatic compounds because its PI-electrons absorb in UV-range (Abbt-Braun and Frimmel 1999). The higher SUVA after hydrothermal treatment suggests the excessive formation of aromatic compounds and melanoidins (Dwyer et al. 2008). Stemann et al. (2013b) found comparable ratios for COD/DOC and SUVA of 2.8 mg O_2/mg C and 1.3 L/(mg·m). Recirculating the liquid phase to the HTC-process five times led to a decrease of both parameters to 2.5 mg O_2/mg C and 0.7 L/(mg·m). Stemann et al. (2013b) concluded, that recirculation leads to an accumulation of aliphatic, organic acids, which were not detected by UV_{254}, whereas reactive components with higher molecular weight tend to polymerize.

Table 9: Sum parameters to characterize the organic load of the untreated liquid phase and the hydrothermally treated liquid phase (Mean values ± STD, n=15)

	COD	**DOC**	**COD/DOC**	**UV_{254}**	**SUVA**
	mg O_2/L	**mg C/L**	**mg O_2/mg C**	**1/m**	**L/(mg·m)**
RS 1 (raw)	3,911	1,458	2.68	1,196	0.82
RS 1 (hydrochars)	26,263	8,506	3.10	13,896	1.63
	±1,221	±614	±0.13	±1,205	±0.05

Regarding NH_4-N (Figure 11 a), opposite trends compared to DOC were observed. Higher temperatures and longer times also led to higher ammonium concentration in the liquid phase. The NH_4-N concentration increased from 535 mg/L at 190 °C to 926 mg/L at 250 °C (0.5 h) with a slight flattening curve with higher temperatures. With an extension of the reaction time up to 4 h the model illustrates an almost linear increase in the ammonium concentration. The share of NH_4-N in TN, referred to as NH_4-N-release in % in Figure 11 b was about 26% at the lowest hydrothermal conditions of 190 °C for 0.5 h. When the reaction temperature was increased to 250 °C, about 45% of the total nitrogen was present as NH_4-N. Prolonging the reaction time to 4 h led to an increased share of 32% at 190 °C and of 54% at 250 °C. As with NH_4-N, higher temperatures and longer reaction times increased the NH_4-N-release. The NH_4-N concentration and

the NH_4-N release follow the discussed trend of a higher influence of the reaction time at higher temperatures.

Since for all experiments the concentration of TN in the liquid phase remained relatively consistent at 2,254 ± 84 mg/L, lower hydrothermal conditions favor hydrolysis of the solid phase nitrogen, while more intense hydrothermal conditions lead to decomposition of dissolved nitrogen into lower molecular products with release of NH_4-N (Yin et al. 2015). Dissolved organic nitrogen compounds are degraded into NH_4-N, for example as a result of deamination. Sun et al. (2013) also used sewage sludge and observed a similar influence of the reaction time at 200 °C, but also discovered a higher increase in NH_4-N concentration with an extension of the reaction time from 60 to 90 minutes at 180 °C by more than 30%. Taking their study and the presented results into account, the reaction time becomes less significant for the nitrogen degradation somewhere between 180 °C and 190 °C. The share of NH_4-N in their study is within approx. 27% at 180 °C for 0.5 h to 51% at 240 °C for 1.5 h and therefore about 15% higher than in our study. Probably the higher nitrogen content of their feedstock of 7.2% (dry basis) in comparison to 5.0% (dry basis) of our feedstock is decisive.

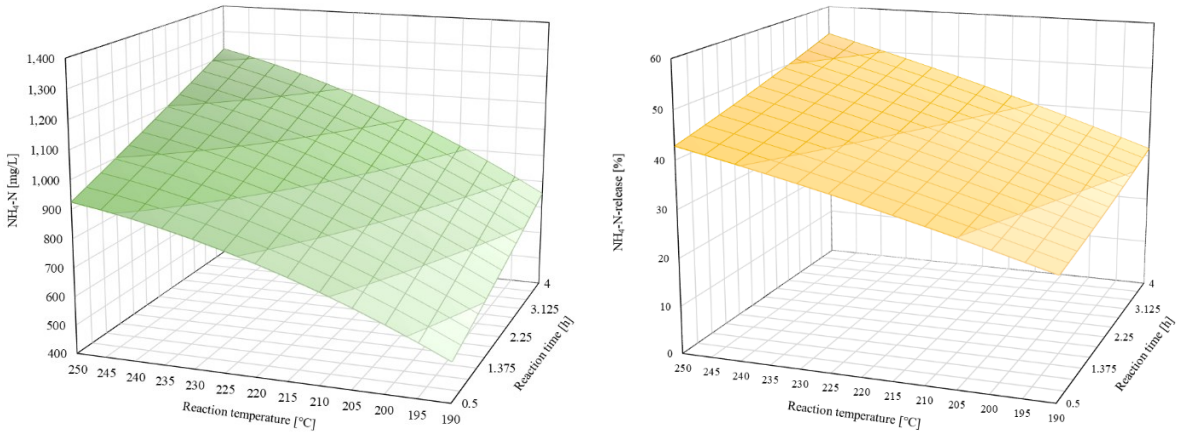

(**a**) (**b**)

Figure 11: Response surface plots of a) NH_4-N at pH = 6.1 and b) NH_4-N release at pH = 6.1

4.3.4 Impact of the volatile solids in feedstock sewage sludge on higher heating value

For sewage sludge and its hydrochars, the HHV (in the range of 10.9 to 22.1 MJ/kg TS), the COD (in the range of 0.75 to 1.52 kg O_2/kg TS) and the carbon content (in the range of 0.26 to 0.49 kg C/kg TS) strongly correlate with each other (Figure 12). The HHV and COD correlated linearly to carbon

content showing high correlation factors $R^2 = 0.98$ and 0.96. These correlations allow only one parameter to be measured and the other parameters to be determined from it, which can be useful in case of limited analytical capabilities. With this in mind, only the HHV was discussed further below. Nonetheless, the relationship between COD, HHV and carbon content must be determined for every series of tests (Heidrich et al. 2011).

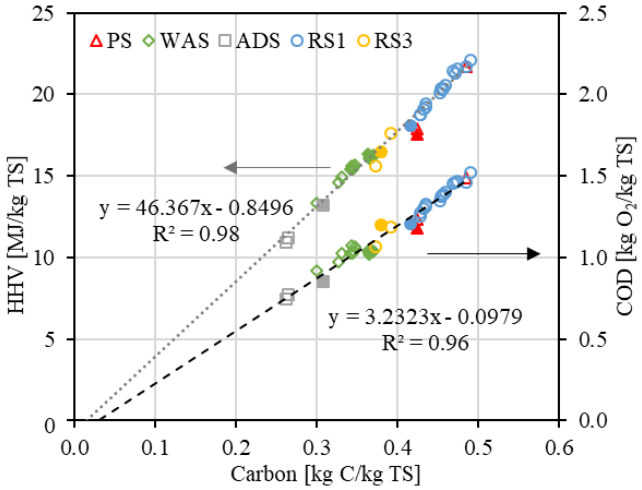

Figure 12: Relation between the HHV and the carbon content of all sewage sludges investigated (filled icons) and their hydrochars (framed icons) resulting from HTC

Figure 12 also shows, that the HHV and carbon content of some hydrochars were higher than the feedstock (e.g. PS and RS1), whereas for some hydrochars these parameters were lower (ADS, WAS) than in feedstock. Hence, the hydrothermal treatment of sewage sludge does not necessarily increase the HHV of hydrochars. Figure 13 depicts the percentage change of the HHV caused by hydrothermal treatment as a function of ash content and thus of volatile solids in the feedstock. At first sight, an increase in HHV appears to become unlikely with increasing ash content in feedstock. On the one hand, organic compounds are dissolved to a certain degree during HTC due to hydrolysis, resulting in decreasing organics content in the solids and a mass loss. On the other hand, dehydration, decarboxylation and polymerization induce carbonization and therefore a higher HHV. An ash content of around 28% seems to mark a turning point where the two effects were balanced and beyond which the hydrothermal treatment no longer affects HHV positively. Even below 28% ash content, lower temperatures of 180 - 190 °C often resulted in only a limited elevation. As expected, higher temperatures mostly led to higher HHVs compared to the feedstock due to decarboxylation and dehydration as well as polymerization reactions. The data also suggest, that the origin of the sewage sludge and therefore it's composition is less relevant for the change in HHV than the ash content of the feedstock since

different sewage sludges behave similarly. Studies by Zhao et al. (2014), Zheng et al. (2019) and our study using WAS all follow the trend described. While Zhao et al. (2014) increased the HHV of sewage sludge with 18.8% ash by up to 7% at the highest temperature of 240 °C, we measured no decrease at 250 °C and a decline of -10% at 190 °C for a WAS with 29.0% ash. The WAS used by Zheng et al. (2019) had an ash content of 41.2% and their data implicates a drop in heating value of -34% at 280 °C. Kim et al. (2014) carbonized ADS with an initial ash content of 26.1% and reached an increase in HHV of up to 18% at 250 °C. In contrast, the hydrothermal treatment of the ADS we used (41.5% ash) reduced the HHV by -18% (at 250 °C) to -20% (at 190 °C). For both types of feedstock (WAS, ADS) the HHV reduces when the ash content is above 20 - 35%. For their study, Danso-Boateng et al. (2013) used PS with minor ash content of 16.0% and increased the HHV by 20% to 22%. The municipal sewage sludge used by Zhang et al. (2014) contained 33.1% ash and resulted in a reduction of the HHV of -5% (at 190 °C) to -2% (at 260 °C). Prolonging the reaction time from 1 h to 24 h led to a percental change of -2% (190°C) to 4% (260°C).

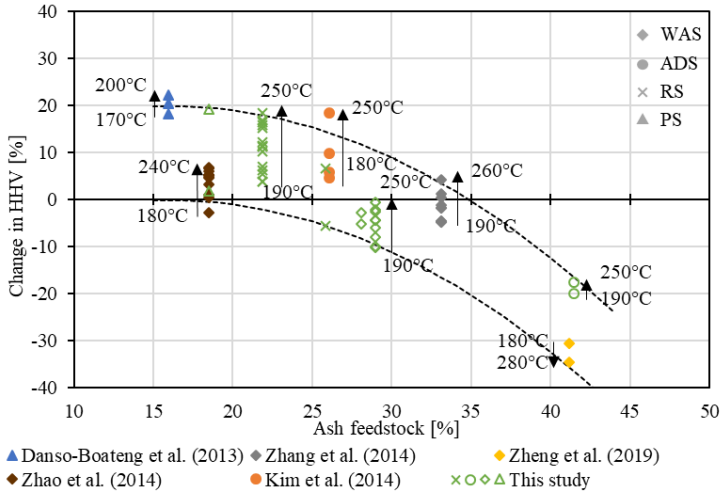

Figure 13: Correlation of the ash content of the feedstock and the change of HHV calculated by ($HHV_{hydrochar}$-$HHV_{feedstock}$)/$HHV_{hydrochar}$·100. Data adapted from: Danso-Boateng et al. (2013): PS, 190 °C, 200 °C, 4 h; Zhang et al. (2014): 190 °C, 260 °C, 1 h; Zhao et al. (2014): WAS, 180 °C, 200 °C, 220 °C, 240 °C, 0.25 h, 0.5 h, 0.45 h; Zheng et al. (2019): WAS, 180 °C, 230 °C, 280 °C, 1 h; Kim et al. (2014): ADS 180 °C, 200 °C, 220 °C, 250 °C, 0.5 h; this study: see Table 6, 190 °C, 220 °C, 250 °C at various reaction times

Although varying experimental setups and hydrothermal conditions make it difficult to objectively compare the results of the studies the data show some coherence among the diverse experiments. With this in mind, it seems reasonable to consider a maximum ash content of the feedstock of 20% to 35%, beyond which an increase in the HHV seems unlikely. This corresponds to a VS of

65 to 80%. According to these findings, not all sewage sludges are suitable to generate a higher calorific product using HTC.

4.3.5 Impact of volatile solids on process water load

The concentrations of DOC or TOC and NH_4-N in process water are related to the VS as well as carbon and nitrogen content of the feedstock sewage sludge. Table 5 summarizes the concentrations of DOC and NH_4-N in the process water after hydrothermal treatment at varying reaction intensities for the different sludges. To obtain process water concentration from hydrothermal treatment only, the concentration change resulting from thawing was deducted.

Table 10: Resulting DOC and NH_4-N in process water of the tested sewage sludges after HTC

	f	**DOC**	**NH_4-N**
	-	**mg/L**	**mg/L**
WWTP A			
RS1	0.13 - 0.42	6,088 - 7,938	483 - 1,130
WWTP B			
PS	0.12 - 0.31	708 - 6,200	53 - 239
WAS	0.12 - 0.41	4,693 - 16,795	522 - 2,765
RS2	0.12 - 0.28	6,610 - 6,835	347 - 684
RS3	0.13 - 0.31	9,510 - 11,485	635 - 1,380
ADS	0.13 - 0.29	2,896 - 4,108	170 - 448

Depending on the reaction intensity, the DOC/VS release ratio in Figure 14 a behaved differently for each type of sewage sludge: The hydrothermal carbonization of WAS resulted in a DOC/VS of 250 mg DOC/g VS at a low reaction intensity (f = 0.13) and decreased to 165 mg DOC/g VS at higher temperatures and longer reaction times (f = 0.41). Polymerization reactions, as mentioned above, can lead to an exponential decrease of the VS-specific release with increasing reaction intensity. Despite variations in VS content resulting from the dilution of WAS (see Table 6) the specific release showed no significant deviations. In contrast, Aragón-Briceño et al. (2020) detected decreasing process water releases with rising solids loading from 2.5% TS to 17.5% TS and a saturation concentration of organics and ammonium beyond 17.5% TS. Presumably, our method of evaluation and smaller variations in solids loading (3.1% to 9.1%) allow no detailed observation of this effect. The DOC/VS for RS1 decreased from 166 mg DOC/g VS at f = 0.13 to 133 mg DOC/g VS at f = 0.42. Although different pH values and their effects on hydrothermal processes were not considered in the calculation of f, the curve fit is good (R^2 = 0.81). A contrary

trend was observed for PS, as a low f (0.12) resulted in an organic load of 19 mg DOC/g VS and a high f (0.33) in an organic load of 153 mg DOC/g VS. This may be attributed to the more structured solids in primary sewage sludge, which are further decomposed with increasing reaction intensity. Similar findings with PS under less harsh reaction conditions were obtained by Danso-Boateng et al. (2015b). The other sewage sludges contain no structured material and a maximum degradation has already been reached at lower reaction intensity than those studied (f < 0.12). This is supported by data from Wang et al. (2019b), who investigated the concentration of several parameters in process water, like TOC, as a function of f using a Chinese raw sewage sludge. They observed higher TOC concentrations up to nearly 21,000 mg/L (f = 0.14) in comparison to our RS1 with DOC = 7,703 mg/L (f = 0.13). When taking into account the VS of sewage sludge, their data agreed with our results at a comparable level: Starting from 230 mg TOC/g VS at f = 0.13, the TOC/VS ratio was reduced to 133 mg TOC/g VS at f = 0.41. In addition, data of Wang et al. (2019b) imply a further reduction of the VS-specific TOC release due to the intensified hydrothermal treatment for f > 0.41. The reduction of their TOC/VS-ratio was more pronounced than in our experiments, possibly because samples were not filtered at 0.45 μm or analytical methods were different. It is important to mention, that the results of Wang et al. (2019b) limit the extrapolation of the regressionlines: The reaction intensity f = 0.14 marks a turning point with the maximum release, indicating the transition between thermal hydrolysis and hydrothermal carbonization.

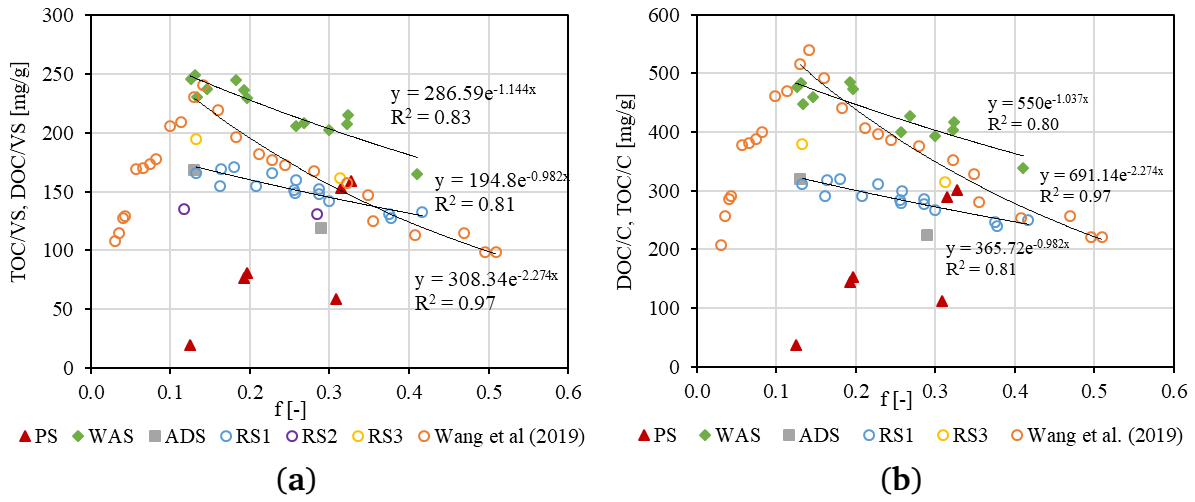

Figure 14: Curves of the ratio a) DOC/VS (TOC/VS: data adapted from Wang et al. (2019b)) and b) DOC/C (TOC/C: data adapted from Wang et al. (2019b)) with increasing reaction intensity during hydrothermal treatment of various sewage sludges

The trends in specific release of DOC/TOC relative to organic carbon in the feedstock sewage sludge, denoted DOC/C and TOC/C in Figure 14 b, behaved very similarly to DOC/VS. The specific C-releases of WAS and RS1 decreased from 476 mg DOC/g C and 311 mg DOC/g C at f = 0.13 to 339 mg DOC/g C and 250 mg DOC/g C at f = 0.41 (WAS) and f = 0.42 (RS1). The C-specific release can also be interpreted as a percentage of organic solids carbon which was dissolved into the process water. Taking RS1 as an example, hydrolysis at lower reaction intensities released 31% carbon into the process water and polymerization reactions at higher reaction intensities reduced share of carbon released to 25%. This caused an increasing carbon content and an associated increasing HHV in the hydrochars, as discussed in section 4.3.2. Comparing the VS specific and C specific release, no major differences of the overall picture can be observed. This suggests that the carbon content is not the only factor affecting the carbon release into the process water and that considering a correlation between the release of carbon in the process water and the carbon in the feedstock is not sufficient. As our analytics provide no detailed insights, further research should be carried out to identify other main drivers for the carbon release resulting from hydrothermal treatment of sewage sludge.

The release of ammonium is also related to the VS and depicted in Figure 15 a. Elevating reaction intensity increased the VS-specific release of NH_4-N for each sewage sludge. For PS, raising f led to a minor increase in the NH_4-N/VS ratio from 3.1 mg NH_4-N/g VS at f = 0.12 to 4.3 mg NH_4-N/g VS at f = 0.33. The increase in NH_4-N/VS as consequence of a more intense reaction was more evident for WAS, as the ratio elevated from 15 mg NH_4-N/g VS at f = 0.13 to 40 mg NH_4-N/g VS at f = 0.41. R^2 is 0.97 for a logarithmic VS-specific correlation, which seems plausible due to the release being limited by nitrogen in the solids. The intensification of hydrothermal conditions of WAS led to a higher NH_4-N concentration by a factor of 2.6 whereas for PS the factor was only 1.4. These observations can be contributed to the different composition of the sewage sludges, as the protein content in WAS is up to 2.3 times higher than in PS in a range of 19 - 41% and 14 - 30%, respectively (Wang et al. 2019a; Wilson and Novak 2009). Besides, WAS contains only few structural materials. As also assumed for DOC-release, hydrothermal treatment could break down these smaller molecules to a greater extend and release more ammonium. The raw sewage sludges RS1, RS2 and RS3 are within the range of WAS and PS. Despite variations in the pH of RS1, the results showed a good correlation with R^2 = 0.95. The NH_4-N/VS of ADS ranged from 7 mg NH_4-N/g VS at f = 0.13 to 18 mg NH_4-N/g VS at f = 0.29. So, the nitrogenous compounds in the in ADS

seem to be degraded to the same extend as for the other sewage sludges, despite the previous biological hydrolysis during anaerobic digestion. The data from Wang et al. (2019b) showed an almost identical curve than our data of WAS and a more linear behavior for f < 0.14. This suggests that similar behavior is likely for our sludges at lower reaction intensities and that the correlation's extrapolation is not valid.

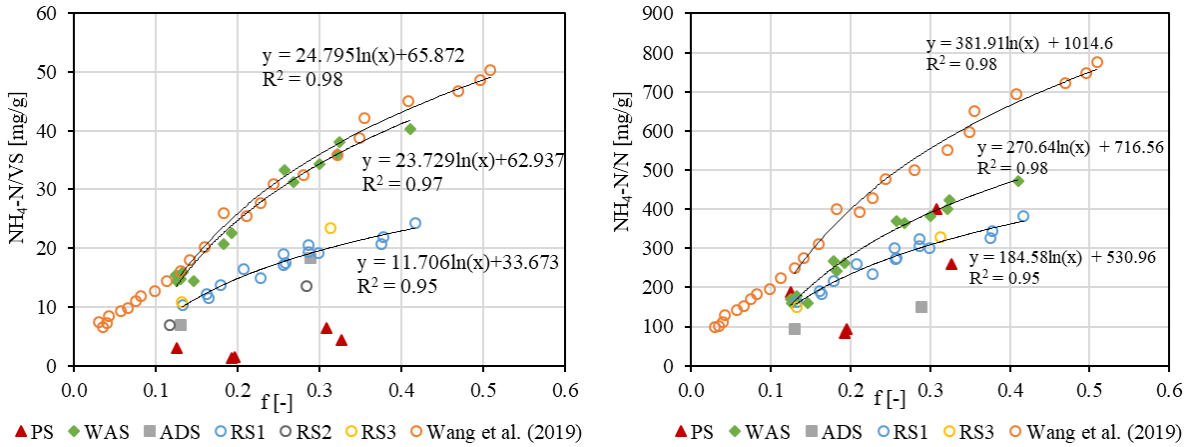

Figure 15: Curves of the ratio a) NH_4-N/VS and b) NH_4-N/N with increasing reaction intensity during hydrothermal treatment of various sewage sludges. Data adapted from Wang et al. (2019b)

Nitrogen-specific release of NH_4-N in feedstock sewage sludges, denoted NH_4-N/N in Figure 15 b, started with 92 - 249 mg NH_4-N/g N at f = 0.12 - 0.13. Depending on the sewage sludge, NH_4-N was released to different degrees and resulted in 309 mg NH_4-N/g N (RS1), 471 mg NH_4-N/g N (WAS) and 695 mg NH_4-N/g N (Liu et al. 2020; Wang et al. 2019b) at f ≈ 0.41. This corresponded to a release of 30.9% to 69.5% of the total nitrogen in the sewage sludge as ammonium. Extrapolating the regressions beyond their maximum tested hydrothermal conditions suggests a limit, which is below the theoretical maximum of 1,000 mg NH_4-N/g N for the sewage sludges investigated in this study. Accordingly, the hydrothermal treatment under the shown hydrothermal conditions did not decompose the entire nitrogen in the feedstock sewage sludge as ammonium. As several other studies consistently indicate no complete breakdown of dissolved nitrogen to ammonium due to hydrothermal carbonization, nitrogen remains as dissolved organic nitrogen on the one hand and in hydrochars on the other hand (Dote et al. 1998; Inoue et al. 1997). Comparing the NH_4-N/VS and the NH_4-N/N some deviations become apparent. For example, the nitrogen-specific NH_4-N-release of PS did not seem to match the VS-specific NH_4-N-release in Figure 15 a, as the spread of the values

measured was larger. A closer look reveals that the percentage spread is identical but is illustrated super elevated in Figure 15 b. These fluctuations might be due to the heterogeneous mixture of PS, which could have affected sampling. Nevertheless, the ratio of the NH_4-N concentration to the nitrogen in the feedstock PS showed that the degree of release is of the same magnitude. The NH_4-N/N accounted for the lower nitrogen in PS and lifted the N-specific release to a comparable level to the other sewage sludges. ADS showed a minor NH_4-N/N than the other sewage sludges. During anaerobic digestion proteins were already hydrolyzed and present as NH_4-N in the process water (which were deducted in the graphs). This seems to limit the degradation of nitrogen resulting from hydrothermal treatment, which was not represented in the NH_4-N/VS. The lower NH_4-N/N illustrates, that bonding forms of nitrogen in the feedstock sewage sludge determine the extent of NH_4-N-release during hydrothermal treatment.

4.4 Conclusions

The main reaction parameters on the hydrothermal treatment of sewage sludge temperature and time were predominantly described by their linear coefficients in the model fits of the BBD. Results of these model fits suggest, that intensifying HTC process conditions favor higher HHV of the hydrochars and hence coalification. Simultaneous polymerization reactions form more hydrochars, which led to lower DOC concentrations in the process water. These reactions were accelerated at pH 3.9, but the effect of pH decreased with increasing intensity of hydrothermal conditions. For a technical application, costs and benefits in the particular case must be weighed up, as it results in a trade-off between higher reaction temperatures by additional energy input and additional operating resources by the addition of acids.

Regarding nitrogen, harsher hydrothermal conditions led to an ongoing deamination and the associated increase in NH_4-N load in the liquid phase. But even with the most intense hydrothermal treatment of 250 °C for 4 h, a fraction of 46% remained as dissolved organic nitrogen. The high carbon and nitrogen concentrations in the process water permit no direct discharge of the process water and require extensive purification. Consistently, the treatment of the process water, the aim of the hydrochars application and the hydrothermal conditions must be adjusted to one another. This adjustment of the process steps with another requires an understanding of the level of process water load, which was shown to be mainly affected by VS as well as carbon and nitrogen content. The specific C and N release illustrated enables the estimation of process water

load as function of the type of sewage sludge and the hydrothermal conditions. This can be a useful tool for the technical application of HTC for sewage sludge treatment within the framework of a holistic management of the produced residues. As an example, anaerobic digestion of process water DOC allows to recover energy, which would not necessarily require low DOC concentrations in the liquid. However, no conclusions about the biodegradability can be drawn from the measurement of organic concentration alone. To remove ammonium, high ammonium concentrations favor stripping or, since phosphorus concentrations are also high, MAP precipitation. A possible alternative could be biological nitrogen removal. In any case, the high concentration of remaining dissolved organic nitrogen has to be mineralized to be eliminated from process water e. g. by nitrification and denitrification. The development of adequate solutions is the subject of current and future research.

Author Contributions: Conceptualization, T.B. and M.E.; methodology, T.B.; formal analysis, T.B.; investigation, T.B.; data curation, T.B.; writing - original draft preparation, T.B.; writing - review and editing, M.E.; visualization, T.B.; supervision, M.E.; project administration, M.E.; funding acquisition, M.E. All authors have read and agreed to the published version of the manuscript.

Funding: This research was funded by the German Federal Ministry of Education and Research (BMBF) within the project “IntenKS”, grant number 02WCL1470A. We acknowledge support by the Deutsche Forschungsgemeinschaft (DFG – German Research Foundation) and the Open Access Publishing Fund of Technical University of Darmstadt.

Acknowledgments: The authors gratefully thank L. Hennemann, K. Pilatus, L. Schreiber and J. Schäfer for conducting parts of the experiments.

Conflicts of Interest: The authors declare no conflict of interest.

4.5 References

Abbt-Braun, G.; Frimmel, F. H. (1999): Basic Characterization of Norwegian NOM Samples - Similarities and Differences. In: Environment International 25 (2/3), S. 161–180. DOI: 10.1016/S0160-4120(98)00118-4.

Ahmad, M.; Rajapaksha, A. U.; Lim, J. E.; Zhang, M.; Bolan, N.; Mohan, D. et al. (2014): Biochar as a sorbent for contaminant management in soil and water. A review. In: Chemosphere 99, S. 19–33.

Akhtar, J.; Amin, Nor A. S. (2011): A review on process conditions for optimum bio-oil yield in hydrothermal liquefaction of biomass. In: Renewable and

Sustainable Energy Reviews 15 (3), S. 1615–1624. DOI: 10.1016/j.rser.2010.11.054.

Aragón-Briceño, C.; Ross, A. B.; Camargo-Valero, M. A. (2017): Evaluation and comparison of product yields and bio-methane potential in sewage digestate following hydrothermal treatment. In: Applied Energy 208, S. 1357–1369. DOI: 10.1016/j.apenergy.2017.09.019.

Aragón-Briceño, C. I.; Grasham, O.; Ross, A. B.; Dupont, V.; Camargo-Valero, M. A. (2020): Hydrothermal carbonization of sewage digestate at wastewater treatment works: Influence of solid loading on characteristics of hydrochar, process water and plant energetics. In: Renewable Energy 157, S. 959–973. DOI: 10.1016/j.renene.2020.05.021.

Asghari, F. S.; Yoshida, H. (2006): Acid-Catalyzed Production of 5-Hydroxymethyl Furfural from d-Fructose in Subcritical Water. In: Industrial & Engineering Chemistry Research 45 (7), S. 2163–2173. DOI: 10.1021/ie051088y.

Bas, D.; Boyaci, I. H. (2007): Modeling and optimization I: Usability of response surface methodology. In: Journal of Food Engineering 78, S. 836–845.

Bergius, F. (1913): Die Anwendung hoher Drücke bei chemischen Vorgängen und eine Nachbildung des Entstehungsprozesses der Steinkohle. Halle a. S.: Wilhelm Knapp.

Chen, H.; Rao, Y.; Cao, L.; Shi, Y.; Hao, S.; Luo, G.; Zhang, S. (2019): Hydrothermal conversion of sewage sludge: Focusing on the characterization of liquid products and their methane yields. In: Chemical Engineering Journal 357, S. 367–375.

Danso-Boateng, E.; Holdrich, R. G.; Martin, S. J.; Shama, G.; Wheatley, A. D. (2015): Process energetics for the hydrothermal carbonisation of human faecal wastes. In: Energy Conversion and Management 105, S. 1115–1124.

Danso-Boateng, E.; Holdrich, R. G.; Shama, G.; Wheatley, A. D.; Sohail, M.; Martin, S. J. (2013): Kinetics of faecal biomass hydrothermal carbonisation for hydrochar production. In: Applied Energy 111, S. 351–357.

Danso-Boateng, E.; Shama, G.; Wheatley, A. D.; Martin, S. J.; Holdrich, R. G. (2015b): Hydrothermal carbonisation of sewage sludge: Effect of process conditions on product characteristics and methane production. In: Bioresource Technology 177, S. 318–327.

Dote, Y.; Inoue, S.; Ogi, T.; Yokoyama, S. (1998): Distribution of Nitrogen to Oil Products from Liquefaction of Amino Acids. In: Bioresource Technology 64, S. 157–160.

Dunne, D. J.; Agnew, J. B. (1992): Thermal Upgrading of Low-Grade, Low-Rank South Australia Coal. In: Energy Sources 14 (2), S. 169–181. DOI: 10.1080/00908319208908718.

Dwyer, J.; Starrenburg, D.; Tait, S.; Barr, K.; Batstone, D. J.; Lant, P. (2008): Decreasing activated sludge thermal hydrolysis temperature reduces product colour, without decreasing degradability. In: Water Research 42, S. 4699–4709.

Escala, M.; Zumbühl, T.; Koller, Ch.; Junge, R.; Krebs, R. (2013): Hydrothermal Carbonization as an Energy-Efficient Alternative to Established Drying Technologies for Sewage Sludge. A Feasibility Study on a Laboratory Scale. In: Energy & Fuels 27 (1), S. 454–460.

Fan, Y.; Hornung, U.; Dahmen, N.; Kruse, A. (2018): Hydrothermal liquefaction of protein-containing biomass: study of model compounds for Maillard reactions. In: Biomass Conversion and Biorefinery 8 (4), S. 909–923. DOI: 10.1007/s13399-018-0340-8.

Heidrich, E. S.; Curtis, T. P.; Dolfing, J. (2011): Determination of the Internal Chemical Energy of Wastewater. In: Environmental Science & Technology (45), S. 827–832. DOI: 10.1021/es103058w.

Holliday, R. L.; King, J. W.; List, G. R. (1997): Hydrolysis of Vegetable Oils in Sub- and Supercritical Water. In: Industrial & Engineering Chemistry Research 36, S. 932–935.

Inoue, S.; Sawayama, S.; Dote, Y.; Ogi, T. (1997): Behaviour of Nitrogen during Liquefaction of Dewatered Sewage Sludge. In: Biomass and Bioenergy 12 (6), S. 473–475.

Kim, D.; Lee, K.; Park, K. Y. (2014): Hydrothermal carbonization of anaerobically digested sludge for solid fuel production and energy recovery. In: Fuel 130, S. 120–125.

Klingler, D.; Berg, J.; Vogel, H. (2007): Hydrothermal reactions of alanine and glycine in sub- and supercritical water. In: The Journal of Supercritical Fluids 43 (1), S. 112–119. DOI: 10.1016/j.supflu.2007.04.008.

Liu, X.; Zhai, Y.; Li, S.; Wang, B.; Wang, T.; Liu, Y. et al. (2020): Hydrothermal carbonization of sewage sludge: Effect of feed-water pH on hydrochar's

physicochemical properties, organic component and thermal behavior. In: Journal of Hazardous Materials 388.

Minowa, T.; Inoue, S.; Hanaoka, T.; Matsumura, Y. (2004): Hydrothermal Reaction of Glucose and Glycine as Model Compounds of Biomass. In: Journal of the Japan Institute of Energy 83, S. 794–798.

Montgomery, D. C. (2001): Design and Analysis of Experiments. 5th Edition. New York: John Wiley & Sons, INC.

Paneque, M.; La Rosa, J. M. de; Kern, J.; Reza, M. T.; Knicker, H. (2017): Hydrothermal carbonization and pyrolysis of sewage sludges: What happen to carbon and nitrogen? In: Journal of Analytical and Applied Pyrolysis 128, S. 314–323. DOI: 10.1016/j.jaap.2017.09.019.

Peterson, A. A.; Vogel, F.; Lachance, R. P.; Fröling, M.; Antal Jr., M. J.; W, Tester J. (2008): Thermochemical biofuel production in hydrothermal media. A review of sub- and supercritical water technologies. In: Energy and Environmental Science 1, S. 32–65.

Reza, M. T.; Becker, W.; Sachsenheimer, K.; Mumme, J. (2014): Hydrothermal carbonization (HTC): Near infrared spectroscopy and partial least-squares regression for determination of selective components in HTC solid and liquid products derived from maize silage. In: Bioresource Technology 161, S. 91–101.

Rogalinski, T.; Liu, K.; Albrecht, T.; Brunner, G. (2008): Hydrolysis kinetics of biopolymers in subcritical water. In: The Journal of Supercritical Fluids 46 (3), S. 335–341. DOI: 10.1016/j.supflu.2007.09.037.

Ruyter, H. P. (1982): Coalification model. In: Fuel 61 (12), S. 1182–1187.

Sevilla, M.; Fuertes, A. B. (2009): The production of carbon materials by hydrothermal carbonization of cellulose. In: Carbon 47, S. 2281–2289.

Shanableh, A. (2000): Production of useful Organic Matter from Sludge using Hydrothermal Treatment. In: Water Research 34 (3), S. 945–951.

Stemann, J.; Putschew, A.; Ziegler, F. (2013): Hydrothermal carbonization. Process water characterization and effects of water recirculation. In: Bioresource Technology 143, S. 139–146.

Sun, X. H.; Sumida H.; Yoshikawa K. (2013): Effects of Hydrothermal Process on the Nutrient Release of Sewage Sludge. In: International Journal of Waste Resources 03 (02). DOI: 10.4172/2252-5211.1000124.

Sun, X. H.; Sumida H.; Yoshikawa K. (2014): Effects of Liquid Fertilizer Produced from Sewage Sludge by the Hydrothermal Process on the Growth of Komatsuna. In: British Journal of Environment & Climate Change 4 (3), S. 261–278.

Titirici, M. M.; Thomas, A.; Yu, S.-H.; Müller, J.-O.; Antonietti, M. (2007a): A Direct Synthesis of Mesoporous Carbons with Bicontinuous Pore Morphology from Crude Plant Material by Hydrothermal Carbonization. In: Chemistry of Materials 19 (17), S. 4205–4212. DOI: 10.1021/cm0707408.

Titirici, M.-M.; Thomas, A.; Antonietti, M. (2007b): Back in the black: hydrothermal carbonization of plant material as an efficient chemical process to treat the CO2 problem? In: New Journal of Chemistry 31 (6), S. 787. DOI: 10.1039/b616045j.

Toor, S. S.; Rosendahl, L.; Rudolf, A. (2011): Hydrothermal liquefaction of biomass. A review of subcritical water technologies. In: Energy 36, S. 2328–2342.

Wang, L.; Chang, Y.; Li, A. (2019a): Hydrothermal carbonization for energy-efficient processing of sewage sludge: A review. In: Renewable and Sustainable Energy Reviews 108, S. 423–440.

Wang, L.; Chang, Y.; Liu, Q. (2019b): Fate and distribution of nutrients and heavy metals during hydrothermal carbonization of sewage sludge with implication to land application. In: Journal of Cleaner Production 225, S. 972–983.

Wang, L.; Li, A. (2015): Hydrothermal treatment coupled with mechanical expression at increased temperature for excess sludge dewatering: the dewatering performance and the characteristics of products. In: Water Research 68, S. 291–303. DOI: 10.1016/j.watres.2014.10.016.

Watanabe, M.; Aizawa, Y.; Iida, T.; Aida, T. M.; Levy, C.; Sue, K.; Inomata, H. (2005): Glucose reactions with acid and base catalysts in hot compressed water at 473 K. In: Carbohydrate Research 340 (12), S. 1925–1930. DOI: 10.1016/j.carres.2005.06.017.

Weiner, B.; Breulmann, M.; Wedwitschka, H.; Fühner, C.; Kopinke, F.-D. (2018): Wet Oxidation of Process Waters from the Hydrothermal Carbonization of Sewage Sludge. In: Chemie Ingenieur Technik 90 (6), S. 872–880. DOI: 10.1002/cite.201700050.

Wilson, C. A.; Novak, J. T. (2009): Hydrolysis of macromolecular components of primary and secondary wastewater sludge by thermal hydrolytic pretreatment. In: Water Research 43 (18), S. 4489–4498. DOI: 10.1016/j.watres.2009.07.022.

Yin, F.; Chen, H.; Xu, G.; Wang, G.; Xu, Y. (2015): A detailed kinetic model for the hydrothermal decomposition process of sewage sludge. In: Bioresource Technology 198, S. 351–357.

Zhai, Y.; Peng, C.; Xu, B.; Wang, T.; Li, C.; Zeng, G.; Zhu, Y. (2017): Hydrothermal carbonisation of sewage sludge for char production with different waste biomass: Effects of reaction temperature and energy recycling. In: Energy 127, S. 167–174.

Zhang, J.-H.; Lin, Q.-M.; Zhao, X.-R. (2014): The Hydrochar Characters of Municipal Sewage Sludge Under Different Hydrothermal Temperatures and Durations. In: Journal of Integrative Agriculture 13 (3), S. 471–482.

Zhao, P.; Shen, Y.; Ge, S.; Yoshikawa, K. (2014): Energy recycling from sewage sludge by producing solid biofuel with hydrothermal carbonization. In: Energy Conversion and Management 78, S. 815–821. DOI: 10.1016/j.enconman.2013.11.026.

Zheng, Chupeng; Ma, Xiaoqian; Yao, Zhongliang; Chen, Xinfei (2019): The properties and combustion behaviors of hydrochars derived from co-hydrothermal carbonization of sewage sludge and food waste. In: Bioresource Technology 285, S. 121347. DOI: 10.1016/j.biortech.2019.121347.

Zhuang, X.; Huang, Y.; Song, Y.; Zhan, H.; Yin, X.; Wu, C. (2017): The transformation pathways of nitrogen in sewage sludge during hydrothermal treatment. In: Bioresource Technology 245, S. 463–470.

Zou, S.; Wu, Y.; Yang, M.; Li, C.; Tong, J. (2009): Thermochemical Catalytic Liquefaction of the Marine Microalgae Dunaliella tertiolecta and Characterization of Bio-oils. In: Energy & Fuels 23 (7), S. 3753–3758. DOI: 10.1021/ef9000105.

4.6 Supplementary material

Table 11: ANOVA for the model of HHV. DF: degrees of freedom, SS: sum of squares, MS: mean squares

Source	DF	Sequential SS	Adjusted SS	Adjusted MS	F-value	P-value
Model	9	16817438	16817438	1868604	16.38	0.003
Linear	3	16545650	16545650	5515217	48.33	0.000
T (Temperature, °C)	1	14284513	14284513	14284513	125.18	0.000
t (time, h)	1	1168156	1168156	1168156	10.24	0.024
pH (pH-value, -)	1	1092981	1092981	1092981	9.58	0.027
Quadratic	3	38745	38745	12915	0.11	0.949
T^2	1	15	218	218	0	0.967
t^2	1	33345	35235	35235	0.31	0.602
pH^2	1	5384	5384	5384	0.05	0.837
2-Way Interactions	3	233044	233044	77681	0.68	0.601
T*t	1	66178	66178	66178	0.58	0.481
T*pH	1	153468	153468	153468	1.34	0.299
t*pH	1	13398	13398	13398	0.12	0.746
Error	5	570565	570565	114113		
Lack of fit	3	535270	535270	178423	10.11	0.091
Pure error	2	35296	35296	17648		
Total	14	17388003				

Table 12: ANOVA for the model of DOC. DF: degrees of freedom, SS: sum of squares, MS: mean squares

Source	DF	Sequential SS	Adjusted SS	Adjusted MS	F-value	P-value
Model	9	5431550	5431550	603506	13.25	0.005
Linear	3	4789919	4789919	1596640	35.06	0.001
T (Temperature, °C)	1	4343878	4343878	4343878	95.38	0.000
t (time, h)	1	161028	161028	161028	3.54	0.119
pH (pH-value, -)	1	285012	285013	285013	6.26	0.054
Quadratic	3	443294	443294	147765	3.24	0.119
T^2	1	210109	198164	198164	4.35	0.091
t^2	1	172770	156433	156433	3.43	0.123
pH^2	1	60416	60416	60416	1.33	0.302
2-Way Interactions	3	198338	198338	66113	1.45	0.333
T*t	1	105625	105625	105625	2.32	0.188
T*pH	1	66306	66306	66306	1.46	0.282
t*pH	1	26406	26406	26406	0.58	0.481
Error	5	227723	227723	45545		
Lack of fit	3	80706	80706	26902	0.37	0.789
Pure error	2	147017	147017	73508		
Total	14	5659273				

Table 13: ANOVA for the model of NH_4-N. DF: degrees of freedom, SS: sum of squares, MS: mean squares

Source	DF	Sequential SS	Adjusted SS	Adjusted MS	F-value	P-value
Model	9	492059	492059	54673	62.54	0.000
Linear	3	475817	475817	158606	181.41	0.000
T (Temperature, °C)	1	394938	394938	394938	451.73	0.000
t (time, h)	1	79501	79501	79501	90.93	0.000
pH (pH-value, -)	1	1378	1378	1378	1.58	0.265
Quadratic	3	10266	10266	3422	3.91	0.088
T^2	1	9891	9896	9896	11.32	0.02
t^2	1	98	74	74	0.08	0.783
pH^2	1	276	276	276	0.32	0.598
2-Way Interactions	3	5977	5977	1992	2.28	0.197
T*t	1	1914	1914	1914	2.19	0.199
T*pH	1	156	156	156	0.18	0.69
t*pH	1	3906	3906	3906	4.47	0.088
Error	5	4371	4371	874		
Lack of fit	3	417	417	139	0.07	0.971
Pure error	2	3954	3954	1977		
Total	14	496431				

Table 14: ANOVA for the model of NH_4-N/TN. DF: degrees of freedom, SS: sum of squares, MS: mean squares

Source	DF	Sequential SS	Adjusted SS	Adjusted MS	F-value	P-value
Model	9	965.646	965.646	107.294	74.06	0.000
Linear	3	955.835	955.835	318.612	219.92	0.000
T (Temperature, °C)	1	823.866	823.866	823.866	568.66	0.000
t (time, h)	1	112.038	112.038	112.038	77.33	0.000
pH (pH-value, -)	1	19.931	19.931	19.931	13.76	0.014
Quadratic	3	4.239	4.239	1.413	0.98	0.474
T^2	1	2.707	2.272	2.272	1.57	0.266
t^2	1	0.511	0.625	0.625	0.43	0.54
pH^2	1	1.022	1.022	1.022	0.71	0.439
2-Way Interactions	3	5.571	5.571	1.857	1.28	0.376
T*t	1	3.801	3.801	3.801	2.62	0.166
T*pH	1	0.149	0.149	0.149	0.1	0.762
t*pH	1	1.622	1.622	1.622	1.12	0.338
Error	5	7.244	7.244	1.449		
Lack of fit	3	6.296	6.296	2.099	4.43	0.19
Pure error	2	0.948	0.948	0.474		
Total	14	972.890				

5 Effect of temperature during the hydrothermal carbonization of sewage sludge on the aerobic treatment of the produced process waters

Authors:	Blach, T.; Lechevallier, P.; Engelhart, M.
Keywords:	Aerobic biodegradation; hydrothermal carbonization; nitrification inhibition; HTC process water; recalcitrant compounds
Published in:	Journal of Water Process Engineering 51 (2023) 103368 https://doi.org/10.1016/j.jwpe.2022.103368
Received:	3 September 2022
Accepted:	17 November 2022
Published:	25 November 2022

Abstract:

The treatment of the highly contaminated process water produced during the hydrothermal carbonization (HTC) of waste activated sludge is of major concern for the full-scale implementation of the HTC process. So far, no satisfying treatment strategies have been elaborated and the biodegradability under aerobic conditions has hardly been studied. To fill these gaps, aerobic tests were first carried out in batches with HTC process waters produced at 190 °C, 218 °C and 249 °C, and two sequencing batch reactors (SBR) were operated simultaneously to treat process waters produced at 190 °C and 217 °C. Both experiments show that the HTC temperature has only a little effect on the elimination of dissolved organic carbon (DOC). In the aerobic batch tests, DOC removal were 80.5 - 81.9%. In the SBR, 28% of the initial DOC was found to be recalcitrant, and 25 - 28% of the initial nitrogen. In the SBR experiments, the nitrification was also monitored, and nitrification inhibtion test were conducted on both process waters obtained at 190 °C and 217 °C. Nitrification the initial SBR reactors was only possible after dilution of the process waters, which indicates the presence of inhibiting substances. The inhibition tests validated those observations, and showed that process waters derived at 217 °C had a higher inhibition potential. This study demonstrates that aerobically treated HTC process waters are still too polluted to be discharged in a wastewater treatment plant: model calculations showed an increase in effluent DOC of 8.3 mg/L.

5.1 Introduction

Hydrothermal carbonization (HTC) is an alternative technology for recovering resources from waste materials such as sewage sludge. It has gained increasing attention in recent years to produce hydrochars, a coal-like solid with high carbon density and high dewatering properties. During HTC, temperatures up to 300 °C break down the sewage sludge structure by mechanisms like dehydration and decarboxylation (Funke and Ziegler 2010; Toor et al. 2011). The higher the reaction temperatures, the higher the coalification of the generated hydrochars. One formation pathway of hydrochars is the polymerization of dissolved reaction by-products (Paneque et al. 2017). However, a substantial amount of slowly or non-polymerizing organic matter remains dissolved and form a high strength wastewater with high amounts of refractory compounds: Aragón-Briceño et al. (2020) reported total organic carbon (TOC) concentrations up to 29,778 mg/L and total Kjeldahl nitrogen (TKN) concentrations of 8,064 mg/L. Also others studies showed the high loading of HTC process waters (Hämäläinen et al. 2021; Blach and Engelhart 2021). Such high concentrations result from various components like volatile fatty acids (VFA), humic-like substances, N-heterocycle compounds, phenols, ketones, or aldehydes (Atallah et al. 2019; Chen et al. 2019b; Cao et al. 2021).

Readily biodegradable substances, such as acetic acid, suggest the use of anaerobic digestion for process water treatment and has been studied intensively (Chen et al. 2019b; Si et al. 2019; Posmanik et al. 2017; Meier et al. 2017). Weide et al. (2019) investigated two-stage anaerobic digestion to treat process waters from the hydrothermal treatment of sewage sludge, using a continuous stirred tank reactor and an expanded granular sludge bed reactor with aerobic downstream treatment. This removed 55 - 58% of the chemical oxygen demand (COD) and the subsequent aerobic digestion led to an overall COD removal of 71 - 78%. In general, increasing hydrothermal reaction temperature lead to a drop in biogas yield during anaerobic digestion (Seyedi et al. 2021; Ariunbaatar et al. 2015), indicating the formation of slow biodegradable or inhibiting substances (Si et al. 2018).

Unlike anaerobic digestion, the use of aerobic processes for HTC process water treatment has not gained much attention yet. Nevertheless, aerobic treatment could be advantageous regarding the removal of recalcitrant compounds, such as polycyclic aromatic hydrocarbons (PAH), phenols, N-heterocyclic compounds, or melanoidins (Haritash and Kaushik 2009). Melanoidins, which are the brownish reaction products from the Maillard reaction, are of particular concern,

as they are formed during thermal sewage sludge treatment and have antimicrobial properties and limited biodegradability (Padoley et al. 2011). As a result, lag phases were prolonged and growth rates were lower (Helou et al. 2014). However, the role of melanoidins and recalcitrant dissolved organic nitrogen (rDON) and their evaluation needs further research (Zhang et al. 2020). The few studies focusing on aerobic treatment used different HTC feedstock, and reported COD removal rates of 58 - 89%, and the inhibition of nitrification. Inhibition could be reduced by anaerobic pretreatment and dilution (Kühni et al. 2015; Eibisch et al. 2013; Fettig et al. 2017). At high dilution, no toxicity of HTC process water to heterotrophic biomass of a municipal wastewater treatment plant (WWTP) was observed and the readily biodegradable compounds could serve as an external carbon supplement (Ferrentino et al. 2021; Langone et al. 2021).

To the best of our knowledge, the aerobic biodegradation and the inhibition of nitrification associated with HTC process water from sewage sludge has not been given much attention in international literature and systematic studies on biodegradation and quantification of refractory compounds are lacking. However, the process water is of major concern for the full scale implementation of the HTC process, but no satisfying treatment strategies have been elaborated so far. Discharge into municipal WWTP must be well evaluated considering the loading and the amount of recalcitrant compounds in the process water. In order to find solutions for the treatment of HTC process water, established strategies for the treatment of high strength wastewaters (e.g. for industrial wastewater or landfill leachate) must also be considered. Against this background, this study aims to assess the effect of the HTC temperature on the aerobic biodegradability of process waters. The total biodegradability of DOC was determined in batch tests. Continuous sequencing batch reactors (SBR) were used to evaluate the recalcitrant DOC (rDOC) and rDON, and the nitrification performance. Subsequent nitrification tests revealed the inhibition potential of process water and aerobically pre-treated process water.

5.2 Materials and methods

5.2.1 Preparation of HTC process water

Waste activated sludge (WAS) was obtained from a nitrifying municipal WWTP in Germany which serves 50,000 people. After sampling, the sludge was frozen in portions at -20 °C to obtain similar feedstock. Before use, the samples were thawed overnight at ambient temperature. Total solids were 9.1 ± 0.1% and

volatile solids 6.8 ± 0.1% (n=7). To produce process water, hydrothermal runs were performed using an electrically heated and water-cooled 0.5 L batch reactor (midiclave Typ 3E / 0,5lt, Büchi AG, Switzerland). The stirrer was set to 2,000 rpm. Hydrothermal temperatures were set to 189 ± 0.6 °C, 218 ± 0.1 °C, and 249 ± 0.3 °C for 30 min (ZW190, ZW218 and ZW249) and average pressures were 16.0, 31.6 and 54.5 bar. Setting cover low, medium and upper temperature range of HTC processes. After hydrothermal treatment, a folded filter (Whatman 520 B 1/2 240mm, GE Healthcare, UK) was used to separate the process water from the coal slurry. As suggested in literature, for continuous tests technical more relevant HTC conditions of 190 ± 1 °C and 217 ± 3 °C for 60 min (Feed SBR190, Feed SBR217) at average pressures of 16.3 bar and 32.2 bar were chosen (Cao et al. 2021; Ahmed et al. 2021).

Table 15: Overview and loading of the HTC process waters tested. Feed SBR190 and Feed SBR217 were analyzed every two weeks, but no changes became apparent

Parameter	ZW190	ZW218	ZW249	Feed SBR190		Feed SBR217	
	Mean	Mean	Mean	Mean	STD[e]	Mean	STD
DOC [mg C/L]	16,621	18,200	14,351	16,881	320	16,468	457
COD [mg O_2/L]	47,275	n.d.[d]	44,050	49,163	866	48,556	1,183
COD/DOC[a] [mg COD/mg C]	2.8	-	3.1	2.9	-	2.9	-
UV_{254} [1/m]	22,553	26,001	18,413	25,165	651	23,640	512
SUVA[b] [L/(mg·m)]	1.36	1.43	1.28	1.49	0.04	1.44	0.05
UV_{475}[1/m]	688	533	532	918	57	578	20
TKN [mg N/L]	n.d.	n.d.	n.d.	4,674	141	5,009	101
TN [mg N/L]	4,170	n.d.	4,508	4,481	130	4,843	73
DON[c] [mg N/L]	n.d.	n.d.	n.d.	3,327	117	3,126	96
NH_4-N [mg N/L]	1,084	1,530	1,867	1,153	37	1,701	41
NO_3-N [mg N/L]	n.d.	n.d.	n.d.	<1	-	<1	-
NO_2-N [mg N/L]	n.d.	n.d.	n.d.	<1	-	<1	-
PO_4-P [mg P/L]	n.d.	n.d.	n.d.	573	11	419	8
Cl^- [mg Cl/L]	n.d.	n.d.	n.d.	132	4	124	1
SO_4^{2-}[mg SO_4/L]	n.d.	n.d.	n.d.	575	39	572	6

[a]COD/DOC was constant during SBR tests and therefore used to calculate effluent COD

[b]specific UV absorbance: SUVA = UV_{254}/DOC

[c]dissolved organic nitrogen: DON = TN - NH_4-N - NO_3-N - NO_2-N

[d]not determined

[e]Standard deviation

At each temperature, 12 hydrothermal runs were carried out and the process waters were mixed after filtration with folded filters. The process waters were stored refrigerated at 4 °C. These process waters were also used for nitrification

inhibition tests. Table 15 gives an overview of the characteristics of the process waters.

5.2.2 Zahn-Wellens tests

Zahn-Wellens tests were performed according to DIN EN ISO 9888 (1999). One day before the experiments, aerobic inoculum from a nitrifying municipal WWTP in Germany was rinsed three times with tap water and sieved (400 μm) to remove coarse particulate substances. In addition, one test (ZW218*) was inoculated with pre-exposed biomass from a previous Zahn-Wellens test, following the same procedure. The inoculum activity was checked using ethylene glycol, and also inoculum blanks were set up. The test vessels (2 L) were filled with inoculum to a total mixed liquid suspended solids concentration (MLSS) of 0.88 g/L. The process waters were diluted to achieve an initial DOC of 350 mg/L. The vessels were mixed with magnetic stirrers and aerated with a diaphragm pump via a wash bottle containing deionized water at 22.2 ± 0.4 °C. To ensure sufficient dissolved oxygen (DO) in the reactors (>2 mg/L), DO was measured using a Multi 3620 IDS and an FDO 925 (Xylem Analytics Germany Sales GmbH & Co. KG), and aeration was regulated if necessary. The pH was adjusted several times a day to 6.7 - 7.8 using H_2SO_4 (0.5 M) or NaOH (0.5 M). Before each sampling, water losses due to evaporation were measured gravimetrically and replaced with deionized water. All tests with process waters were carried out in triplicates, with blanks in duplicates, and with references in singles. The DOC removal of the reference compound was almost 100% after 15 days of incubation, which proves a sufficient activity of the inoculum.

To calculate the DOC removal rate, the initial DOC in the suspensions was used. This differs from EN ISO 9888 (1999), which recommends using the DOC 2.5 to 3.5 hours after starting the experiments to account for adsorption processes at the beginning. During the first 3 hours, the DOC removal was already 15 - 26% indicating, as expected, a high concentration of readily biodegradable substances. Such high organics removal was considered unlikely for adsorption only and was therefore attributed to biological degradation.

5.2.3 SBR setup

Two continuous activated sludge reactors (SBR190 and SBR217) were operated simultaneously. Each vessel had a reaction volume of 300 mL and was aerated and mixed in the same way as the Zahn-Wellens tests. The SBRs were inoculated with nitrifying activated sludge from a lab-scale reactor, which was fed with HTC-process water. Temperature, electrical conductivity, redox potential, and

pH were measured continuously using Condumax CLS21D and Memosens CPS16D sensors (Endress+Hauser Conducta GmbH+Co. KG, Germany). A pH-controlled peristaltic pump (Ismatec ISMB833C, Cole-Parmer GmbH, Germany) dispensed H_2SO_4 (0.5 M) or NaOH (0.5 M) to ensure a pH between 6.8 and 7.5. The temperature was 19.7 - 20.5 °C. The DO was controlled manually several times a day to assure sufficient DO in the reactors (>2 mg/L). The SBRs had one cycle per day: (i) the reactor was filled manually with a volumetric pipette with 30 mL or 60 mL, which depended on the operation phase (see Table 16) (ii) aeration and mixing started for 23 h (iii) settling for 30 minutes (iv) effluent was removed manually with a volumetric pipette. Again, losses due to evaporation were recorded gravimetrically and replaced with deionized water before step iv. The effluent was analyzed 2-3 times a week, and the influent once every two weeks. Samples for MLSS and mixed liquor volatile suspended solids (MLVSS) were taken from the fully mixed suspension once a week. Beyond that, no additional sludge was removed from the systems and the sludge retention time (SRT) should be sufficiently high for nitrification. Due to strong foaming, 10 μL silicon-free defoaming agent based on fatty alcohols was added daily (ECSO 8361, EnviroChemie GmbH, Germany).

Table 16: Operation conditions in phases 1 - 3 during SBR treatment

Reactor	Parameter	Phase 1	Phase 2	Phase 3
Both	Operation days [d]	44	43	21
	Dilution of process water	-	10	10
	HRT [d]	10	10	5
	Exchange ratio [%]	10	10	20
SBR190	MLSS [g/L]	8.9	4.9	5.7
	F/M_C [mg C/(g MLSS·d)]	190	34	60
SBR217	MLSS [g/L]	8.0	4.5	5.0
	F/M_C [mg C/(g MLSS·d)]	212	38	67

The test reactors were operated in 3 phases with different process water share and hydraulic retention times (HRT), according to Table 16. In phase 2 and 3, process water was diluted 1:10 with deionized water. Data evaluation was done 2.5 HRTs after changing the influent regime.

The activity of ammonium oxidizing bacteria (AOB) and nitrite oxidizing bacteria (NOB) measured during SBR treatment were used to calculate the AOB rate (R_{AOB}) in mg N/(g MLSS·h) and the nitrification rate (R_N) in mg N/(g MLSS·h) with equation (5) and (6).

$$R_{AOB} = \frac{c_{NO_2-N} + c_{NO_3-N}}{c_{MLSS} \cdot t} \quad (5)$$

$$R_N = \frac{c_{NO_3-N}}{c_{MLSS} \cdot t} \quad (6)$$

c_{NO2-N}: Nitrite concentration, mg/L
c_{NO3-N}: Nitrate concentration, mg/L
c_{MLSS}: MLSS concentration, g/L
t: Reaction time, t = 23 h

5.2.4 Nitrification inhibition

To assess the nitrogen inhibition of the process waters, tests were performed according to DIN EN ISO 9509 in 150 mL glass vessels (DIN EN ISO 9509, 2006). The inoculum was taken from the same WWTP and prepared the same way as described in section 5.2.2. Mixing, aeration and temperature were also similar. The DO was checked regularly and ensured to be above 3 mg/L, and the pH was checked at the beginning and the end of the tests. All tests ran for 3.5 h starting with the addition of inoculum. MLSS was adjusted to 2.3 - 3.3 g/L and the initial ammonium concentration was 50 mg/L to avoid ammonia inhibition. $(NH_4)_2SO_4$ was added to set the different shares of process water to 50 mg/L in each batch. However, the high NH_4-N concentrations in the process waters only allowed a process water share of 4%. Therefore, a second series was conducted with an initial NH_4-N concentration of 250 mg/L, allowing a share of up to 22%. In addition to Feed SBR190 and Feed SBR217, the treated effluents of the SBRs during phase 1 were tested on nitrification inhibition again. The tests needed to be performed with a defoaming agent as described in section 5.2.3. After each test, the samples were filtered (0.45 μm) and stored at 4 °C before being analyzed for oxidized nitrogen (nitrite and nitrate). The inhibition rates (I_N) in % and maximum nitrification rate R_N in mg N/(g MLSS·h) were calculated according to equations (7) and (8). The concentrations of NO_2-N and NO_3-N at the beginning of a test were subtracted from $c_{ON,c}$, $c_{ON,t}$ and $c_{ON,b}$.

$$I_N = \left(\frac{c_{ON,c} - c_{ON,t}}{c_{ON,c} - c_{ON,b}}\right) \cdot 100 \quad (7)$$

$c_{ON,c}$: Oxidized nitrogen in blank suspension without inhibitor at t = 3.5 h, mg/L
$c_{ON,t}$: Oxidized nitrogen in test suspension without inhibitor at t = 3.5 h, mg/L
$c_{ON,b}$: Oxidized nitrogen in reference suspension with inhibitor at t = 3.5 h, mg/L

$$R_N = \left(\frac{c_{ON,t} - c_{ON,b}}{c_{MLSS} \cdot t}\right) \cdot 100 \quad (8)$$

c_{MLSS}: Concentration of MLSS, g/L
t: Reaction time, t = 3.5 h

5.2.5 Chemical analysis

Solids were analyzed either in terms of total solids and volatile solids according to DIN EN 12880:2001 and DIN EN 15936:2012, or in terms of MLSS and MLVSS according to DIN 38409:1987 at 105 °C and 550 °C. The process water samples were filtered via 0.45 μm PES syringe filters before analysis. Dissolved organic carbon (DOC) was analyzed using a vario TOC cube (Elementar Analysensysteme GmbH, Germany). Nitrite (NO_2-N), nitrate (NO_3-N) were analyzed with a Compact IC Flex and a Metrosep A Supp 7 column (Metrohm AG, Suisse). For COD, total nitrogen (TN) and ammonium (NH_4-N) HACH tests LCK 514, LCK 338 and LCK 303 as well as a HACH Photometer DR 3900 were used (Hach Lange GmbH, Germany). UV_{254} and UV_{475} were determined with a HACH Photometer DR 5000 with a cell length of 10 mm (100-QS, Hellma GmbH, Germany). The ratio of UV_{254}/DOC (SUVA) was used to quantify the aromaticity. The brownish color of samples, which is mostly caused by melanoidins, was evaluated by measuring specific UV absorbance at 475 nm as proposed by Arimi et al. (2015).

5.2.6 Assessing the effect of HTC on the effluent of a WWTP

For this estimation, SBR treatment of the HTC process water was considered as a pretreatment step before discharge into an exemplary full-scale WWTP. From this WWTP we obtained the WAS for HTC experiments. The inflow (Q_{WWTP}) was 5,400 m^3/d and the WAS flow (Q_{WAS}) was 11.1 m^3/d with 9.2% total solids on average in 2020 and 2021. DOC and DON after SBR treatment were expected to be recalcitrant for biodegradation in the WWTP and therefore increase the effluent concentrations of the WWTP. Assuming constant mass during HTC and 65% total solids after dewatering the HTC coal slurry (Wang and Li 2015), the mass balance in equation (9) was used to determine the volume of the dewatered hydrochar. The effluent concentrations of recalcitrant compounds were calculated according to equation (10).

$$Q_{Hydrochar} = Q_{WAS} \cdot \frac{9.2\%}{65\%} \quad (9)$$

$$DOC = \left(\frac{(Q_{WAS} - Q_{Hydrochar}) \cdot rDOC}{Q_{WWTP}} \right) \quad (10)$$

DOC: DOC (or DON) in the WWTP effluent, mg/L
rDOC: Recalcitrant DOC (or DON) after SBR treatment, mg/L

5.3 Results and discussion

5.3.1 Total biodegradability

The evolution of DOC removal and SUVA for ZW218 and ZW218* (with pre-exposed inoculum) are depicted in Figure 16 a.

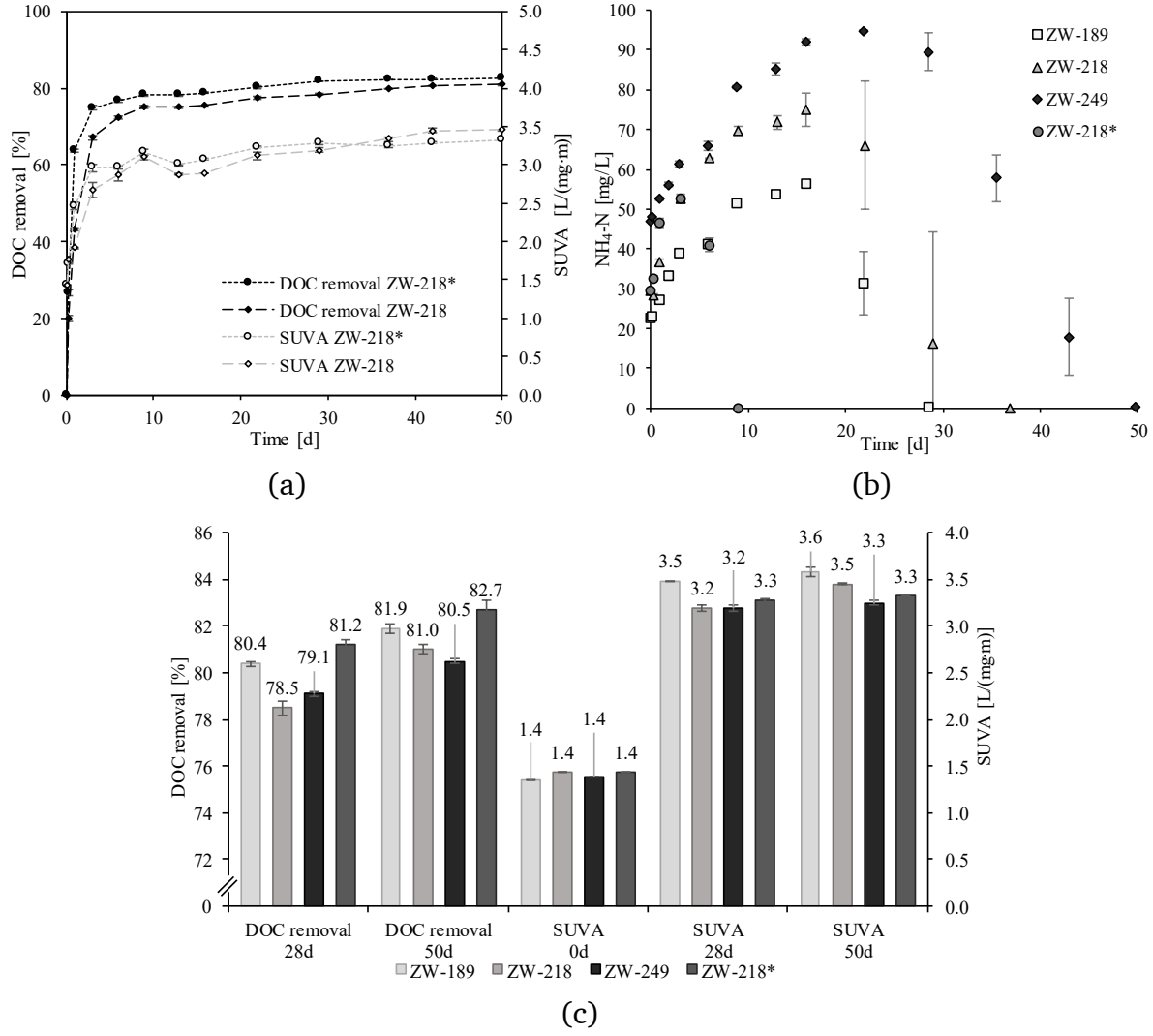

Figure 16: Evolution of a) DOC removal and SUVA during Zahn-Wellens tests for ZW218 and ZW218*, b) NH_4-N, and c) DOC removal and SUVA for the process waters after 28 d and 50 d incubation time

Both batches show that the HTC process waters contain a large fraction of readily biodegradable organics, which resulted in a DOC removal of 67.1 ± 1.5% and

74.9 ± 0.7% within 3 days of incubation. Between day 3 and 10 the DOC removal was lower, which indicates the presence of a slowly biodegradable fraction. From day 10 on, DOC was only marginally reduced, implying that biodegradable DOC had been almost completely removed. Pre-exposed inoculum in ZW218* showed a slightly faster and further reduction of DOC. This indicates that adaption of aerobic microorganisms enables a faster removal of readily biodegradable compounds and additional removal of some of the slowly biodegradable compounds. On day 28, the regular test duration to identify non-biodegradable compounds according to EN ISO 9888 (1999), DOC was removed by 78.5 ± 0.3% and 81.9 ± 0.2% for ZW218 and ZW218*, respectively. Extending the test period to 50 days had no significant effect on DOC removal.

The SUVA increased from 1.4 L/(mg·m) to 3.2 and 3.3 L/(mg·m) for ZW218 and ZW218* on day 28. It followed the overall trend of DOC removal by already reaching values above 3 L/(mg·m) after 8 days and by showing only a minor raise in the further course of tests. Increasing SUVAs indicate the removal of compounds that do not absorb UV light, and the enrichment of hydrophobic, humic-like compounds (Abbt-Braun and Frimmel 1999), which are not available for biological treatment. This could be caused by heterocyclic and aromatic structure of melanoidins, which show a high UV quenching and therefore a high SUVA (Dwyer et al. 2008). Accordingly, the SUVA curve shows that a majority of readily biodegradable substances were degraded in the first days. Gupta et al. (2015) obtained similar results by investigating the removal of organic matter from return liquors from dewatering thermal hydrolysis digestate. After 28 days of aerated incubation, they observed a humic substances (UV_{254}) removal of 15 - 20% and a DOC removal of 35 - 40%. With this, an increase in SUVA from 1.5 to 2.1 L/(mg·m) can be calculated.

All batches using non-pre-exposed biomass (ZW190, ZW218, ZW249) lead to very similar maximum DOC removal (Figure 16, c). So, the increasing HTC reaction temperatures had only little impact on aerobic biodegradation. This is quite surprising, as lower biodegradability with increasing HTC temperature was shown for anaerobic digestion of HTC process waters (Chen et al. 2021). Aerobic microorganisms degrade the compounds that can form at elevated HTC temperature to the same extent. For example, Yeom et al. (1997) and Pradeep et al. (2015) showed the adaption of biomass and biodegradation of phenols, which are present in HTC process water (Cao et al. 2021). Also PAHs were shown to be aerobically degraded (Ma et al. 2017).

The degradation of N-containing compounds was also shown in the evolution of ammonium (Figure 16 b), which was similar for all tests with non-pre-exposed biomass. The increase in ammonium concentration with increasing HTC temperature results from deamination, which is the breakdown of dissolved nitrogen into lower molecular products releasing NH_4-N (Yin et al. 2015). The evolution of NH_4-N resulted from two simultaneous processes which cannot clearly be distinguished from each other: the ammonification, which releases ammonium due to the degradation of nitrogenous compounds, and the nitrification, which consumes ammonium. The increase in NH_4-N in the beginning of the tests shows that the rate of ammonification was higher than the rate of nitrification. After 16 to 22 days, ammonification slowed down and nitrification led to the decrease of NH_4-N. Ammonia stripping could not be quantified in the tests, but the pH and temperature (see section 5.2.2) suggest that it is of minor importance. Comparing ZW190, ZW218 and ZW249, higher HTC temperatures seem to produce either nitrogenous compounds harder to degrade or more nitrification inhibition substances, or both. The evolution of NH_4-N in ZW218* shows the positive effect of biomass pre-exposition. NH_4-N in ZW218* increased until day 3 and was not detectable any longer after day 9. For ZW218 with non-pre-exposed biomass, the removal of NH_4-N lasted beyond day 30. Overall, the tests show that nitrification can be achieved once microorganisms are adapted to HTC process water.

5.3.2 Biodegradability in SBRs

Similar to the Zahn-Wellens test, the HTC temperature had only a small effect on the DOC removal and the SUVA in SBR190 and SBR217, but a slight dependence on the F/M_C ratio was observed (Figure 17). For F/M_C ratios from 31 to 76 mg C/(g MLSS·d), the DOC removal varied between 70 - 74% and the SUVA between 2.9 - 3.1 L/(mg·m). These F/M_C ratios were set during phases 2 and 3 with a 1:10 dilution of feed. For higher F/M_C ratios of 185 - 263 mg C/(g MLSS·d), which resulted from the undiluted process water in phase 1, DOC removal was 68 - 74%, and SUVA was 2.5 - 2.7 L/(mg·m). The lower SUVAs for higher F/M_C ratios imply that despite comparable DOC removal, fewer non-aromatic compounds were removed in phase 1 (Dwyer et al. 2008).

Since the COD/DOC ratio of the feed and the SBR effluent was 2.9 mg COD/mg C during each phase, the COD removal can also be calculated from the DOC. Fettig et al. (2017) reported a COD removal of about 80% at a sludge loading of 0.08 - 0.2 g COD/(g MLSS·d) during the aerobic treatment of HTC process water. At a similar sludge loading of 0.09 to 0.23 g COD/(g MLSS·d) in SBR190 and

SBR217, the DOC removal was roughly 72%. This lower DOC removal may be attributed to the use of different feedstock for HTC and consequently, differences in the process water composition. The average DOC removal of 72% equals rDOC of 28%.

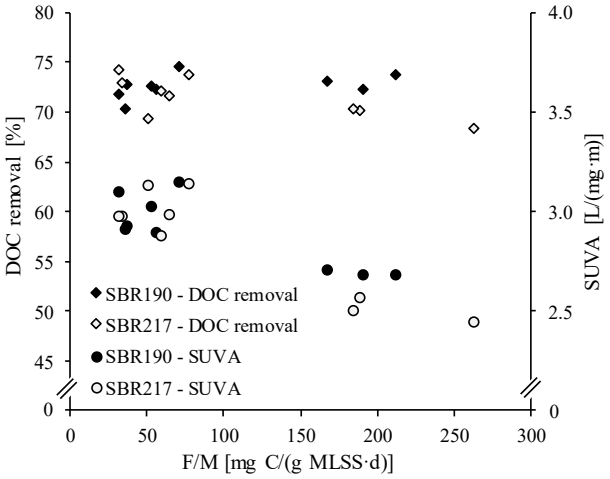

Figure 17: DOC removal and SUVA in SBRs

5.3.3 Nitrification performance and rDON in SBRs

The type and concentration of nitrogen species during the different phases are summarized in Figure 18 a and b. During phase 1 and for both SBRs, nitrogen was present as ammonium and DON. No nitrification was observed in phase 1, probably due to inhibiting compounds, but also due to NH_3 which inhibits Nitrosomonas in the range of 10 - 150 mg/L (Anthonisen et al. 1976). The DON concentration was 770 - 830 mg/L and 470 - 830 mg/L for SBR190 and SBR217. NH_4-N was higher than in Feed SBR190 and Feed SBR217 suggesting that ammonification took place, but was not complete. With 69 - 75% NH_4-N and 25 - 27% DON for SBR190 and 75 - 85% NH_4-N and 15 - 26% for SBR217, the degree of mineralization was almost similar. Similar mineralization rates have been observed in anaerobic batch tests (Ahmed et al. 2021). The observation of limited mineralization was also reported in literature, as some melanoidins like pyridines and pyrazines were shown to mineralize to ammonium (Bai et al. 2009; Padoley et al. 2006; Müller and Rappert 2010), whereas no complete biological removal of coloring melanoidins was reported (Chandra et al. 2008).

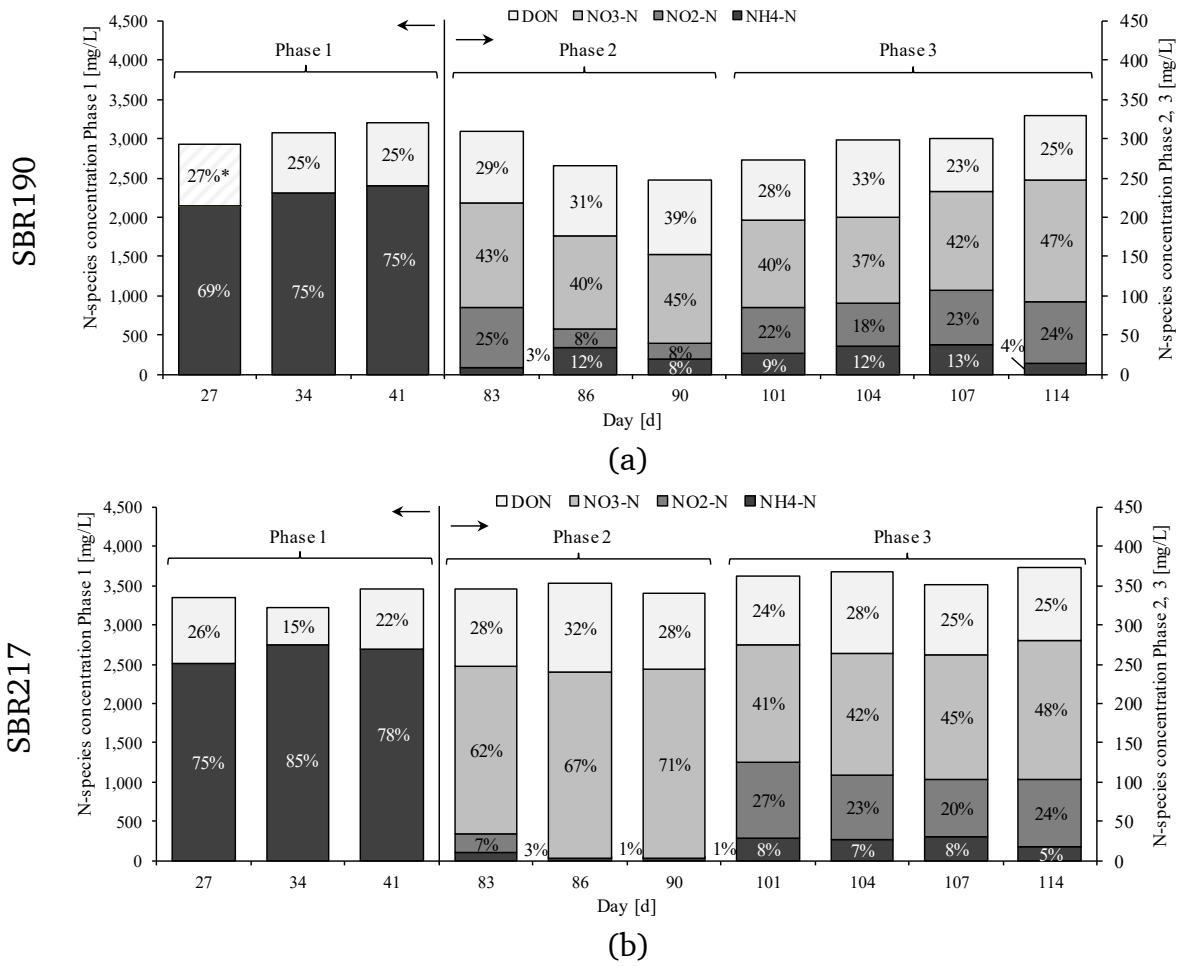

Figure 18: Different nitrogen species in phases 1-3 for a) SBR190 and b) SBR217. *TN was not measured on this day; therefore, DON was calculated by the average DON

The DON was removed to an almost similar extent, despite the proportion of NH_4-N in Feed SBR217 (35%) compared to Feed SBR190 (26%) (see Table 15) being higher. This differences are due to the increased decomposition of organic nitrogen compounds into ammonium at higher hydrothermal temperatures (Alimoradi et al. 2020). Still, DON in Feed SBR190 could be degraded to the same extent as Feed SBR217 at higher hydrothermal reaction temperatures. In addition, HTC temperature didn't affect the overall biodegradability of DON. However, higher reaction temperatures than in our study (270 °C to 345 °C) were reported to cause a lower biodegradability of DON and higher rDON (Alimoradi et al. 2020). Compared to the TN in Feed SBR190 (4,400 mg/L) and Feed SBR217 (4,800 mg/L), concentrations in both SBRs were noticeable lower (around 3,000 mg/L and 3,350 mg/L, respectively). This gap in TN of approx. 1,500 mg/L can partly be attributed to biomass growth: With the given feed COD and TN and at 20 °C, the estimated nitrogen for cell growth would be somewhere between 950 to 1.700 mg/L depending on the assumed biomass growth rates (Tchobanoglous et al. 2014). In addition, stripping of NH_3 could explain some of

the differences in TN. Although NH_4 dominates at a pH of 7.5 according to the ammonium-ammonia equilibrium, NH_3 was also present. For both SBRs, NH_3 was calculated to be 41 - 45 mg/L (Anthonisen et al. 1976). Ammonia stripping could not be quantified, but probably contributed to the nitrogen loss.

In the Zahn-Wellens tests it could not be clarified whether nitrification or ammonification is the limiting step. However, the comparison with the SBR test suggests that nitrification was the limiting step and not ammonification.

In phase 2 and 3, ratio DON/TN of SBR190 ranged between 23 - 39% (69 - 103 mg/L). For SBR217, DON was 24 - 32% (87 - 113 mg/L). As the DON was very similar for SBR190 and SBR217 at different operation settings, the remaining DON seems to be non-biodegradable. Coloring substances such as Maillard products were not or only slightly removed, as the UV_{475} (see Table 17) remained constant during biodegradation. A decolorization due to the biological removal of melanoidins as summarized by Chandra et al. (2008) could not be observed. On average, the recalcitrant DON/TN was 28% for SBR190 and 25% for SBR217.

Table 17: Mean R_{AOB}, R_N and UV_{475} ± standard deviation

Reactor	Parameter	Phase 1	Phase 2	Phase 3
SBR190	F/M_N [mg TN/(g MLSS·d)]	50.6±5.9	9.1±0.8	16.0±2.6
	R_{AOB} [mg N/(g MLSS·h)]	n.d.[a]	1.4±0.4	1.5±0.2
	R_N [mg N(g MLSS·h)]	n.d.	1.1±0.1	1.0±0.2
	UV_{475} [1/m]	895±52	87±10	84±5
SBR217	F/M_N [mg TN/(g MLSS·d)]	62.4±13.0	11.3±3.0	19.6±2.7
	R_{AOB} [mg N/(g MLSS·h)]	n.d.	2.0±0.0	2.1±0.1
	R_N [mg N/(g MLSS·h)]	n.d.	2.0±0.1	1.4±0.1
	UV_{475} [1/m]	683±21	72±12	71±8

[a]not determinable

The TN sludge loading significantly decreased due to the dilution of process water to 1:10 in phase 2, and nitrification set in. No notable concentrations of ammonium and nitrite were measured in SBR217, indicating a high level of nitrification. R_{AOB} and R_N were almost identical with 2.05 mg N/(g MLSS·h) and 1.98 mg N/(g MLSS·h), respectively. Although the TN loading rate was lower than in SBR217, a lower level of nitrification could be achieved in SBR190. Both ammonium and nitrite were not completely oxidized, and R_{AOB} and R_N were lower at 1.4 and 1.5 mg N/(g MLSS·h), respectively.

In phase 3, TN loading was increased to 16 - 19 mg TN/(g MLSS·d), which led to partial nitrification in both SBRs. Shares of nitrogen species were present on

a similar scale in SBR190 and SBR217 of 4 - 13%, 18 - 27%, and 37 - 48% for ammonium, nitrite and nitrate, respectively. R_{AOB} of both SBRs in phase 3 was only slightly higher than in phase 2. Consequently, nitrification was unlikely to be limited by ammonium shortage, but the maximum AOB activity seems to have been reached. Lower R_N in phase 3 suggest a greater inhibition of NOBs with increasing sludge loading.

Calculated according to Anthonisen et al. (1976) free ammonia (FA) and free nitrous acid (FNA) reached 0.15 mg/L and 0.18 mg/L during phase 2, as well as 0.02 mg/L and 0.05 mg/L during phase 3 (SBR190). For SBR217, FA reached 0.03 mg/L and 0.13 mg/L, and FNA 0.01 mg/L and 0.06 mg/L during phase 2 and 3, respectively. Accordingly, FA and FNA should have no significant effect on nitrification. Even though SBR217 showed a slightly better nitrification performance, the inhibition of nitrification could not be further differentiated in SBR tests. Therefore, subsequent inhibition tests were initiated to clarify whether lower nitrogen conversion in SBR190 was due to increased inhibition of nitrification.

5.3.4 Nitrification inhibition

The inhibition of nitrification by Feed SBR190 starts at low DON sludge loadings and rapidly increases with raising DON sludge loading (Figure 19 a). 50% inhibition (IC_{50}) was reached at around 28 mg DON/g MLSS. For Effluent SBR190, the IC_{50} dropped 10 mg DON/g MLSS. This is equivalent to volumetric shares of 2 - 3% for Feed SBR190 and about 5% for Effluent SBR190. For Feed SBR217 and Effluent SBR217 (Figure 19 b), inhibition followed a similar trend but was more pronounced. The IC_{50} was at 16 mg DON/g MLSS and at 7 mg DON/g MLSS, respectively. The volumetric shares were 1 - 2% for Feed SBR217 and 4% for Effluent SBR217, indicating that higher HTC temperatures seem to lead to the increased formation of nitrification inhibiting substances. Accordingly, low HTC temperatures are favorable for lower inhibition of nitrification. However, even at lower temperatures, the process water has a strong inhibitory effect. Looking at the volumetric shares, the inhibitory effect has been halved by the biological treatment, but was still strong. The specific inhibition in mg DON/g MLSS, on the other hand, shows a different result: The SBR effluents inhibited nitrification more than the HTC process waters themselves. This indicates that the inhibiting substances were still present after biodegradation and that these recalcitrant compounds were primarily responsible for nitrification inhibition.

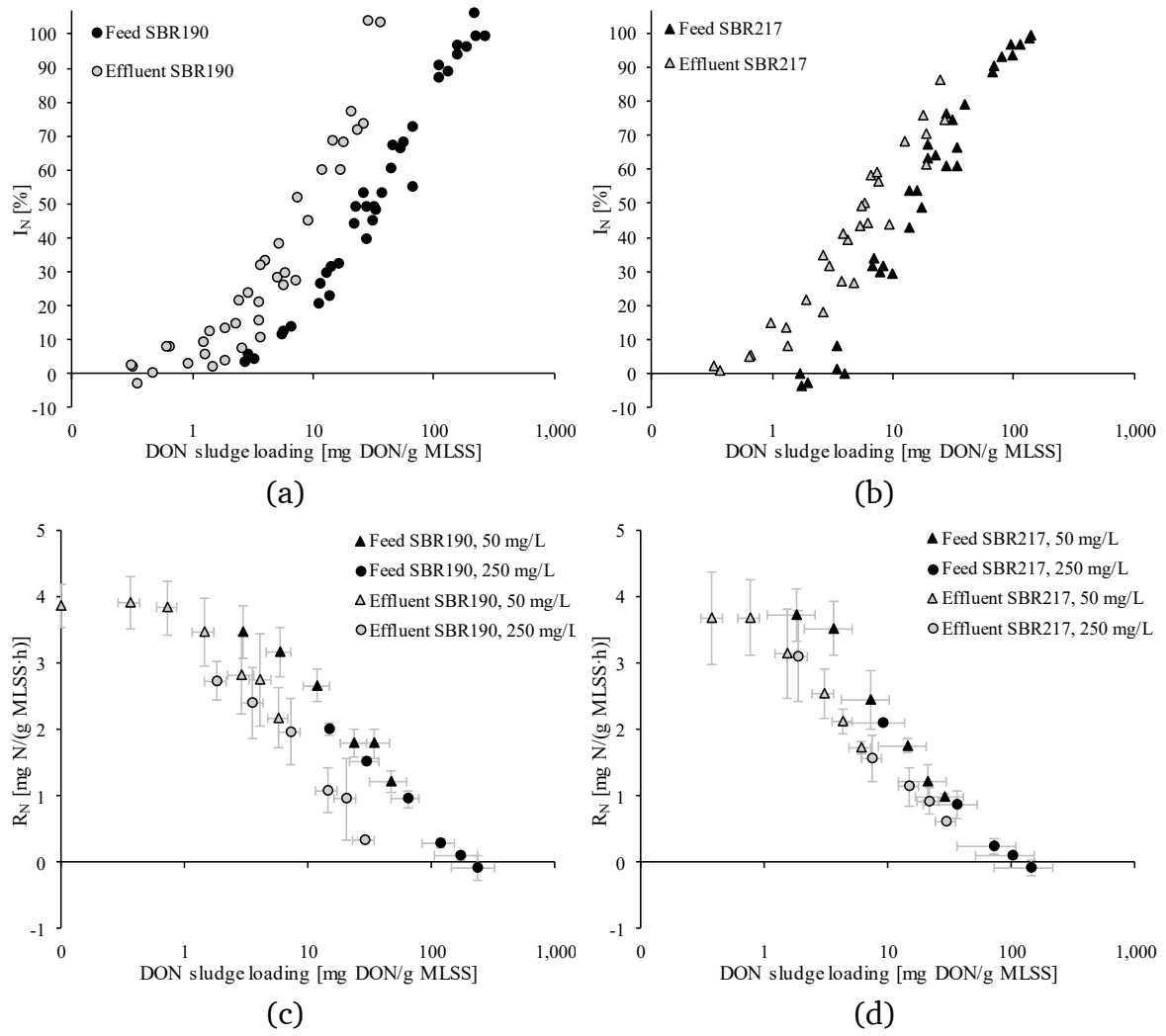

Figure 19: Nitrification inhibition of feed and phase 1 effluent process waters for a) SBR190 and b) SBR217 and corresponding average nitrification rates with STD at different NH_4-N concentrations for a) 50 mg/L and b) 250 mg/L

Pagga et al. (2006) reported similar findings, as nitrification inhibition caused by poorly degradable compounds was more severe compared to biodegradable ones. Nitrification inhibition of HTC process waters could also not be reduced by ultrafiltration pretreatment as shown by Kühni et al. (2015). In addition, the authors recommend a 100-fold dilution of process water before discharging into nitrifying wastewater treatment plans to avoid inhibition. In contrast to the aerobic pretreatment in this study, the anaerobic pretreatment of brewer's grain HTC process water could reduce the inhibition from 90 to 35% at a dilution of 1:50 (Fettig et al. 2017). Beyond that, no further studies dealing with nitrification inhibition of HTC process waters are available. The obtained results indicate that even biologically pre-treated process water is of major concern for WWTPs, as HTC process water not only contains recalcitrant DOC and DON but also disturbs nitrification.

As illustrated in Figure 19 c and d, R_N reached 3.8 mg N/(g MLSS·h) at low DON sludge loadings. With increasing DON sludge loadings, nitrification rates declined and dropped to zero at 240 mg DON/g MLSS (Feed SBR190) and 145 mg DON/g MLSS (Feed SBR217). Standard deviations were quite high for the tests, which is due to the use of new inoculum with different nitrification rates for each series of tests. However, each inoculum was within the required range between 2 and 6.5 mg N/(g MLSS·h).

Batch inhibition tests do not directly relate to continuous tests, since no long-term effects can be deducted. Still, they give an idea of the extent of inhibition. Even though Feed SBR190 was less inhibiting than Feed SBR217, the nitrification rate in SBR190 was lower than in SBR217 (Table 17). A possible explanation for those differences may be amount of nitrifying biomass present in the tests or the degree of adaption.

5.3.5 Effect of HTC on WWTP effluent

rDOC and rDON were used to calculate the effect of HTC on the effluent of a full-scale WWTP. Since there were no major differences, the refractory concentrations across all phases 1 - 3 were used. Concentrations were lower in phase 2 and 3 due to the dilution. The results of these calculations indicate that the effluent concentrations of the WWTP could be increased to a considerable extent, especially for phase 1 effluent (Table 18).

Table 18: Predicted effluent concentrations for DOC, COD and DON after SBR treatment

Parameter	SBR190	SBR217
rDOC[1] [mg/L]	4,727	4,611
rCOD[2] [mg/L]	13,766	13,596
rDON[3] [mg/L]	1,255	1,211
Increase in effluent DOC [mg/L]	8.3	8.1
Increase in effluent COD[a] [mg/L]	24.1	23.5
Increase in effluent DON [mg/L]	2.2	2.1

[1]28% of DOC was recalcitrant in SBR190 and SBR217

[2]average COD/DOC was 2.9 mg COD/mg C during the tests

[3]28% and 25% DON was recalcitrant in SBR190 and SBR217

In particular, the increase in effluent DOC by up to 8.3 mg/L and effluent COD by up to 24.1 mg/L may cause serious problems with regard to legal discharge limits. For example, the discharge limit of the model wastewater treatment plant is 40 mg/L, which would be difficult to meet if the HTC process water was recirculated. Higher effluent DON is of minor importance as the concentrations

were lower and dilution would be high enough to avoid inhibition of nitrification. In general, this approximation is not transferable to other WWTPs, as boundary conditions such as inflow conditions, treatment steps or effluent regulations vary. Yet, the results suggest that an aerobic biological treatment step alone is not sufficient for the treatment of HTC process water. Additional treatment steps such as advanced oxidation processes are necessary.

Similar results were found by Toutian et al. (2020), who calculated an increase in effluent COD for thermal hydrolysis and anaerobic digestion. Reactions resemble those of HTC, but the lower temperatures lead to less recalcitrant compounds. They found a sharp increase in effluent COD at 170 °C of 12 - 21 mg/L compared to lower temperatures, which is within the range of our predicted increase in effluent COD. Elevating the temperature from 170 °C to 190 °C does not seem to increase recalcitrant compounds significantly.

5.4 Conclusions

To make HTC a proper alternative for the treatment of sewage sludge, solutions to deal with the produced HTC process water must be developed. In summary, this study showed that aerobic treatment cannot achieve satisfactory purification of the process water and further post-treatment steps are required. The following findings were obtained:

- Increasing HTC temperature had basically no effect on the DOC removal, but increased the potential inhibition of nitrification.
- DOC removal in continuously operated SBRs was around 72%, resulting in an effluent rDOC of 28%.
- The effluent rDON/TN ratio was 25 - 28%.
- Nitrification was inhibited to a large extent by substances that could not be effectively biodegraded.
- Higher hydrothermal reaction temperatures increased the inhibitory potential for nitrification.
- Discharging the undiluted, pretreated HTC process water in a WWTP plant could increase the effluent DOC by 8.3 mg/L, and the effluent COD by 24.1 mg/L.

Funding

This research was funded by the German Federal Ministry of Education and Research (BMBF) within the project “IntenKS”, grant number 02WCL1470A.

Acknowledgment

The authors gratefully thank L. Hennemann and J. Huang.

Author contributions

Conceptualization: TB; Data curation: TB, PL; Formal analysis: TB; Investigations: TB, PL; Methodology: TB, Writing - original draft preparation: TB; Writing - review and editing: PL, ME; Visualization: TB; Funding acquisition: ME; Project administration TB; Supervision: ME

5.5 References

Abbt-Braun, G.; Frimmel, F. H. (1999): Basic Characterization of Norwegian NOM Samples - Similarities and Differences. In: Environment International 25 (2/3), S. 161–180. DOI: 10.1016/S0160-4120(98)00118-4.

Ahmed, M.; Andreottola, G.; Elagroudy, S.; Negm, M. S.; Fiori, L. (2021): Coupling hydrothermal carbonization and anaerobic digestion for sewage digestate management: Influence of hydrothermal treatment time on dewaterability and bio-methane production. In: Journal of Environmental Management 281, S. 111910. DOI: 10.1016/j.jemman.2020.111910.

Alimoradi, S.; Stohr, H.; Stagg-Williams, S.; Sturm, B. (2020): Effect of temperature on toxicity and biodegradability of dissolved organic nitrogen formed during hydrothermal liquefaction of biomass. In: Chemosphere 238, S. 124573. DOI: 10.1016/j.chemosphere.2019.124573.

Anthonisen, A. C.; Loehr, R. C.; Prakasam, T. B. S.; Srinath, E. G. (1976): Inhibition of Nitrification by Ammonia and Nitrous Acid. In: Journal (Water Pollution Control Federation) 48 (5), S. 835–852.

Aragón-Briceño, C. I.; Grasham, O.; Ross, A. B.; Dupont, V.; Camargo-Valero, M. A. (2020): Hydrothermal carbonization of sewage digestate at wastewater treatment works: Influence of solid loading on characteristics of hydrochar, process water and plant energetics. In: Renewable Energy 157, S. 959–973. DOI: 10.1016/j.renene.2020.05.021.

Arimi, M. M.; Zhang, Y.; Götz, G.; Geißen, S.-U. (2015): Treatment of melanoidin wastewater by anaerobic digestion and coagulation. In: Environmental Technology 36 (19), S. 2410–2418. DOI: 10.1080/09593330.2015.1032366.

Ariunbaatar, J.; Panico, A.; Yeh, D. H.; Pirozzi, F.; Lens, P. N. L.; Esposito, G. (2015): Enhanced mesophilic anaerobic digestion of food waste by thermal pretreatment: Substrate versus digestate heating. In: Waste Management (46), S. 176–181. DOI: 10.1016/j.wasman.2015.07.045.

Atallah, E.; Kwapinski, W.; Ahmad, M. N.; Leahy, J. J.; Al-Muhtaseb, A. H.; zeaiter, J. (2019): Hydrothermal carbonization of olive mill wastewater: Liquid phase product analysis. In: Journal of Environmental Chemical Engineering 7.

Bai, Yaohui; Sun, Qinghua; Zhao, Cui; Wen, Donghui; Tang, Xiaoyan (2009): Aerobic degradation of pyridine by a new bacterial strain, Shinella zoogloeoides BC026. In: Journal of Industrial Microbiology & Biotechnology 36 (11), S. 1391–1400. DOI: 10.1007/s10295-009-0625-9.

Blach, T.; Engelhart, M. (2021): Optimizing the Hydrothermal Carbonization of Sewage Sludge - Response Surface Methodology and the Effect of Volatile Solids. In: Water 13 (9), S. 1225. DOI: 10.3390/w13091225.

Cao, Z.; Hülsemann, B.; Wüst, D.; Oechsner, H.; Lautenbach, A.; Kruse, A. (2021): Effect of residence time during hydrothermal carbonization of biogas digestate on the combustion characteristics of hydrochar and the biogas production of process water. In: Bioresource Technology 333, S. 125110.

Chandra, R.; Bharagava, R. N.; Rai, V. (2008): Melanoidins as major colourant in sugarcane molasses based distillery effluent and its degradation. In: Bioresource Technology 99 (11), S. 4648–4660. DOI: 10.1016/j.biortech.2007.09.057.

Chen, H.; Rao, Y.; Cao, L.; Shi, Y.; Hao, S.; Luo, G.; Zhang, S. (2019): Hydrothermal conversion of sewage sludge: Focusing on the characterization of liquid products and their methane yields. In: Chemical Engineering Journal 357, S. 367–375.

Chen, Z.; Rao, Y.; Usman, M.; Chen, H.; Bialowiec, A.; Zhang, S.; Luo, G. (2021): Anaerobic fermentation of hydrothermal liquefaction wastewater of dewatered sewage sludge for volatile fatty acids production with focuses on the degradation of organic components and microbial community compositions. In: Science of the Total Environment 777 (146077).

DIN EN ISO 9509 (2006): Water quality - Toxicity test for assessing the inhibition of nitrification of activated sludge microorganisms, 2006.

DIN EN ISO 9888 (1999): Evaluation of ultimate aerobic biodegradability of organic compounds in aqueous medium - Static test (Zahn-Wellens method), 1999.

Dwyer, J.; Starrenburg, D.; Tait, S.; Barr, K.; Batstone, D. J.; Lant, P. (2008): Decreasing activated sludge thermal hydrolysis temperature reduces product colour, without decreasing degradability. In: Water Research 42, S. 4699–4709.

Eibisch, N.; Helfrich, M.; Don, A.; Mikutta, R.; Kruse, A.; Ellerbrock, R.; Flessa, H. (2013): Properties and Degradability of Hydrothermal Carbonization Products. In: Journal of Environmental Quality 42 (5), S. 1565–1573. DOI: 10.2134/jeq2013.02.0045.

Ferrentino, R.; Merzari, F.; Grigolini, E.; Fiori, L.; Andreottola, G. (2021): Hydrothermal carbonization liquor as external carbon supplement to improve biological denitrification in wastewater treatment. In: Journal of Water Process Engineering (44), S. 102360. DOI: 10.1016/j.jwpe.2021.10236O.

Fettig, J.; Liebe, H.; Busch, A.; Austermann-Haun, U.; Meier, J. F. (2017): Entwicklung eines technischen Verwertungs- und Entsorgungskonzeptes für HTC-Prozesswasser. Abschlussbericht. Höxter/Detmold.

Funke, A.; Ziegler, F. (2010): Hydrothermal carbonization of biomass: A summary and discussion of chemical mechanisms for process engineering. In: Biofuels, Bioproducts and Biorefining 4, S. 160–177.

Gupta, A.; Novak, J. T.; Thao, R. (2015): Characterization of organic matter in the thermal hydrolysis pretreated anaerobic digestion return liquor. In: Journal of Environmental Chemical Engineering (3), S. 2631–2636.

Hämäläinen, A.; Kokko, M.; Kinnunen, V.; Hilli, T.; Rintala, J. (2021): Hydrothermal carbonisation of mechanically dewatered digested sewage sludge-Energy and nutrient recovery in centralised biogas plant. In: Water Research 201, S. 117284. DOI: 10.1016/j.watres.2021.117284.

Haritash, A. K.; Kaushik, C. P. (2009): Biodegradation aspects of polycyclic aromatic hydrocarbons (PAHs): a review. In: Journal of Hazardous Materials 169 (1-3), S. 1–15. DOI: 10.1016/j.jhazmat.2009.03.137.

Helou, C.; Marier, D.; Jacolot, P.; Abdennebi-Najar, L.; Niquet-Léridon, C.; Tessier, F. J.; Gadonna-Widehem, P. (2014): Microorganisms and Maillard

reaction products: a review of the literature and recent findings. In: Amino Acids 46 (2), S. 267–277. DOI: 10.1007/s00726-013-1496-y.

Kühni, M.; Wanner, R.; Baier, U.; Krebs, R. (2015): Behandlung des Prozesswassers aus hydrothermal karbonisiertem Klärschlamm vor der Einleitung in eine Abwasserreinigungsanlage. In: gwf - Wasser/Abwasser 156 (10), S. 1004–1011.

Langone, A.; Sabia, G.; Petta, L.; Zanetti, L.; Leoni, L.; Basso, D. et al. (2021): Evaluation of the aerobic biodegradability of process water produced by hydrothermal carbonization and inhibition effects on the heterotrophic biomass of an activated sludge system. In: Journal of Environmental Management 299 (299), S. 113561. DOI: 10.1016/j.jenvman.2021.113561.

Ma, Weiwei; Han, Y.; Ma, W.; Han, H.; Zhou, H.; Xu, C. et al. (2017): Enhanced nitrogen removal from coal gasification wastewater by simultaneous nitrification and denitrification (SND) in an oxygen-limited aeration sequencing batch biofilm reactor. In: Bioresource Technology 244 (84-91).

Meier, J. F.; Austermann-Haun, U.; Fettig, J.; Liebe, H.; Wichern, M. (2017): Operation of an anaerobic filter compared with an anaerobic moving bed bioreactor for the treatment of waste water from hydrothermal carbonisation of fine mulch. In: Water Science & Technology 76 (7-8), S. 2065–2074. DOI: 10.2166/wst.2017.379.

Müller, R.; Rappert, S. (2010): Pyrazines: occurrence, formation and biodegradation. In: Applied Microbiology and Biotechnology 85 (5), S. 1315–1320. DOI: 10.1007/s00253-009-2362-4.

Padoley, K. V.; Mudliar, S. N.; Banerjee, S. K.; Deshmukh, S. C.; Pandey, R. A. (2011): Fenton oxidation: A pretreatment option for improved biological treatment of pyridine and 3-cyanopyridine plant wastewater. In: Chemical Engineering Journal 166 (1), S. 1–9. DOI: 10.1016/j.cej.2010.06.041.

Padoley, K. V.; Rajvaidya, A. S.; Subbarao, T. V.; Pandey, R. A. (2006): Biodegradation of pyridine in a completely mixed activated sludge process. In: Bioresource Technology 97 (10), S. 1225–1236. DOI: 10.1016/j.biortech.2005.05.020.

Pagga, U.; Bachner, J.; Strotmann, U. (2006): Inhibition of nitrification in laboratory tests and model wastewater treatment plants. In: Chemosphere 65, S. 1–8.

Paneque, M.; La Rosa, J. M. de; Kern, J.; Reza, M. T.; Knicker, H. (2017): Hydrothermal carbonization and pyrolysis of sewage sludges: What happen to carbon and nitrogen? In: Journal of Analytical and Applied Pyrolysis 128, S. 314–323. DOI: 10.1016/j.jaap.2017.09.019.

Posmanik, R.; Labatut, R. A.; Kim, A. H.; Usack, J. G.; Tester, J. W.; Angenent, L. T. (2017): Coupling hydrothermal liquefaction and anaerobic digestion for energy valorization from model biomass feedstocks. In: Bioresource Technology 233, S. 134–143. DOI: 10.1016/j.biortech.2017.02.095.

Pradeep, N. V.; Anupama, S.; Navya, K.; Shalini, H. N.; Idris, M.; Hampannavar, U. S. (2015): Biological removal of phenol from wastewaters: a mini review. In: Appl Water Sci 5 (2), S. 105–112. DOI: 10.1007/s13201-014-0176-8.

Seyedi, S.; Venkiteshwaran, K.; Zitomer, D. (2021): Current status of biomethane production using aqueous liquid from pyrolysis and hydrothermal liquefaction of sewage sludge and similar biomass. In: Reviews in Environmental Science and Bio/Technology 20 (1), S. 237–255. DOI: 10.1007/s11157-020-09560-y.

Si, B.; Li, J.; Zhu, Z.; Shen, M.; Lu, J.; Duan, N. et al. (2018): Inhibitors degradation and microbial response during continuous anaerobic conversion of hydrothermal liquefaction wastewater. In: The Science of the total environment 630, S. 1124–1132. DOI: 10.1016/j.scitotenv.2018.02.310.

Si, B.; Yang, L.; Zhou; Watson, J.; Tommaso, G.; Chen, W.-T. et al. (2019): Anaerobic conversion of the hydrothermal liquefaction aqueous phase: fate of organics and intensification with granule activated carbon/ozone pretreatment. In: Green Chemistry 21 (6), S. 1305–1318. DOI: 10.1039/C8GC02907E.

Tchobanoglous, G.; Stensel, H. D.; Tsuchihashi, R.; Burton, F. (2014): Wastewater Engineering. Treatment and Resource Recovery. Fifth Edition. New York: McGraw-Hill Education.

Toor, S. S.; Rosendahl, L.; Rudolf, A. (2011): Hydrothermal liquefaction of biomass. A review of sub-critical water technologies. In: Energy 36, S. 2328–2342.

Toutian, V.; Barjenbruch, M.; Unger, T.; Loderer, C.; Remy, C. (2020): Effect of temperature on biogas yield increase and formation of refractory COD during thermal hydrolysis of waste activated sludge. In: Water Research 171, S. 115383. DOI: 10.1016/j.watres.2019.115383.

Wang, L.; Li, A. (2015): Hydrothermal treatment coupled with mechanical expression at increased temperature for excess sludge dewatering: the dewatering performance and the characteristics of products. In: Water Research 68, S. 291–303. DOI: 10.1016/j.watres.2014.10.016.

Weide, T.; Brügging, E.; Wetter, C. (2019): Anaerobic and aerobic degradation of wastewater from hydrothermal carbonization (HTC) in a continuous, three-stage and semi-industrial system. In: Journal of Environmental Chemical Engineering 7.

Yeom, S. H.; Kim, S. H.; Yoo, J. Y.; Yoo, I. S. (1997): Microbial adaptation in the degradation of phenol by Alcaligenes xylosoxidans Y234. In: Korean Journal of Chemical Engineering 14 (1), S. 37–40.

Yin, F.; Chen, H.; Xu, G.; Wang, G.; Xu, Y. (2015): A detailed kinetic model for the hydrothermal decomposition process of sewage sludge. In: Bioresource Technology 198, S. 351–357.

Zhang, D.; Feng, Y.; Huang, H.; Khunjar, W.; Wang, Z.-W. (2020): Recalcitrant dissolved organic nitrogen formation in thermal hydrolysis pretreatment of municipal sludge. In: Environment International 138, S. 105629. DOI: 10.1016/j.envint.2020.105629.

6 Limitations of treating hydrothermal carbonization process water in a membrane bioreactor and a sequencing batch reactor on pilot scale

Authors: Blach, T.; Engelhart, M.

Keywords: Biodegradability; hydrothermal carbonization; HTC; membrane bioreactor; nitrification inhibition; process water; sequencing batch reactor

Published in: Journal of Environmental Chemical Engineering 13 (2025) 115304
https://doi.org/10.1016/j.jece.2024.115304

Received: 1 April 2024

Accepted: 31 December 2024

Published: 31 December 2024

Abstract:

Hydrothermal carbonization (HTC) is a promising technology for treating waste materials like sewage sludge. However, HTC generates highly contaminated process water that contains many poorly biodegradable, inhibitory, or toxic substances. So far, there are no studies on the aerobic biodegradation and nitrification/denitrification for treatment in pilot scale. Therefore, we investigated the treatment of process water from HTC of sewage sludge on a pilot scale using a membrane bioreactor (MBR) and a sequencing batch reactor (SBR). The MBR achieved a slightly higher removal of chemical oxygen demand (COD) (74.8 ± 1.9%) than the SBR (71.4 ± 2.6%) due to the filtration of the effluent until a COD sludge loading of 270 mg COD/(g MLSS·d). Stable nitrification could be established up to a total nitrogen (TN) sludge loading (F/MN) of 20 mg TN/(g MLSS·d) in both reactors. To ensure this F/MN, however, the high load of the process water required a minimum dilution of 1:5 and/or very long hydraulic retention times of >4 d. Nitrification inhibition tests showed that nitrifiers in non-adapted activated sludge was inhibited by 50 % (IC50) at already 0.4% volumetric process water share. Biomass taken from the SBR adapted to the inhibitors, resulting in an increase in IC50 of 4% v/v process water share. Additionally, some inhibitors could be degraded biologically, allowing a significantly higher process water share. Our study demonstrates the feasibility of nitrification and denitrification, but follow-up treatment is necessary to avoid

negative environmental impacts due to the high concentrations of recalcitrant COD and organic nitrogen.

6.1 Introduction

The sustainable management of sewage sludge from wastewater treatment plants (WWTPs) is a topical issue that is receiving more and more attention. Safe treatment and disposal are the top priorities due to heavy metals, pathogens and organic contaminants present in sewage sludge. However, sewage sludge contains nutrients and energy, which are valuable resources and make recycling of the sewage sludge necessary in the sense of a circular economy approach (DWA 2020; European Comission 2020).

One solution to these challenges could be the hydrothermal carbonization (HTC) process. During HTC, wet sewage sludge is treated at 180 °C to 250 °C for a few minutes up to several hours in a pressurized reactor (Blach and Engelhart 2021). The resulting hydrochar usually features higher calorific value and easier mechanical dewaterability than raw sewage sludge (Saha 2021; Namoika et al. 2009). This could lead to significant energy savings compared to thermal drying (Zhao et al. 2014; Knötig et al. 2021). As a result of HTC, some of the particulate organic matter breaks down into soluble organic components and nutrients, which are released to the aqueous phase. These components include a variety of readily biodegradable substances such as organic acids (Wang and Li 2015; Julien et al. 1993; Ender et al. 2024). However, poorly biodegradable and inhibiting substances such as phenols and various polycyclic aromatic hydrocarbons are also among the dissolved reaction by-products (Li et al. 2017).

Nitrogeneous compounds such as proteins are broken down and converted during HTC and have a special significance. The chemical reaction of reduced sugars and amines, the Maillard reaction, is a key reaction, as refractory organic compounds and humic-like products such as pyrrole derivates and pyrazines are formed (Chen et al. 2019; Xu et al. 2022c). These can disorder the metabolic pathways, destruct cell walls and membranes and change the physiochemical properties of cell walls thereby inducing antibacterial effects (Xu et al. 2022b).

Currently, there is growing interest in recovering nutrients or valuable materials from the HTC aqueous phase, such as struvite or 5-hydroxymethylfurfural (Malhotra and Garg 2020; Jamal-Uddin et al. 2023), or H_2 by aqueous phase reforming (Oliveira et al. 2022; Cortright et al. 2002). Anaerobic digestion also enables energy recovery and is intensively studied at present (Park et al. 2021).

Nevertheless, anaerobic digestion lacks conclusive studies for full-scale implementations (Ipiales et al. 2021).

Aerobic biodegradation has received little attention in the scientific literature. Organic substances could be removed, even though the removal of the chemical oxygen demand (COD) was limited (Ferrentino et al. 2021; Mantovani et al. 2022). Furthermore, nitrogen-containing heterocyclic compounds could be degraded into ammonium and aromatic compounds could be reduced (Hu et al. 2022). Nonetheless, a high dilution for treating process water in the co-treatment in a municipal WWTP was necessary to avoid a short-term toxicity towards heterotrophic microorganisms (Langone et al. 2021).

To date, there have been no systematic pilot-scale studies on the treatment of HTC process water using activated sludge processes focusing on refractory organic matter and nitrification inhibition. If these cannot be removed in a treatment stage, a negative impact on the aquatic environment can be expected. To close this gap, we have investigated the limits of biodegradation and the performance of nitrification during a one-year-operation of a membrane bioreactor (MBR) and a sequencing batch reactor (SBR). Both technologies are highly suitable for treating high loaded and inhibiting wastewaters (Dvorak et al. 2013). The high biomass concentration in a MBR allows high organic loading rates and the membrane provides a high quality effluent. In a SBR, the duration of the cycles is highly flexible and the substrate gradient after feeding favors floc-forming biomass. Since we expected a strong inhibition of nitrification, we gradually reduced the dilution from 1:20 to 1:1 (undiluted) to increase the load of nitrogen and inhibitors. In addition, we quantified the inhibition of nitrification by determining the EC_{50} values. This explored the adaptation of activated sludge biomass to process water constituents and the biodegradability of inhibitory compounds.

6.2 Materials and methods

6.2.1 Characteristics of HTC process water

The HTC process water was obtained from a large-scale, steam-driven HTC plant in batch mode. Sewage sludge after anaerobic digestion from a WWTP was dewatered to 19.8% TS and subsequently carbonized for 1 h at 197 °C. After HTC, a chamber filter press dewatered the hydrochar slurry to 39.6% TS and separated the HTC process water. The characteristics of the anaerobically digested sewage sludge and the hydrochars can be found in the supplementary

material (Table 22). The MBR and the SBR treated the process water at different dilutions, resulting in varying concentrations (Table 19). During operation, dilution of the process water was reduced stepwise. The feed concentration at 1:1 reflects the raw and undiluted process water and was tested in the MBR only. The dilution 1:5* was the result of a previous breakdown of nitrification in the SBR aiming to investigate the regrowth of ammonium oxidizing bacteria (AOB).

Table 19: Feed characteristics in dilution 1:20 to 1:1 (Mean values ± STD[a])

Parameter	Dilution 1:20	Dilution 1:10	Dilution 1:5	Dilution 1:1	Dilution 1:5*
COD [mg O_2/L]	1,158	2,680	5,264	30,381	5,040
	±49	±134	±680	±1.119	±680
TOC [mg C/L]	396	882	1,692	9,950	1,600
	±57	±105	±187	±950	±209
UV_{254} [1/m]	574	1,140	2,285	12,365	2,084
	±25	±81	±174	±377	±139
SUVA [L/(mg C·m)]	1.5±0,2	1.5±0,1	1.5±0,2	1.2±0,1	1.3±0,2
TN [mg N/L]	148	293	555	3,148	537
	±8	±19	±44	±126	±44
NH_4-N [mg N/L]	91±5	179±21	370±28	1,819±99	349±18
NO_2-N [mg N/L]	<0.5	<0.5	<1.5	-	<1.5
NO_3-N [mg N/L]	<0.02	<0.2	<0.2	0,7	<0.2
DON [mg N/L]	58	106	182	1,329	189
	±11	±26	±30	±150	±37
PO_4-P [mg P/L]	3±4	5±1	7±2	61±5	8±2

[a]Standard deviation

We diluted the HTC process water with tap water due to the better handling. Another option was using the treated wastewater from the MBR or the SBR. However, preliminary tests have shown that the effluent contains non-biodegradable inhibitors. These could affect nitrification in addition to the inhibitors in the untreated process water. The second option was using the effluent from a municipal WWTP, which is usually low polluted (COD< 50 mg/L) compared to HTC process water. Accordingly, the HTC process water mainly determines the composition of the mixture.

6.2.2 SBR setup

The SBR had a volume of V = 300 L and was fully automated (Figure 20). Feed, effluent and waste activated sludge (WAS) were pumped using progressive cavity pumps (MD Series, Seepex GmbH, Germany). The effluent tank stored the treated process water for sampling, after which it was emptied (3 to 4 times a

week). The WAS discharge ensured a constant biomass concentration in the reactor and was recorded gravimetrically. Temperature (T), pH value, oxidation reduction potential (ORP), dissolved oxygen (DO), mixed liquor suspended solids (MLSS), electrical conductivity (ECO), Ammonium and Nitrate (Endress+Hauser Conducta GmbH & Co. KG, Germany) were continously measured in the reactor. The DO was set to 4 to 5 mg O_2/L to guarantee unlimited oxygen supply during nitrification and was controlled by the run time of the blower. A stirrer ensured sufficient mixing as soon as the blower switched off, which was either when the set oxygen concentration was reached or during denitrification. The pH ranged between 6.9 and 7.6 and was adjusted, if necessary, using H_2SO_4 (2 mol/L) and NaOH (2 mol/L). 20% Acetic acid (VWR International GmbH, Germany) was added during denitrification without focusing on the minimal addition of external carbon source. Each day, the SBR completed one cycle consisting of (i) feeding, (ii) 140 minutes of nitrification and 55 minutes of denitrification, alternating several times, (iii) 30 minutes of sedimentation and (iv) about 20 - 40 minutes of WAS removal, depending on the demand. In the beginning, the SBR was inoculated with activated sludge from a nitrifying and denitrifying municipal wastewater treatment plant (MLSS 3 g/L, sludge retention time (SRT) >15 d).

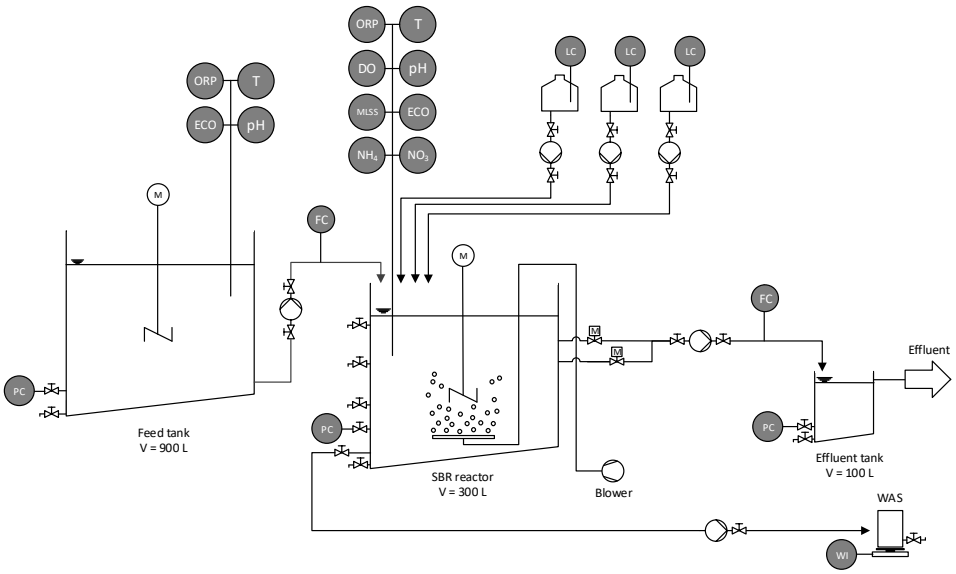

Figure 20: Flow scheme of the SBR

6.2.3 MBR setup

The MBR had a volume of V = 170 L, was also fully automated and had the same pumps, instrumentation, aeration and stirring control as well as the same acid and caustic dosing as the SBR (Figure 21). WAS was discharged whenever the set MLSS concentration of 9.5 g/L was reached. The intermittent operation

consisted of alternating phases of nitrification (140 min) and denitrification (55 min). The MBR was fed quasi-continuously whenever the water level fell below a certain threshold (volume filled with every feed: 3% of the MBR volume) and independently of nitrification or denitrification. The membrane unit used was an externally mounted rotating disk filter (CRD02) operated in bypass mode with a maximum of 6 ceramic filtration disks made of α-Al_2O_3 (novoflow GmbH, Rain, Germany). Each filter disc had an area of about 0.04 m^2 and a pore size of 0.2 μm. Rotation of the filter discs at 140 rpm produced the crossflow of the membrane, resulting in a crossflow velocity of 0.2 - 1.1 m/s over the radius of the discs. The recycle flow to the membrane circulated the MBR volume every 5 hours and was approx. 20 times the permeate flow. Rotating filter discs did not rely on crossflow aeration like submerged membranes, therefore minimizing the negative effects on denitrification. The filter discs were mounted on a hollow shaft through which the permeate was withdrawn by suction using a displacement pump. Permeate was removed independently of nitrification or denitrification and quantified using a flow control. Backwashing of the membrane with permeate was performed periodically every 10 min for 30 sec. The membrane was operated below the critical flux all the time and chemical cleaning of the membrane was not necessary. The inoculum of the MBR was the same as for the SBR.

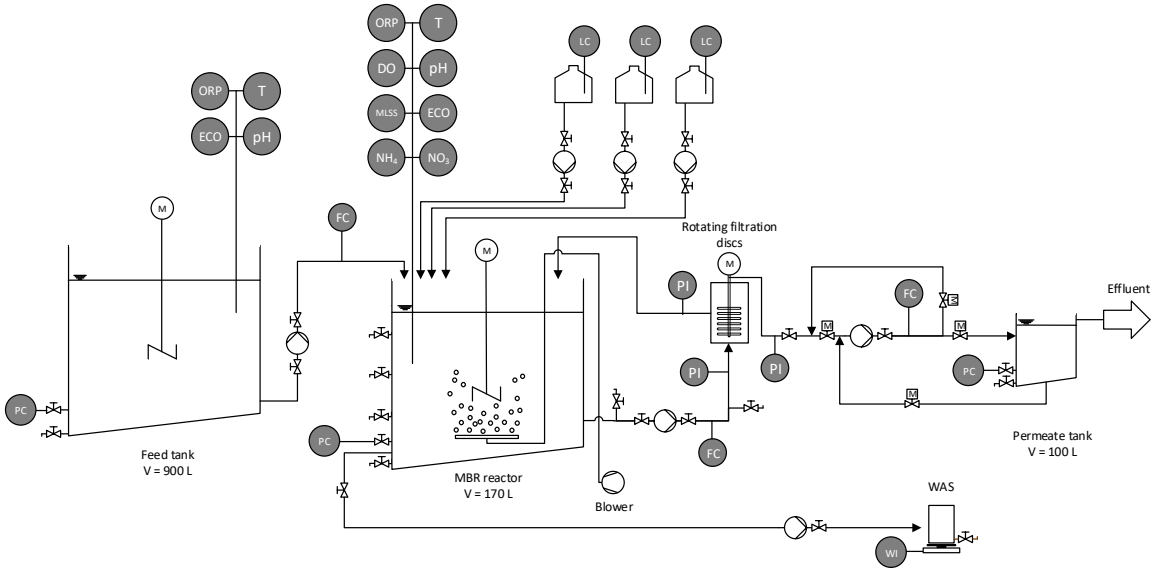

Figure 21: Flow scheme of the MBR

6.2.4 Operation settings

Operating settings of SBR and MBR in all phases show that the hydraulic retention times (HRT) were exceptionally high in both reactors (Table 20). These were necessary to adjust the usual F/M ratios for biological processes and

resulted from the high loading of the process water. The operating time with each dilution was governed by the HRT, as 3 HRTs were required for steady state operation. Once the reactors reached the steady state, operation was continued for 2 - 3 weeks to collect data before the F/M was increased.

Table 20: Operation settings for MBR and SBR (Mean values ± STD)

Parameter	MBR	SBR
HRT [d]	2 - 8	4 - 32
SRT [d]	24 - 51	31 - 56
Exchange ratio [%]	3	3 - 25
MLSS [g/L]	9.3±1.4	4.0±0.7
MLVSS [g/L]	8.6±1.3	3.8±0.7
Temperature [°C]	25.4±2.2	24.9±1.8
pH [-]	7.5±0.3	7.4±0.2
SVI [mL/g]	-	88±26

The exchange ratio is the volumetric percentage exchanged during each feeding. The SRTs, temperature and pH were at all times kept within a range suitable for nitrification. The sludge volume index (SVI) in SBR indicates a good settleability of the activated sludge. Due to strong foaming, a silicon-free defoaming agent based on fatty alcohols was added to the reactors several times a day (ECSO 8361, EnviroChemie GmbH, Germany).

Due to the high percentage of volatile MLSS (MLVSS) of 92 to 95%, the MLSS was used to calculate the F/M instead of the MLVSS. Accordingly, calculation of F/M was based on mean feed concentration of each dilution step multiplied with the daily feed volume flow and divided by the daily determined sludge mass of the reactors (Table 21). The F/M was adjusted by either increasing or reducing the flow rate to the reactors.

Table 21: Sludge loadings during dilutions

Parameter	Dilution and corresponding sludge loading			
MBR	**1:20**	**1:10**	**1:5**	**1:1**
Day	53 to 89	90 to 178	179 to 304	305 to 371
F/M_{COD} [mg COD/(g MLSS·d)]	29 - 43	60 - 268	48 - 147	700 - 753
F/M_C [mg C/(g MLSS·d)]	10 - 15	20 - 88	14 - 47	229 - 246
F/M_N [mg TN/(g MLSS·d)]	4 - 6	7 - 30	5 - 16	10 - 78
SBR	**1:20**	**1:10**	**1:5**	**1:5***
Day	99 to 149	150 to 241	242 to 367	368 to 433
F/M_{COD} [mg COD/(g MLSS·d)]	25 - 31	58 - 268	32 - 147	33 - 40
F/M_C [mg C/(g MLSS·d)]	8 - 10	19 - 88	10 - 47	10 - 13
F/M_N [mg TN/(g MLSS·d)]	3 - 4	6 - 31	3 - 16	3 - 4

6.2.5 Zahn-Wellens tests

Zahn-Wellens tests to deduct maximum biodegradability of the HTC process water were performed in 2 L glas vessels according to EN ISO 9888 (1999). The test procedure has previously been explained in detail (Blach et al. 2023).

6.2.6 Nitrification rate and inhibition

To assess the nitrification inhibition of the process waters, tests were performed according to DIN EN ISO 9509 (2006) in 150 mL glass vessels at 20.7 - 21.5 °C. One day before the experiments, aerobic inoculum from a nitrifying municipal WWTP in Germany was rinsed three times with tap water and sieved (400 μm) to remove coarse particulate substances. Inoculum from the SBR was used to study the biomass adaptation to the HTC process water and equally prepared. The DO was checked regularly and ensured to be above 3 mg O_2/L and the pH was checked at the beginning and the end of the tests. The initial NH_4-N concentration was 50 mg N/L to avoid ammonia inhibition. $(NH_4)_2SO_4$ was added to set the different shares of process water to 50 mg NH_4-N/L in each batch. However, the high NH_4-N concentrations in the HTC process waters only allowed a process water share of 3%. Therefore, a second series was conducted with an initial NH_4-N concentration of 100 mg N/L, allowing a share of up to 6%. In addition to the raw HTC process waters, the treated MBR effluent of dilution 1:5 was tested. To counteract the dilution, 5 L MBR effluent was evaporated at 50 °C for 2 days to obtain 1 L. During this process, of course, stripping of ammonia or volatilization of organic substances may have occurred, but were assumed to be negligible. After each test, the samples were filtered (0.45 μm) and stored at 4 °C before being analyzed for nitrite and nitrate. The

inhibition rate (I_N) in % was calculated according to equation (11). The concentrations of NO_2-N and NO_3-N at the beginning of a test were subtracted from $c_{ON,c}$, $c_{ON,t}$ and $c_{ON,b}$.

$$I_N = \left(\frac{c_{ON,c} - c_{ON,t}}{c_{ON,c} - c_{ON,b}}\right) \cdot 100 \quad (11)$$

$c_{ON,c}$: Oxidized nitrogen in blank suspension without inhibitor, mg/L
$c_{ON,t}$: Oxidized nitrogen in test suspension without inhibitor, mg/L
$c_{ON,b}$: Oxidized nitrogen in reference suspension with inhibitor, mg/L

The nitrification rate (R_N) was calculated according to equation (12).

$$R_N = \left(\frac{c_{ON,t} - c_{ON,b}}{c_{MLSS} \cdot t}\right) \cdot 100 \quad (12)$$

c_{MLSS}: Concentration of MLSS, g/L
t: Reaction time, h

6.2.7 Chemical analysis

Total solids (TS) and volatile solids (VS) of the sewage sludge were analyzed at 105 °C and 550 °C according to DIN EN ISO 18134-2:2017-05 and DIN EN ISO 18122:2016-03, respectively. The MLSS and mixed liquor volatile suspended solids (MLVSS) were analyzed according to DIN 38409:1987 at 105 °C and 550 °C. The SVI was determined by settling 1 L of suspended activated sludge in a cylinder for 30 minutes divided by the MLSS (DIN EN 14702-1). For COD, total organic carbon (TOC), total nitrogen (TN) and ammonium (NH_4-N) HACH tests LCK 514, LCK 386, LCK 338 and LCK 303 as well as a HACH Photometer DR 6000 were used (Hach Lange GmbH, Germany). Nitrite (NO_2-N), nitrate (NO_3-N) were analyzed using a Compact IC 930 Flex (Metrohm AG, Suisse) with Anion column SykroGel Ax 300 (Sykam Chromatographie Vertriebs GmbH, Germany). The dissolved organic nitrogen (DON) was determined by subtracting NH_4-N, NO_3-N and NO_2-N from TN. UV_{254} were determined with a HACH Photometer DR 6000 with a cell length of 10 mm (100-QS, Hellma GmbH, Germany). The SUVA as the ratio UV_{254}/Dissolved organic carbon (DOC) was used to quantify the aromaticity. Samples of Feed and SBR were not filtrated before analysis of COD and TOC, but 0.45 μm polyethersulfone syringe filters were used for the other parameters. MBR samples were not filtered because the effluent was already filtered through the membrane (0.2 μm). All parameters of the feed and the SBR and MBR effluents were analyzed 2 to 4 times a week.

6.3 Results and discussion

6.3.1 Nitrogen removal in MBR and SBR

To explore the limits of nitrification in the MBR, the concentrations of nitrogen species with the stepwise ramp up of TN sludge loading during the different dilutions were monitored. To account for the increasing MLSS concentration up to day 200, the feed volume flow was regularly readjusted for a constant F/M_N (Figure 22). After startup on day 55, it took the nitrification 20 days to start and the ammonium concentration to decrease. As the MBR was inoculated with AOB biomass from a municipal WWTP, this can be attributed to adaptation of microorganisms to the HTC process water. Increasing the F/M_N to 14 mg TN/(g MLSS·d) led to a minor accumulation of ammonium (1.7 mg N/L) and nitrate (5.3 mg N/L), while still removing more than 99% ammonium. An increase in both concentrations resulted from the reactor design and the intermittent operation of the MBR. Permeate was continuously drawn off during both nitrification and denitrification, so minor residual ammonium and nitrate concentrations were present. Further raising the F/M_N resulted in a significant ammonium increase. Consequently, the sludge loading exceeded the nitrification capacity, resulting in an accumulation of ammonium (see Figure 28).

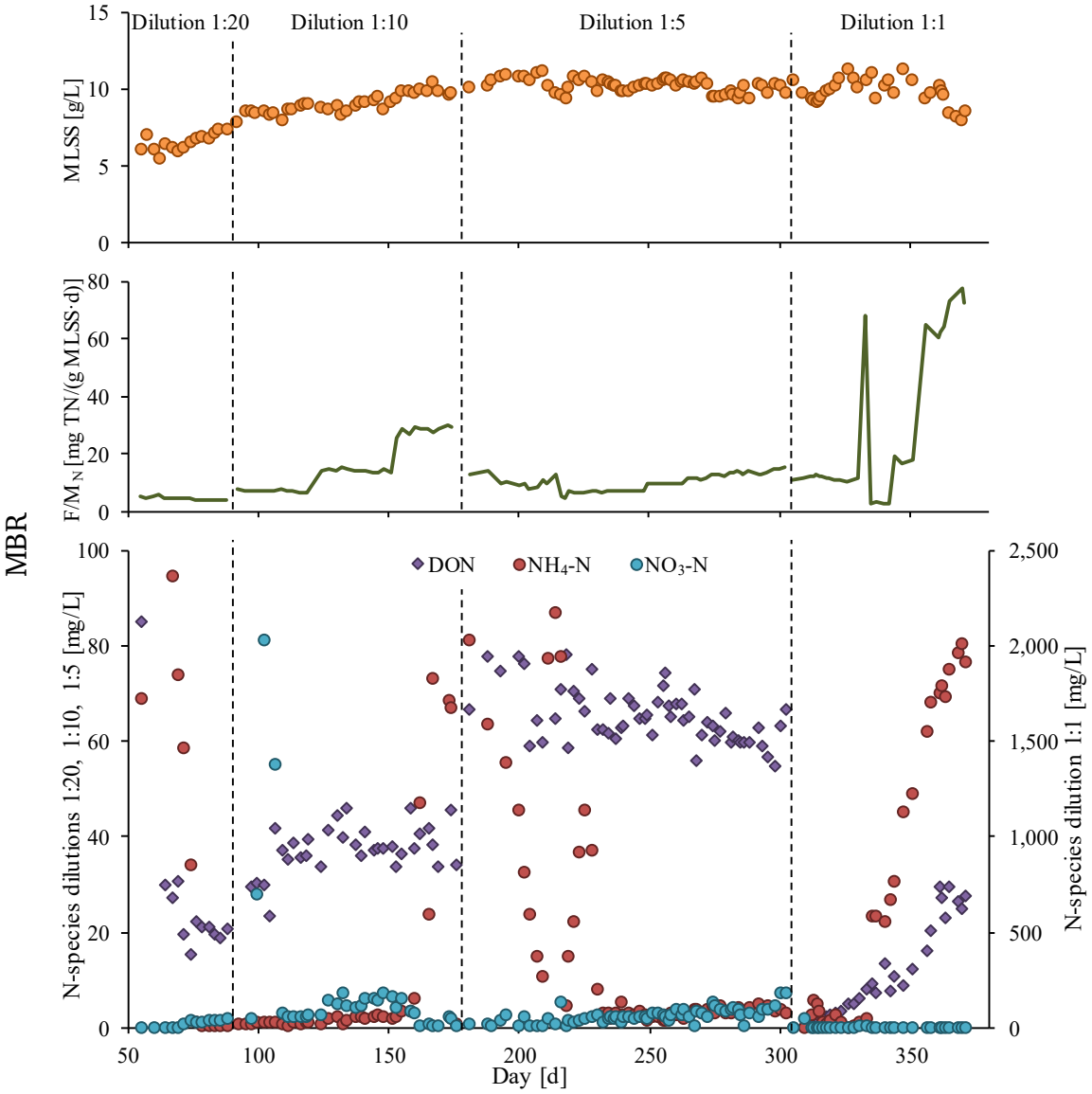

Figure 22: MLSS, F/M$_N$ and nitrogen species during the operation of the MBR. NO$_2$-N is not shown, since it was <0.6 mg N/L at any time.

The dilution 1:5 was started with F/M$_N$ = 8 - 12 mg TN/(g MLSS·d) to F/M$_N$, which had shown stable nitrification at the dilution 1:10. Even though it took almost 50 days before the nitrification was stable again. This was probably the consequence of the doubled inhibitor concentration, which may have affected the AOB activity. From day 230, stable nitrification re-established and the F/M$_N$ was slowly ramped up with 99% ammonium removal. When treating undiluted process water, nitrification initially worked. Setting a low F/M$_N$, however, required a very long HRT of 28 d, which had considerable operational difficulties. The higher COD concentration was associated with a higher growth of heterotrophic microorganisms and, to keep the MLSS constant, the feed volume (6.1 L/d) was almost discharged with the WAS volume (5.3 L/d). This observation suggests that aerobic activated sludge processes are not or not

entirely suitable for such high COD concentrations in the undiluted HTC process water due to the high biomass growth. Anaerobic digestion processes could be more feasible for higher COD concentrations and have already been studied (Weide et al. 2019), but the reduction of only COD was not the intention of our study. During operation of the MBR, a false high concentration measurement from the MLSS sensor at day 333 caused a large WAS volume to be withdrawn. To keep the level of the reactor constant, the feed pump fed the MBR for one day with 38.9 L/d process water, which corresponds to 68 mg TN/(g MLSS·d). This overloaded the AOBs resulting in the collapse of nitrification. Even pausing the feed for 10 days could not re-establish nitrification. As a result, the research focus for dilution 1:1 was placed on COD removal rather than nitrification and denitrification. On day 362, steady state with dilution 1:1 was reached.

The nitrate concentration in the MBR peaked between day 95 and 104 as the result of a supply bottleneck for acetic acid, but dropped rapidly after resuming dosing. For complete denitrification, a sufficient acetic acid dosing was approx. 4.7 g COD/g TN_{Feed} (Dilution 1:10) and 6.1 g COD/g TN_{Feed} (Dilution 1:5), although the acetic acid dosing was no subject for optimization.

The stepwise ramp up of the F/M_N in the SBR and the resulting N species concentrations are depicted in Figure 23. Nitrification set in 20 days after start up (day 134) and ammonium decreased below 0.3 mg N/L at first. After starting with dilution 1:10, the DON gradually accumulated until steady state was reached on day 181. As the MLSS and therefore the volume flow were lower, this effect is more visible than in the MBR. With increasing F/M_N, the nitrification capacity was exceeded from day 220 and ammonium accumulated in the effluent. When reducing the dilution to 1:5, nitrification stabilized due to a lower F/M_N. Further on the F/M_N remained stable, but on day 305 a renewed accumulation of ammonium necessitated to stop the feed temporarily. This decreased the accumulated ammonium in the short term, but it increased again once feeding was restarted. The background for the breakdown of nitrification performance could not be identified, since the F/M_N was even lowered and other operating parameters remained unchanged. Washout of AOBs seems unlikely considering the long SRT and the unchanged ratio of MLSS/MLVSS (Table 20).

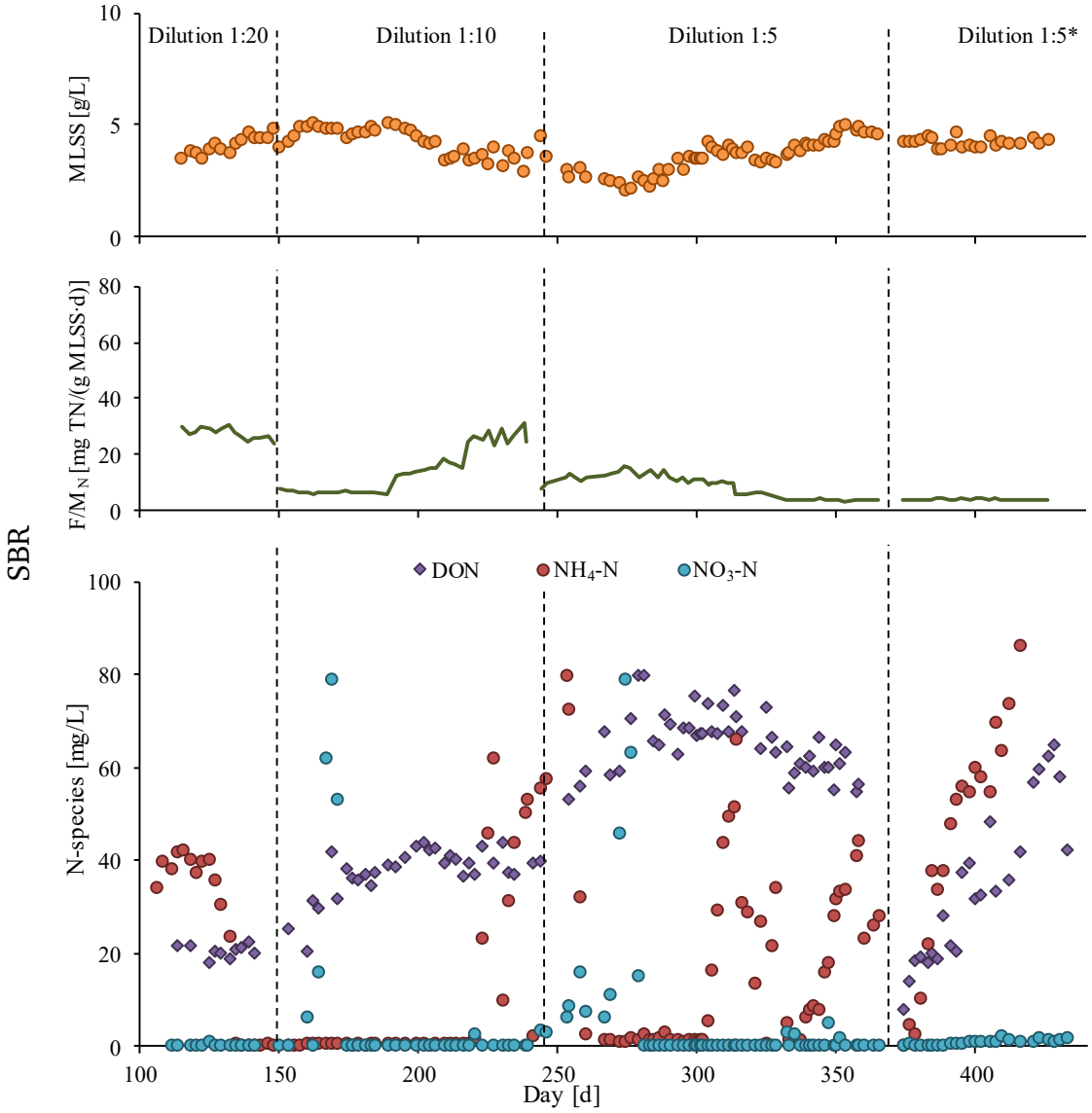

Figure 23: MLSS, F/M$_N$ and nitrogen species during the operation of the SBR. NO$_2$-N is not shown, since it was <0.6 mg N/L at any time

This event indicates that nitrification in the presence of various inhibitors in the HTC process water is a sensitive process. From literature it is known that potentially inhibiting or toxic substances in HTC process water are, among others, phenols, aldehydes or heterocylcic nitrogen compounds (Xu et al. 2022a). These substances already have an antibacterial effect as single substances due to various mechanisms such as disruption of metabolic circuits, depletion of crucial components or damage to cell membranes (Jayakody et al. 2018). For the mixture of the substances, a stronger effect than for the single substances was observed, suggesting their synergistic inhibition due to multiple inhibition pathways (Xu et al. 2022b). Due to the complex composition of sewage sludge for HTC feedstock, the generated process water contains a variety of differently active inhibitors. As a result, the regrowth of AOBs in the SBR during dilution

1:5* was investigated. Repeated settling of the biomass, removal of the supernatant and refilling with tap water should flush out the inhibitors. As indicated by the rise of ammonium concentration from day 374, no nitrification returned. Apparently, the AOBs were inactivated or inhibited to such a large extent that they could not re-grow despite the low F/M_N. In a full-scale application, renewed inoculation of the SBR is therefore recommended.

Due to the acetic acid supply bottleneck, nitrate increased between day 162 and day 174. Between day 246 and 272, the added COD was reduced to 3.4 g COD/g TN_{Feed}. Apparently, this COD/TN ratio was insufficient for denitrifying the nitrate formed. Optimization could, for example, include feeding only during denitrification to use the easily biodegradable organic matter in the process water for denitrification. The availability of the carbon of HTC process water for denitrification was shown by Ferrentino et al. (2021). Moreover, denitrifying microorganisms are more robust to inhibitors generated during hydrothermal processes (Macêdo et al. 2023) compared to nitrifying microorganisms.

Figure 24 depicts the nitrogen removal depending on the F/M_N for data from the steady-state phases and with acetic acid dosing. In both reactors, the removal of TN ranged between 82 and 89% up to an F/M_N of 20 mg TN/(g MLSS·d). The ratio MLSS/MLVSS was fairly constant at 92 - 95% throughout the operation. Accordingly, the 21 mg TN/(g MLVSS·d) calculated for stable nitrification deviates little from the reference to MLSS. Residual ammonium and nitrate in the MBR effluent are negligible. In a study by Hu et al. (2022), the organic nitrogen in HTC process water was released as ammonium to about 83% by *E.coli*. From this, the recalcitrant DON can be calculated to be 17%, which is similar to our results. It is likely that melanoidins from the HTC reaction, which are only partially biodegradable, contribute to the recalcitrant DON (Chandra et al. 2010; Chandra et al. 2008; Müller and Rappert 2010). Increasing the F/M_N to 31 mg TN/(g MLSS·d) caused the TN removal to drop in both reactors due to AOB overload. As the F/M_N was similar for both reactors, the MBR was superior to the SBR due to the higher nitrogen loading rate resulting from the higher MLSS concentration. For a stable nitriciation at F/M_N = 20 mg TN/(g MLSS·d) and the mean MLSS in Table 20, the nitrogen loading rate was 0.19 kg TN/(m^3·d) for the MBR but only 0.08 kg COD/(m^3·d) for the SBR. Accordingly, the required reactor volume and the footprint of the MBR are smaller by a factor of 2.3, which is useful in confined spaces.

Further elevating the F/M_N in the MBR without dilution reduced the TN removal efficiency to 16 - 17%, which equals about 530 mg N/L. Since no nitrification

was achieved, TN removal can be attributed to the incorporation of nitrogen into biomass, i.e., biomass growth. Considering the feed COD and the TN concentrations at 25.4 °C, the required nitrogen for cell growth can be estimated to be 470 to 540 mg/L depending on the assumed kinetic parameters (Tchobanoglous et al. 2014). Further TN loss could be due to stripping of ammonia, which cannot be quantified in more detail. Our observed F/M_N for stable nitrification was similar to a study treating inhibitory wastewater from chemical and pharmaceutical industry, which F/M_N was approx. 16 mg TN/(g MLSS·d) (Dvorak et al. 2013).

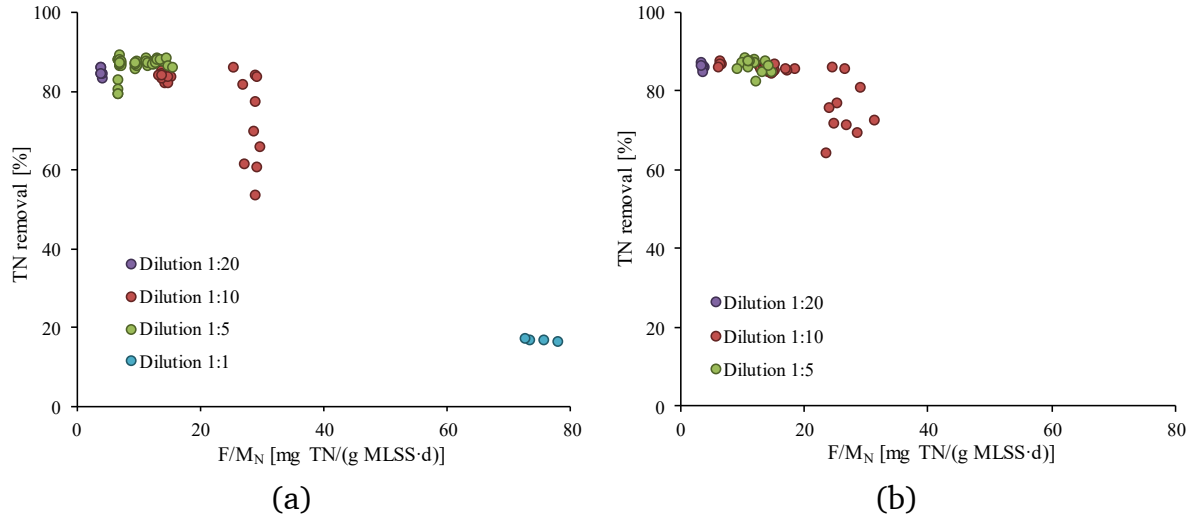

Figure 24: TN removal depending on the F/M_N in mg TN/(g MLSS·d) for a) the MBR and b) the SBR

During an SBR cycle, ammonium concentration increased sharply after feeding (t = 0 h), then first remained constant and only decreased noticeably after the third nitrification phase (Figure 25). Since nitrate was formed throughout all nitrification phases, DON appears to have been mineralized. The release as ammonium apparently occurred at the same rate as the conversion of ammonium to nitrate, keeping the ammonium concentration constant. The concentration decreased when less DON was mineralized than ammonium oxidized. From about 17 hours, the ammonium concentration remained at a very low level while nitrate continued to be formed. This indicates that DON continued to be mineralized, but at a much slower rate than nitrification. Consequently, the released ammonium was converted directly to nitrate. This suggests that the duration of treatment must be long enough to achieve the most extensive mineralization of DON. It should be noted that the sum of nitrate formed does not equal the sum of ammonium, which could have been caused by a suboptimal calibration of the sensor or the fact, that nitrite was not measured.

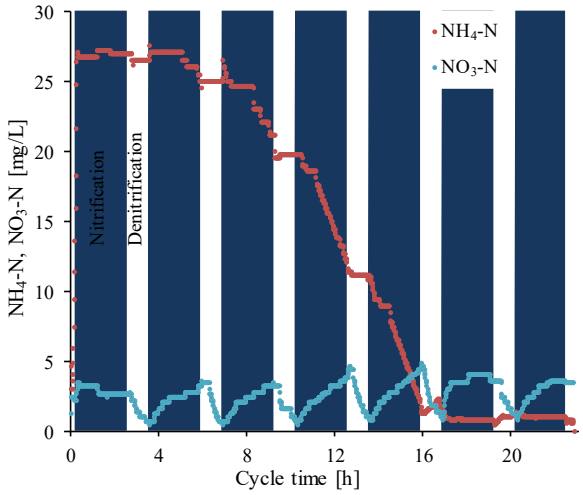

Figure 25: Evolution of ammonium and nitrate during one SBR cycle

6.3.2 Nitrification inhibition

Figure 26 a shows that microorganisms were able to adapt to the inhibitors in the HTC process water. While non pre-exposed inoculum from the WWTP was inhibited by 50% (IC_{50}) at 6.6 mg DON, the pre-exposed inoculum from the SBR was only inhibited by 50% at the 7.5-fold. The IC_{50} correspond to volumetric shares of about 0.4% v/v for WWTP inoculum and 4% v/v for SBR inoculum. Similar inhibition was reported by Farru et al. (2022b) with IC_{50} values ranging from 0.34 to 1.37% v/v for non-pre-exposed inoculum and process water generated during HTC of various feedstocks.

Biological treatment in the MBR reduces the nitrification-inhibiting substances in the process water to a substantial degree. As a result, IC_{50} for WWTP inoculum increased to 25 mg DON, corresponding to almost 40% v/v of the effluent with dilution 1:5 (Figure 26 b). The inhibition of the evaporated effluent lines up seamlessly with the diluted effluent when correlating to the DON. Accordingly, no inhibiting substances evaporated due to the enrichment of the MBR effluent. For the SBR inoculum, inhibition up to 39 mg DON was below 10%, which is equivalent to 60% v/v of the MBR effluent. The evaporated effluent could not be measured with SBR inoculum, since its nitrification activity dropped before the inhibition tests were completed.

The results indicate, firstly, that some of the nitrification-inhibiting compounds are biodegradable and, secondly, that nitrifying microorganisms can adapt to inhibitory nitrogen compounds. In a previous study, we observed IC_{50} of 15 - 16 mg DON for biologically pre-treated HTC process water, which is within the range of the current study (Blach et al. 2023). The reduction of inhibition could be attributed to the degradation of biodegradable phenols. For example, Farru et al. (2022a) demonstrated the correlation of phenols' concentration and

inhibition. Milia et al. (2016) observed the inhibition of nitrification by trichlorophenol, which could be degraded biologically resulting in a great inhibition reduction.

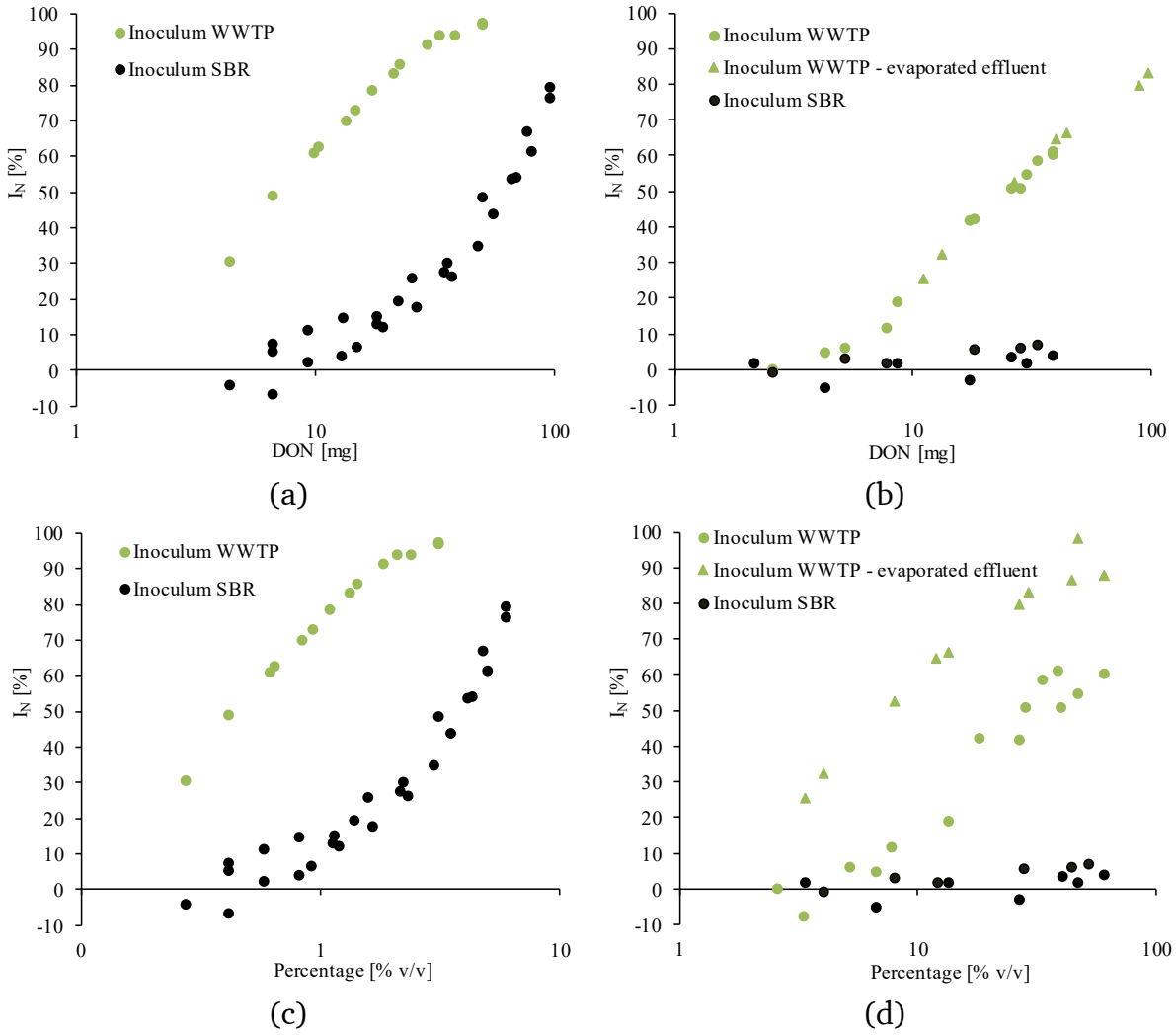

Figure 26: Nitrification inhibition of a) the feed and b) the MBR effluent of dilution 1:5 with non-pre-exposed inoculum and pre-exposed inoculum from the SBR

6.3.3 COD removal in MBR and SBR

For the F/M_{COD}, again, only values during steady states are depicted. Initially, a slight decrease in COD removal could be observed in MBR (Figure 27 a), which was 74.8 ± 1.9% up to 270 mg COD/(g MLSS·d). However, the increasing F/M_{COD} caused the COD removal to drop to 62.5%. On the one hand, as a result of the high load, only readily degradable organics such as sugars and volatile fatty acids were removed (Stemann et al. 2013; Hoekman et al. 2013), while less readily degradable substances were not. This is supported by the SUVA, defined by the ratio of UV_{254} to DOC, which reduced from 3.4 ± 0.1 L/(mg·m) to 2.7 L/(mg·m). This suggests that aromatic compounds such as melanoidins (Dwyer et al. 2008) have not been removed to the maximum extent possible. The high

SUVA of aromatic substances is due to their strong absorption at low UV wavelengths (Langhals et al. 2000). On the other hand, the intermittent operation causes the discharge of potentially degradable COD via the permeate, in analogy to the presence of ammonium and nitrate (Figure 23). The COD removal with increasing F/M_{COD} in the SBR was similar to the MBR, although the COD was reduced by only 71.4 ± 2.6% (Figure 27 b). This can be attributed to particulate organic matter contained in unfiltered effluent. Despite the good settleability of the activated sludge (see SVI in Table 20), this could have been caused, for example, by sludge flocs in the effluent. This may be assumed at dilution 1:5, during which the SBR nitrified stably, but COD removal dropped to about 66% in places. Accordingly, the MBR was superior to the SBR in terms of COD removal. Additionally, as already discussed for nitrogen, the MBR reached higher MLSS concentrations and thus the higher organic loading rate (OLR) than the SBR. For F/M_{COD} = 200 mg COD/(g MLSS·d) and the mean MLSS concentration in each reactor (Table 20), the OLR was 1.9 kg COD/(m^3·d) for the MBR and 0.8 kg COD/(m^3·d) for the SBR.

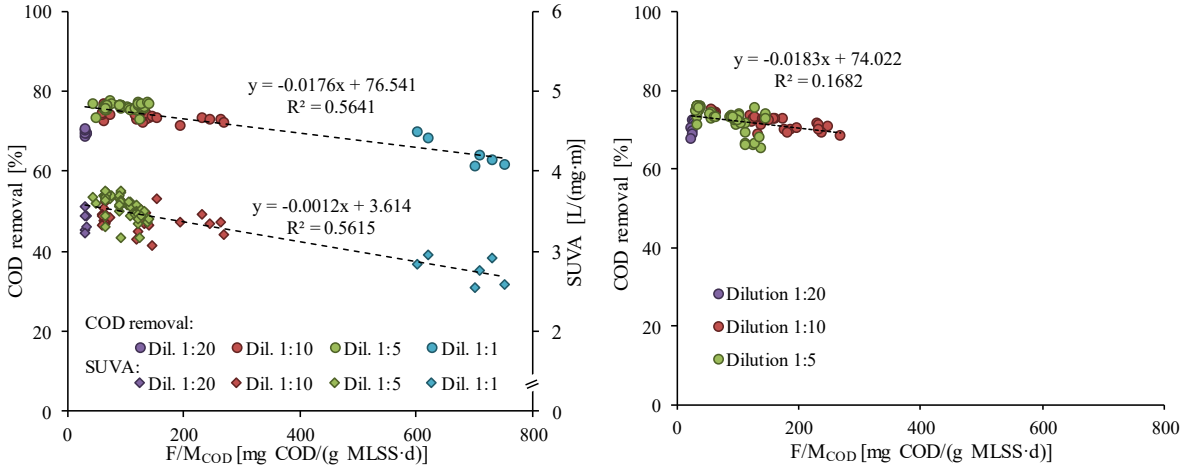

Figure 27: COD removal depending on the COD sludge loading in mg COD/(g MLSS·d) for a) the MBR and b) the SBR

Removal of DOC in the MBR was 73.7 ± 1.6% and of TOC in the SBR was 70.8 ± 2.6% and similar to COD (Figure 30). The DOC reduction in continous MBR and SBR was below the ultimate biodegradability of 81.7 ± 0.8% after 35 days of incubation in the Zahn-Wellens tests (Figure 29). Accordingly, the organic substances in the HTC process water are not completely biodegradable. Depending on the dilution, the effluent COD ranges from 351 to 11,403 mg/L and the effluent DON from 20 to 676 mg/L. The effluent concentrations are summarized in the supplementary material in detail (Table 23 and Table 24). As

a consequence, discharging the biologically treated process water into natural waters could adversely affect their quality. To avoid negative environmental impact, downstream treatment steps for removing refractory substances are necessary. We addressed this issue using electrochemical oxidation in a previous study (Blach and Engelhart 2024). Here we used the effluents obtained from operating the MBR at dilution 1:10 and dilution 1:1.

When treating the undiluted HTC process water without nitrification, ammonium has to be considered in addition to the refractory compounds. High ammonium concentration could open the opportunity for recovering nitrogen using ammonia stripping (Alrbai et al. 2024). Such a scenario would not require nitrification at all, but only COD reduction.

6.4 Conclusions

This study shows the basic feasibility of pilot-scale nitrification and denitrification of HTC process water. However, the operation is not a trivial matter due to nitrification inhibitors and the overall treatment performance is limited by refractory organic matter:

- MBR and SBR achieved a high degree of nitrification and denitrification if the F/M_N was below 20 mg TN/(g MLSS·d). Due to the high load of the process water, the F/M_N had to be set by very long HRT and/or by diluting the process water.
- When the process water was diluted and nitrification was established, the MBR was superior to the SBR regarding the COD removal (MBR: 74.8%, SBR: 71.4%). The removal of TN was similar in both reactors and between 82 and 89%.
- No nitrification could be established without diluting the process water.
- The MBR achieved 2.3 times higher loading rates compared to the SBR due to the higher MLSS concentration.

The findings indicate that simply treating HTC process water biologically is not sufficient. When removing nitrogen (with dilution), for example, a downstream treatment for reducing refractory COD and DON is necessary. If nitrification and denitrification (without dilution) are not used but only COD is removed, the recovery of nitrogen might be feasible. Nevertheless, refractory COD and DON must be reduced in a downstream treatment to avoid these substances to enter the environment. Consequently, future studies should develop holistic concepts considering the HTC processes itself in combination with the process water

treatment focusing on biodegradable as well as refractory substances and nitrogen recovery.

Funding

This research was funded by the German Federal Ministry of Education and Research (BMBF) within the project “IntenKS”, grant number 02WCL1470A.

Author contributions

Conceptualization, T.B.; methodology, T.B.; validation, T.B. and M.E.; investigation, T.B.; data curation, T.B.; writing - original draft preparation, T.B.; writing - review and editing, M.E.; visualization, T.B.; supervision, M.E.; project administration, T.B. and M.E.; funding acquisition, M.E. All authors have read and agreed to the published version of the manuscript.

6.5 References

Alrbai, M.; Al-Dahidi, S.; Shboul, B.; Abusorra, M.; Hayajneh, H. (2024): Techno-economic feasibility study of ammonia recovery from sewage sludge digestate in wastewater treatment plants. In Cleaner Environmental Systems 15, p. 100235. DOI: 10.1016/j.cesys.2024.100235.

Blach, T.; Engelhart, M. (2021): Optimizing the Hydrothermal Carbonization of Sewage Sludge - Response Surface Methodology and the Effect of Volatile Solids. In Water 13 (9), p. 1225. DOI: 10.3390/w13091225.

Blach, T.; Engelhart, M. (2024): Electrochemical oxidation of refractory compounds from hydrothermal carbonization process waters. In *Chemosphere* 352, p. 141310. DOI: 10.1016/j.chemosphere.2024.141310.

Blach, T.; Lechevallier, P.; Engelhart, M. (2023): Effect of temperature during the hydrothermal carbonization of sewage sludge on the aerobic treatment of the produced process waters. In Journal of Water Process Engineering 51, p. 103368. DOI: 10.1016/j.jwpe.2022.103368.

Chandra, R.; Bharagava, R. N.; Rai, V. (2008): Melanoidins as major colourant in sugarcane molasses based distillery effluent and its degradation. In Bioresource Technology 99 (11), pp. 4648–4660. DOI: 10.1016/j.biortech.2007.09.057.

Chandra, R.; Yadav, S.; Bharagava, R. N. (2010): Biodegradation of pyridine raffinate by two bacterial co-cultures of Bacillus cereus (DQ435020) and Alcaligenes faecalis (DQ435021). In World Journal of Microbiology and Biotechnology 26 (4), pp. 685–692. DOI: 10.1007/s11274-009-0223-z.

Chen, H.; Rao, Y.; Cao, L.; Shi, Y.; Hao, S.; Luo, G.; Zhang, S. (2019): Hydrothermal conversion of sewage sludge: Focusing on the characterization of liquid products and their methane yields. In Chemical Engineering Journal 357, pp. 367–375.

Cortright, R. D.; Davda, R. R.; Dumesic, J. A. (2002): Hydrogen from catalytic reforming of biomass-derived hydrocarbons in liquid water. In Nature 418 (6901), pp. 964–967. DOI: 10.1038/nature01009.

DIN EN ISO 9509 (2006): Water quality - Toxicity test for assessing the inhibition of nitrification of activated sludge microorganisms, 2006.

DIN EN ISO 9888 (1999): Evaluation of ultimate aerobic biodegradability of organic compounds in aqueous medium - Static test (Zahn-Wellens method), 1999.

Dvorak, L.; Svojitka, J.; Wanner, J.; Wintgens, T. (2013): Nitrification performance in a membrane bioreactor treating industrial wastewater. In *Water Research* 47, pp. 4412–4421.

DWA (2020): DWA-Position: The Revision of the European Urban Wastewater Directive, March 2020. Available online at https://de.dwa.de/de/positionspapiere-5979.html.

Dwyer, J.; Starrenburg, D.; Tait, S.; Barr, K.; Batstone, D. J.; Lant, P. (2008): Decreasing activated sludge thermal hydrolysis temperature reduces product colour, without decreasing degradability. In Water Research 42, pp. 4699–4709.

Ender, T.; Ekanthalu, V. S.; Jalalipour, H.; Sprafke, J.; Nelles, M. (2024): Process Waters from Hydrothermal Carbonization of Waste Biomasses like Sewage Sludge: Challenges, Legal Aspects, and Opportunities in EU and Germany. In Water 16 (7), p. 1003. DOI: 10.3390/w16071003.

European Comission (2020): A new Circular Economy Action Plan for a cleaner and more competitive Europe. In Communication 2020, 3/11/2020 (COM(2020) 98 final).

Farru, G.; Asquer, C.; Cappai, G.; Gioannis, G. de; Melis, E.; Milia, S. et al. (2022a): Hydrothermal carbonization of hemp digestate: influence of operating parameters. In Biomass Conversion and Biorefinery. DOI: 10.1007/s13399-022-02831-4.

Farru, G.; Cappai, G.; Carucci, A.; Gioannis, G. de; Milia, S.; Muntoni, A. (2022b): Valorisation and suitable treatment of process waters from

hydrothermal carbonization of agro-industrial residues. In 11th IWA International Symposium of Waste Management Problems in Agro-Industry, 26-28th October 2022, 2022.

Ferrentino, R.; Merzari, F.; Grigolini, E.; Fiori, L.; Andreottola, G. (2021): Hydrothermal carbonization liquor as external carbon supplement to improve biological denitrification in wastewater treatment. In Journal of Water Process Engineering (44), p. 102360. DOI: 10.1016/j.jwpe.2021.10236O.

Hoekman, S. K.; Broch, A.; Robbins, C.; Zielinska, B.a; Felix, L. (2013): Hydrothermal carbonization (HTC) of selected woody and herbaceous biomass feedstocks. In Biomass Conversion and Biorefinery 3 (2), pp. 113–126. DOI: 10.1007/s13399-012-0066-y.

Hu, Z.-Y.; Jiang, S.-F.; Shi, X.-Y.; Jiang, H. (2022b): Simultaneous recovery of nutrients and improving the biodegradability of waste algae hydrothermal liquid. In Environmental Pollution 307, p. 119556. DOI: 10.1016/j.envpol.2022.119556.

Ipiales, R. P.; La Rubia, M. A. de; Diaz, E.; Mohedano, A. F.; Rodriguez, Juan J. (2021): Integration of Hydrothermal Carbonization and Anaerobic Digestion for Energy Recovery of Biomass Waste: An Overview. In Energy & Fuels 35 (21), pp. 17032–17050. DOI: 10.1021/acs.energyfuels.1c01681.

Jamal-Uddin, A.-T.; Reza, M. T.; Norouzi, O.; Salaudeen, S. A.; Dutta, A.; Zytner, R. G. (2023): Recovery and Reuse of Valuable Chemicals Derived from Hydrothermal Carbonization Process Liquid. In Energies 16 (2), p. 732. DOI: 10.3390/en16020732.

Jayakody, L. N.; Johnson, C. W.; Whitham, J. M.; Giannone, R. J.; Black, B. A.; Cleveland, N. S. et al. (2018): Thermochemical wastewater valorization via enhanced microbial toxicity tolerance. In Energy Environ. Sci. 11 (6), pp. 1625–1638. DOI: 10.1039/c8ee00460a.

Julien, S.; Chornet, E.; Overend, R. P. (1993): Influence of acid pretreatment (H2SO4, HCl, HNO3) on reaction selectivity in the vacuum pyrolysis of cellulose. In Journal of Analytical and Applied Pyrolysis 27 (1), pp. 25–43. DOI: 10.1016/0165-2370(93)80020-Z.

Knötig, P.; Etzold, H.; Wirth, B. (2021): Model-Based Evaluation of Hydrothermal Treatment for the Energy Efficient Dewatering and Drying of Sewage Sludge. In Processes 9 (8), p. 1346. DOI: 10.3390/pr9081346.

Langhals, H.; Abbt-Braun, G.; Frimmel, F. H. (2000): Association of Humic Substances: Verification of Lambert-Beer Law. In Acta hydrochimica et hydrobiologica 28 (6), pp. 329–332. DOI: 10.1002/1521-401X(200012)28:6<329::AID-AHEH329>3.0.CO;2-E.

Langone, A.; Sabia, G.; Petta, L.; Zanetti, L.; Leoni, L.; Basso, D. et al. (2021): Evaluation of the aerobic biodegradability of process water produced by hydrothermal carbonization and inhibition effects on the heterotrophic biomass of an activated sludge system. In Journal of Environmental Management 299 (299), p. 113561. DOI: 10.1016/j.jenvman.2021.113561.

Li, Y.; Zhai, Y.; Zhu, Y.; Peng, C.; Wang, T.; Zeng, G. et al. (2017): Distribution and Conversion of Polycyclic Aromatic Hydrocarbons during the Hydrothermal Treatment of Sewage Sludge. In Energy & Fuels 31 (9), pp. 9542–9549. DOI: 10.1021/acs.energyfuels.7b01523.

Macêdo, W. V.; Schmidt, J. S.; Jensen, S. B.; Biller, P.; Vergeynst, L. (2023): Is nitrification inhibition the bottleneck of integrating hydrothermal liquefaction in wastewater treatment plants? In J Environ Manage 348, p. 119046. DOI: 10.1016/j.jenvman.2023.119046.

Malhotra, M.; Garg, A. (2020): Hydrothermal carbonization of centrifuged sewage sludge: Determination of resource recovery from liquid fraction and thermal behaviour of hydrochar. In Waste Management 117, pp. 114–123.

Mantovani, M.; Collina, E.; Marazzi, F.; Lasagni, M.; Mezzanotte, V. (2022): Microalgal treatment of the effluent from the hydrothermal carbonization of microalgal biomass. In Journal of Water Process Engineering 49, p. 102976. DOI: 10.1016/j.jwpe.2022.102976.

Milia, S.; Porcu, R.; Rossetti, S.; Carucci, A. (2016): Performance and Characteristics of Aerobic Granular Sludge Degrading 2,4,6-Trichlorophenol at Different Volumetric Organic Loading Rates. In Clean Soil Air Water 44 (6), pp. 615–623. DOI: 10.1002/clen.201500127.

Müller, R.; Rappert, S. (2010): Pyrazines: occurrence, formation and biodegradation. In Applied Microbiology and Biotechnology 85 (5), pp. 1315–1320. DOI: 10.1007/s00253-009-2362-4.

Namoika, T.; Morohashi, Y.; Yamane, R.; Yoshikawa, K. (2009): Hydrothermal Treatment of Dewatered Sewage Sludge Cake for Solid Fuel Production. In Journal of Environment and Engineering 4 (1), pp. 68–77. DOI: 10.1299/jee.4.68.

Oliveira, A. S.; Sarrión, A.; Baeza, J. A.; Diaz, E.; Calvo, L.; Mohedano, A. F.; Gilarranz, M. A. (2022): Integration of hydrothermal carbonization and aqueous phase reforming for energy recovery from sewage sludge. In Chemical Engineering Journal 442, p. 136301. DOI: 10.1016/j.cej.2022.136301.

Park, M.; Kim, N.; Jung, S.; Jeong, T.-Y.; Park, D. (2021): Optimization and comparison of methane production and residual characteristics in mesophilic anaerobic digestion of sewage sludge by hydrothermal treatment. In Chemosphere 264, p. 128516.

Saha, N. (2021): Behavior of selective oxygen functional groups upon hydrothermal carbonization and pyrolysis of biomass and their roles on selective applications. Dissertation. Florida Institute of Technology, Melbourne, Florida. Department of Biomedical and Chemical Engineering and Sciences.

Stemann, J.; Putschew, A.; Ziegler, F. (2013): Hydrothermal carbonization. Process water characterization and effects of water recirculation. In Bioresource Technology 143, pp. 139–146.

Tchobanoglous, G.; Stensel, H. D.; Tsuchihashi, R.; Burton, F. (2014): Wastewater Engineering. Treatment and Resource Recovery. Fifth Edition. New York: McGraw-Hill Education.

Wang, L.; Li, A. (2015): Hydrothermal treatment coupled with mechanical expression at increased temperature for excess sludge dewatering: the dewatering performance and the characteristics of products. In Water Research 68, pp. 291–303. DOI: 10.1016/j.watres.2014.10.016.

Weide, T.; Brügging, E.; Wetter, C. (2019): Anaerobic and aerobic degradation of wastewater from hydrothermal carbonization (HTC) in a continuous, three-stage and semi-industrial system. In Journal of Environmental Chemical Engineering 7.

Xu, Y.; Wang, Y.; Lu, J.; Yuan, C.n; Zhang, L.; Liu, Z. (2022a): Understand the antibacterial behavior and mechanism of hydrothermal wastewater. In Water Research 226, p. 119318. DOI: 10.1016/j.watres.2022.119318.

Xu, Z.-X.; Ma, X.-Q.; Zhou, J. Duan, P.-G.; Zhou, W.-Y.; Ahmad, A.; Luque, R. (2022b): The influence of key reactions during hydrothermal carbonization of sewage sludge on aqueous phase properties: A review. In Journal of Analytical and Applied Pyrolysis 167, p. 105678. DOI: 10.1016/j.jaap.2022.105678.

Zhao, P.; Shen, Y.; Ge, S.; Yoshikawa, K. (2014): Energy recycling from sewage sludge by producing solid biofuel with hydrothermal carbonization. In Energy Conversion and Management 78, pp. 815–821. DOI: 10.1016/j.enconman.2013.11.026.

6.6 Supplementary material

Table 22: Analysis of the anaerobically digested sewage sludge and it's hydrochars after HTC for 1h at 197 °C

Parameter	Raw sewage sludge	Hydrochar	Method
Total solids [%]	19.8	39.6	DIN EN ISO 18134-2
Volatile solids [%]	12.5	19.4	DIN EN ISO 18122
Higher heating value [MJ/kg TS]	14.7	15.0	DIN EN ISO 18125
C [%]	33.3	33.4	DIN EN ISO 16948
H [%]	4.7	3.9	DIN EN ISO 16948
N [%]	5.0	2.5	DIN EN ISO 16948
S [%]	1.6	1.2	DIN EN ISO 16994
O [%]	18.5	8.0	By difference

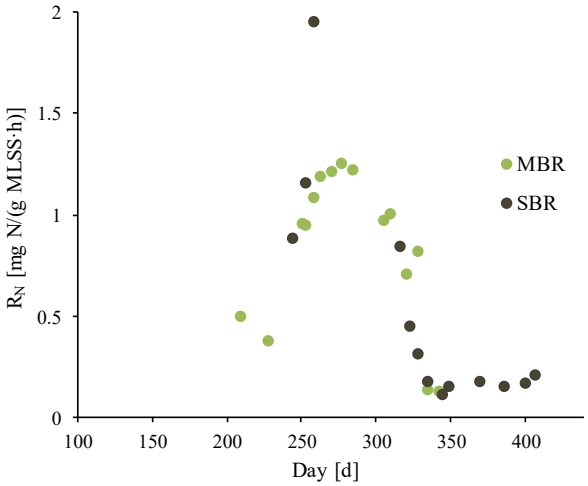

Figure 28: Nitrification rates in MBR and SBR during the operation (n = 2)

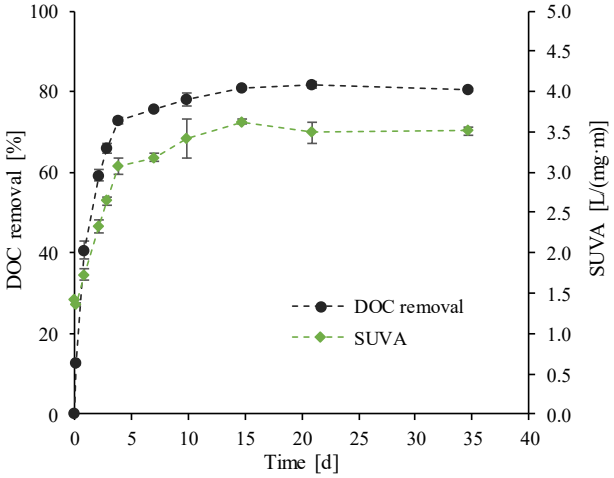

Figure 29: Evolution of DOC and SUVA during the Zahn-Wellens test. DOC removal was 81.7 ± 0.8% after 35 days of incubation and SUVA increased from initially 1.4 to 3.5 ± 0.1 L/(mg·m) (Mean values ± STD, n = 3)

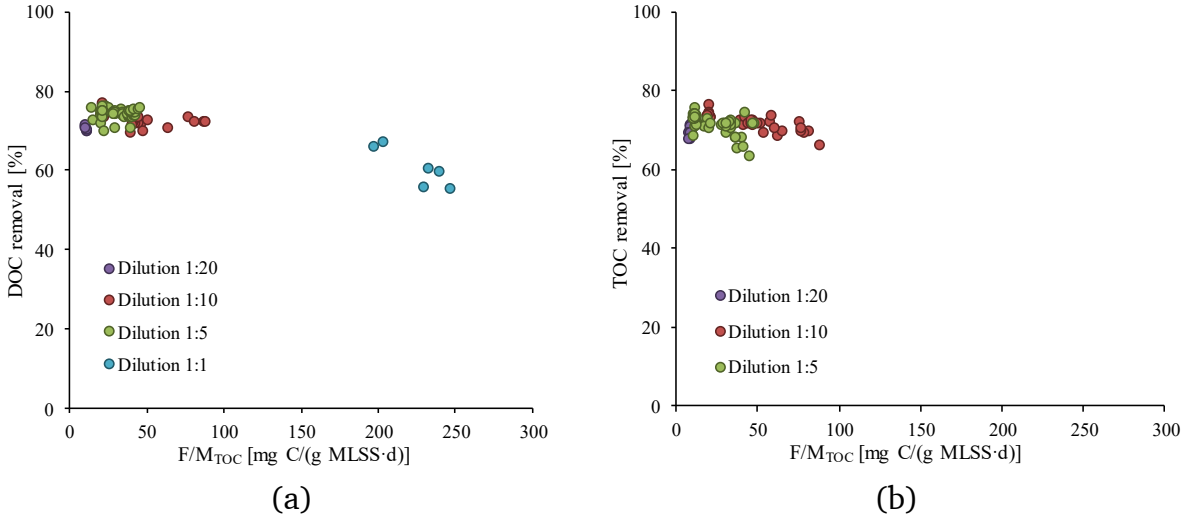

Figure 30: DOC and TOC removal depending on the TOC sludge loading in mg C/(g MLSS·d) for a) the MBR and b) the SBR

Table 23: MBR Effluent concentrations

Parameter	Dilution 1:10	Dilution 1:5	Dilution 1:10	Dilution 1:1
COD [mg O_2/L]	351±8	704±25	1,257±33	11,403±372
DOC [mg C/L]	109±3	240±8	433±12	4,195±261
UV_{254} [1/m]	392±14	817±21	1,512±64	11,311±330
SUVA [L/(mg C·m)]	3.4±0.1	3.4±0.1	3.5±0.1	2.7±0.2
TN [mg N/L]	22±2	47±4	69±4	2,618±14
NH_4-N [mg N/L]	0.4±0.3	1.8±0.4	3.5±0.8	1,941±56
NO_2-N [mg N/L]	<0,2	0.3±0.1	0.5±0.2	<0.3
NO_3-N [mg N/L]	1.3±0.2	5.3±1.3	3.3±1.5	<0.2
DON [mg N/L]	21±1	39±4	62±4	676±46
PO_4-P [mg P/L]	4±1	<1.6	3±2	17±2

Table 24: SBR Effluent concentrations

Parameter	Dilution 1:20	Dilution 1:10	Dilution 1:5
COD [mg O_2/L]	357± 12	743±32	1,582±163
TOC [mg C/L]	119± 4	248±8	515±50
UV_{254} [1/m]	379± 7	814±18	1,670±49
TN [mg N/L]	21± 1	41±2	74±9
NH_4-N [mg N/L]	<0.3	<0.7	1.6±0.5
NO_2-N [mg N/L]	<0.1	<0.3	<0.3
NO_3-N [mg N/L]	<0.2	<0.2	<0.2
DON [mg N/L]	20±1	40±2	70±5
PO_4-P [mg P/L]	0.8±0.4	2.4±0.5	8.2±3.5

7 Electrochemical oxidation of refractory compounds from hydrothermal carbonization process waters

Authors:	Blach, T.; Engelhart, M.
Keywords:	BDD; Electrochemical oxidation; HTC; Hydrothermal carbonization; Process water; Aqueous phase
Published in:	Chemosphere 352 (2024) 141310 https://doi.org/10.1016/j.chemosphere.2024.141310
Received:	12 October 2023
Accepted:	25 January 2024
Published:	4 February 2024

Abstract:

Hydrothermal carbonization (HTC) is an emerging technology for treating sewage sludge. However, the resulting HTC process water is heavily contaminated with various carbonaceous and nitrogenous components, some of them being non-biodegradable. To implement HTC as a full-scale treatment alternative for sewage sludge, effective concepts for treating process water are crucial. This study focuses on the electrochemical oxidation (EO) using a boron-doped diamond electrode to treat one HTC process waters with different pretreatments: (i) without pretreatment, (ii) biologically pretreated with chemical oxygen demand (COD) removal, (iii) biologically pretreated with nitrification and denitrification. The EO removed COD of all HTC process waters by over 97%, but as COD concentrations decreased, the instantaneous current efficiency (ICE) dropped below 5% and energy consumption increased. The organically bound and refractory nitrogen was completely mineralized and converted to mainly NO3-N. After EO of process waters without nitrification/ denitrification, nitrogen was present as NO3-N with up to 730 mg/L and NH4-N with up to 1,813 mg/L. Such high ammonium concentrations treatment could be interesting for nitrogen recovery. In addition, the toxicity towards *Vibrio fischeri* could be reduced to a large extent. The findings suggest that EO after a biological step with COD removal is a viable solution for HTC process water treatment.

7.1 Introduction

For the protection and sustainable management of natural resources, the resource recovery of waste materials such as sewage sludge is a key issue. As an alternative to established technologies for sewage sludge treatment, hydrothermal carbonization (HTC) produces a hydrochar with various recycling possibilities (Fang et al. 2018). Dewatering the hydrochar slurry, however, separates a highly contaminated process water. This liquid stream contains many dissolved pollutants formed during thermal treatment such as volatile fatty acids, aldehydes, phenols, and ammonium (Huang et al. 2021a; Shrestha et al. 2021; Huang et al. 2021b). The loading strongly depends on the HTC feedstock and the HTC process conditions, resulting in a chemical oxygen demand (COD) of up to 63.9 g/L and total nitrogen (TN) of up to 12 g/L (He et al. 2015; Langone and Basso 2020). Anaerobic digestion of process waters has been used to recover energy as biogas and to improve the energy balance of HTC (Gaur et al. 2020; Zhao et al. 2020). Nevertheless, the biodegradability of HTC process waters is limited due to the formation of refractory substances such as humic-like substances and heterocyclic nitrogen compounds, especially at higher HTC temperatures (Li et al. 2017; Shrestha et al. 2021). In addition, inhibitors such as phenols or ammonium restrict anaerobic digestion, but also aerobic biodegradation (Wang et al. 2021; Blach et al. 2023). Removing the inhibiting and recalcitrant compounds from HTC process water requires further treatment steps. Oxidation and coagulation using Fe(II)/persulfates reduced the dissolved organic carbon (DOC) of HTC process water by up to 35% (Liu et al. 2022). Also coagulation was successfully used for treating the process water by increasing its biodegradability (Hu et al. 2022). Fettig et al. (2019) proposed a multistage treatment for the HTC process using anaerobic and aerobic treatment followed by activated carbon adsorption with optional ozonation.

Electrochemical oxidation (EO) may be a feasible technology for treating process waters from HTC, as it is suitable treating for highly contaminated wastewaters and poor biodegradability (Garcia-Rodriguez et al. 2020) Boron-doped diamond (BDD) electrodes are often used as anode material due to the high potential for oxygen evolution overpotential and therefore high reactivity towards oxidation of organics. BDD also show high corrosion resistance compared to other electrode materials (Shestakova and Sillanpää 2017; Patel et al. 2013; Carboneras et al. 2020). Recent studies focus on improving the synthesis of BDD and improving the reactor design of BDD (Vernasqui et al. 2022; Montenegro-Ayo et al. 2023).

Besides direct anodic oxidation, oxidation by heterogeneous reactive oxygen species such as •OH, H_2O_2, and O_3 and indirect oxidation by oxidants generated during the EO process reinforce the oxidation process (Moreira et al. 2017). BDD anodes have high oxygen overpotentials, leading to the generation of •OH according to equation (13) (Groenen-Serrano et al. 2013; Barrera-Díaz et al. 2014).

$$BDD + H_2O \rightarrow BDD\,(\cdot OH) + H^+ + e^- \qquad (13)$$

Assuming that the oxidation process is primarily driven by the generated •OH, organic compounds (R) are degraded and ultimately mineralized according to equation (14) (Kapalka et al. 2010). The oxidation of organic matter during EO is divided in two different regimes: In the kinetic controlled regime, the applied current is below the limiting current. The rate constant is theoretically independent from COD concentration and the COD decreases linearly at maximum instantaneous current efficiency (ICE) of 100% (Panizza and Cerisola 2009). During mass transfer limitation, the oxidation rate strongly depends on the COD concentration as diffusion governs the transport of organics towards the anode. As a result, low COD concentrations lead to undesirable side reactions such as the formation of oxygen (equation (15)) and the efficiency of the oxidation process declines (Kapalka et al. 2008).

$$BDD(\bullet OH) + R \rightarrow BDD + Degradation\ products + H^+ + e^- \qquad (14)$$

$$BDD(\bullet OH) \rightarrow BDD + \frac{1}{2}O_2 + H^+ + e^- \qquad (15)$$

The indirect oxidation can improve EO process by electrochemically generating oxidants from ions in the bulk solution. These include chlorine, hypochlorous acid, hypochlorite, hydrogen peroxide, ozone, persulphate, and peroxophosphate, which are electrochemically formed from chloride, sulphate, phosphate, and oxygen (Rajkumar and Kim 2006; Guinea et al. 2010; Serrano et al. 2002; Bensalah et al. 2012). The electrochemical formation of these oxidants favors EO over other advanced oxidation processes, as intermediates that are refractory to one of the radicals are also mineralized (Cañizares et al. 2009). The presence of chlorides is of special interest, as its electrochemically formed oxidants are potentially toxic and persistent (Periyasamy et al. 2022; Chatzisymeon et al. 2006). For this reason, it is important to monitor the

ecotoxicity of electrochemically oxidized wastewater to organisms such as luminescent bacteria.

To date, no studies have been conducted on the holistic treatment of HTC process water using a combination of different technologies. Therefore, this study aims to evaluate EO using BDD for the treatment of raw HTC process water and two biologically pre-treated process waters to assess oxidation and energy efficiency. Of the two biologically pretreated process waters, one was treated with COD removal and one was diluted and treated with nitrification. Additional ecotoxicity tests using luminescent bacteria revealed the effects of EO on toxicity. With these results, three scenarios to treat HTC process water could be developed.

7.2 Materials and methods

7.2.1 Characteristics of HTC process water

The HTC process water was obtained from a full-scale demonstration HTC plant in Germany. Anaerobically digested sludge from a municipal wastewater treatment plant (WWTP) was dewatered to a total solids (TS) content of 19.8% and subsequently carbonized for 1 h at 197 °C. Volatile solids (VS) of the sludge were 12.5%. After HTC, a chamber filter press dewatered the hydrochar slurry to 39.6% TS (19.4% VS) and separated the HTC process water (PW-AD). PW-AD was first subjected to EO experiments. To obtain the pre-treated process waters, PW-AD was treated aerobically in a pilot-scale membrane bioreactor with a volume of 170 L coupled with a ceramic rotating disc filter with membrane pore size of 0.2 μm. Aerobic biodegradation removed approx. 60% of chemical oxygen demand (COD) and dissolved organic carbon (DOC), and 22% of total nitrogen (TN). Since no nitrification could be established, reduction of TN can mainly be attributed to biomass growth. This process water is referred to as MBR 1-1. By diluting the process water 10 times with tap water before treatment, nitrification and denitrification (N+DN) could be established. Biodegradation removed 76% COD and DOC, and 87% TN. This process water is referred to as MBR 1-10. Table 25 gives an overview of the process waters characteristics.

Table 25: Characteristics of the tested HTC process waters (Mean values ± STD[a], n>3)

Parameter	PW-AD	MBR 1-1	MBR 1-10
pH [-]	6.9	8.1	7.3
EC [μS/cm]	12,071	11,039	1,145
DOC [mg C/L]	9,125±177	3,773±50	217±3
COD [mg O_2/L]	28,050±532	11,233±51	675±15
UV_{254} [1/m]	13,284±434	10,887±246	769±10
SUVA[b] [L/(mg·m)]	1.5±0.1	2.9±0.1	3.5±0.1
TN [mg N/L]	3,162±67	2,435±35	43.0±1.2
DON[c] [mg N/L]	1,130±121	628±35	34.1±1.9
NH_4-N [mg N/L]	2,030±56	1,843±57	1.3±0.9
NO_2-N [mg N/L]	1.2±0.4	0.4±0.2	0.9±0.8
NO_3-N [mg N/L]	0.9±0.3	<0.3	6.7±2.6
PO_4-P [mg P/L]	61±5	17±2	<1.6
Cl^- [mg Cl/L]	70.7	99.5±1.5	40.6±0.5
SO_4^{2-}[mg SO_4/L]	700	1,307±57[d]	170±2.5

[a]Standard deviation

[b]specific UV absorbance: SUVA = UV_{254}/DOC

[c]dissolved organic nitrogen: DON = TN - NH_4-N - NO_3-N - NO_2-N

[d]SO_4^{2-} concentrations were higher since pH in the MBR was adjusted using H_2SO_4

7.2.2 Electro-oxidation setup

For each EO test, the feed volume was set to 5 L (see Figure 31). Redox potential (ORP), pH and electrical conductivity (EC) were measured every five minutes using Orbisint CSPS11D and Condumax CLS21D (Endress+Hauser Conducta GmbH+Co. KG, Germany). Dissolved oxygen (DO) was measured manually using the O_2 sensor FDO 925 and a multi-parameter portable meter (Multi 3620 IDS, Xylem Analytics Germany Sales GmbH & Co. KG, Germany). Evaporation of water was taken into account, but was negligible. The electrode stack consisted of an anode coated with a 12 μm boron-doped diamond based on niobium with a surface area of 0.016 m², and two stainless steel cathodes. The gap between the electrodes was 2 mm (Type “Susi”, DiaCCon GmbH, Germany). A pump (Type “1046”, Eheim GmbH & Co.KG, Germany) ensured a flow rate of $\dot{v}$ = 2.5 L/min and $\dot{v}$ = 6 L/min in the electrode stack. Galavanostatic conditions were 5.5 A and 10.5 A using a DC supply type “6226” (PeakTech Prüf- und Messtechnik GmbH, Germany) resulting in current densities of j = 34 mA/cm² and j = 66 mA/cm². A heat exchanger kept system temperature at 23 - 26 °C during each experiment. After each experiment, the system was rinsed for 30 minutes with 1.5% citric acid to remove inorganic residues on the electrodes.

As the oxidation of PW-AD lasted for several days, once a day the tests were paused and the system was cleaned. Each process water and each setting was tested three times, except for MBR 1-10 with 5.5 A. Test results are presented as the mean values of the experiments with standard deviation.

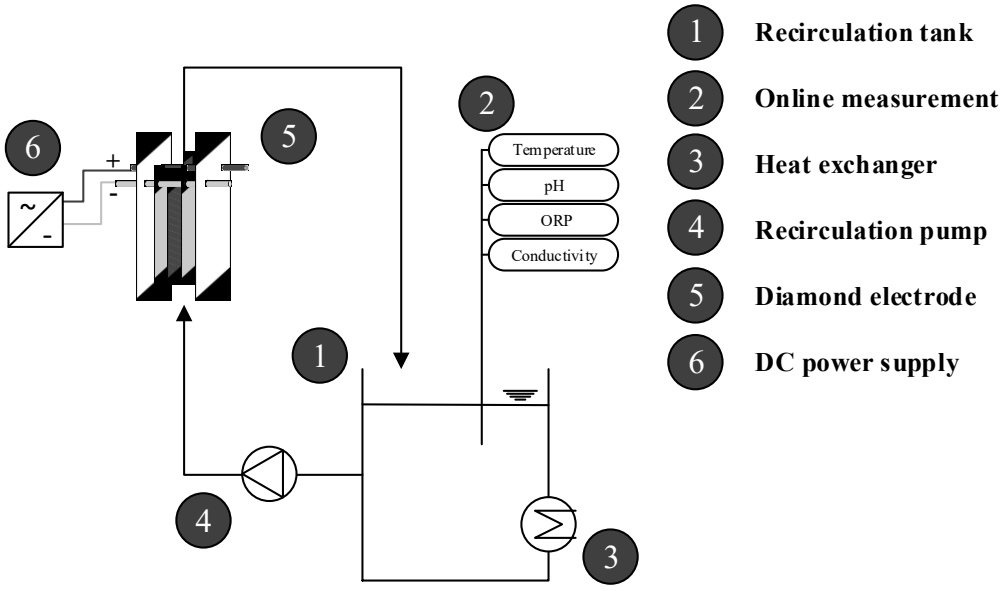

Figure 31: Flow scheme of the oxidation setup

7.2.3 Calculations

The volumetric flow rate of $\dot{v} = 6$ L/min resulted in an approximate Reynold's number of Re ≈ 1,100 using equation (16). Herein, the estimated density is $\rho = 1{,}000$ kg/m³, the estimated viscosity is $\eta = 1$ mPa·s, and the hydraulic diameter is $d = 0.76$ cm.

$$Re = \frac{\rho \cdot v \cdot d}{\eta} \tag{16}$$

The volume flow of $\dot{v} = 6$ L/min resulted in Re ≈ 2,600.

Equation (17) describes the evolution of COD if the applied current is high and it is $\alpha > 1$ from the start (Liakos et al. 2017). Herein A is the anode area in m², t the oxidation time in s, V_R the electrolyte volume in m³ and the factor 32 g/mol to convert the COD from mol/m³ into mg/L.

$$COD(t) = COD_0 \cdot exp\left(-\frac{A \cdot k_m}{V_R} t\right) \cdot 32 \tag{17}$$

The efficiency of the process was determined using the ICE in equation (18) (Kapalka et al. 2010), where I is the applied current in A.

$$ICE = \frac{F \cdot V_R \cdot (COD_t - COD_{t+\Delta t})}{8 \cdot I \cdot \Delta t} \quad (18)$$

For calculating the energy consumption, only the energy demand of the electrode was considered. Energy consumption of the pump and the cooling unit was neglected. The electrical energy per mass of COD (EE/M) in kWh/kg COD was calculated according to equation (19), where U is the average voltage during the oxidation in V and 3.6 a factor in (s·m³)/(h·L) to convert the units.

$$EE/M = \frac{I \cdot U}{(COD_0 - COD_t) \cdot V_R \cdot 3.6} \cdot t \quad (19)$$

7.2.4 Toxicity tests

To measure toxicity, inhibition of bioluminescence of *Vibrio fischeri* NRRL-B-11177 was assessed according to DIN ISO 11348-2 (LCK 482, Hach Lange GmbH, Germany). NaCl was added to provide osmotic protection of the bacteria (electrical conductivity about 34 - 35 mS/cm). Toxicity was defined as the first dilution level of the samples causing less than 20% inhibition (G_L-value). In addition, the percentage of process water for 50% inhibition was given (EC_{50}). The inhibition of bioluminescence was calculated based on 30 minutes of exposure.

7.2.5 Chemical analysis

Total solids were analyzed according to DIN EN ISO 18134-2:2017-05 and volatile solids according to DIN EN ISO 18122:2016-03 at 105 °C and 550 °C. The process water samples were filtered via 0.45 μm polyethersulfone syringe filters (VWR International GmbH, Germany) before analysis. For COD, DOC, total nitrogen (TN) and ammonium (NH_4-N) HACH tests LCK 514, LCK 386, LCK 338 and LCK 303 with HACH Photometer DR 3900 were used (Hach Lange GmbH, Germany). Nitrite (NO_2-N) and nitrate (NO_3-N) were analyzed with a Compact IC 930 Flex (Metrohm AG, Suisse) and Anion column SykroGel Ax 300 (Sykam Chromatographie Vertriebs GmbH, Germany). The DOC was further characterized with liquid chromatography and continuous organic carbon detection (LC-OCD, DOC Labor Huber, Germany) (Huber et al. 2011). UV_{254} was determined with HACH Photometer DR 6000 at a cell length of 10 mm (100-QS, Hellma GmbH, Germany). Each parameter was analyzed only one time, as the experiments were already conducted three times. The ratio of UV_{254}/DOC (SUVA) was used to quantify the aromaticity of organic matter.

7.3 Results and discussion

7.3.1 Defining the operating parameters

The evolution of COD for different current densities and flow rates was tested with MBR 1-10. Exhibiting similar patterns, COD was reduced from initially 675 mg/L to 22 mg/L at 20 Ah/L (Figure 32 a).The COD reduction followed an exponential curve, indicating a mass transfer limitation during the oxidation. Accordingly, the data were fitted with equation (17) using the method of least squares. The apparent rate constants for j = 66 mA/cm^2 were 8.4×10^{-5} and 8.2×10^{-5} m/s for $\dot{v}$ = 2.5 L/min and $\dot{v}$ = 6 L/min, respectively. For j = 34 mA/cm^2 these were 8.8×10^{-5} and 1.05×10^{-4} m/s for $\dot{v}$ = 2.5 L/min and $\dot{v}$ = 6 L/min. k_m was slightly higher for the lower current density and $\dot{v}$ = 6 L/min, but the overall effect of flow rate was small. At lower current densities, in general, fewer side reactions take place (Bensalah et al. 2012; Moreira et al. 2017; Panizza et al. 2001). The small differences suggest that j = 34 mA/cm^2 already caused significant side reactions such as the generation of oxygen (equation (15)). Lower current densities were not used in the experiments, since the oxidation time increases with decreasing current density, which was not practical for further investigations.

The side reactions during mass transport-controlled oxidation reduced the energy efficiency, as shown by the ICE in Figure 32 b. As a result, the ICE decreased from initially 24% to less than 5% in all experiment without significant benefits at higher flow rates. Even though, increasing the flow rate during mass transfer limitation regime can raise the ICE by accelerating the mass-transfer (Souza and Ruotolo 2013; Yao et al. 2019).

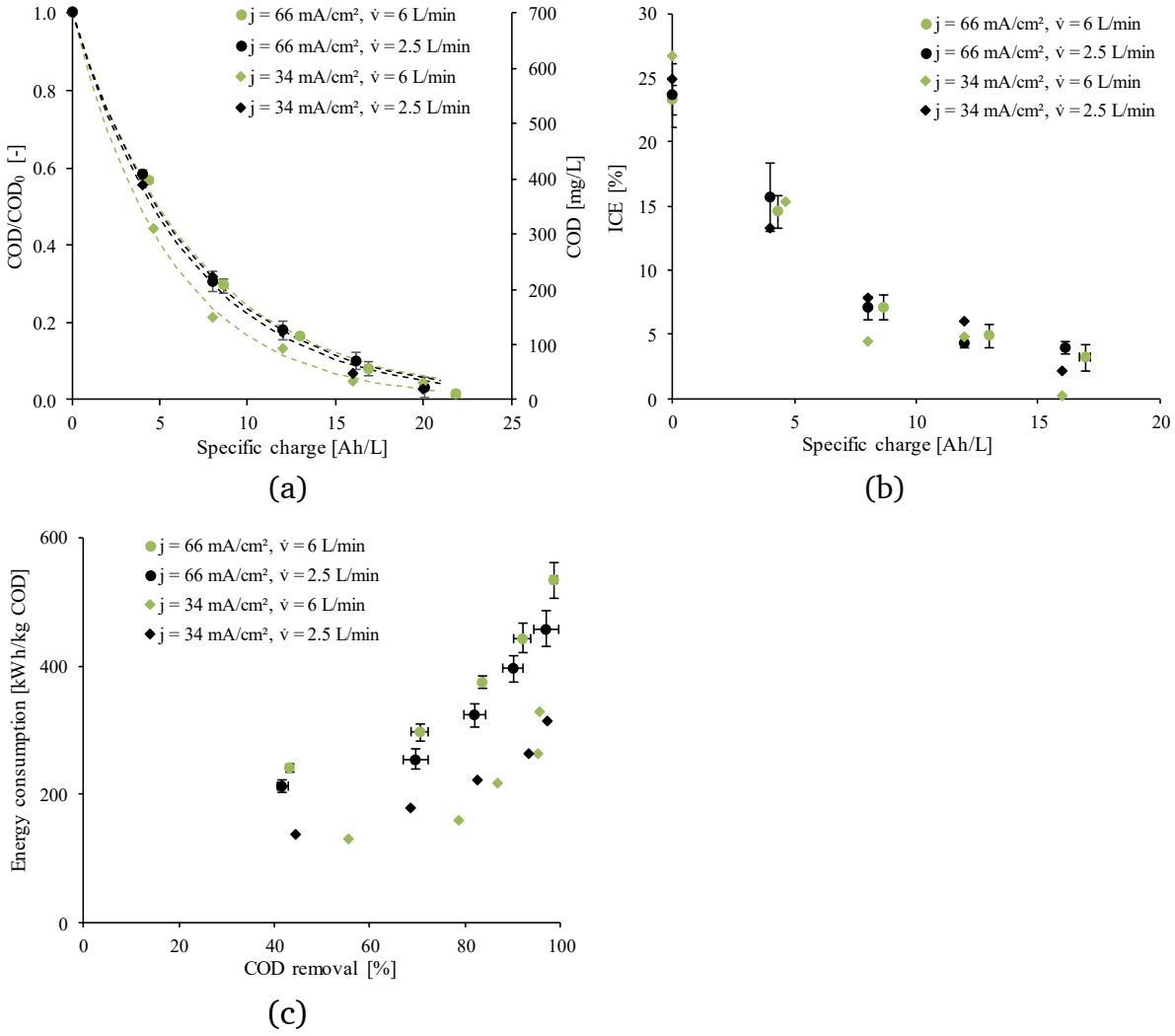

Figure 32: Evolution of a) COD, b) ICE, and c) energy consumption for different current densities and flow rates using MBR 1-10. Mean values ± STD, n=3 for 66 mA/cm² and n=2 for j = 34 mA/cm²

Energy consumption for oxidation increased excessively with increasing COD removal, especially from about 60 - 70% (Figure 32 c). This reflects the reduction in ICE with lowering COD concentrations. The lower current density j = 34 mA/cm² resulted in less energy consumption compared to j = 66 mA/cm². This resulted from the lower mean cell voltage of 10.4 ± 0.2 V compared to 16.1 ± 1.1 V at j = 66 mA/cm². However, less energy consumed comes at the cost of a longer treatment time for reaching the same charge input in Ah/L. The halved current density doubled the treatment time from 9.5 h to 18.2 h. This could be compensated by a larger anode area, but at higher investment costs. Hence, the optimum application of an EO must be assessed case by case.

It is generally agreed that different operating parameters of EO strongly influence the mineralization of wastewater contaminants (Kick et al. 2022; Matayeva and Biller 2021). We could not find such dependencies and suppose, that the range

of operation parameter variation could have been too little. Since a positive effect of a higher flow rate could not be ruled out, the flow rate was set to $\dot{v} = 6$ L/min for turbulent conditions (Re ≈ 2,600) in the flow cell. However, especially in a full-scale application, the trade-off between pump energy and transfer limitation has to be made. Besides, the higher current density of $j = 66$ mA/cm^2 was used.

7.3.2 Comparing the HTC process waters

7.3.2.1 COD removal and efficiency

The evolution of COD concentration during EO of PW-AD, MBR 1-1 and MBR 1-10 ($j = 66$ mA/cm^2 and $\dot{v} = 6$ L/min) is depicted in Figure 33 a. EO has succeeded in almost completely removing the COD from all process waters. Final COD concentrations were 109 mg/L and 184 mg/L in PW-AD and MBR 1-1, respectively. Despite an excessive charge input, COD of PW-AD and MBR 1-1 could not be decreased as low as for MBR 1-10. This indicates the formation of intermediates such as oxalic, oxamic, or formic acid, which can only hardly be mineralized by BDD(•OH) ((Brillas et al. 2010; Montenegro-Ayo et al. 2023; Olvera-Vargas et al. 2021). The COD decreased linearly at high COD concentrations. With lower COD concentrations, the linear reduction changed to exponential. This behaviour is characteristic for the electrochemical oxidation using constant current and assuming a hydroxyl radical or a direct electrochemical oxidation (Nasr et al. 2009). High COD concentrations are strongly related to current limitation, where a zero order kinetic defines the process. At lower COD concentrations, however, the mass transfer is limiting and determines the mineralization rate (Rodrigo et al. 2010). Accordingly, the behaviour of COD in PW-AD and MBR 1-1 shows the shift from current controlled to mass transport controlled operation. EO of MBR 1-10 was under mass transport controlled operation from the very beginning. The mineralization of COD could be facilitated by electrochemically generated oxidants, known as mediated or indirect oxidation. The presence of Cl^- lead to the formation of reactive chlorine species (RCS), which are the main agents of indirect oxidation (Sirés et al. 2014). This could ultimately lead to the formation of less reactive oxidants such as ClO_3^- and ClO_4^-, which are known to be toxic or hazardous (Brown and Gu 2006). We could not detect ClO_3^- and ClO_4^- due to the strong matrix of the process waters. Their formation could reflect in a raising toxicity, which did actually not increase during EO but even decreased (see section 7.3.2.3). However, we could measure initial Cl^- concentrations of up to 99.5 mg/L (Table 25). Chloride was below quantification limit (10 mg/L) after

EO, which could indicate the formation of RCS. The formation of RCS could not be ruled out, but appears to be less significant.

The shift from current controlled to mass transport controlled operation also reflects in the ICE, which remained at a high level close to 100% for PW-AD before rapidly dropping below 30% (see Figure 33 b). The ICE of MBR 1-1 was initially also 100%. However, due to the biological pretreatment and the associated lower COD concentration, the ICE dropped already at a lower specific charge. The severity of mass transfer limitation becomes even more evident when looking at MBR 1-10 with the lowest initial COD concentration and only 23% ICE. Organic contaminants could be reduced to low levels in all process waters, but at the expense of efficiency at little COD concentrations. The dropping ICE was strongly associated with the increase in side reactions, especially the formation of oxygen according to equation (15) (see Figure 38).

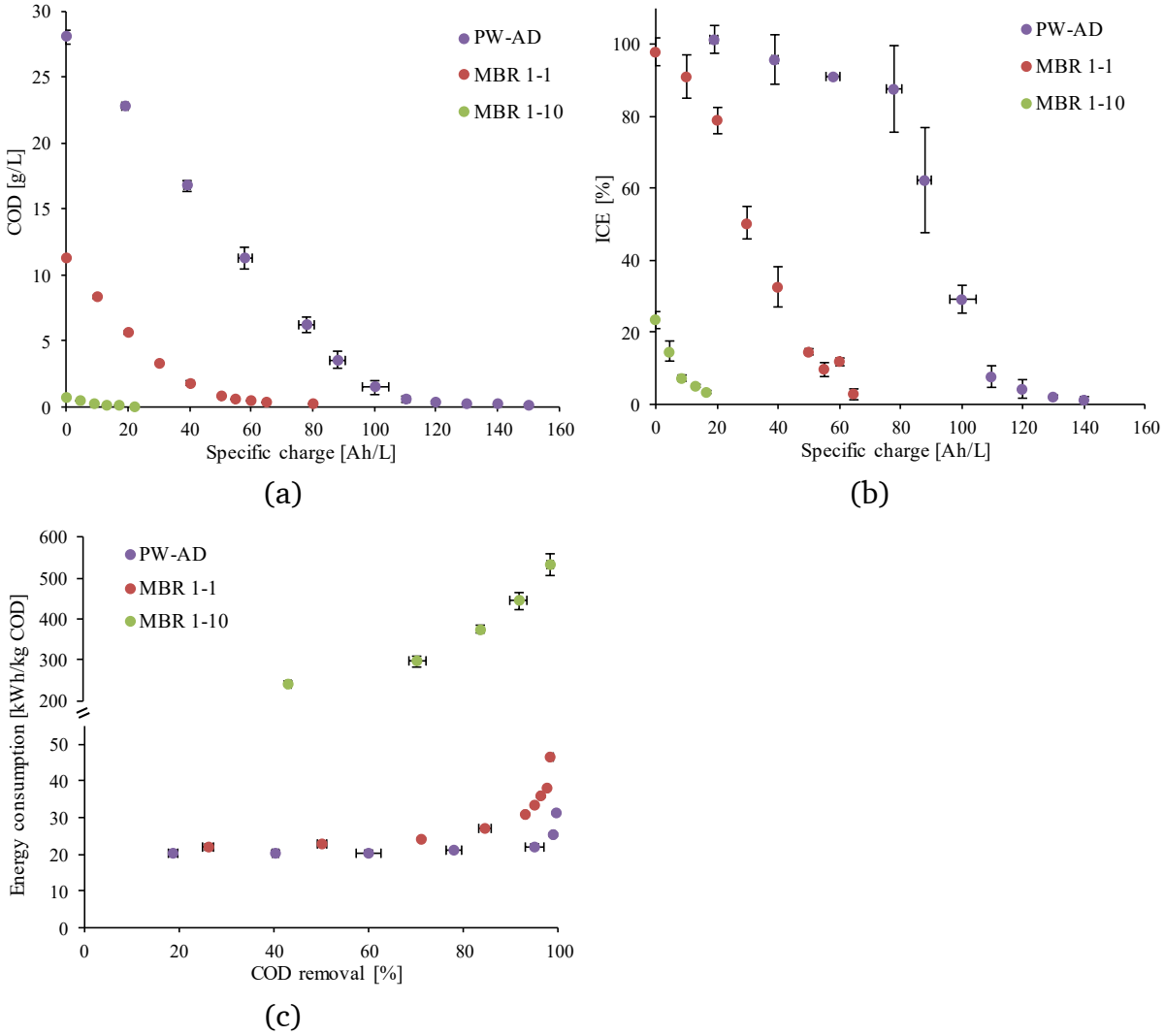

Figure 33: Comparison of a) COD, b) ICE, and c) EE/M for PW-AD, MBR 1-1, and MBR 1-10 (j = 66 mA/cm², $\dot{v}$ = 6 L/min). Mean values ± STD, n=3

The declining ICE with decreasing COD is reflected in the energy consumption (Figure 33, c). PW-AD had the lowest EE/M, which was relatively constant at 20.2 kWh/kg COD up to 95% COD removal. The EE/M jumped to 31.3 kWh/kg COD at higher COD removals. The mean cell voltage was 5.8 ± 0.2 V. MBR 1-1 had a higher voltage of 6.5 ± 0.1 V, which was responsible for the slightly higher energy consumption. EE/M started at 22.1 kWh/kg COD and significantly raised to 46.6 kWh/kg COD with higher COD removal. Previous studies reported comparable EE/M, such as 27.9 to 33.6 kWh/kg COD with $j = 30$ - 50 mA/cm^2 and COD removal of 95 - 99% for post-hydrothermal liquefaction wastewater (Ciarlini et al. 2020). For the aqueous phase of pyrolyzed sewage sludge, Kick et al. (2022) determined energy consumptions between 39.5 - 58.3 kWh/kg COD at $j = 50$ - 100 mA/cm^2 and COD removal of 87.9 - 97.7%. The energy consumption of EO for PW-AD and MBR 1-1 was similar to ozonation: Fettig et al. (2019) investigated the ozonation of the refractory substances of HTC process water from spent grain and swine mulch using an ozone dose of 2.5 kg O_3/kg COD. Assuming an energy consumption of 10 kWh/kg O_3 to provide the ozone (Hostachy et al. 2014), 25 kWh/kg COD would be necessary to oxidize the process water compounds.

The energy consumption of MBR 1-10 started at 241 kWh/kg COD for 41% COD removal and increased to 534 kWh/kg COD for 99% COD removal. Although this is within the range of literature values, e.g. 134 kWh/kg COD for landfill leachate (Anglada et al. 2011), the EO of MBR 1-10 consumed about ten times more energy compared to PW-AD and MBR 1-1. On the one hand, this resulted from the previously described mass transport limitation due to low COD concentration, which resulted in a low efficiency of EO. Therefore, higher COD concentrations are favorable regarding energetic costs (Fernandes et al. 2012). On the other hand, the voltage of 16.8 ± 0.5 V was more than doubled compared to PW-AD and MBR 1-1. This was caused by the lower concentration of the electrolyte, which also resulted in a significantly lower electrical conductivity (see Table 25). Adding supporting electrolytes such as $NaSO_4$ or NaCl would be beneficial for lowering the cell voltage and therefore the energy consumption. Though, some supporting electrolytes could significantly affect degradation kinetics by the formation of $SO^{\bullet-}_4$ and RCS (Moreira et al. 2017). Especially the addition of chlorides should be avoided due to the electrochemical formation of chlorinated compounds (Anglada et al. 2011). Treating MBR 1-10 using EO does not seem to be a viable solution from an energy point of view.

The removal of DOC during EO was similar to the removal of COD (data not shown). The DOC and the UV_{254} allows to calculate the SUVA as an indicator of aromaticity. For PW-AD, the SUVA increased from initially 1.5 L/(mg·m) to 2.7 L/(mg·m). Either substances with low aromaticity such as VFAs could be mineralized, while higher aromatic substances such as humic-like substances were mineralized less. A second possibility is the formation of aromatic by-products such as Benzaldehyde, 1,3,5-Benzenetriol or 1,2-benzenediol during EO (González-Arias et al. 2023). The SUVA of MBR 1-1 was higher at 2.9 L/(mg·m), because low aromatic compounds such as VFAs were removed during biological treatment. EO could lower the SUVA to 2.7 L/(mg·m) and therefore its aromaticity, which was confirmed in other studies (Matayeva and Biller 2021). The SUVAs of both wastewaters end up at 2.7 L/(mg·m). It could be hypothesized that similar substances have accumulated during EO of the wastewaters. For phenol, operating under current limitation was shown to lead to the formation of aromatic compounds. The low concentration of •OH relative to phenol led to the formation benzoquinone, hydroquinone and catechol. When mass transport was limited and the concentration of •OH relative to phenol high, phenol was directly mineralized to CO_2 (Kapalka et al. 2010; Iniesta et al. 2001). This could explain that the SUVA of MBR 1-10, which was operated under mass transfer limitation, decreased from 3.4 to 1.6 L/(mg·m).

For further characterizing the organics, the fractions of the non-adsorbable DOC were determined in the process water. In the chromatograms, the molecular weight of organics decreases from fraction I to V. Accordingly, many compounds with a low molecular weight were present (Fraction V), but almost no compounds with a very high molecular weight (Fraction I) (Figure 34 a). Aldehydes, sugars and amino acids, for example, which are present in large quantities in the process water, have a low molecular weight (Huang et al. 2021b; Huber et al. 2011). For this fraction, and also for the peak in fraction IV, the MBR effluent had a significantly lower signal in the chromatogram, whereas higher molecular weight compounds, especially fraction II, remained almost unchanged. After the EO of the MBR effluent, the overall signal decreased significantly and only minor peaks became apparent. The distribution of DOC fractions (Figure 34 b) of HTC process water and MBR effluent confirms that the lowest molecular weight fraction V is the one that is primarily biodegradable. Its percentage reduced from 58% in the process water to 36% in the MBR effluent. As higher molecular weight molecules (especially fraction II and III) were removed biologically to a lesser extent, their share doubled from 18% in the process water to 37% in the MBR effluent. Comparing MBR effluent and EO

effluent shows an almost identical distribution of fractions. This indicates that the EO was not very selective in removing organic matter with respect to its molecular weight.

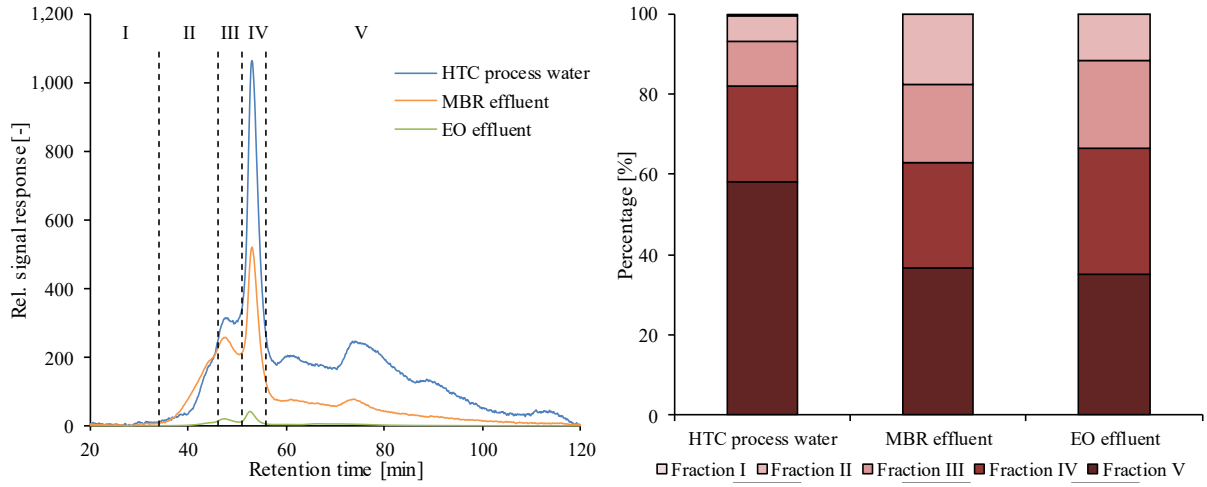

Figure 34: a) LC-OCD chromatogram and b) DOC fractions according to the retention time (I: 20 - 34 min, II: 34 -46 min, III: 46-51 min, IV: 51 - 56 min, V: >56 min)

7.3.2.2 Evolution of nitrogen species

In PW-AD and MBR 1-1, nitrogen was present as NH_4-N and DON (Figure 35 a, b). As a result of biomass growth and incorporation of nitrogen into biomass during biological treatment, nitrogen concentrations in MBR 1-1 were lowered compared to PW-AD. Nitrogen species in MBR 1-10 were mainly DON and small amounts of NH_4-N, NO_3-N and NO_2-N due to nitrification and denitrification (Figure 35 c). The behaviour of the nitrogen species during EO treatment was similar for all process waters: With higher charge input, the DON reduced and NO_3-N accumulated. NH_4-N increased until the middle of EO, but then declined again. Besides, NO_2-N was formed, but at insignificant concentrations compared to the other nitrogen species.

The results demonstrate, that EO can completely mineralize the refractory DON formed during HTC. Removing refractory N-heterocyclic compounds and melanoidins such as pyrrole and pyrazine using EO is in accordance with literature (Hiwarkar et al. 2017; Ciarlini et al. 2020; Cañizares et al. 2009). The oxidation pathway of organic nitrogen into nitrate in the absence of chloride is suggested via •OH. In the presence of chloride, the electrochemically generated hypochlorous acid oxidizes organic nitrogen to mainly chloramines and nitrogen gas (Schranck and Doudrick 2020).

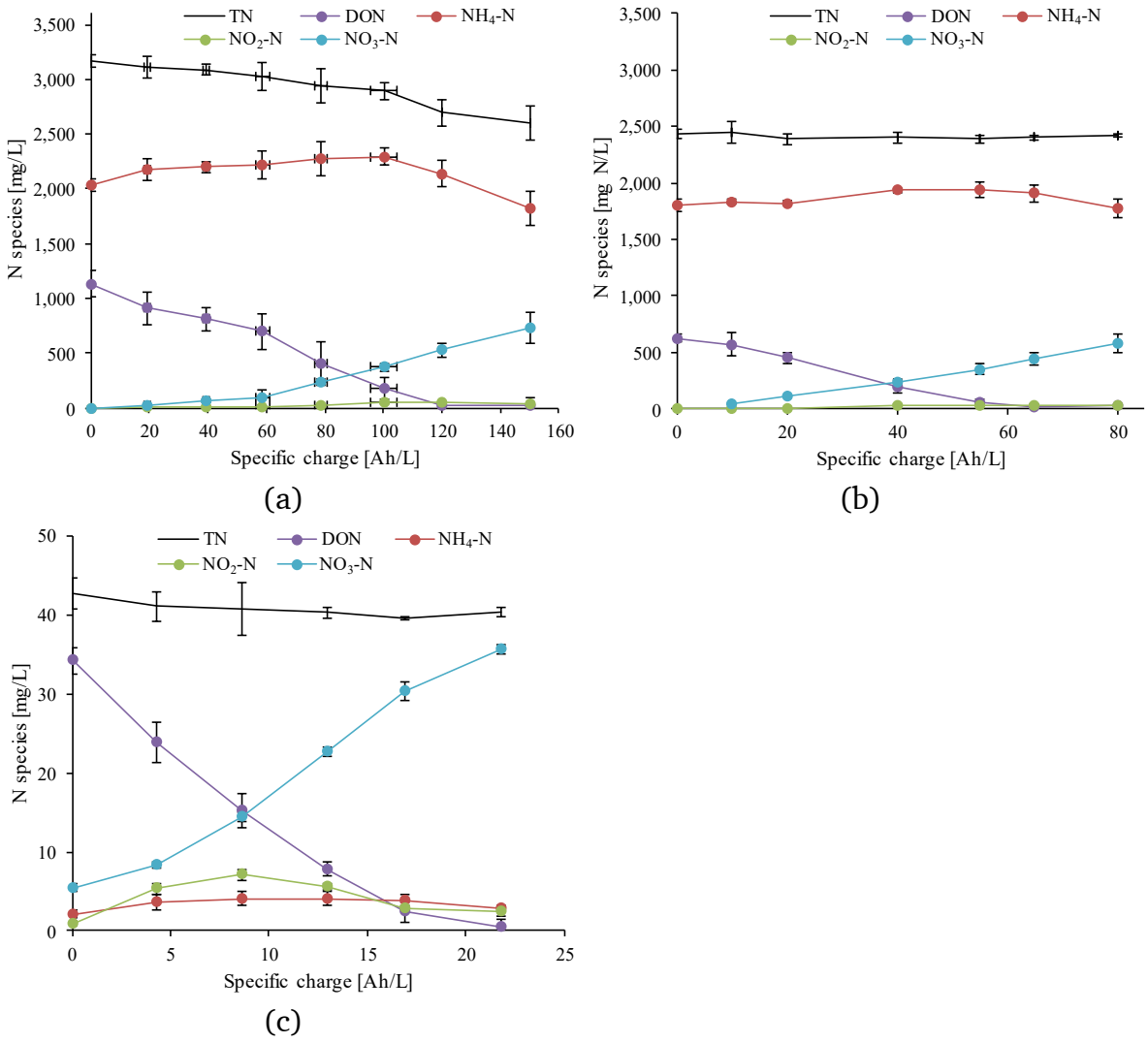

Figure 35: Evolution of N species during the EO of a) PW-AD, b) MBR 1-1, and c) MBR 1-10. Mean values ± STD, n=3

For each process water we observed a smaller increase of NO_3-N at the beginning of the EO than at the end. This could be attributed to the electrochemical reduction of nitrate ions at the cathode, which leads to the formation of ammonium and nitrite (Panizza and Cerisola 2005) according to equation (20) to (22).

$$NO_3^- + H_2O + 2e^- = NO_2^- + 2OH^- \quad (20)$$

$$NO_3^- + 3H_2O + 5e^- = \frac{1}{2}N_2 + 6OH^- \quad (21)$$

$$NO_3^- + 7H_2O + 8e^- = NH_4OH + 9OH^- \quad (22)$$

This could explain the temporary observed accumulation of NH_4-N and NO_2-N. Nitrite was described as an intermediate product, which can be electrochemically reduced to ammonia and nitrogen gas, but also oxidized back to nitrate

(Ghazouani et al. 2017). This could least partly explain the stronger increase in NO_3-N concentration in the second half of the experiments. Ciarlini et al. (2020) observed a similar elevated accumulation of nitrate above a certain electrical charge for a comparable wastewater, without finding the cause. The NO_3-N concentration in PW-AD and MBR 1-1 continued raising, even when the DON was already oxidized. As NH_4-N decreased simultaneously, nitrate seems to have been formed from ammonium. However, this is no favored reaction pathway in anodic oxidation (Lacasa et al. 2011; Martin de Vidales, M. J. et al. 2016). The conversion of ammonium to nitrate is described predominantly via hypochlorous acid according to equation (23), which requires the presence of chloride (Jermakka et al. 2021).

$$4HOCl + NH_4 = NO_3^- + H_2O + 6H^+ + 4Cl^- \quad (23)$$

In literature, ratios of chloride to ammonium in the range of 0.16 - 1.35 mg Cl^-/mg N were reported (Zöllig et al. 2017; Jermakka et al. 2021). Perhaps the lower ratio of 0.05 mg Cl^-/mg N in our tests was already sufficient. The mediated oxidation of ammonium to nitrate was proposed by Yang et al. (2022) via sulfate radicals, which are electrochemically generated from sulfate. However, this oxidation pathway seems appears to take place to a limited extent.

During EO, TN in PW-AD was removed, indicating the formation and removal of volatile nitrogen species such as mainly N_2, but also N_xO_y in small shares (Michels et al. 2010; Garcia-Segura et al. 2017). The removal of ammonium was described not via •OH but via the direct anodic oxidation of ammonia at the electrode surface according to equation (24) (Michels et al. 2010).

$$2NH_3 \rightarrow N_2 + 6H^+ + 6e^- \quad (24)$$

To shift the ammonium/ammonia dissociation equilibrium towards ammonia requires an alkaline pH. From 115 Ah/L, the pH was 8.1 (see Figure 39), where only a small share was present as ammonia (Kapałka et al. 2010). Considering the high concentrations of ammonium and compared to MBR 1-1 the longer oxidation time, this seems not unrealistic. The second and much faster conversion pathway of ammonium is again via RCS, particularly HOCl (equation (25) (Michels et al. 2010; Jermakka et al. 2021; Martin de Vidales, M. J. et al. 2016; Zöllig et al. 2017).

$$3HOCl + 2NH_4^+ \rightarrow N_2 + 3H_2O + 5H^+ + 3Cl^- \quad (25)$$

The mediated conversion of ammonium in the experiments by RCS cannot be generally ruled out, but cannot be quantified either. The decreasing TN for similar complex wastewaters has been reported and was attributed to lower current densities (Ciarlini et al. 2020; Kick et al. 2022; Matayeva and Biller 2021), but no reaction mechanisms were described.

7.3.2.3 Toxicity of the HTC process waters

The toxicity of PW-AD was $G_L < 254$, which was reduced slightly to $G_L < 192$ by biological pre-treatment. Due to the additional dilution of MBR 1-10, its toxicity was $G_L < 16$. This corresponds to EC_{50} of 1.9%, 2.2%, and 20.1%. For raw HTC process water, Mihajlović et al. (2018) and Mantovani et al. (2022) reported values for EC_{50} of 0.7 - 1.3% and 1.8%, respectively. Interestingly, the EC_{50} is of same magnitude despite their different HTC feedstock (*Miscanthus x giganteus* and microalgae). After EO, the toxicity was significantly reduced to 57.7% (PW-AD) and 50.6% (MBR 1-1). EO of MBR 1-10 showed no inhibition of bioluminescence against *Vibrio fischeri* at all. Whether EO can reduce toxicity at all strongly depends on the wastewater constituents. Accordingly, opposite trends in toxicity were observed (Carboneras Contreras et al. 2020; Trellu et al. 2016), especially when highly toxic chlorinated by-products were formed (Periyasamy et al. 2022). Our results suggest no formation of toxic by-products such as chlorate and perchlorate, even though the toxicity of PW-AD and MBR 1-1 could not be completely removed.

7.3.3 Integrating EO into a treatment concept for HTC process water

An effective application of EO strongly depends on the pretreatment of HTC process water. Therefore, several opportunities for integrating EO with BDD for HTC process water treatment have to be evaluated (Figure 36). High concentrations of ammonium in the oxidized PW-AD and MBR 1-1 allow nitrogen recovery. Considering the increasing importance of resource protection, this seems to be more appropriate than the removal of nitrogen by nitrification and denitrification (MBR 1-10).

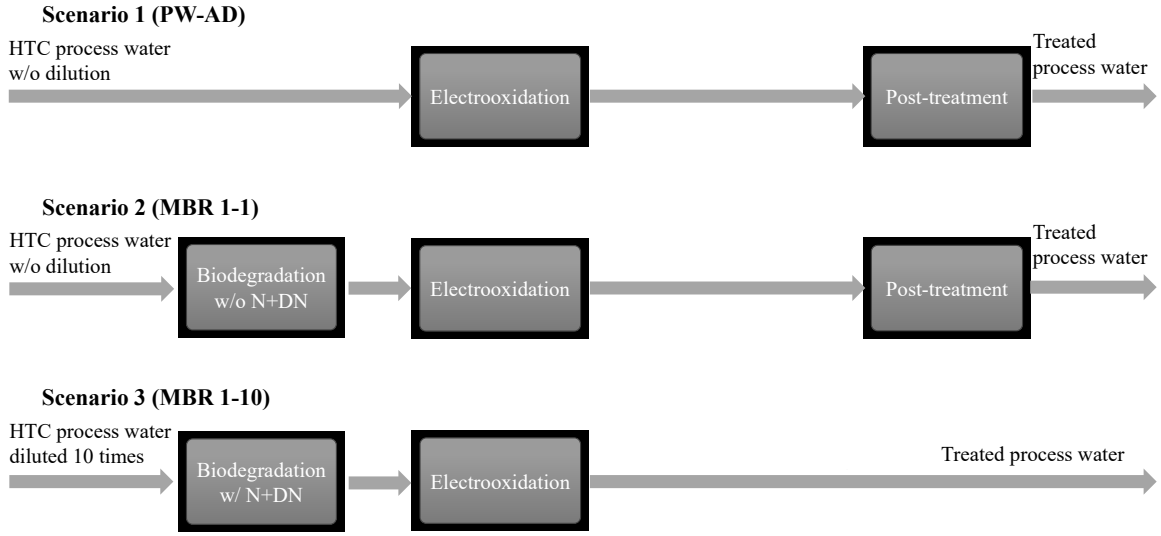

Figure 36: Scenarios for integrating the BDD into a treatment concept for HTC process water

Scenario 1 (PW-AD): BDD only

BDD achieved superior performance in terms of COD and DON removal. The COD was oxidized at the highest energy efficiency of all scenarios, but the load of organic substances to be oxidized was the highest. Post-treatment e.g. by adsorption would be necessary to further reduce COD, which would also remove some of the oxidation by-products and probably toxicity. High ammonium concentrations in the effluent allow the recovery of nitrogen e.g. by air stripping or membrane processes.

Scenario 2 (MBR 1-1): Biodegradation without N+DN and BDD

Biological pretreatment reduced the process waters organics to a limited extent. Since no nitrification and denitrification was reached, ammonium concentrations remained also high. Due to lower initial COD, the EO of MBR 1-1 was less efficient than the EO of PW-AD. Again, post-treatment of the oxidized MBR 1-1 would be necessary and the recovery of nitrogen is recommended.

Scenario 3 (MBR 1-10): Biodegradation with N+DN and BDD

Due to dilution before biological treatment, nitrification and denitrification was established and refractory COD and DON were significantly lower than in scenario 1 and 2. This was associated with a lower oxidation efficiency and a higher specific energy consumption of the EO. In return, the COD was reduced to very low concentrations. Since nitrification removed ammonium almost completely, no nitrogen recovery would be possible. Considering the very low effluent COD and toxicity, a post-treatment seems not mandatory.

The most viable scenario seems to be scenario 2. Compared to scenario 1, the energy consumption is only a little bit higher, but 60% of COD was already removed during less energy consuming biological treatment. The high energy demand suggests that scenario 3 is unrealistic for a full-scale application. For the optimization of scenario 2, less extensive EO could be considered. The EO was quite efficient (ICE = 33%) up to 40 Ah/L, where the COD removal was 84%, the residual COD 1,760 mg/L, and the energy consumption 27.2 kWh/kg COD. Further COD reduction by downstream treatment technologies such as activated carbon adsorption would be required, depending on the required discharge limits. In exchange, a higher residual COD after EO is associated with a higher loading of the post-treatment and therefore a higher demand of activated carbon. In addition, a review shows that EO could increase the biodegradability, which would be most interesting for a treatment concept (Mousset et al. 2021). The ecologically and economically most viable process concept is to be examined considering various boundary conditions and should be the subject of future studies.

7.4 Conclusions

The treatment of sewage sludge by HTC produces highly contaminated process water. To establish HTC as a sustainable alternative for sludge treatment, strategies for treating process water must be developed. Electrochemical oxidation using BDD is a promising technology to remove a large amount of the organic load and the refractory components. The following conclusions can be drawn:

- EO could remove COD and DON of the raw HTC process water as well as the refractory COD and DON of the pre-treated process waters by more than 97%.
- The significantly lower energy consumption for PW-AD and MBR 1-1 resulted from the high COD concentrations and therefore current limited operation.
- DON was mainly converted to nitrate and to a small extent to nitrite and ammonium.
- EO significantly reduced the toxicity of the tested process water, whereas biological treatment was only marginally effective.

- The results indicate two approaches for treating the process water: One is the recovery of nitrogen (Scenario 1 and 2) and the other is the maximized removal of pollutants (Scenario 3).

The scenario pursued ultimately depends on the objective of the treatment and boundary conditions. In any case, the full-scale application of BDD for treating HTC process water needs further optimization. Reducing the current density would result in lower operating costs, but at the expense of longer treatment times or larger anode areas and thus higher capital costs. Furthermore, additives might be added to increase the electrical conductivity of the electrolyte.

Funding

This research was funded by the German Federal Ministry of Education and Research (BMBF) within the project “IntenKS”, grant number 02WCL1470A.

Author contributions

Conceptualization, T.B.; methodology, T.B.; validation, T.B. and M.E.; investigation, T.B.; data curation, T.B.; writing - original draft preparation, T.B.; writing - review and editing, M.E.; visualization, T.B.; supervision, M.E.; project administration, T.B. and M.E.; funding acquisition, M.E. All authors have read and agreed to the published version of the manuscript.

7.5 References

Anglada, A.; Urtiaga, A.; Ortiz, I.; Mantzavinos, D.; Diamadopoulos, E. (2011): Boron-doped diamond anodic treatment of landfill leachate: evaluation of operating variables and formation of oxidation by-products. In Water Res. 45 (2), pp. 828–838. DOI: 10.1016/j.watres.2010.09.017.

Barrera-Díaz, C.; Canizares, P.; Fernández, F. J.; Natividad, R.; Rodrigo, M. A. (2014): Electrochemical Advanced Oxidation Processes: An Overview of the Applications to Actual Industrial Effluents. In J. Mex. Chem. Soc. 58 (3), pp. 256–275.

Bensalah, N.; Louhichi, B.; Abdel-Wahab, A. (2012): Electrochemical oxidation of succinic acid in aqueous solutions using boron doped diamond anodes. In Int. J. Environ. Sci. Technol. 9 (1), pp. 135–143. DOI: 10.1007/s13762-011-0007-5.

Blach, T.; Lechevallier, P.; Engelhart, M. (2023): Effect of temperature during the hydrothermal carbonization of sewage sludge on the aerobic treatment of

the produced process waters. In J. Water Process. Eng. 51, p. 103368. DOI: 10.1016/j.jwpe.2022.103368.

Brillas, E.; Garcia-Segura, S.; Skoumal, M.; Arias, C (2010): Electrochemical incineration of diclofenac in neutral aqueous medium by anodic oxidation using Pt and boron-doped diamond anodes. In Chemosphere 79 (6), pp. 605–612. DOI: 10.1016/j.chemosphere.2010.03.004.

Brown, G. M.; Gu, B. (2006): The Chemistry of Perchlorate in the Environment. In B. Gu, J. D. Coates (Eds.): Perchlorate. Boston: Kluwer Academic Publishers, pp. 17–47.

Cañizares, P.; Hernández-Ortega, M.; Rodrigo, M. A.; Barrera-Díaz, C. E.; Roa-Morales, G.; Sáez, C. (2009): A comparison between Conductive-Diamond Electrochemical Oxidation and other Advanced Oxidation Processes for the treatment of synthetic melanoidins. In J. Hazard. Mater. 164 (1), pp. 120–125. DOI: 10.1016/j.jhazmat.2008.07.134.

Carboneras, M. B.; Villaseñor, J.; Fernández, F. J.; Rodrigo, M. A.; Cañizares, P. (2020): Selection of anodic material for the combined electrochemical-biological treatment of lindane polluted soil washing effluents. In J. Hazard. Mater. 384, p. 121237. DOI: 10.1016/j.jhazmat.2019.121237.

Carboneras Contreras, M. B.; Villaseñor C., J.; Fernández-Morales, F. J.; Cañizares, P. C.; Rodrigo, M. A. R. (2020): Biodegradability improvement and toxicity reduction of soil washing effluents polluted with atrazine by means of electrochemical pre-treatment: Influence of the anode material. In J. Environ. Manage. 255, p. 109895. DOI: 10.1016/j.jenvman.2019.109895.

Chatzisymeon, E.; Xekoukoulotakis, N. P.; Coz, A.; Kalogerakis, N.; Mantzavinos, D. (2006): Electrochemical treatment of textile dyes and dyehouse effluents. In J. Hazard. Mater. 137 (2), pp. 998–1007. DOI: 10.1016/j.jhazmat.2006.03.032.

Ciarlini, J.; Alves, L.; Rajarathnam, G. P.; Haynes, B. S.; Montoya, A. (2020): Electrochemical oxidation of nitrogen-rich post-hydrothermal liquefaction. In Algal Res. (48), p. 101919. DOI: 10.1016/j.algaI.2020.101919.

Fang, J.; Zhan, L.; Ok, Y. S.; Gao, B. (2018): Minireview of potential applications of hydrochar derived from hydrothermal carbonization of biomass. In J. Ind. Eng. Chem. 57, pp. 15–21.

Fernandes, A.; Pacheco, M. J.; Ciríaco, L.; Lopes, A. (2012): Anodic oxidation of a biologically treated leachate on a boron-doped diamond anode. In J. Hazard. Mater. 199-200, pp. 82–87. DOI: 10.1016/j.jhazmat.2011.10.074.

Fettig, J.; Austermann-Haun, U.; Meier, J.-F.; Busch, A.; Gilbert, E. (2019): Options for Removing Refractory Organic Substances in Pre-Treated Process Water from Hydrothermal Carbonization. In Water 11 (4), p. 730. DOI: 10.3390/w11040730.

Garcia-Rodriguez, O.; Mousset, E.; Olvera-Vargas, H.; Lefebvre, O. (2020): Electrochemical treatment of highly concentrated wastewater: A review of experimental and modeling approaches from lab- to full-scale. In Cri. Rev. Environ. Sci. Technol. 52 (2), pp. 240–309. DOI: 10.1080/10643389.2020.1820428.

Garcia-Segura, S.; Mostafa, E.; Baltruschat, H. (2017): Could NOx be released during mineralization of pollutants containing nitrogen by hydroxyl radical? Ascertaining the release of N-volatile species. In Appl. Catal. B: Environ. 207, pp. 376–384. DOI: 10.1016/j.apcatb.2017.02.046.

Gaur, R. Z.; Khoury, O.; Zohar, M.; Poverenov, E.; Darzi, R.; Laor, Y.; Posmanik, R. (2020): Hydrothermal carbonization of sewage sludge coupled with anaerobic digestion: Integrated approach for sludge management and energy recycling. In Energy Convers. Manag. 224, p. 113353.

Ghazouani, M.; Akrout, H.; Bousselmi, L. (2017): Nitrate and carbon matter removals from real effluents using Si/BDD electrode. In Environ. Sci. Pollut. Res. 24 (11), pp. 9895–9906. DOI: 10.1007/s11356-016-7563-7.

González-Arias, J.; La Rubia, M. A. de; Sánchez, M. E.; Gómez, X.; Cara-Jiménez, J.; Martínez, E. J. (2023): Treatment of hydrothermal carbonization process water by electrochemical oxidation: Assessment of process performance. In Environ. Res. 216 (Pt 4), p. 114773. DOI: 10.1016/j.envres.2022.114773.

Groenen-Serrano, K.; Weiss-Hortala, E.; Savall, A.; Spiteri, P. (2013): Role of Hydroxyl Radicals During the Competitive Electrooxidation of Organic Compounds on a Boron-Doped Diamond Anode. In Electrocatalysis 4 (4), pp. 346–352. DOI: 10.1007/s12678-013-0150-5.

Guinea, E.; Garrido, J. A.; Rodríguez, R. M.; Cabot, P.-L.; Arias, C.; Centellas, F.; Brillas, E. (2010): Degradation of the fluoroquinolone enrofloxacin by electrochemical advanced oxidation processes based on hydrogen peroxide

electrogeneration. In Electrochim. Acta 55 (6), pp. 2101–2115. DOI: 10.1016/j.electacta.2009.11.040.

He, C.; Wang, K.; Yang, Y.; Amaniampong, P. N.; Wang, J.-Y. (2015): Effective nitrogen removal and recovery from dewatered sewage sludge using a novel integrated system of accelerated hydrothermal deamination and air stripping. In Environ. Sci. Technol. 49 (11), pp. 6872–6880. DOI: 10.1021/acs.est.5b00652.

Hiwarkar, A. D.; Singh, S.; Srivastava, V. C.; Mall, I. D. (2017): Mineralization of pyrrole, a recalcitrant heterocyclic compound, by electrochemical method: Multi-response optimization and degradation mechanism. In J. Environ. Manag. 198, pp. 144–152. DOI: 10.1016/j.jenvman.2017.04.051.

Hostachy, J.-C.; van Wyk, B.; Metais, A. (2014): Use of Ozone in the Pulp and Paper Industry. In Paper Asia 30 (2), pp. 22–28.

Hu, R.; Liu, Y.; Zhu, G.; Chen, C.; H., Dwi; Yan, M. (2022): COD removal of wastewater from hydrothermal carbonization of food waste: Using coagulation combined activated carbon adsorption. In J. Water Process. Eng. 45, p. 102462. DOI: 10.1016/j.jwpe.2021.102462.

Huang, F.; Liu, H.; Wen, J.; Zhao, C.; Dong, L. (2021a): Underestimated humic acids release and influence on anaerobic digestion during sludge thermal hydrolysis. In Water Res. 201, p. 117310. DOI: 10.1016/j.watres.2021.117310.

Huang, J.; Wang, Z.; Qiao, Y.; Wang, B.; Yu, Y.; Xu, M. (2021b): Transformation of nitrogen during hydrothermal carbonization of sewage sludge: Effects of temperature and Na/Ca acetates addition. In P. Combust. Inst. 38 (3), pp. 4335–4344. DOI: 10.1016/j.proci.2020.06.075.

Huber, Stefan A.; Balz, Andreas; Abert, Michael; Pronk, Wouter (2011): Characterisation of aquatic humic and non-humic matter with size-exclusion chromatography--organic carbon detection--organic nitrogen detection (LC-OCD-OND). In Water Res. 45 (2), pp. 879–885. DOI: 10.1016/j.watres.2010.09.023.

Iniesta, J.; Michaud, P. A.; Panizza, M.; Cerisola, G.; Aldaz, A.; Comninellis, C. (2001): Electrochemical oxidation of phenol at boron-doped diamond electrode. In Electrochim. Acta 46 (23), pp. 3573–3578. DOI: 10.1016/S0013-4686(01)00630-2.

Jermakka, J.; Freguia, S.; Kokko, M.; Ledezma, P. (2021): Electrochemical system for selective oxidation of organics over ammonia in urine. In Environmental Science: Water Res. Technol. 7 (5), pp. 942–955. DOI: 10.1039/D0EW01057J.

Kapalka, A.; Fóti, G.; Comninellis, C. (2008): Kinetic modelling of the electrochemical mineralization of organic pollutants for wastewater treatment. In J. Appl. Electrochem. (38), pp. 7–16. DOI: 10.1007/s10800-007-9365-6.

Kapalka, A.; Fóti, G.; Comninellis, C. (2010): Basic Principles of the Electrochemical Mineralization of Organic Pollutants for Wastewater Treatment. In Christos Comninellis, Guohua Chen (Eds.): Electrochemistry for the Environment. New York, NY: Springer New York, pp. 1–23.

Kapałka, A.; Joss, L.; Anglada, Á.; Comninellis, C.; Udert, K. M. (2010): Direct and mediated electrochemical oxidation of ammonia on boron-doped diamond electrode. In Electrochem. Commun. 12 (12), pp. 1714–1717. DOI: 10.1016/j.elecom.2010.10.004.

Kick, C.; Uchaikina, A.; Apfelbacher, A.; Daschner, R.; Helmreich, B.; Hornung, A. (2022): Aqueous phase of thermo-catalytic reforming of sewage sludge – quantity, quality, and its electrooxidative treatment by a boron-doped diamond electrode. In Sep. Purif. Technol. 286, p. 120392. DOI: 10.1016/j.seppur.2021.120392.

Lacasa, E.; Cañizares, P.; Llanos, J.; Rodrigo, M. A. (2011): Removal of nitrates by electrolysis in non-chloride media: Effect of the anode material. In Sep. Purif. Technol. 80 (3), pp. 592–599. DOI: 10.1016/j.seppur.2011.06.015.

Langone, Michela; Basso, Daniele (2020): Process Waters from Hydrothermal Carbonization of Sludge: Characteristics and Possible Valorization Pathways. In Int. J. Environ. Res. Pub. He. 17 (18). DOI: 10.3390/ijerph17186618.

Li, C.; Wang, X.; Zhang, G.; Yu, G.; Lin, J.; Wang, Y. (2017): Hydrothermal and alkaline hydrothermal pretreatments plus anaerobic digestion of sewage sludge for dewatering and biogas production: Bench-scale research and pilot-scale verification. In Water Res. (117), pp. 49–57. DOI: 10.1016/j.watres.2017.03.047.

Liakos, T. I.; Sotiropoulos, S.; Lazaridis, N. K. (2017): Electrochemical and bio-electrochemical treatment of baker's yeast effluents. In J. Environ. Chem. Eng. (5), pp. 699–708. DOI: 10.1016/j.jece.2016.12.048.

Liu, L.; Zhai, Y.; Liu, X.; Wang, Z.; Zhu, Y.; Xu, M. (2022): Features and mechanisms of sewage sludge hydrothermal carbonization aqueous phase after ferrous/persulfate-based process: The selective effect of oxidation and coagulation. In J. Clean. Prod. 366, p. 132831. DOI: 10.1016/j.jclepro.2022.132831.

Mantovani, M.; Collina, E.; Marazzi, F.; Lasagni, M.; Mezzanotte, V. (2022): Microalgal treatment of the effluent from the hydrothermal carbonization of microalgal biomass. In J. Water Process. Eng. 49, p. 102976. DOI: 10.1016/j.jwpe.2022.102976.

Martin de Vidales, M. J.; Millán, M.; Sáez, C.; Cañizares, P.; Rodrigo, M. A. (2016): What happens to inorganic nitrogen species during conductive diamond electrochemical oxidation of real wastewater? In Electrochem. Commun. 67, pp. 65–68. DOI: 10.1016/j.elecom.2016.03.014.

Matayeva, A.; Biller, P. (2021): Hydrothermal liquefaction aqueous phase treatment and hydrogen production using electro-oxidation. In Energy Convers. Manag. 244, p. 114462. DOI: 10.1016/j.enconman.2021.114462.

Michels, N.-L.; Kapałka, A.; Abd-El-Latif, A. A.; Baltruschat, H.; Comninellis, C. (2010): Enhanced ammonia oxidation on BDD induced by inhibition of oxygen evolution reaction. In Electrochem. Commun. 12 (9), pp. 1199–1202. DOI: 10.1016/j.elecom.2010.06.018.

Mihajlović, Marija; Petrović, Jelena; Maletić, Snežana; Isakovski, Marijana Kragulj; Stojanović, Mirjana; Lopičić, Zorica; Trifunović, Snežana (2018): Hydrothermal carbonization of Miscanthus × giganteus: Structural and fuel properties of hydrochars and organic profile with the ecotoxicological assessment of the liquid phase. In Energy Convers. Manag. 159, pp. 254–263. DOI: 10.1016/j.enconman.2018.01.003.

Montenegro-Ayo, R.; Pérez, T.; Lanza, M. R.V.; Brillas, E.; Garcia-Segura, S.; Dos Santos, A. J. (2023): New electrochemical reactor design for emergent pollutants removal by electrochemical oxidation. In Electrochim. Acta 458, p. 142551. DOI: 10.1016/j.electacta.2023.142551.

Moreira, F. C.; Boaventura, R. A. R.; Brillas, E.; Vilar, V. J. P. (2017): Electrochemical advanced oxidation processes: A review on their application to synthetic and real wastewaters. In Appl. Catal. B: Environ. 202, pp. 217–261. DOI: 10.1016/j.apcatb.2016.08.037.

Mousset, E.; Trellu, C.; Olvera-Vargas, H.; Pechaud, Y.; Fourcade, F.; Oturan, M. A. (2021): Electrochemical technologies coupled with biological treatments. In Curr. Opin. Electrochem. 26, p. 100668. DOI: 10.1016/j.coelec.2020.100668.

Nasr, B.; Hsen, T.; Abdellatif, G. (2009): Electrochemical treatment of aqueous wastes containing pyrogallol by BDD-anodic oxidation. In J. Environ. Manag. 90 (1), pp. 523–530. DOI: 10.1016/j.jenvman.2007.12.007.

Olvera-Vargas, H.; Gore-Datar, N.; Garcia-Rodriguez, O.; Mutnuri, S.; Lefebvre, O. (2021): Electro-Fenton treatment of real pharmaceutical wastewater paired with a BDD anode: Reaction mechanisms and respective contribution of homogeneous and heterogeneous OH. In Chem. Eng. J. 404, p. 126524. DOI: 10.1016/j.cej.2020.126524.

Panizza, M.; Cerisola, G. (2005): Application of diamond electrodes to electrochemical processes. In Electrochim. Acta 51 (2), pp. 191–199. DOI: 10.1016/j.electacta.2005.04.023.

Panizza, M.; Cerisola, G. (2009): Direct And Mediated Anodic Oxidation of Organic Pollutants. In Chem. Rev. 109 (12), pp. 6541–6569. DOI: 10.1021/cr9001319.

Panizza, M.; Michaud, P. A.; Cerisola, G.; Comninellis, C. (2001): Anodic oxidation of 2-naphthol at boron-doped diamond electrodes. In J. Electroanal. Chem. (507), pp. 206–214. DOI: 10.1016/S0022-0728(01)00398-9.

Patel, P.S.; Bandre, N.; Saraf, A.; Ruparelia, J. P. (2013): Electro-catalytic Materials (Electrode Materials) in Electrochemical Wastewater Treatment. In Procedia Eng. 51, pp. 430–435. DOI: 10.1016/j.proeng.2013.01.060.

Periyasamy, S.; Lin, X.; Ganiyu, S. O.; Kamaraj, S.-K.; Thiam, A.; Liu, D. (2022): Insight into BDD electrochemical oxidation of florfenicol in water: Kinetics, reaction mechanism, and toxicity. In Chemosphere 288, p. 132433. DOI: 10.1016/j.chemosphere.2021.132433.

Rajkumar, D.; Kim, Jong Guk (2006): Oxidation of various reactive dyes with in situ electro-generated active chlorine for textile dyeing industry wastewater treatment. In J. Hazard. Mater. 136 (2), pp. 203–212. DOI: 10.1016/j.jhazmat.2005.11.096.

Rodrigo, M. A.; Cañizares, P.; Sánchez-Carretero, A.; Sáez, C. (2010): Use of conductive-diamond electrochemical oxidation for wastewater treatment. In Catal. Today 151 (1-2), pp. 173–177. DOI: 10.1016/j.cattod.2010.01.058.

Särkkä, H.i; Bhatnagar, A.; Sillanpää, M. (2015): Recent developments of electro-oxidation in water treatment — A review. In J. Electroanal. Chem. 754, pp. 46–56. DOI: 10.1016/j.jelechem.2015.06.016.

Schranck, A.; Doudrick, K. (2020): Effect of reactor configuration on the kinetics and nitrogen byproduct selectivity of urea electrolysis using a boron doped diamond electrode. In Water Res. 168, p. 115130. DOI: 10.1016/j.watres.2019.115130.

Serrano, K.; Michaud, P. A.; Comninellis, C.; Savall, A. (2002): Electrochemical preparation of peroxodisulfuric acid using boron doped diamond thin film electrodes. In Electrochim. Acta (48), pp. 432–436. DOI: 10.1016/S0013-4686(02)00688-6.

Shestakova, M.; Sillanpää, M. (2017): Electrode materials used for electrochemical oxidation of organic compounds in wastewater. In Rev. Environ. Sci. Bio/Technol. 16 (2), pp. 223–238. DOI: 10.1007/s11157-017-9426-1.

Shrestha, A.; Acharya, B.; Farooque, A. A. (2021): Study of hydrochar and process water from hydrothermal carbonization of sea lettuce. In Renew. Energy 163, pp. 589–598. DOI: 10.1016/j.renene.2020.08.133.

Sirés, I.; Brillas, E.; Oturan, M. A.; Rodrigo, M. A.; Panizza, M. (2014): Electrochemical advanced oxidation processes: today and tomorrow. A review. In Environ. Sci. Pol. Res. Int. 21 (14), pp. 8336–8367. DOI: 10.1007/s11356-014-2783-1.

Souza, R. B. A.; Ruotolo, L. A. M. (2013): Electrochemical treatment of oil refinery effluent using boron-doped diamond anodes. In J. Environ. Chem. Eng. 1 (3), pp. 544–551. DOI: 10.1016/j.jece.2013.06.020.

Trellu, C.; Ganzenko, O.; Papirio, S.; Pechaud, Y.; Oturan, N.; Huguenot, D. et al. (2016): Combination of anodic oxidation and biological treatment for the removal of phenanthrene and Tween 80 from soil washing solution. In Chem. Eng. J. 306, pp. 588–596. DOI: 10.1016/j.cej.2016.07.108.

Vernasqui, L. G.; Dos Santos, A. J.; Fortunato, G. V.; Kronka, M. S.; Barazorda-Ccahuana, H. L.; Fajardo, A. S. et al. (2022): Highly porous seeding-free boron-doped ultrananocrystalline diamond used as high-performance anode for electrochemical removal of carbaryl from water. In Chemosphere 305, p. 135497. DOI: 10.1016/j.chemosphere.2022.135497.

Wang, P.; Sakhno, Y.; Adhikari, S.; Peng, H.; Jaisi, D.; Soneye, T. et al. (2021): Effect of ammonia removal and biochar detoxification on anaerobic digestion of aqueous phase from municipal sludge hydrothermal liquefaction. In Biores. Technol. (326). DOI: 10.1016/j.biortech.2021.124730.

Yang, S.; Hu, X.; You, X.; Zhang, W.; Liu, Y.; Liang, W. (2022): Removal of Ammonia Using Persulfate during the Nitrate Electro-Reduction Process. In Int. J. Env. Res. Pub. He. 19 (6). DOI: 10.3390/ijerph19063270.

Yao, J.; Mei, Y.; Xia, G.; Lu, Y.; Xu, D.; Sun, N. et al. (2019): Process Optimization of Electrochemical Oxidation of Ammonia to Nitrogen for Actual Dyeing Wastewater Treatment. In Int. J. Env. Res. Pub. He. 16 (16). DOI: 10.3390/ijerph16162931.

Zhao, J.; Hou, T.; Zhang, Z.; Shimizu, K.; Lei, Z.; Lee, D.-J. (2020): Anaerobic co-digestion of hydrolysate from anaerobically digested sludge with raw waste activated sludge: Feasibility assessment of new sewage sludge management strategy in the context of a local wastewater treatment plant. In Biores. Technol. 314, p. 123748.

Zöllig, H.; Remmele, A.; Morgenroth, E.; Udert, K. M. (2017): Removal rates and energy demand of the electrochemical oxidation of ammonia and organic substances in real stored urine. In Water Res. Technol. 3 (3), pp. 480–491. DOI: 10.1039/c7ew00014f.

7.6 Supplementary material

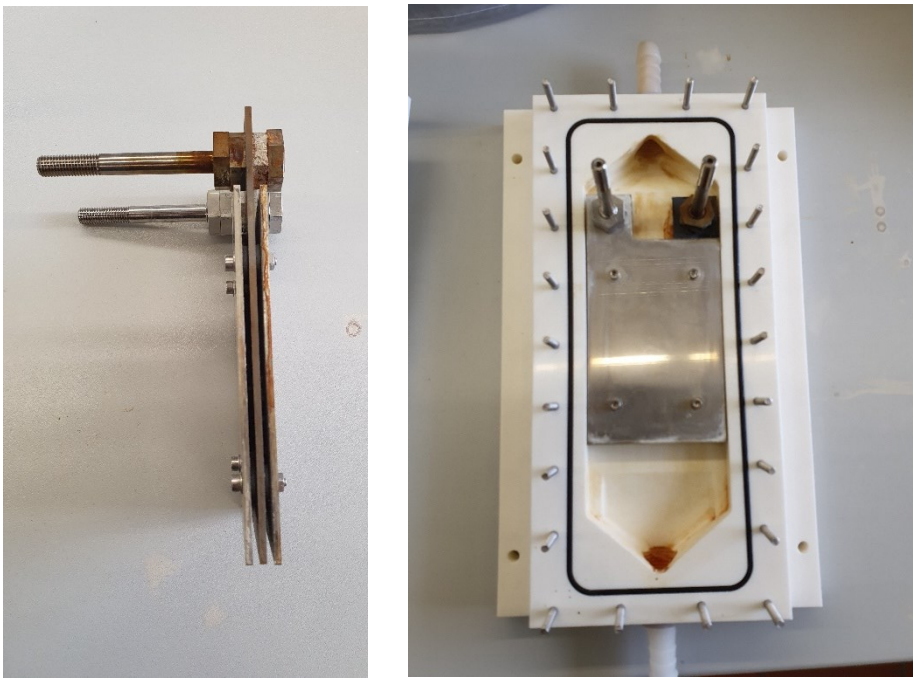

(a) (b)

Figure 37: Electrode stack (a) and electrode stack in the flow cell (b)

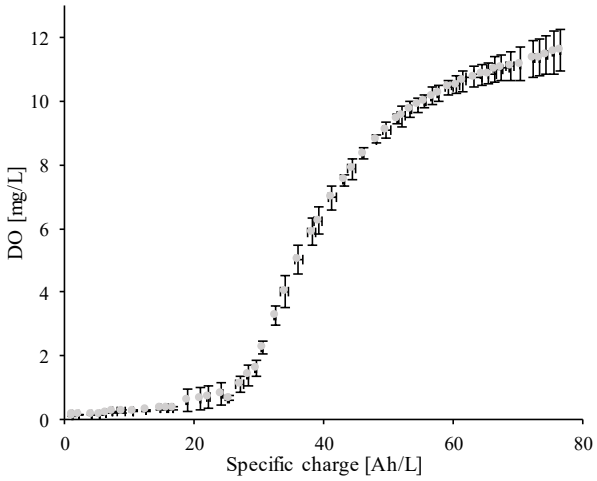

Figure 38: Evolution of DO during the EO of MBR 1-1. Mean values ± STD, n=3

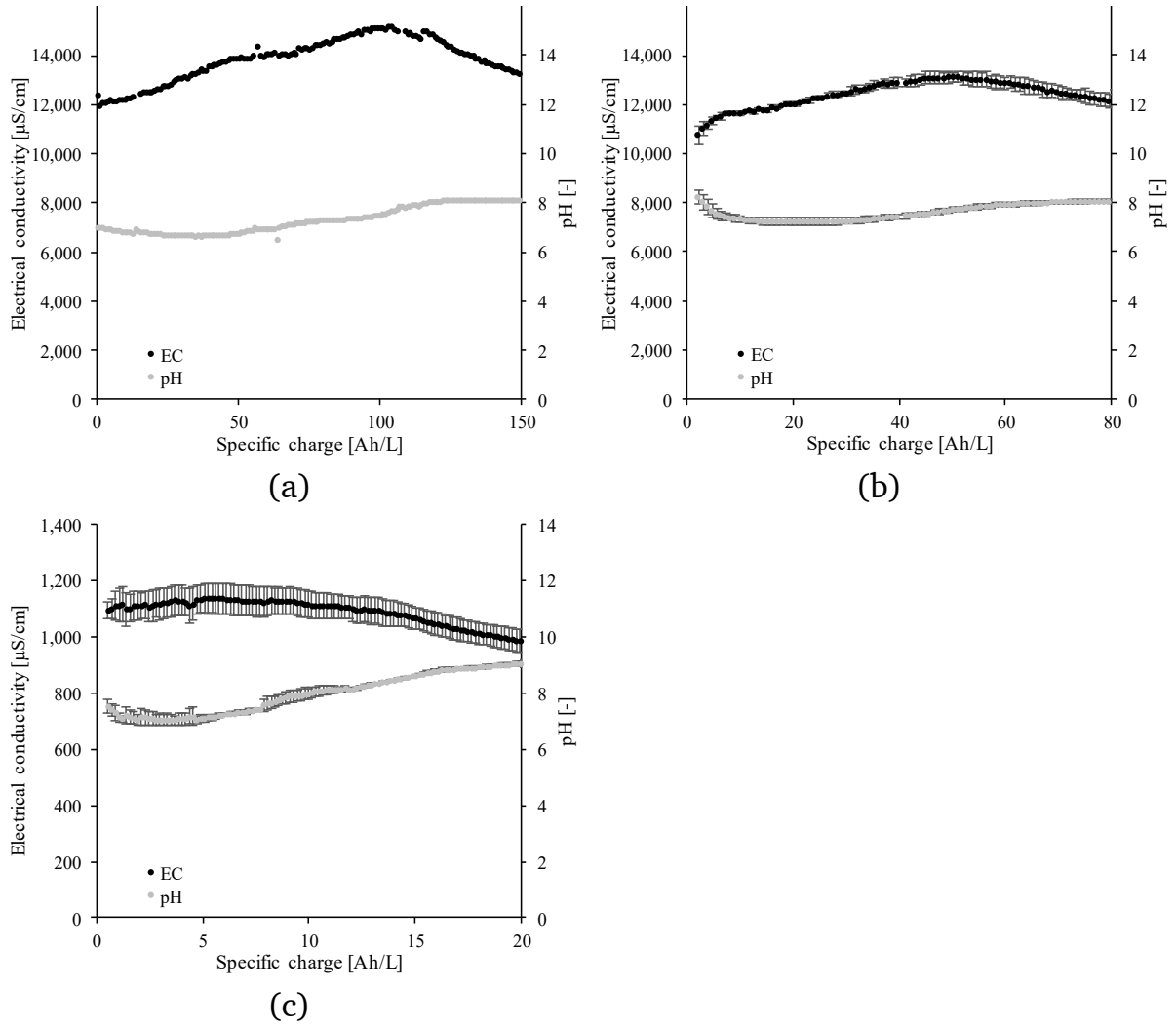

Figure 39: Evolution of electrical conductivity and the pH for a) PW-AD, b) MBR 1-1, and c) MBR 1-10 (Mean values and standard deviation). No standard deviation was given for PW-AD, since the recording of one test failed. Mean values ± STD, n=3

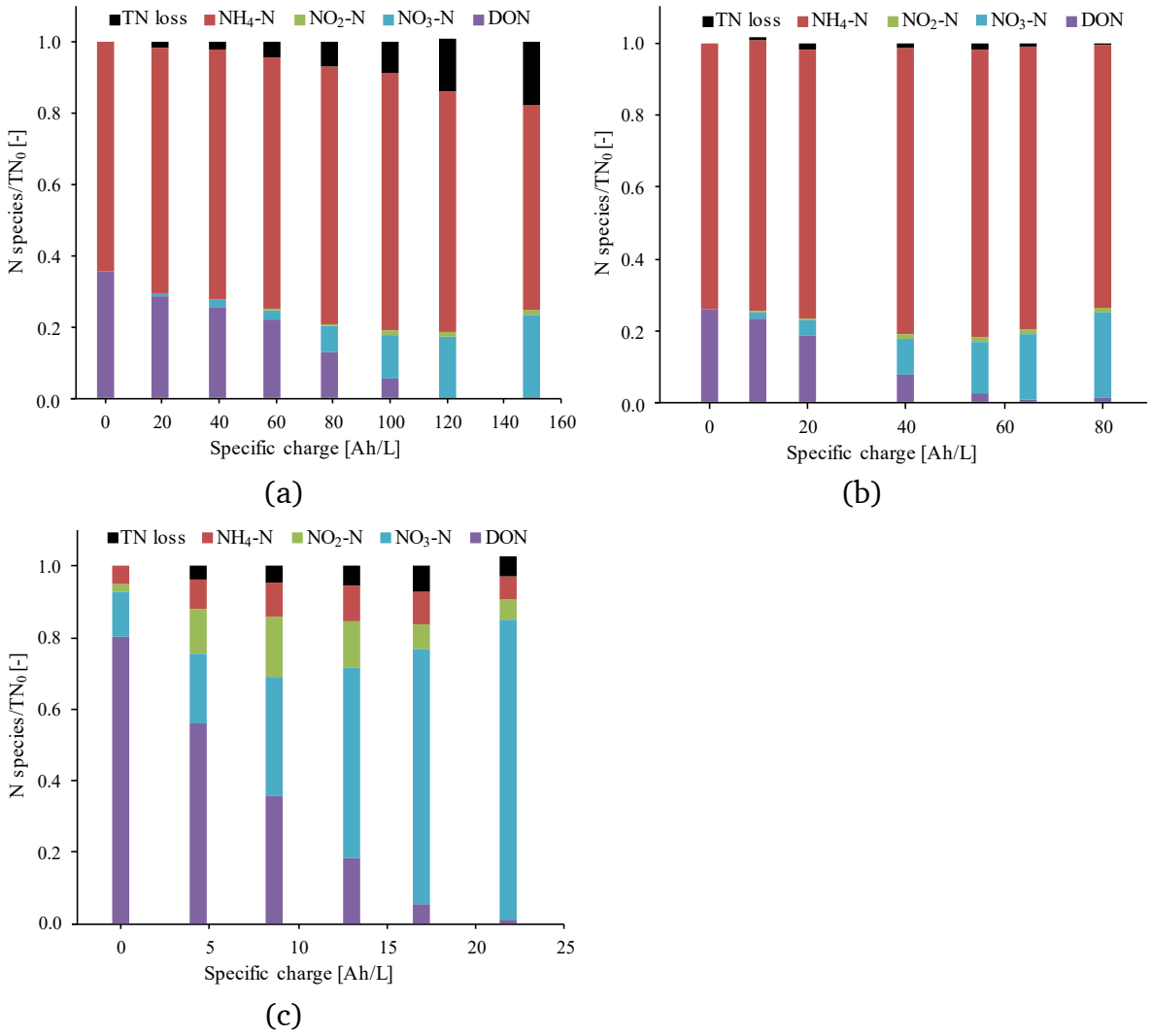

Figure 40: Nitrogen balances during the EO of a) PW-AD, b) MBR 1-1, and c) MBR 1-10. The single measured N species were related to the TN concentration at the beginning (TN_0). Mean values ± STD, n=3

Table 26: Toxicity of the HTC process waters before and after EO

Parameter	PW-AD	MBR 1-1	MBR 1-10
$G_{L,\ before\ EO}$	256	192	16
$G_{L,\ after\ EO}$[a]	6	6	≤2
$EC_{50,\ before\ EO}$	1.9%	2.2%	20.1%
$EC_{50,\ after\ EO}$[a]	57.7%	50.6%	n.d.[b]

[a]150 Ah/L for PW-AD, 80 Ah/L for MBR 1-1, 22 Ah/L for MBR 1-10

[b]not detectable

8 Proposed concept for process water treatment

The previous findings raise questions about how the processes of biological treatment and electrochemical oxidation can be combined most efficiently. For this purpose, the results obtained in each paper are supplemented by literature references for an exemplary HTC application on a wastewater treatment plant. Subsequently, the most viable concept results from balances for COD, nitrogen, and energy. Concepts are those described in section 7:

Scenario I: Electrooxidation only

Scenario II: Biodegradation using MBR without nitrification/denitrification and electrooxidation

Scenario III: Biodegradation using MBR with nitrification/denitrification and electrooxidation

The calculation is based on an exemplary wastewater treatment plant serving 100,000 inhabitants (Table 27). Assuming the specific anaerobic digested sewage sludge production and the TS after dewatering the formed hydrochars, 13.3 m^3 of HTC process water (PW) is produced each day.

Table 27: Calculation of the process water production of an example HTC plant for a population of 100,000

	Parameter	Value	Remarks
A	Specific sludge production [g TS/(P·d)]	38	Annual average of anaerobic digested sewage sludge production according to DWA-M 368 (DWA-M 368 2014)
B	Population [P]	100,000	Assumption
C	Total sludge production [t TS/d]	3.8	= A · B / (1,000,000 g/t)
D	Sewage sludge TS after dewatering [%]	19.8	TS of the sludge used in section 6
E	Sludge volume flow [m^3/d]	19.2	= C · (100% / D)
F	Hydrochar TS after dewatering [%]	65	Assumption based on section 2.2.1 and 5
G	Hydrochar volume flow [m^3/d]	5.8	= E · E / F
H	Process water flow [m^3/d]	13.3	= F - G

For scenarios I to III, the feed concentrations to the pilot plant (see 6.2.1) were adopted (Table 28). The dilution of the process water in Scenario III is based on

the ratio of the COD concentration of dilution 1:1 and 1:10 ($COD_{1:1}/COD_{1:10}$), which results in a process water flow rate of 150.8 m^3/d.

Table 28: Characteristics of the HTC process waters for the scenarios I, II, and III

Parameter	Scenario		
	I	II	III
Feed[a,b]			
Q_{PW} [m^3/d]	13.3[c]	13.3[c]	150.8[d]
COD [mg O_2/L]	30,381	30,381	2,680
TN [mg N/L]	3,148	3,148	293
NH_4-N [mg N/L]	1,819	1,819	179
DON [mg N/L]	1,329	1,329	106

[a]Concentrations of phase 2 and 4a feed from the pilot plant studies
[b]Nitrite and nitrate were neglected due to their low concentrations
[c]Calculation according to Table 27
[d]Dilution based on COD concentration; 13.3 $m^3/d \cdot COD_{1:1}/COD_{1:10}$

The MBR volume was calculated using the sludge loading (Table 29).

Table 29: MBR calculations for scenario II, and III

	Parameter	Scenario		Remarks
		II	III	
A	F/M_{COD} [g COD/(kg MLSS·d)]	723	130	Findings from section 6
B	MLSS [g/L]	9.3	9.3	Findings from section 6
C	OLR_{MBR}[g COD/(L·d)]	6.7	1.2	= A · B / (1,000 g/kg)
D	V_{MBR} [m^3]	60	334	= 404 kg/d[a] / C
E	$EC_{MBR,COD}$ [kWh/kg COD][c]	0.68	0.68	DWA-M 227[b]
F	EC_{MBR} [kWh/d]	172	203	= $COD_{removed}$[d] · E

[a]COD removal according to COD balance in kg/d
[b]Assuming 0.68 kWh/m^3 and a COD of 1 g/L (calculated from 120 g COD/(E·d) and 120 L/(E·d))
[c]The fact, that N+DN consumes more energy than carbon removal was neglected due to the MBR's low impact on the total energy consumption (MBR + EO)
[d]$COD_{removed}$ depends on the scenario according to the COD balance in kg/d

The EO anode area was calculated using the EO operation settings (Table 30).

Table 30: EO calculations for scenarios I, II, and III

	Parameter	Scenario			Remarks
		I	II	III	
A	Q_{EO} [Ah/L][a]	100	40	17	Findings from section 7
B	j [A/m²]	660	660	660	Setting in section 7
C	A_{Anode} [m²]	84	34	162	= (Q_{PW}[b] · A) / (24 h/d · B)
D	$EC_{EO,COD}$ [kWh/kg COD]	22	27	444	Findings from section 7
E	EC_{EO} [kWh/d]	8,436	3,480	43,363	= $COD_{removed}$[c] · D

[a] Q_{EO} was reduced for the benefit of higher efficiency, but to the disadvantage of higher effluent COD.
[b] Q_{PW} from Table 28 in L/d
[c] $COD_{removed}$ depends on the scenario according to the COD balance in kg/d

8.1 COD and nitrogen balance

The results of the COD balances are shown in Figure 41. Considering the presented boundary conditions, the COD load in the feed was calculated to 404 kg/d. The EO in Scenario I would remove 383 kg/d to an effluent load of 21 kg/d. In Scenario II, the EO reduces the COD to a similar extent (24 kg/d). Due to the upstream biological treatment in Scenario II, only 128 kg/d COD need to be oxidized. In Scenario I and II, EO was assumed not to remove COD completely in exchange for lower energy consumption, although an EO would be able of doing so (Section 7). The MBR removes 252 kg/d by biological conversion to CO_2 and biomass growth. The lower sludge loading in Scenario III results in a higher COD removal of 298 kg/d compared to Scenario II. Consequently, the load to be oxidized in Scenario III is the lowest at 98 kg/d and the effluent is lowest at 8 kg/d. However, reaching the low COD load requires diluting the feed, which leads to a higher volume flow and finally a larger MBR volume (334 m³) compared to Scenario II (60 m³). The higher volume flow additionally requires an almost 5-fold increase in the EO anode surface. Both entail considerably higher investment costs, which are not estimated at this point. Although the lowest COD load is oxidized in Scenario III, the energy consumption of 43,000 kWh/d is the highest by far among all scenarios. The lower efficiency as a consequence of the low COD concentration of the diluted and biologically treated process water is responsible for this. Such high energy consumption presumably cannot justify the low effluent load in Scenario III. An EO is not an energetically feasible technology for post-treatment of diluted HTC process water.

Scenario II requires a smaller anode area and only 3,652 kWh/d compared to 8,436 kWh/d in Scenario I. This is attributed to the biological pretreatment in

Scenario II, which already reduced the COD load. At the same time, the EO is operated at high efficiency in both scenarios. Accordingly, Scenario II is the most favorable regarding energy aspects.

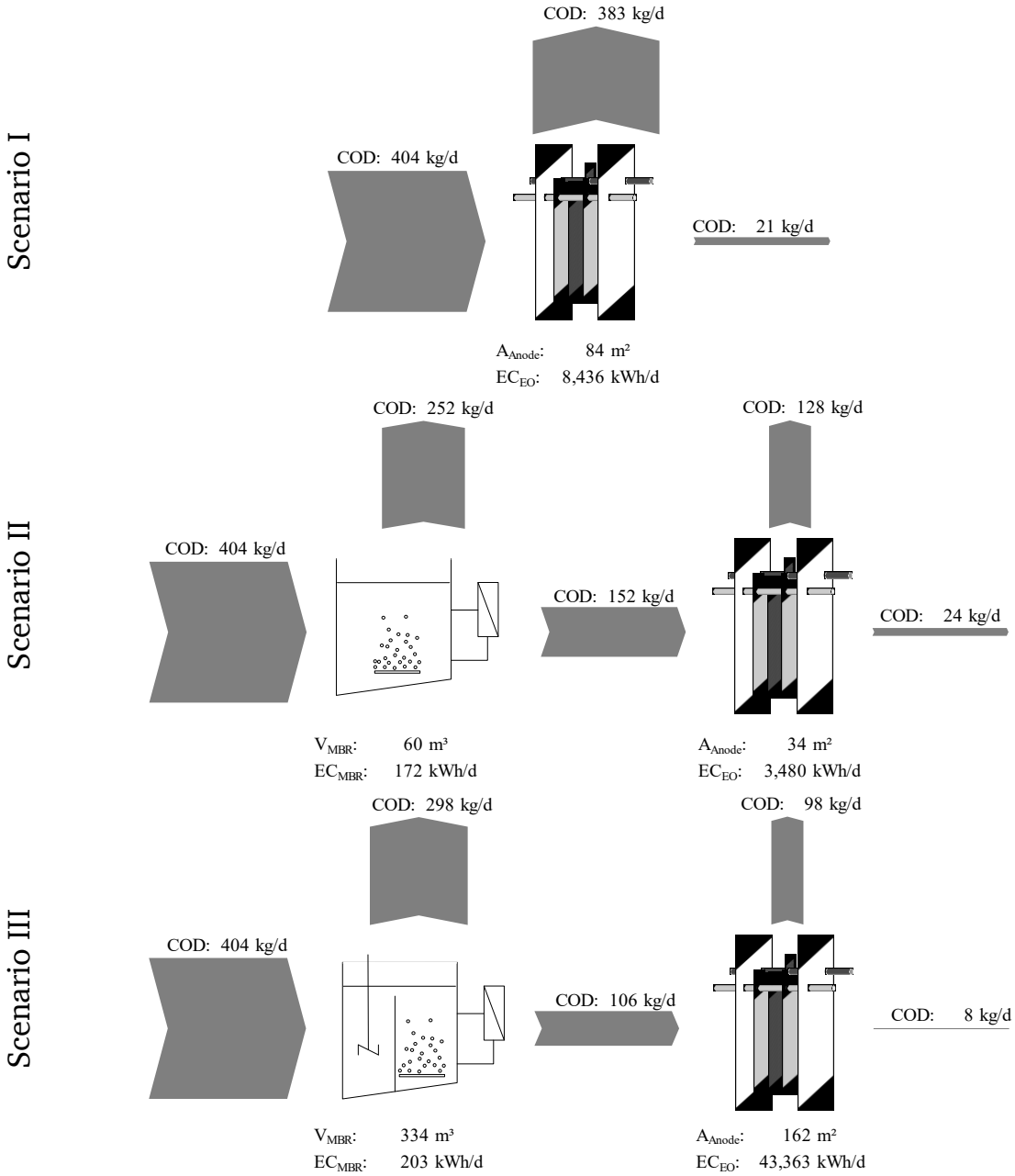

Figure 41: COD balances and energy consumptions for scenarios I, II, and III

Nitrogen is present in the HTC process water organically bound as DON and as ammonium with 17.7 kg/d and 24.2 kg/d, respectively (Figure 42). The EO in Scenario I converts most of the DON into ammonium and nitrate, which amount to 28.5 kg/d and 5.0 kg/d, respectively. As a result of N_2 formation during EO, the total nitrogen decreases by 4.0 kg/d. The DON is not completely converted by the EO because higher effluent loads were accepted in return for low energy consumption, analogous to the COD. The lower ammonium and nitrate in

Scenario II are due to the removal of nitrogen in the MBR as a result of biomass growth and possibly stripping. In total, both reduce nitrogen by 7.1 kg/d. With nitrification and denitrification in Scenario III, total nitrogen can be removed by 36.3 kg/d. The recalcitrant DON in the MBR effluent is 6.5 kg/d, while the other nitrogen species are less critical. The EO converts the DON almost completely to nitrate and smaller portions of ammonium and nitrite.

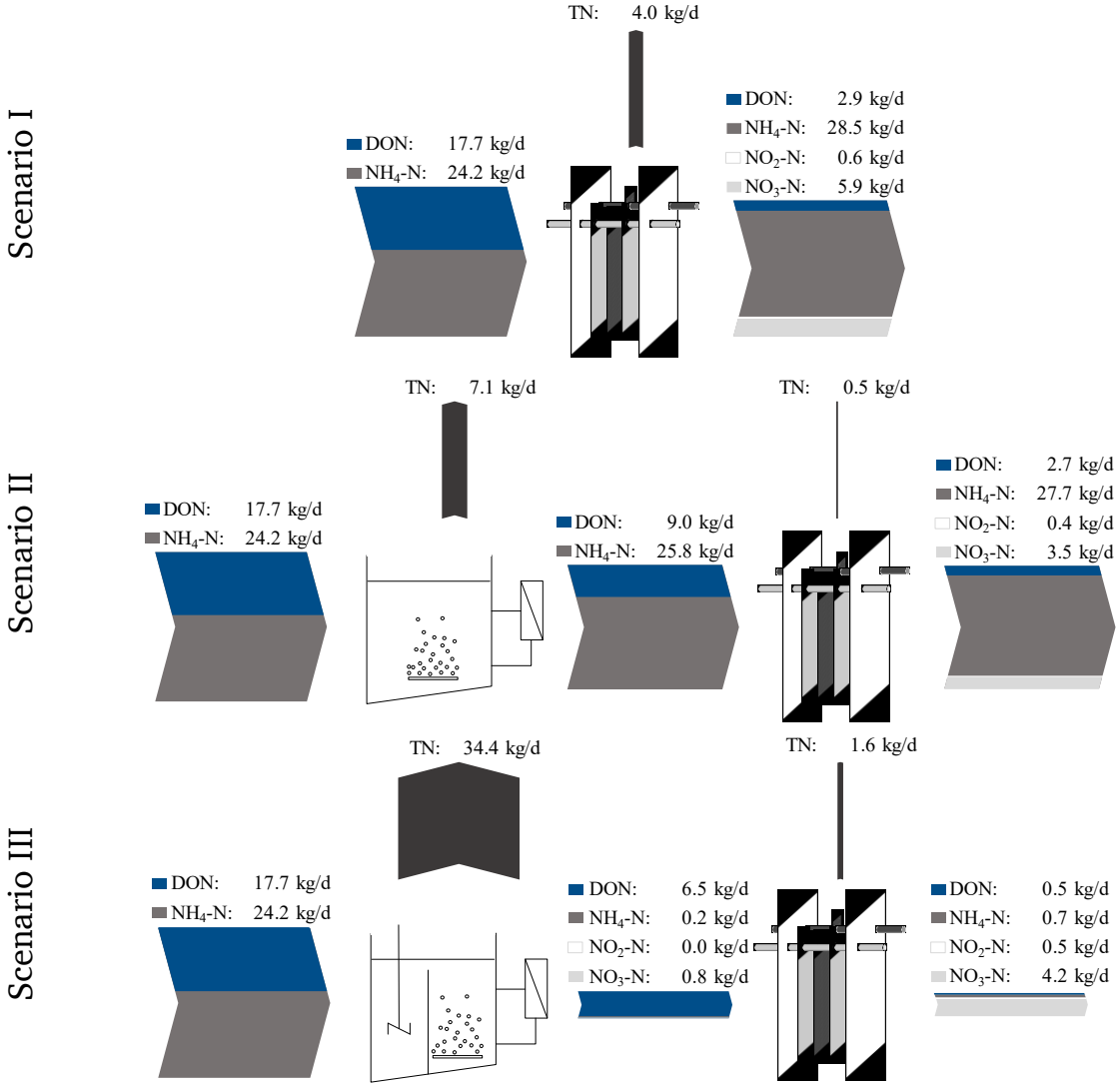

Figure 42: Nitrogen balances for scenarios I, II, and III

8.2 Implications

The preceding balances demonstrate the opportunities and limitations of the analyzed scenarios. The effluent concentrations after each treatment step are summarized in Table 31. In Scenario I, the EO consumes a lot of energy at low COD concentrations and other advanced oxidation processes or adsorption should be considered for post-treatment. However, the effluent COD concentration in Scenario I of 1.551 mg/L is not higher than that of process water

separated from dewatering anaerobically digested sludge at municipal WWTPs. Process water COD concentrations range between 809 and 5,000 mg/L and it is recirculated to the WWTP in many cases and can increase the WWTP's discharge concentrations (Rosenwinkel et al. 2015; DWA-M 349 2019). With this in mind, the follow-up treatment of HTC process water does not appear to be essential. Nevertheless, the absence of follow-up treatment would also lead to an increase in the discharge concentrations of the WWTP. Recirculating the EO-treated HTC process water to the WWTP could negatively affect its nitrification due to high ammonium concentrations of 2.144 mg/L. A more sophisticated approach to removing nitrogen would be its recovery. For recovering nitrogen as ammonium sulfate, ammonia stripping with subsequent acidic scrubbing or membrane distillation is conceivable (Klein 2015; Herb et al. 2021). High temperatures are advantageous for both processes, since the NH_4-NH_3 equilibrium favors ammonia and benefits stripping, and for membrane distillation it is needed to establish the vapor pressure gradient. Since EO heats up the process water during oxidation, less cooling of the EO and optimizing the nitrogen recovery would be a starting point for further research.

Scenario II is similar to Scenario I in terms of COD and ammonium concentrations, resulting in similar considerations for follow-up treatment and nitrogen recovery. However, the energy consumption in Scenario II is less than halved because the COD load to be oxidized is significantly lower.

In Scenario III, the very high energy consumption of the EO causes electrooxidation processes to be literally unfeasible. As aforementioned for low COD concentrations, other advanced oxidation processes or adsorption should be considered. As the COD concentrations are even lower than in Scenario I and II, post-treatment may not be necessary at all. Additionally, in Scenario III ammonium and nitrate concentrations are very low at 2 mg/L and 5 mg/L, respectively. Consequently, no negative effect on any nitrification of the WWTP is expected. For process water from a municipal digester, ammonium ranges from 455 to 1,200 mg/L (Rosenwinkel et al. 2015; DWA-M 349 2019). If discharging the pre-treated HTC process water in a WWTP is no option, further treating the process water is required in any case.

Table 31: Characteristics of the HTC process waters and the effluent concentrations after biodegradation (MBR) and oxidation (EO) for scenarios I, II, and III

	Scenario		
Parameter	**I**	**II**	**III**
Effluent MBR			
COD [mg O_2/L]	-	11,403	704
TN [mg N/L]	-	2,618	47
NH_4-N [mg N/L]	-	1,941	2
NO_2-N [mg N/L]	-	<0.3	0
NO_3-N [mg N/L]	-	<0.2	5
DON [mg N/L]	-	676	39
Effluent EO			
COD [mg O_2/L]	1,551	1,785	56
TN [mg N/L]	2,848	2,583	43
NH_4-N [mg N/L]	2,144	2,081	4
NO_2-N [mg N/L]	48	32	3
NO_3-N [mg N/L]	440	262	30
DON [mg N/L]	215	206	3

9 Conclusions and perspectives

"What is the effectiveness of aerobic biological processes and electro-chemical oxidation in treating process water generated from hydrothermal carbonization of sewage sludge?"

This research question can be answered by the challenges defined in section 3 as follows:

Challenge 1	*How do different HTC operating parameters affect the process water contamination?*

For keeping the loads of the process water as low as possible, higher reaction intensities or the addition of acid should be aimed for. High HTC temperatures and the addition of H_2SO_4 reduced the DOC concentration of the process water. The addition of H_2SO_4 was beneficial mainly at low reaction intensities. For a full-scale application, this implies a trade-off between higher energy consumption for higher temperatures and higher consumption of acids. In addition, higher reaction intensities break down DON, resulting in higher ammonium concentrations.

Challenge 2	*What is the effect of reaction temperature as key parameter of HTC on biodegradability and nitrification?*

HTC Temperature has a limited effect on aerobic biological treatment. For different temperatures (190 to 249 °C), the DOC removal in batch tests was almost similar (80.5 to 81.9%). In continuous SBRs, higher temperatures lowered the DOC removal at high sludge loadings by a few percent. Furthermore, higher temperatures inhibited nitrifying microorganisms more strongly. Nevertheless, both could only be detected to a minor extent.

Challenge 3	*Can the discharge of pretreated HTC process water deteriorate the effluent quality of municipal wastewater treatment plants?*

Refractory substances in the process water can considerably worsen the effluent quality. The deterioration of the effluent concentrations depends significantly on the boundary conditions, e.g. the load of the process water, the volume flow, the kind of sewage sludge for HTC, or the dilution of process water for pretreatment. A case study for non-diluted process water showed, that refractory substances could increase the effluent COD by up to 24.1 mg/L. For comparison, the COD limit for the category 4 WWTP, on which the mixing calculation was carried out, is 90 mg/L according to the German Wastewater Ordinance.

Challenge 4	*What are the limitations of biological treatment using MBR and SBR?*

The nitrogen sludge loading is the decisive parameter for operating nitrification and denitrification. For nitrogen removal, the F/M_N should be maximum 20 - 25 mg TN/(g MLSS·d), regardless of MBR or SBR. This F/M_N was associated with a COD removal of 74.8 ± 1.9% (MBR) and 71.4 ± 2.6% (SBR). Increasing the nitrogen sludge loading up to 78 mg TN/(g MLSS·d) caused nitrification breakdown, and also COD removal decreased to 62.5% (MBR). The effluent filtration by the MBR resulted in lower COD concentrations and smaller reactor volumes compared to the SBR.

Challenge 5	*Can nitrifying microorganisms acclimatize to process water contaminants?*

Nitrifying microorganisms can acclimatize remarkably to the inhibitory process water constituents. The IC_{50} for pre-exposed activated sludge was 10 times higher than the IC_{50} for non-pre-exposed activated sludge using raw HTC process water. Likewise, the refractory substances in pre-treated HTC process water were significantly less inhibitory towards pre-exposed activated sludge compared to non-pre-exposed activated sludge. Nevertheless, the nitrification rate of the pre-exposed activated sludge was mostly below 1.3 mg N/(g MLSS·h), which is lower than that of activated sludge from municipal wastewater treatment plants (2 - 6 mg N/(g MLSS·h)).

Challenge 6	*What is the efficiency of removing refractory compounds using electrochemical oxidation?*

The efficiency of the EO significantly depends on the organic matter content in the process water. At high organic concentrations, the ICE was 100% and dropped to below 2% at low organic concentrations. The decreasing efficiency sharply increased the energy consumption for oxidizing the process waters at different COD concentrations from 22 - 27 kWh/kg COD to 444 kWh/kg COD. Anyway, refractory compounds were removed to a high extent and the organic nitrogen was mainly converted into nitrate.

Challenge 7	*Which process combinations of biological treatment and oxidation are suitable for the treatment of HTC process water?*

From an energy point of view, biological pretreatment without nitrification and denitrification with downstream oxidation is the most effective solution. In addition, this process combination provides the opportunity to recover nitrogen. To achieve COD concentrations below approx. 2,000 mg/L, other processes than electrooxidation should be used.

Further perspectives

The results of this work demonstrate that HTC process water can be effectively treated with aerobic biological treatment followed by electrochemical oxidation. However, due to high inhibitors concentrations, nitrification can in fact only be established by diluting the process water. Without dilution, only the removal of carbon can be achieved. Considering the high concentrations of organic acids in the process water and the energy required for aeration, anaerobic processes seem to provide a better solution for removing carbon only. The produced biogas additionally improves the overall energy balance. However, due to the variety of inhibitors, the operation of anaerobic reactors is also sensitive to failures and yet there are no conclusive studies for full-scale implementations of anaerobic digestion available. In any case, when removing carbon only, the recovery of nitrogen is a promising approach and should be pursued. For removing the refractory matter, additional treatment steps are necessary. Electrooxidation turned out to achieve low effluent concentrations, although its energy consumption is very high. Removal of refractory compounds and achieving low effluent concentrations should receive further attention. Overall, the energy consumption for process water treatment reduces the savings resulting from improved dewaterability and thermal drying. Whether HTC including process water treatment can still lead to savings in energy and costs should be investigated in further studies.

10 References

Akiya, N.; Savage, P. E. (2002): Roles of Water for Chemical Reactions in High-Temperature Water. In Chemical Reviews 102, pp. 2725–2750.

Antal, M. J.; Mok, W. S.L.; Richards, G. N. (1990): Four-carbon model compounds for the reactions of sugars in water at high temperature. In Carbohydrate Research 199 (1), pp. 111–115. DOI: 10.1016/0008-6215(90)84097-E.

Aragón-Briceño, C. I.; Grasham, O.; Ross, A. B.; Dupont, V.; Camargo-Valero, M. A. (2020): Hydrothermal carbonization of sewage digestate at wastewater treatment works: Influence of solid loading on characteristics of hydrochar, process water and plant energetics. In Renewable Energy 157, pp. 959–973. DOI: 10.1016/j.renene.2020.05.021.

Aragón-Briceño, C. I.; Ross, A. B.; Camargo-Valero, M. A. (2021): Mass and energy integration study of hydrothermal carbonization with anaerobic digestion of sewage sludge. In Renewable Energy 167, pp. 473–483. DOI: 10.1016/j.renene.2020.11.103.

Aruoja, V.; Sihtmäe, M.; Dubourguier, H.-C.; Kahru, A. (2011): Toxicity of 58 substituted anilines and phenols to algae Pseudokirchneriella subcapitata and bacteria Vibrio fischeri: comparison with published data and QSARs. In Chemosphere 84 (10), pp. 1310–1320. DOI: 10.1016/j.chemosphere.2011.05.023.

Asghari, F. S.; Yoshida, H. (2006): Acid-Catalyzed Production of 5-Hydroxymethyl Furfural from d -Fructose in Subcritical Water. In Industrial & Engineering Chemistry Research 45 (7), pp. 2163–2173. DOI: 10.1021/ie051088y.

Baccile, N.; Laurent, G.; Babonneau, F.; Fayon, F.; Titirici, M.-M.; Antonietti, M. (2009): Structural Characterization of Hydrothermal Carbon Spheres by Advanced Solid-State MAS 13 C NMR Investigations. In The Journal of Physical Chemistry C 113 (22), pp. 9644–9654. DOI: 10.1021/jp901582x.

Bär, F. (2018): Hydrothermale Carbonisierung von holzartiger Biomasse und Modellsubstanzen. Dissertation. Technische Universität Darmstadt, Darmstadt.

Baskyr, I.; Weiner, B.; Riedel, G.; Poerschmann, J.; Kopinke, F.-D. (2014): Wet oxidation of char–water-slurries from hydrothermal carbonization of paper and brewer's spent grains. In Fuel Process Technology 128, pp. 425–431.

Bauer, A.; Lizasoain, J.; Theuretzbacher, F.; Agger, J. W.; Rincón, M.; Menardo, S. et al. (2014): Steam explosion pretreatment for enhancing biogas production of late harvested hay. In Bioresource Technology 166, pp. 403–410. DOI: 10.1016/j.biortech.2014.05.025.

Bergius, F. (1913): Die Anwendung hoher Drücke bei chemischen Vorgängen und eine Nachbildung des Entstehungsprozesses der Steinkohle. Halle a. S.: Wilhelm Knapp.

Blöhse, D. (2016): Karbonisate durch hydrothermale Verfahren. In P. Quicker, K. Weber (Eds.): Biokohle - Herstellung, Eigenschaften und Verwertung von Biomassekarbonisaten. Wiesbaden: Springer Vieweg.

Blöhse, D. (2017): Hydrothermale Karbonisierung – Nutzen dieser Konversationstechnik für optimierte Entsorgung feuchter Massenreststoffe. Duisburg-Essen, Universität, Essen. Fakultät für Ingenieurwissenschaften.

Chen, H.; Rao, Y.; Cao, L.; Shi, Y.; Hao, S.; Luo, G.; Zhang, S. (2019a): Hydrothermal conversion of sewage sludge: Focusing on the characterization of liquid products and their methane yields. In Chemical Engineering Journal 357, pp. 367–375.

Chen, H.; Rao, Y.; Cao, L.; Shi, Y.; Hao, S.; Luo, G.; Zhang, S. (2019b): Hydrothermal conversion of sewage sludge: Focusing on the characterization of liquid products and their methane yields. In Chemical Engineering Journal 357, pp. 367–375.

Ciarlini, J.; Alves, L.; Rajarathnam, G. P.; Haynes, B. S.; Montoya, A. (2020): Electrochemical oxidation of nitrogen-rich post-hydrothermal liquefaction. In Algal Research (48), p. 101919. DOI: 10.1016/j.algaI.2020.101919.

Danso-Boateng, E.; Shama, G.; Wheatley, A. D.; Martin, S. J.; Holdrich, R. G. (2015): Hydrothermal carbonisation of sewage sludge: Effect of process conditions on product characteristics and methane production. In Bioresource Technology 177, pp. 318–327.

Destatis (2021): Klärschlamm-entsorgung aus der öffentlichen Abwasser-behandlung. Available online at www.destatis.de, checked on 4/11/2023.

Dinjus, E.; Kruse, A.; Tröger, N. (2011): Hydrothermale Karbonisierung: 1. Einfluss des Lignins in Lignocellulosen. In Chemie Ingenieur Technik 83 (10), pp. 1734–1741. DOI: 10.1002/cite.201100092.

DWA-IG-5.1 (2012): 8. Arbeitsbericht der DWA-Arbeitsgruppe IG-5.1. Auswahl

und Bewertung von Systemen und Reaktoren zur anaeroben Industrieabwasserbehandlung. In Korrespondez Abwasser (59 (1)), pp. 1147–1152.

DWA-M 349 (2019): Biologische Stickstoffelimination von Schlammwässern der anaeroben Schlammstabilisierung. Hennef, Deutschland: Deutsche Vereinigung für Wasserwirtschaft Abwasser und Abfall e.V (DWA-Regelwerk).

DWA-M 368 (2014): Biologische Stabilisierung von Klärschlamm. Hennef, Deutschland: Deutsche Vereinigung für Wasserwirtschaft Abwasser und Abfall e.V (DWA-Regelwerk).

Dwyer, J.; Starrenburg, D.; Tait, S.; Barr, K.; Batstone, D. J.; Lant, P. (2008): Decreasing activated sludge thermal hydrolysis temperature reduces product colour, without decreasing degradability. In Water Research 42, pp. 4699–4709.

Escala, M.; Zumbühl, T.; Koller, Ch.; Junge, R.; Krebs, R. (2013): Hydrothermal Carbonization as an Energy-Efficient Alternative to Established Drying Technologies for Sewage Sludge. A Feasibility Study on a Laboratory Scale. In Energy & Fuels 27 (1), pp. 454–460.

Falco, C.; Baccile, N.; Titirici, M.-M. (2011): Morphological and structural differences between glucose, cellulose and lignocellulosic biomass derived hydrothermal carbons. In Green Chemistry 13 (11), p. 3273. DOI: 10.1039/c1gc15742f.

Fang, J.; Zhan, L.; Ok, Y. S.; Gao, B. (2018): Minireview of potential applications of hydrochar derived from hydrothermal carbonization of biomass. In Journal of Industrial and Engineering Chemistry 57, pp. 15–21.

Ferrentino, R.; Ceccato, R.; Marchetti, V.; Andreottola, G.; Fiori, L. (2020): Sewage Sludge Hydrochar: An Option for Removal of Methylene Blue from Wastewater. In Applied Sciences 10 (10), p. 3445. DOI: 10.3390/app10103445.

Ferrentino, R.; Merzari, F.; Grigolini, E.; Fiori, L.; Andreottola, G. (2021): Hydrothermal carbonization liquor as external carbon supplement to improve biological denitrification in wastewater treatment. In Journal of Water Process Engineering (44), p. 102360. DOI: 10.1016/j.jwpe.2021.10236O.

Fettig, J.; Austermann-Haun, U.; Meier, J.-F.; Busch, A.; Gilbert, E. (2019): Options for Removing Refractory Organic Substances in Pre-Treated Process Water from Hydrothermal Carbonization. In Water 11 (4), p. 730. DOI:

10.3390/w11040730.

Fettig, J.; Liebe, H. (2013): Analytik und physikalisch-chemische Behandlung von Prozesswässern aus der hydrothermalen carbonisierung von organischen Abfällen – erste Ergebnisse. In C. Grimm (Ed.): Hydrothermale Carbonisierung von Biomasse. Ergebnisse und Perspektiven. Berlin: Schmidt, Erich (Initiativen zum Umweltschutz 87).

Fettig, J.; Liebe, H.; Busch, A.; Austermann-Haun, U.; Meier, J. F. (2017): Entwicklung eines technischen Verwertungs- und Entsorgungskonzeptes für HTC-Prozesswasser. Abschlussbericht. Höxter/Detmold.

FiW e.V. (Ed.) (2023): BMBF Fördermaßnahme Regionales Phosphor-Recycling. Statusseminar. With assistance of Forschungsinstitut für Wasserwirtschaft und Klimazukunft an der RWTH Aachen (FiW) e.V. Frankfurt am Main, 03.-04.05.2023.

Foladori, P.; Bruni, L.; Tamburini, S. (2014): Toxicant inhibition in activated sludge: fractionation of the physiological status of bacteria. In Journal of Hazardous Materials 280, pp. 758–766. DOI: 10.1016/j.jhazmat.2014.09.003.

Franck, H.-G.; Knop, A. (1979): Kohleveredlung: Chemie und Technologie. Berlin, Heidelberg, New York: Springer-Verlag.

Fuchs, G.; Mohamed, M.; Altenschmidt, U.; Koch, J.; Lack, A.; Brackmann, R. et al. (1993): Biochemistry of anaerobic biodegradation of aromatic compounds. In C. Ratledge (Ed.): Biochemistry of Microbial Degradation. Dordrecht: Springer, pp. 513–553.

Funke, A. (2012): Hydrothermale Karbonisierung von Biomasse. Reaktionsmechanismen und Reaktionswärme. Berlin, Technische Universität, Berlin. Fakultät III - Prozesswissenschaften.

Funke, A.; Ziegler, F. (2010): Hydrothermal carbonization of biomass: A summary and discussion of chemical mechanisms for process engineering. In Biofuels, Bioproducts and Biorefining 4, pp. 160–177.

Garcia-Rodriguez, O.; Mousset, E.; Olvera-Vargas, H.; Lefebvre, O. (2020): Electrochemical treatment of highly concentrated wastewater: A review of experimental and modeling approaches from lab- to full-scale. In Critical Reviews in Environmental Science and Technology 52 (2), pp. 240–309. DOI: 10.1080/10643389.2020.1820428.

Gaur, R. Z.; Khoury, O.; Zohar, M.; Poverenov, E.; Darzi, R.; Laor, Y.; Posmanik, R. (2020): Hydrothermal carbonization of sewage sludge coupled with

anaerobic digestion: Integrated approach for sludge management and energy recycling. In Energy Conversion and Management 224, p. 113353.

González-Arias, J.; La Rubia, M. A. de; Sánchez, M. E.; Gómez, X.; Cara-Jiménez, J.; Martínez, E. J. (2023): Treatment of hydrothermal carbonization process water by electrochemical oxidation: Assessment of process performance. In Environmental research 216 (Pt 4), p. 114773. DOI: 10.1016/j.envres.2022.114773.

Großkopf, B. (2009): Einfluss von Produkten der Maillard-Reaktion und Salzen kurzkettiger Fettsäuren auf die Aktivität und Expression des Effluxtransporters P-Glykoprotein. In vitro-Untersuchungen an den humanen Kolonkarzinomzelllinien Caco-2 und LS180. Dissertation. Freie Universität Berlin, Berlin. Fachbereich Biologie, Chemie, Pharmazie.

Hämäläinen, A.; Kokko, M.; Kinnunen, V.; Hilli, T.; Rintala, J. (2021): Hydrothermal carbonisation of mechanically dewatered digested sewage sludge-Energy and nutrient recovery in centralised biogas plant. In Water Research 201, p. 117284. DOI: 10.1016/j.watres.2021.117284.

Herb, J.; Ebrahimi, M.; Winter, D.; Schwantes, R.; Lorenz, M.; Prenzel, T. (2021): Verfahren zur Rückgewinnung von Ammonium aus Abwasser mittels Membrandestillation. Abschlussbericht. Aktenzeichen: 34167/01. Edited by Deutsche Bundesstiftung Umwelt (DBU).

Hodge, J. E. (1953): Dehydrated Foods, Chemistry of Browning Reactions in Model Systems. In Journal of Agricultural and Food Chemistry 1 (15), pp. 928–943. DOI: 10.1021/jf60015a004.

Horn, S. J.; Estevez, M. M.; Nielsen, H. K.; Linjordet, R.; Eijsink, V. G. H. (2011): Biogas production and saccharification of Salix pretreated at different steam explosion conditions. In Bioresour Technol 102 (17), pp. 7932–7936. DOI: 10.1016/j.biortech.2011.06.042.

Hu, B.; Wang, K.; Wu, L.; Yu, S.-H.; Antonietti, M.; Titirici, M.-M. (2010): Engineering carbon materials from the hydrothermal carbonization process of biomass. In Advanced Materials 22 (7), pp. 813–828. DOI: 10.1002/adma.200902812.

Hu, R.; Liu, Y.; Zhu, G.; Chen, C.; H., Dwi; Yan, M. (2022a): COD removal of wastewater from hydrothermal carbonization of food waste: Using coagulation combined activated carbon adsorption. In Journal of Water Process Engineering 45, p. 102462. DOI: 10.1016/j.jwpe.2021.102462.

Huang, F.; Liu, H.; Wen, J.; Zhao, C.; Dong, L. (2021a): Underestimated humic acids release and influence on anaerobic digestion during sludge thermal hydrolysis. In Water Research 201, p. 117310. DOI: 10.1016/j.watres.2021.117310.

Huang, J.; Wang, Z.; Qiao, Y.; Wang, B.; Yu, Y.; Xu, M. (2021b): Transformation of nitrogen during hydrothermal carbonization of sewage sludge: Effects of temperature and Na/Ca acetates addition. In Proceedings of the Combustion Institute 38 (3), pp. 4335–4344. DOI: 10.1016/j.proci.2020.06.075.

Kim, D.; Lee, K.; Park, K. Y. (2014): Hydrothermal carbonization of anaerobically digested sludge for solid fuel production and energy recovery. In Fuel 130, pp. 120–125.

Klein, D. (2015): Bewertung der Stickstoff- und Phosphorrückgewinnung im Gesamtsystem aus Abwasserreinigung und Landwirtschaft. Dissertation. Technische Universität Braunschweig, Braunschweig. Institut für Siedlungswasserwirtschaft.

Klima, M. S.; DeHart, I.; Coffman, R. (2011): Baseline Testing of a Filter Press and Solid-Bowl Centrifuge for Dewatering Coal Thickener Underflow Slurry. In International Journal of Coal Preparation and Utilization 31 (5), pp. 258–272. DOI: 10.1080/19392699.2011.558548.

Knežević, D. (2009): Hydrothermal Conversion of Biomass. Dissertation. University of Twente, Enschede.

Krebs, R.; Baier, U.; Deller, A.; Escala, M.; Floris, J.; Gerner, G. et al. (2013): Weiterentwicklung der hydrothermalen Karbonisierung zur CO2-sparenden und kosteneffizienten Trocknung von Klärschlamm im industriellen Massstab sowie der Rückgewinnung von Phosphor. Schlussbericht UTF 387.21.11./ IDM 2006.2423.222. Schweiz.

Kruse, A.; Dinjus, E. (2007): Hot compressed water as reaction medium and reactant. 2. Degradation reactions. In The Journal of Supercritical Fluids 41 (3), pp. 361–379. DOI: 10.1016/j.supflu.2006.12.006.

Kruse, A.; Funke, A.; Titirici, M.-M. (2013): Hydrothermal conversion of biomass to fuels and energetic materials. In Current Opinion in Chemical Biology 17 (3), pp. 515–521. DOI: 10.1016/j.cbpa.2013.05.004.

Lachos-Perez, D.; Torres-Mayanga, P. C.; Abaide, E. R.; Zabot, G. L.; Castilhos, F. de (2022): Hydrothermal carbonization and Liquefaction: differences, progress, challenges, and opportunities. In Bioresour Technol 343, p. 126084.

DOI: 10.1016/j.biortech.2021.126084.

Langone, A.; Sabia, G.; Petta, L.; Zanetti, L.; Leoni, L.; Basso, D. et al. (2021): Evaluation of the aerobic biodegradability of process water produced by hydrothermal carbonization and inhibition effects on the heterotrophic biomass of an activated sludge system. In Journal of Environmental Management 299 (299), p. 113561. DOI: 10.1016/j.jenvman.2021.113561.

Langone, Michela; Basso, Daniele (2020): Process Waters from Hydrothermal Carbonization of Sludge: Characteristics and Possible Valorization Pathways. In International journal of environmental research and public health 17 (18). DOI: 10.3390/ijerph17186618.

Liebeck, M. (2015): Untersuchung zur Hydrothermalen Carbonisierung an Modellsubstanzen. Dissertation. Technische Universität Darmstadt, Darmstadt. Ernst-Berl-Institut für Technische und Makromolekulare Chemie.

Liu, L.; Zhai, Y.; Liu, X.; Wang, Z.; Zhu, Y.; Xu, M. (2022): Features and mechanisms of sewage sludge hydrothermal carbonization aqueous phase after ferrous/persulfate-based process: The selective effect of oxidation and coagulation. In Journal of Cleaner Production 366, p. 132831. DOI: 10.1016/j.jclepro.2022.132831.

Macêdo, W. V.; Schmidt, J. S.; Jensen, S. B.; Biller, P.; Vergeynst, L. (2023): Is nitrification inhibition the bottleneck of integrating hydrothermal liquefaction in wastewater treatment plants? In Journal of Environmental Management 348, p. 119046. DOI: 10.1016/j.jenvman.2023.119046.

Mannarino, G.; Caffaz, S.; Gori, R.; Lombardi, L. (2022): Environmental Life Cycle Assessment of Hydrothermal Carbonization of Sewage Sludge and Its Products Valorization Pathways. In Waste and Biomass Valorization 13 (9), pp. 3845–3864. DOI: 10.1007/s12649-022-01821-x.

Marin-Batista, J. D.; Mohedano, A. F.; Rodriguez, J. J.; La Rubia, M. A. de (2020): Energy and phosphorous recovery through hydrothermal carbonization of digested sewage sludge. In Waste Management 105, pp. 566–574.

Matissek, R. (2016): Kohlenhydrate. In R. Matissek, W. Baltes (Eds.): Lebensmittelchemie. Berlin, Heidelberg: Springer Berlin Heidelberg, pp. 131–175.

Meng, D.; Jiang, Z.; Kunio, Y.; Mu, H. (2012): The effect of operation parameters on the hydrothermal drying treatment. In Renewable Energy 42, pp. 90–94.

DOI: 10.1016/j.renene.2011.09.011.

Merzari, F.; Goldfarb, J.; Andreottola, G.; Mimmo, T.; Volpe, M.; Fiori, L. (2020): Hydrothermal Carbonization as a Strategy for Sewage Sludge Management: Influence of Process Withdrawal Point on Hydrochar Properties. In Energies 13 (11), p. 2890. DOI: 10.3390/en13112890.

Miyazawa, T.; Ohtsu, S.; Funazukuri, T. (2008): Hydrothermal degradation of polysaccharides in a semi-batch reactor: product distribution as a function of severity parameter. In Journal of Materials Science 43 (7), pp. 2447–2451. DOI: 10.1007/s10853-007-2014-y.

Mottet, A.; Steyer, J. P.; Déléris, S.; Vedrenne, F.; Chauzy, J.; Carrère, H. (2009): Kinetics of thermophilic batch anaerobic digestion of thermal hydrolysed waste activated sludge. In Biochemical Engineering Journal 46 (2), pp. 169–175. DOI: 10.1016/j.bej.2009.05.003.

Nelson, D. A.; Molton, P. M.; Russell, J. A.; Hallen, R. T. (1984): Application of direct thermal liquefaction for the conversion of cellulosic biomass. In Industrial & Engineering Chemistry Product Research and Development 23 (3), pp. 471–475. DOI: 10.1021/i300015a029.

Neyens, E.; Baeyens, J.; Dewil, R.; Heyder, B. de (2004): Advanced sludge treatment affects extracellular polymeric substances to improve activated sludge dewatering. In J Hazard Mater 106 (2-3), pp. 83–92. DOI: 10.1016/j.jhazmat.2003.11.014.

Ohlert, J. (2015): Hydrothermale Carbonisierung (HTC) von Klär- und Faulschlämmen. Oldenburg, Universität.

Oliveira, A. S.; Sarrión, A.; Baeza, J. A.; Diaz, E.; Calvo, L.; Mohedano, A. F.; Gilarranz, M. A. (2022): Integration of hydrothermal carbonization and aqueous phase reforming for energy recovery from sewage sludge. In Chemical Engineering Journal 442, p. 136301. DOI: 10.1016/j.cej.2022.136301.

Park, M.; Kim, N.; Jung, S.; Jeong, T.-Y.; Park, D. (2021): Optimization and comparison of methane production and residual characteristics in mesophilic anaerobic digestion of sewage sludge by hydrothermal treatment. In Chemosphere 264, p. 128516.

Peterson, A. A.; Vogel, F.; Lachance, R. P.; Fröling, M.; Antal Jr., M. J.; W, Tester J. (2008): Thermochemical biofuel production in hydrothermal media. A review of sub- and supercritical water technologies. In Energy and Environmental Science 1, pp. 32–65.

Pham, M.; Schideman, L.; Scott, J.; Rajagopalan, N.; Plewa, M. J. (2013): Chemical and biological characterization of wastewater generated from hydrothermal liquefaction of Spirulina. In Environmental Science & Technology 47 (4), pp. 2131–2138. DOI: 10.1021/es304532c.

Reißmann, D.; Thrän, D.; Bezama, A. (2018): Hydrothermal processes as treatment paths for biogenic residues in Germany. A review of the technology, sustainability and legal aspects. In Journal of Cleaner Production 172, pp. 239–252. DOI: 10.1016/j.jclepro.2017.10.151.

Reißmann, D.; Thrän, D.; Blöhse, D.; Bezama, A. (2021): Hydrothermal carbonization for sludge disposal in Germany: A comparative assessment for industrial-scale scenarios in 2030. In Journal of Industrial Ecology 25 (3), pp. 720–734. DOI: 10.1111/jiec.13073.

Reza, M. T.; Freitas, A.; Yang, X.; Coronella, C. J. (2016): Wet Air Oxidation of Hydrothermal Carbonization (HTC) Process Liquid. In ACS Sustainable Chemistry & Engineering 4 (6), pp. 3250–3254. DOI: 10.1021/acssuschemeng.6b00292.

Rosenwinkel, K.-H.; Kroiss, H.; Dichtl, N.; Seyfried, C.-F.; Weiland, P. (Eds.) (2015): Anaerobtechnik: Springer-Verlag Berlin Heidelberg.

Roskosch, A.; Heidecke, P. (2019): Sewage Sludge Disposal in the Federal Republic of Germany. Edited by Umweltbundesamt.

Roy, U. K.; Radu, T.; Wagner, J. L. (2021): Carbon-negative biomethane fuel production: Integrating anaerobic digestion with algae-assisted biogas purification and hydrothermal carboinsation of digestate. In Biomass and Bioenergy 128, p. 106029.

Sangave, P. C.; Gogate, P. R.; Pandit, A. B. (2007): Combination of ozonation with conventional aerobic oxidation for distillery wastewater treatment. In Chemosphere 68 (1), pp. 32–41. DOI: 10.1016/j.chemosphere.2006.12.053.

Särkkä, H.i; Bhatnagar, A.; Sillanpää, M. (2015): Recent developments of electro-oxidation in water treatment — A review. In Journal of Electroanalytical Chemistry 754, pp. 46–56. DOI: 10.1016/j.jelechem.2015.06.016.

Scherzinger, M.; Kaltschmitt, M. (2021): Thermal pre-treatment options to enhance anaerobic digestibility – A review. In Renewable and Sustainable Energy Reviews 137, p. 110627. DOI: 10.1016/j.rser.2020.110627.

Schnell, M.; Horst, T.; Quicker, P. (2020): Thermal treatment of sewage sludge

in Germany: A review. In Journal of Environmental Management 263, p. 110367. DOI: 10.1016/j.jenvman.2020.110367.

Schwarz, G.; Lingens, F. (1993): Bacterial degradation of N-heterocyclic compounds. In C. Ratledge (Ed.): Biochemistry of Microbial Degradation. Dordrecht: Springer, pp. 459–486.

Scragg, A. H. (2006): The effect of phenol on the growth of Chlorella vulgaris and Chlorella VT-1. In Enzyme and Microbial Technology 39 (4), pp. 796–799. DOI: 10.1016/j.enzmictec.2005.12.018.

Sevilla, M.; Fuertes, A. B. (2009): The production of carbon materials by hydrothermal carbonization of cellulose. In Carbon 47, pp. 2281–2289.

Seyedi, S.; Venkiteshwaran, K.; Zitomer, D. (2021): Current status of biomethane production using aqueous liquid from pyrolysis and hydrothermal liquefaction of sewage sludge and similar biomass. In Reviews in Environmental Science and Bio/Technology 20 (1), pp. 237–255. DOI: 10.1007/s11157-020-09560-y.

Smith, A. M.; Singh, S.; Ross, A. B. (2016): Fate of inorganic material during hydrothermal carbonisation of biomass: Influence of feedstock on combustion behaviour of hydrochar. In Fuel 169, pp. 135–145. DOI: 10.1016/j.fuel.2015.12.006.

Spataru, A.; Jain, R.; Chung, J. W.; Gerner, G.; Krebs, R.; Lens, P. N. L. (2016): Enhanced adsorption of orthophosphate and copper onto hydrochar derived from sewage sludge by KOH activation. In RSC Advances 6 (104), pp. 101827–101834. DOI: 10.1039/C6RA22327C.

Stemann, J. (2013): Hydrothermale Carbonisierung: Stoffliche und energetische Kreislaufführung. Dissertation. Technische Universität Berlin, Berlin. Fakultät III - Prozesswissenschaften.

Takagi, K. (2015): Polymerization Reactions (Overview). In S. Kobayashi, K. Müllen (Eds.): Encyclopedia of Polymeric Nanomaterials. Berlin, Heidelberg: Springer Berlin Heidelberg, pp. 1982–1987.

TerraNova Energy GmbH (2023). Available online at https://www.terranova-energy.com/technologie/, updated on 2/14/2023.

Titirici, M. M.; Thomas, A.; Yu, S.-H.; Müller, J.-O.; Antonietti, M. (2007): A Direct Synthesis of Mesoporous Carbons with Bicontinuous Pore Morphology from Crude Plant Material by Hydrothermal Carbonization. In Chemistry of Materials 19 (17), pp. 4205–4212. DOI: 10.1021/cm0707408.

Urbanowska, A.; Kabsch-Korbutowicz, M.; Wnukowski, M.; Seruga, P.; Baranowski, M.; Pawlak-Kruczek, H. et al. (2020): Treatment of Liquid By-Products of Hydrothermal Carbonization (HTC) of Agricultural Digestate Using Membrane Separation. In Energies 13 (1), p. 262. DOI: 10.3390/en13010262.

Vesilind, P. A. (1994): The role of water in sludge dewatering. In Water Environment Research 66 (1), pp. 4–11. DOI: 10.2175/WER.66.1.2.

Villamil, J. A.; Mohedano, A. F.; Rodriguez, J. J.; La Rubia, M. A. de (2018): Valorisation of the liquid fraction from hydrothermal carbonisation of sewage sludge by anaerobic digestion. In Journal of Chemical Technology & Biotechnology 93 (2), pp. 450–456. DOI: 10.1002/jctb.5375.

Vogel, F. (2016): Hydothermale Verfahren. In M. Kaltschmitt, H. Hartmann, H. Hofbauer (Eds.): Energie aus Biomasse, 3. Auflage: Springer-Verlag Berlin Heidelberg.

Wang, L.; Chang, Y.; Li, A. (2019a): Hydrothermal carbonization for energy-efficient processing of sewage sludge: A review. In Renewable and Sustainable Energy Reviews 108, pp. 423–440.

Wang, L.; Chang, Y.; Liu, Q. (2019b): Fate and distribution of nutrients and heavy metals during hydrothermal carbonization of sewage sludge with implication to land application. In Journal of Cleaner Production 225, pp. 972–983.

Wang, L.; Li, A. (2015): Hydrothermal treatment coupled with mechanical expression at increased temperature for excess sludge dewatering: the dewatering performance and the characteristics of products. In Water Research 68, pp. 291–303. DOI: 10.1016/j.watres.2014.10.016.

Wang, L.; Zhang, L.; Li, A. (2014): Hydrothermal treatment coupled with mechanical expression at increased temperature for excess sludge dewatering: influence of operating conditions and the process energetics. In Water Research 65, pp. 85–97. DOI: 10.1016/j.watres.2014.07.020.

Wang, W.; Chen, W.-H.; Jang, M.-F. (2020): Characterization of Hydrochar Produced by Hydrothermal Carbonization of Organic Sludge. In Future Cities and Environment 6 (1), Article 13. DOI: 10.5334/fce.102.

Weide, T.; Brügging, E.; Wetter, C. (2019): Anaerobic and aerobic degradation of wastewater from hydrothermal carbonization (HTC) in a continuous, three-stage and semi-industrial system. In Journal of Environmental Chemical

Engineering 7.

Wilén, B.-M.; Jin, B.; Lant, P. (2003): Impacts of structural characteristics on activated sludge floc stability. In Water Research 37 (15), pp. 3632–3645. DOI: 10.1016/S0043-1354(03)00291-4.

Wilk, M.; Gajek, M.; Śliz, M.; Czerwińska, K.; Lombardi, L. (2022): Hydrothermal Carbonization Process of Digestate from Sewage Sludge: Chemical and Physical Properties of Hydrochar in Terms of Energy Application. In Energies 15 (18), p. 6499. DOI: 10.3390/en15186499.

Wirth, B. (2021): Anaerobic treatment of liquid by-products from hydrothermal carbonization of biomass. Technische Universität Berlin, Berlin. Fakultät III – Prozesswissenschaften.

Wirth, B.; Reza, M. T.; Mumme, J. (2015): Influence of digestion temperature and organic loading rate on the continuous anaerobic treatment of process liquor from hydrothermal carbonization of sewage sludge. In Bioresource Technology 198, pp. 215–222.

Xu, Y.; Lu, J.; Wang, Y.; Yuan, C.; Liu, Z. (2022a): Construct a novel anti-bacteria pool from hydrothermal liquefaction aqueous family. In Journal of Hazardous Materials 423, p. 127162. DOI: 10.1016/j.jhazmat.2021.127162.

Xu, Yongdong; Wang, Yueyao; Lu, Jianwen; Yuan, Changbin; Zhang, Leli; Liu, Zhidan (2022b): Understand the antibacterial behavior and mechanism of hydrothermal wastewater. In Water Research 226, p. 119318. DOI: 10.1016/j.watres.2022.119318.

Xu, Z.-X.; Ma, X.-Q.; Zhou, J. Duan, P.-G.; Zhou, W.-Y.; Ahmad, A.; Luque, R. (2022c): The influence of key reactions during hydrothermal carbonization of sewage sludge on aqueous phase properties: A review. In Journal of Analytical and Applied Pyrolysis 167, p. 105678. DOI: 10.1016/j.jaap.2022.105678.

Yang, G.; Liu, H.; Li, Y.; Zhou, Q.; Jin, M.; Xiao, H.; Yao, H. (2022b): Kinetics of hydrothermal carbonization of kitchen waste based on multi-component reaction mechanism. In Fuel 324, p. 124693. DOI: 10.1016/j.fuel.2022.124693.

Young, J. C. (1991): Factors Affecting the Design and Performance of Upflow Anaerobic Filters. In Water Science & Technology 24 (8), pp. 133–155. DOI: 10.2166/wst.1991.0222.

Yuan, Y.; Yu, Y.; Xi, H.; Zhou, Y.; He, X. (2019): Comparison of four test methods for toxicity evaluation of typical toxicants in petrochemical wastewater on

activated sludge. In Science of the Total Environment 685, pp. 273–279. DOI: 10.1016/j.scitotenv.2019.05.389.

Zhao, P.; Shen, Y.; Ge, S.; Yoshikawa, K. (2014): Energy recycling from sewage sludge by producing solid biofuel with hydrothermal carbonization. In Energy Conversion and Management 78, pp. 815–821. DOI: 10.1016/j.enconman.2013.11.026.

Zheng, X.; Huang, J.; Ying, Z.; Ji, S.; Feng, Y.; Wang, B.; Dou, B. (2021): Thermochemical conversion of sewage sludge-derived hydrochars: Volatile release and char gasification kinetics. In Journal of Analytical and Applied Pyrolysis 156, p. 105138.

Zhuang, X.; Huang, Y.; Song, Y.; Zhan, H.; Yin, X.; Wu, C. (2017): The transformation pathways of nitrogen in sewage sludge during hydrothermal treatment. In Bioresource Technology 245, pp. 463–470.

Zhuang, X.; Zhan, H.; Huang, Y.; Song, Y.; Yin, X.; Wu, C. (2018): Conversion of industrial biowastes to clean solid fuels via hydrothermal carbonization (HTC): Upgrading mechanism in relation to coalification process and combustion behavior. In Bioresour Technol 267, pp. 17–29. DOI: 10.1016/j.biortech.2018.07.002.